



INAOE

# Spectroscopic search for multiple stellar populations in the Main Sequence of the globular cluster M3

by

Julio César Mendoza Cervantes

A thesis submitted to the Instituto Nacional de Astrofísica, Óptica y Electrónica for the degree of Master of Science in the department of Astrophysics.

Supervisors:

Dr. Miguel Chávez Dagostino  
Dr. Emanuele Bertone

Santa María Tonantzintla, Puebla  
September, 2017

©INAOE 2017

El autor otorga al INAOE el permiso de reproducir y distribuir copias parcial o totalmente de esta tesis.





# Abstract

We present preliminary results on the investigation of the nature of multiple stellar populations in Main Sequence stars (this is, in stars in an evolutionary stage that still preserves their natal chemical composition because they have not yet experienced chemical mixing through deep convection processes) of the Globular Cluster M3 (NGC 5272) by means of a theoretical study using stellar model atmospheres, synthetic spectra and spectroscopic indices.

The work is composed of two main parts that include: (i) The calculation of new Opacity Distribution Functions (ODFs) appropriate for the chemical mix observed in evolved stars of globular clusters, and their use in the creation of a new grid of theoretical spectra at very high resolution. (ii) The computation of a set of theoretical absorption line spectroscopic indices and their correlation with the three leading atmospheric parameters: effective temperature, surface gravity and global metallicity ( $T_{\text{eff}}/\log g/[{\text{Fe}}/{\text{H}}]$ ).

For the first part we implemented a series of numerical routines within the code DFSYNTHE to calculate the distribution of opacities in agreement with the chemical partitions used by [Sbordone et al. \(2011\)](#) which represent, to some extent, the prototypical elemental abundance combinations of globular clusters with multiple stellar populations. Namely, these partitions were an  $\alpha$ -enhanced solar-scaled Reference abundance of  $[{\text{Fe}}/{\text{H}}] = -1.62$  dex ( $Z = 0.001$ ), compatible with the metallicity of M3 of -1.5 ([Harris 1996](#), 2010 Edition) and a Helium fraction of  $Y = 0.246$  and three other combinations that were labeled as CNONa1Y2, CNONa2Y2 and CNONa1Y4, and incorporate an abundance enhancement of N and Na and depletion of C and O, as well as, for the latter, an enhancement of Helium ( $Y = 0.400$ ).

The newly created ODFs were subsequently implemented as input in the ATLAS9 code to build a grid of 3,472 stellar atmosphere models in a range of effective temperature from 4,300 to 7,000 K, at steps of 100 K, surface gravity  $\log g$  from 2.0 to 5.0, at steps of 0.1 dex, and the four different chemical compositions from [Sbordone et al. \(2011\)](#). Finally, the set of model atmospheres were used in the code SYNTHE to calculate synthetic spectra at a resolution of  $R = \lambda/\Delta\lambda = 500,000$  and subsequently

broadened to a resolution of  $R = 2,500$  compatible with the multi-object spectroscopic mode of the instrument OSIRIS on the Gran Telescopio Canarias (GTC). The numerical codes used in this work were developed by R. L. Kurucz of the Harvard-Smithsonian Center for Astrophysics (CfA).

The second part is devoted to the calculation of spectroscopic indices, either as defined in the literature as part of the Lick/IDS system ([Trager et al. 1998](#)) or those reported by [Pancino et al. \(2010\)](#), and additionally, a set of new 10 indices introduced in this thesis. The later set was assembled by identifying features that vary the most among the four different chemical compositions. We explored the effects of atmospheric parameters on the index values and identified the optimal spectral diagnostics that allow to trace the signatures of two stellar populations. We specifically found that the indices involving molecular bands (in particular CN and CH, but also NH, OH and NO) and hydrogen features are very promising for separating stellar populations in globular clusters.

As an addition to the theoretical work, we present, in the last part, preliminary results from an observing program. Spectroscopic data of relatively low luminosity stars of M3 were obtained for the first time. Observations were carried out with the MOS mode of OSIRIS on the GTC. We used two grisms: R2500U and R2500V to observe a sample of 71 stars members of M3 that included 44 main sequence stars, 24 objects at the Turn-off and 3 stars of the red giant branch. The sample was selected by matching the catalogs from [Ferraro et al. \(1997\)](#) and Gaia ([Gaia-Collaboration et al. 2016](#)) in a region of  $1 \times 7.5$  arcmin $^2$  placed as close as possible to center of M3 but avoiding the most crowded part of the cluster. We present preliminary results of these observations.

*A mi familia*

# **Agradecimientos**

Al Instituto Nacional de Astrofísica, Óptica y Electrónica, INAOE, por la beca de excelencia académica otorgada durante el periodo enero - mayo de 2017.

Al Dr. Emanuele Bertone y al Dr. Miguel Chávez por el apoyo y las facilidades brindadas para la realización de esta Tesis.

A mis amigos Sandy, Andrea y Edgar.

# Contents

|  |            |
|--|------------|
| <b>Contents</b>  | <b>vii</b> |
| <b>1 Introduction</b>  | <b>1</b>   |
| 1.1 Globular Clusters . . . . .  | 1          |
| 1.1.1 General properties of Globular Clusters . . . . .  | 1          |
| 1.2 Globular Clusters as single stellar population systems. . . . .                            | 3          |
| 1.3 Globular Cluster with multiple stellar populations. . . . .                                | 4          |
| 1.3.1 Spectroscopic evidence of multiple stellar population. . . . .                           | 5          |
| 1.3.2 Photometric evidence of multiple stellar population. . . . .                             | 9          |
| 1.4 The chemical composition and the origin of multiple stellar populations<br>in GCs. . . . . | 11         |
| 1.5 Chemical partitions of multiple stellar populations in Galactic GCs . . .                  | 13         |
| 1.6 Description of this dissertation . . . . .   | 16         |
| <b>2 The Globular Cluster M3</b>   | <b>19</b>  |
| 2.1 General Properties . . . . .   | 19         |
| 2.2 Multiple population in M3 . . . . .  | 19         |
| <b>3 Model atmospheres and synthetic spectra</b>   | <b>25</b>  |
| 3.1 The library of Kurucz's codes . . . . .  | 26         |
| 3.2 ODF computation . . . . .  | 28         |
| 3.3 ATLAS9 model computation . . . . .   | 28         |
| 3.4 SYNTHE theoretical spectra . . . . .   | 36         |
| <b>4 Spectroscopic indices</b>   | <b>39</b>  |
| 4.1 Lick/IDS system . . . . .  | 39         |
| 4.2 CN and CH indices . . . . .  | 41         |
| 4.3 New indices . . . . .  | 42         |
| 4.3.1 Index error and sensitivity . . . . .  | 44         |
| <b>5 Results</b>   | <b>49</b>  |
| 5.1 Global properties of the spectroscopic indices. . . . .                                    | 49         |
| 5.2 Suitable indices for identifying multiple population in M3 . . . . .                       | 58         |

|                         |  |            |
|-------------------------|--|------------|
| 5.2.1                   | The Main Sequence . . . . .                              | 63         |
| 5.2.2                   | The Red Giant Branch . . . . .                           | 69         |
| 5.2.3                   | The Horizontal Branch . . . . .                          | 72         |
| <b>6</b>                | <b>GTC Observations of M3</b>                            | <b>75</b>  |
| 6.1                     | GTC and the MOS of OSIRIS . . . . .                      | 75         |
| 6.2                     | Definition of the stellar sample . . . . .               | 76         |
| 6.3                     | Preliminary observation data . . . . .                   | 86         |
| <b>7</b>                | <b>Conclusions</b>                                       | <b>89</b>  |
| <b>A</b>                | <b>Abundances of the four chemical compositions</b>      | <b>91</b>  |
| <b>B</b>                | <b>Theoretical indices calculated for the case of M3</b> | <b>95</b>  |
| <b>Index of Figures</b> |  | <b>109</b> |
| <b>Index of Tables</b>  |  | <b>115</b> |
| <b>References</b>       |  | <b>117</b> |

# Chapter 1

## Introduction

### 1.1 Globular Clusters

Globular Clusters (GCs) are nearly spherical systems of stars bounded by gravity, with a high concentration of stars near their centers, that orbit the core of a galaxy as satellites. In spiral galaxies as the Milky Way, these systems are found in the halo and the bulge, and are usually composed hundreds of thousands of old stars of low metallicity. GCs do not contain significant amounts of gas and therefore lack signs of current star formation.

Due to their old age, GCs are considered to carry on the imprints of the formation of the Milky Way and therefore may preserve valuable information about the initial conditions with which the Galaxy was formed and of its early evolutionary processes. The study of globular clusters has played a key role in the understanding of the overall properties, including clues of fundamental questions such as the age of the Universe and its early history.

#### 1.1.1 General properties of Globular Clusters

Although GCs have a circular appearance, most of them have a certain grade of ellipticity, up to 0.27 as in the case of M19 (NGC 6273) that is the most elongated GC of the Milky Way. Other GCs with a high grade of ellipticity are NGC 6144 and NGC 7492 with 0.25 and 0.24, respectively, while many others have zero ellipticity, such as NGC 6093 (M80), NGC 6121 (M4), NGC 6254 (M10), NGC 6569, NGC 6723 and NGC 6838 (M71) ([Harris 1996](#), 2010 Edition).<sup>1</sup>

---

<sup>1</sup>Hereafter this reference corresponds to the 2010 of the edition of the catalogue.

As mentioned above, in spiral galaxies, the GCs are mostly found in the halo. In the Milky Way, the halo has an approximately spherical shape and is extended to a distance of  $\sim 60$  kpc, comparable to the distance to the Magellanic Clouds, with a decrease in density with distance from the galactic center. Unlike the galactic disk, the most outstanding properties of the halo are its low metallicity, the lack of gas and its old age of 10-12 Gyr ([Jofré & Weiss 2011](#)), characteristic of Population II stars according to [Baade \(1944\)](#).

Stars in GCs are in general metal-poor: in the Milky Way, the stellar metallicity  $[\text{Fe}/\text{H}]$ <sup>2</sup> varies from -2.40 to 0.0 dex. Figure 1.1 shows the metallicity distribution of 152 GCs out of the 157 systems reported in [Harris \(1996\)](#).

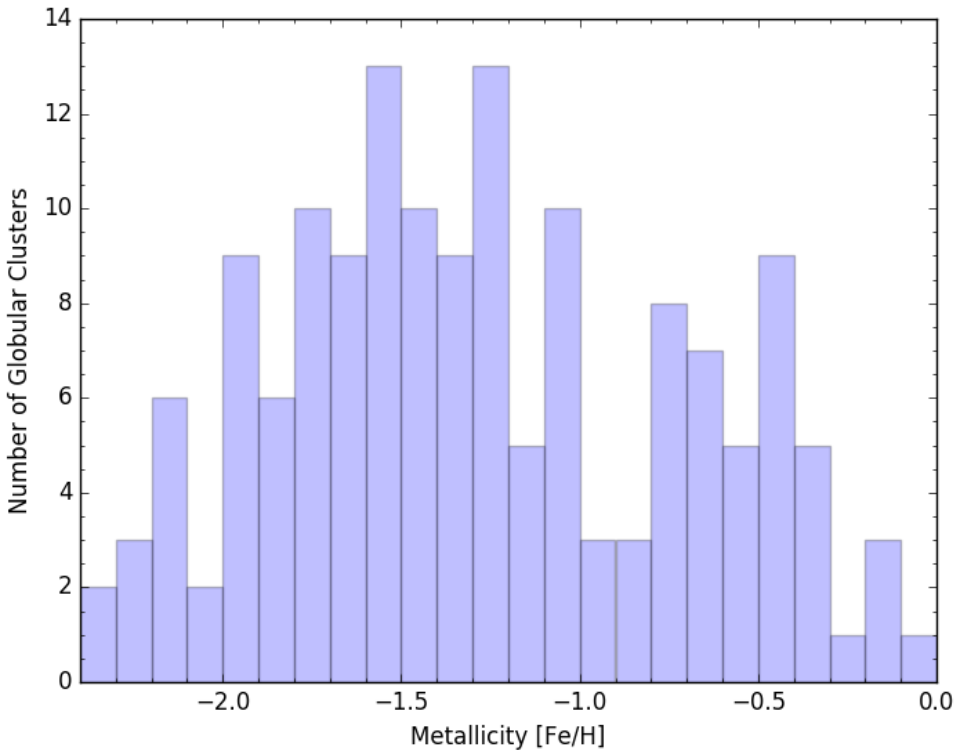


Figure 1.1: Distribution of metallicity  $[\text{Fe}/\text{H}]$  of 152 globular clusters of the Milky Way. The data were extracted from the catalog of [Harris \(1996\)](#).

---

<sup>2</sup>This abundance ratio is defined as the logarithm of the ratio between the number of iron  $n_{\text{Fe}}$  and hydrogen  $n_{\text{H}}$  atoms per unit of volume in the stellar photosphere compared with that of the Sun and is expressed as:

$$[\text{Fe}/\text{H}] = \log_{10} \left( \frac{n_{\text{Fe}}}{n_{\text{H}}} \right)_* - \log_{10} \left( \frac{n_{\text{Fe}}}{n_{\text{H}}} \right)_{\odot} \quad (1.1)$$

As it can be seen in Figure 1.1, two populations of GCs can be distinguished: a metal-poor one with a metallicity distribution that peaks at  $[Fe/H] \sim -1.5$ , and metal-rich systems with  $[Fe/H] \sim -0.5$ . Thus, for the 152 globular cluster considered, there are 110 metal-poor and 42 metal-rich.

A typical GC has an absolute magnitude  $M_V \simeq -7.3$  and half-light radius  $R_e \simeq 3$  pc (Binney & Merrifield 1998). The average of the absolute magnitude of the 157 globular clusters reported by Harris (1996), is  $M_V = -6.89$ . GCs have typical masses of  $\sim 10^3 - 10^6 M_\odot$  with a peak in  $2 \times 10^5 M_\odot$  dominated by the oldest GCs ( $> 12$  Gyr) (Fall & Zhang 2001) but despite their large masses, they contribute only to a small fraction ( $\sim 2\%$ ) of the total mass of the galactic halo which is actually dominated by field stars.

Massive GCs ( $\sim 10^6 M_\odot$ ), such as  $\omega$  Cen and M54, require a timescale of  $\sim 30$  Myr for the formation of First Generation stars, while less massive GCs require about 10 - 20 Myr (Gratton et al. 2012). Knowing the current state of GCs as well as their relationship with field stars is a key point to understand their origin, formation and evolution.

## 1.2 Globular Clusters as single stellar population systems.

A single stellar population (SSP) is a set of stars of different masses that have the same age and initial chemical composition, distributed according to an initial mass function (IMF) and can be represented by a single isochrone in the colour-magnitude diagram (CMD) (Gratton et al. 2012). GCs have long been considered as prototypes of the observational counterparts of the concept of SSP, i.e. stellar aggregates with a generation of coeval stars that were born with a homogeneous chemical composition. As such, GCs represent the best observational basis of stellar evolution and the building blocks in the synthesis of stellar populations to study more complex systems such as galaxies which have been found to be well-represented by suitably weighted sums of SSP of different ages and metallicities.

In Figure 1.2 we show the comparison of an isochrone calculated for a metallicity  $Z = 0.001$  and an age of 12 Gyr and the stellar distribution for the particular case of M3 (NGC 5272), the main target in this thesis. From this figure it is clear that M3 (and many other GCs) can be described by a single isochrone in the CMD, to within the uncertainties of the plotted observational data of Sarajedini et al. (2007).

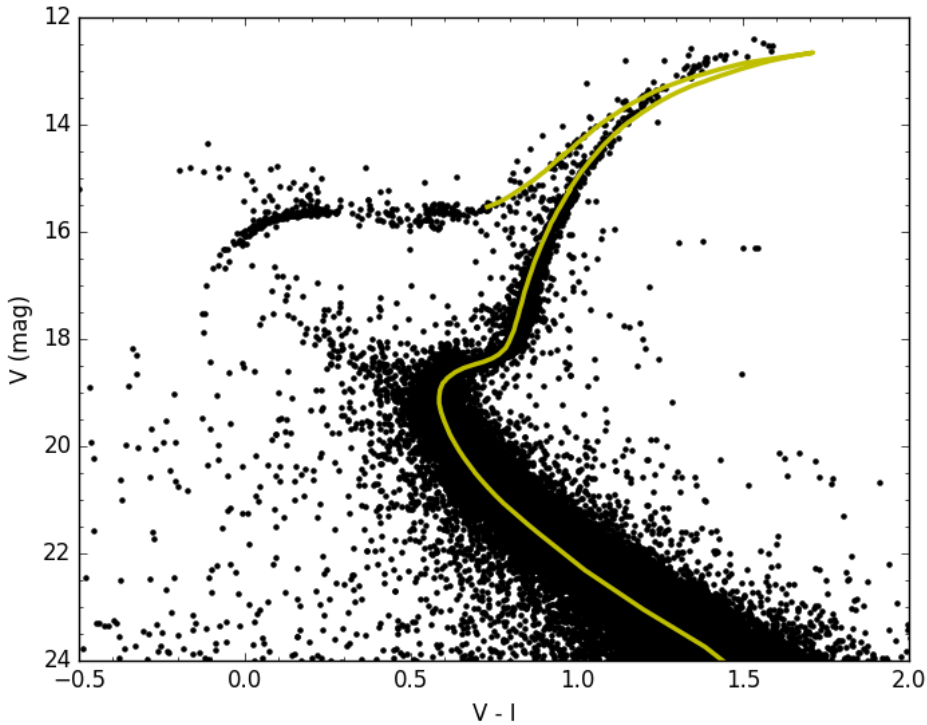


Figure 1.2: Color-magnitude diagram of M3 which is described with an isochrone calculated for a metallicity  $Z = 0.001$  and an age of 12 Gyr. Data for CMD were extracted from the Advanced Camera for Surveys (ACS) of galactic GC ([Sarajedini et al. 2007](#)) and the isochrone was calculated using the Padova and Trieste Stellar Evolution Code (PARSEC) ([Bressan et al. 2012](#)) (<http://stev.oapd.inaf.it/cmd>).

### 1.3 Globular Cluster with multiple stellar populations.

Until recently, GCs were considered as stellar system hosting a single generation of stars. Nevertheless, early studies of GCs already demonstrated that some objects showed significant dispersion in the chemical abundance of their members ([Freeman & Rodgers 1975](#)), as well as quite different morphologies of the CMD at advanced evolutionary stages such as the Horizontal Branch (HB).

Recent studies of GCs have shown that they are not necessarily composed of a simple stellar population, but they are rather made up of multiple stellar populations ([Gratton et al. 2012](#)). They have a much more complex star-formation history than previously thought. Most of GCs (perhaps all) appear to have two (or more) approximately coeval subpopulations, or rather, generations of stars produced by two or even more star-formation phases, which causes a peculiar chemical self-enrichment pattern ([Sbordone et al. 2011](#)).

The multiple population phenomenon is very complex and not yet well understood. Numerous efforts have been directed to resolve the enigma on the origin of the different populations. Until now, the most common chemical signature of GCs is the star-to-star variations in light elements such as C, N, O, Na, Mg, Al, that show anti-correlations and bi- or multi- modality. In the following, we present some studies conducted on several GCs where evidence of population multiplicity has been found.

### 1.3.1 Spectroscopic evidence of multiple stellar population.

Before the multiple stellar populations were photometrically discovered, [Osborn \(1971\)](#) had already detected chemical abundance anticorrelations between strength of CN and CH bands in Messier 5 and Messier 10. This first evidence of chemical inhomogeneity was detected in studies of the more easily accessible stars, i.e., the stars of the right Red Giant Branch (RGB). The unusual chemical pattern was detected as a bimodal distribution of the strength of CN (cyanogen). For example, [Norris et al. \(1981\)](#) found this bimodality in NGC 6752 for 69 RGB stars, and shortly after [Norris \(1981\)](#) and [Smith & Norris \(1982\)](#) detected a similar distribution in M4 and NGC 3201, respectively. A comparison among these three studies, carried out by [Smith & Norris \(1982\)](#), is presented in Figure 1.3. The x-axis in this figure corresponds to the cyanogen excess  $\delta S(3839)$  measured through the spectral index defined by [Norris \(1981\)](#).

More recent studies, carried out by [Kayser et al. \(2008\)](#) and [Pancino et al. \(2010\)](#), demonstrated the existence of multiple stellar populations in stars from Main Sequence (MS) to RGB in 14 GCs through the anticorrelation between CN and CH bands. [Kayser et al. \(2008\)](#) found CN variations in MS stars in M22, M55, NGC 288 and NGC 362 (see Figure 1.4) while [Pancino et al. \(2010\)](#) detected anticorrelations between CN and CH band strengths for MS stars in the metal-rich GCs: Pal 12, 47 Tuc, NGC 5927 and NGC 6352; however, only one of the metal-poor GCs of the [Pancino et al. \(2010\)](#) sample presented a bimodal anticorrelation: M15. Nevertheless, the evolutionary effects alone can not explain these observed chemical anomalies in unevolved stars. Both works support a self-enrichment (see below) scenario as possible origin. More probable causes of multiplicity of stellar populations are presented in Section 1.4.

Figure 1.4 shows two histograms for the  $\delta CN$  measurements of the [Kayser et al. \(2008\)](#) clusters sample. In this Figure a bimodal distribution with CN-strong and CN-weak stars can be easily distinguished, being CN-strong stars those that have a CN excess  $> 0.46$ , i.e. the minimum value between the fitting of the two Gaussians drawn in the plot.

The CN-CH anticorrelation is now accepted as a characteristic of GCs containing different stellar populations, since neither field stars nor open cluster members present such anticorrelation, on the contrary, they display weak CN bands and strong CH bands ([Gratton et al. 2004](#)).

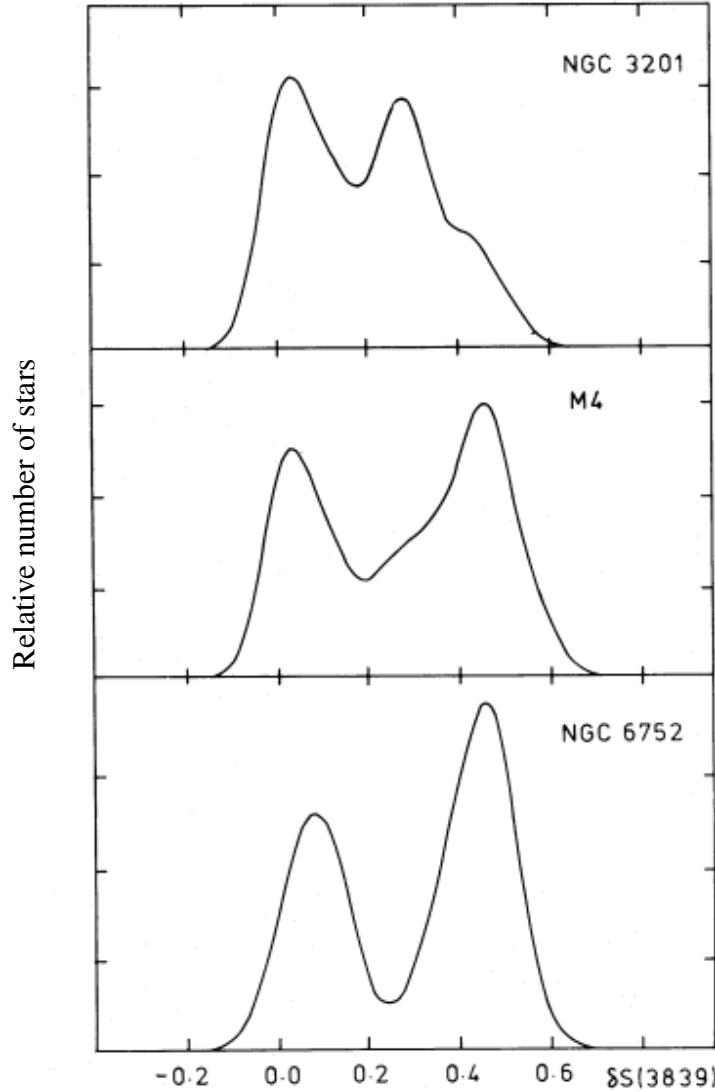


Figure 1.3: Comparison of the cyanogen distribution for RGB stars in the GCs NGC 3201 ([Smith & Norris 1982](#)), M4 ([Norris 1981](#)) and NGC 6752 ([Norris et al. 1981](#)). The abscissa indicates the cyanogen excess  $\delta S(3839)$  on the CN index defined in [Norris \(1981\)](#), while the scale on the ordinate is arbitrary. Plot adapted from [Smith & Norris \(1982\)](#).

Other abundance anticorrelation that also suggest the existence of multiple stellar populations is the one found between Na and O. Such trends have been identified in, for example: a) the high resolution studies of RGB stars of M3 and M13

by Cohen & Meléndez (2005), b) in the analysis of about 1,960 RGB stars in 19 Southern GCs in a range of metallicity  $-2.4 \leq [\text{Fe}/\text{H}] \leq -0.4$  dex conducted by Carretta et al. (2009) (see Figure 1.5), c) more recently in RGB stars of NGC 6139 (Bragaglia et al. 2015) and M28 (Villanova et al. 2017), and d) in studies on not evolved stars in 47 Tuc (Carretta et al. 2004) or in M13 (Cohen & Meléndez 2005). It has been suggested that the Na-O anticorrelation in not evolved stars can not be due to nuclear reactions, but it must be already present in the pristine material from which stars were formed (Lardo 2013). This material can have been polluted by ejecta of evolved stars of an older generation (Na-poorer and O-richer) to form the subsequent generation of stars (Na-richer and O-poorer). This is the so-called multiple population phenomenon (Villanova et al. 2017). The Na-O anticorrelation, as well as the detected between Mg and Al, has not been observed in all GCs, but it tends to be evident in metal-poor and/or massive clusters (Johnson et al. 2005).

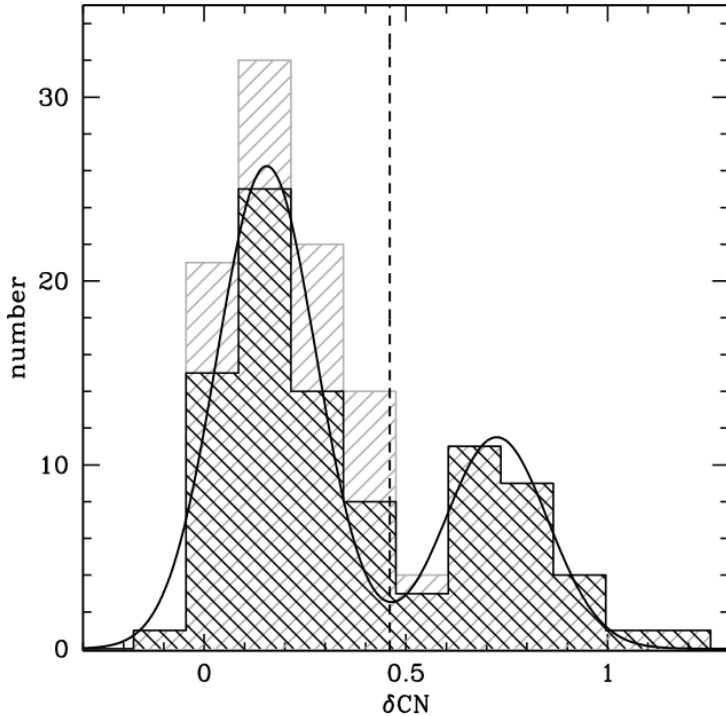


Figure 1.4: Combined histograms of the CN-excess parameter for stars on the lower RGB of the clusters sample from Kayser et al. (2008). The gray histogram includes all eight clusters (M 15, M 22, M 55, NGC 288, NGC 362, NGC 5286, Palomar 12, and Terzan 7). In the black histogram Pal 12 and Ter 7 are not included because they are believed to belong to the Sgr dSph.  $\delta\text{CN}$  shows a bimodal distribution, which was fitted by two Gaussians. The minimum between the two Gaussians marks the criterion to differentiate between CN-strong and CN-weak stars. Figure from Kayser et al. (2008).

$\omega$  Cen, a GC that present the most complex stellar populations has been subject of many studies. For example, once [Bedin et al. \(2004\)](#) demonstrated that it has two MS branches shifted by up to  $\sim 0.3 - 0.5$  mag, [Piotto et al. \(2005\)](#) through a spectroscopic analysis showed that the bluer sequence is more metal-rich than the redder one by a factor of two. To fit an isochrone along the bluer MS was necessary to include a greatly enriched ( $0.35 < Y < 0.45$ ) He composition; in fact the best fit required an isochrone with  $Y = 0.38$ . This result is similar to that reported by [Norris \(2004\)](#), however it is important to remark that the work by [Piotto et al. \(2005\)](#) is based on the measured MS metallicities and on more up-to-date stellar models.

In addition to  $\omega$  Cen and NGC 2808, the two massive GCs NGC 6441 and NGC 6388 also present a helium-rich stellar population, that include  $\sim 10$  and  $\sim 20\%$  of stars, respectively ([D'Ercole et al. 2008](#)). While populations of GCs have, in general, a moderate helium content ( $0.26 < Y < 0.30$ ), the extreme helium-rich sequences appear to be exclusive from the most massive GCs ([Piotto et al. 2007](#)).

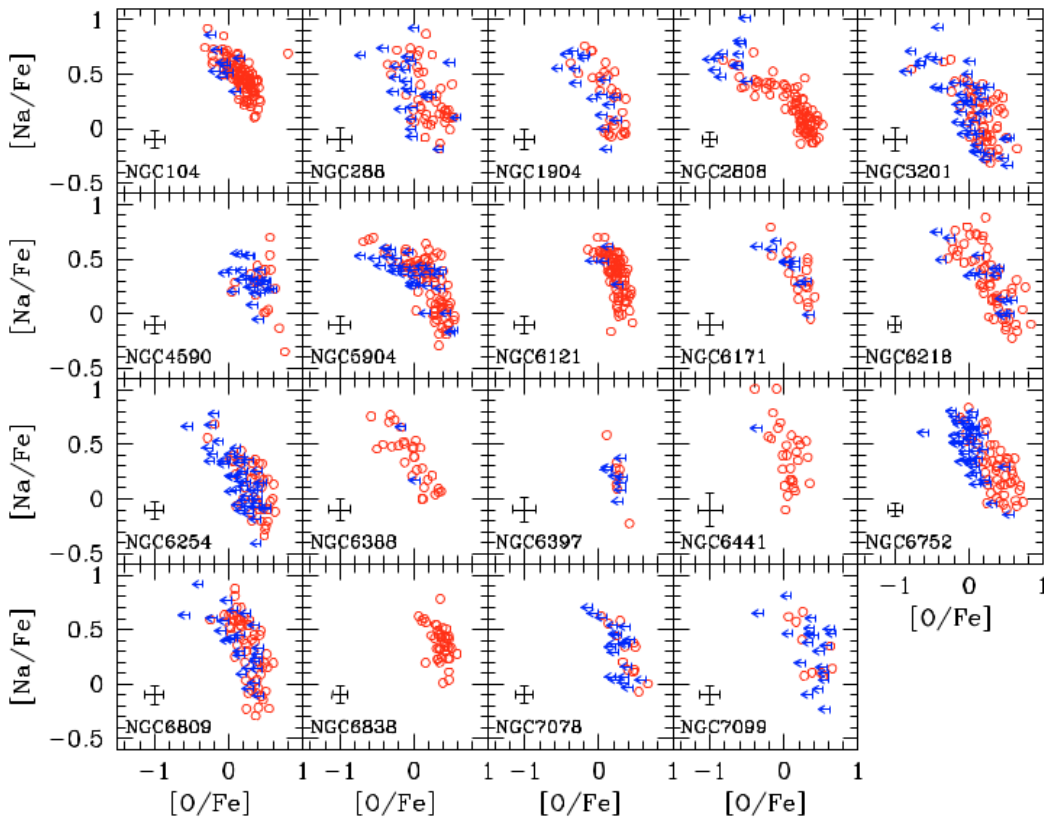


Figure 1.5: Na-O anticorrelation observed in the 19 galactic GCs studied by [Carretta et al. \(2009\)](#). Upper limits in O abundances are shown as arrows and detections are indicated as open circles. Figure from [Carretta et al. \(2009\)](#).

### 1.3.2 Photometric evidence of multiple stellar population.

The better photometric sensitivity of the current generation of ground based 8-10 m telescopes and that of the Hubble Space Telescope (HST) have made possible to clearly separate the different stellar sequences in the CMDs of several clusters that should, in principle, be explained by the different chemical composition among cluster stars, in particular of light elements such as He, C, N, and O (Sbordone et al. 2011; Milone et al. 2012; Piotto et al. 2015).

The photometric discovery of multiple stellar populations in GCs started with  $\omega$  Cen (Lee et al. 1999; Bedin et al. 2004; Villanova et al. 2007; Bellini et al. 2010), one of the first GCs that showed a significant variation in the chemical composition of its member stars (Freeman & Rodgers 1975). Once thought to be a unique and peculiar case, since it is the most massive of the GCs of the Milky Way ( $\sim 3.9 \times 10^6 M_{\odot}$ ) (Pryor & Georges 1993), today the presence of multiple stellar populations appear to be an increasingly more common phenomenon.

Perhaps the most striking examples of population multiplicity are  $\omega$  Cen and M2 (NGC 7089). The massive cluster  $\omega$  Cen was recently studied by Bellini et al. (2010) who carried out high precision photometry using multi-band HST observations obtained with the Wide Field Camera 3 in the UV-optical channel confirming the presence of as many as four distinct stellar populations in the CMD, from the MS to the RGB, as shown in Figure 1.6.

The star-to-star dispersion in metallicity, age and abundances of light and  $\alpha$  elements can be reflected in a multimodal or distinct branches in the CMD of GCs (Bedin et al. 2004; Piotto et al. 2007). This is particularly true for the cluster M2 (NGC 7089), for which it has been possible to distinguish up to seven stellar populations using an adequate combination of ultraviolet and optical filters, namely,  $C_{F275W,F336W,F438W}$  and the pseudo-colour  $m_{F275W} - m_{F814W}$  (Milone et al. 2015). It has been demonstrated that the appropriate combination of filters maximizes the separation of stellar populations along the MS and the RGB (Milone et al. 2012, 2013; Piotto et al. 2013; Bastian & Lardo 2015; Piotto et al. 2015), with a notable sensitivity of the UV magnitudes. As an example, the properties of the seven stellar population of M2 reported by Milone et al. (2015) are listed in Table 1.1.

Similarly, using photometric data from HST ACS, Piotto et al. (2007) found that the MS of the CMD of NGC 2808 splits into three separate branches, that result was attributed to successive rounds of star formation.

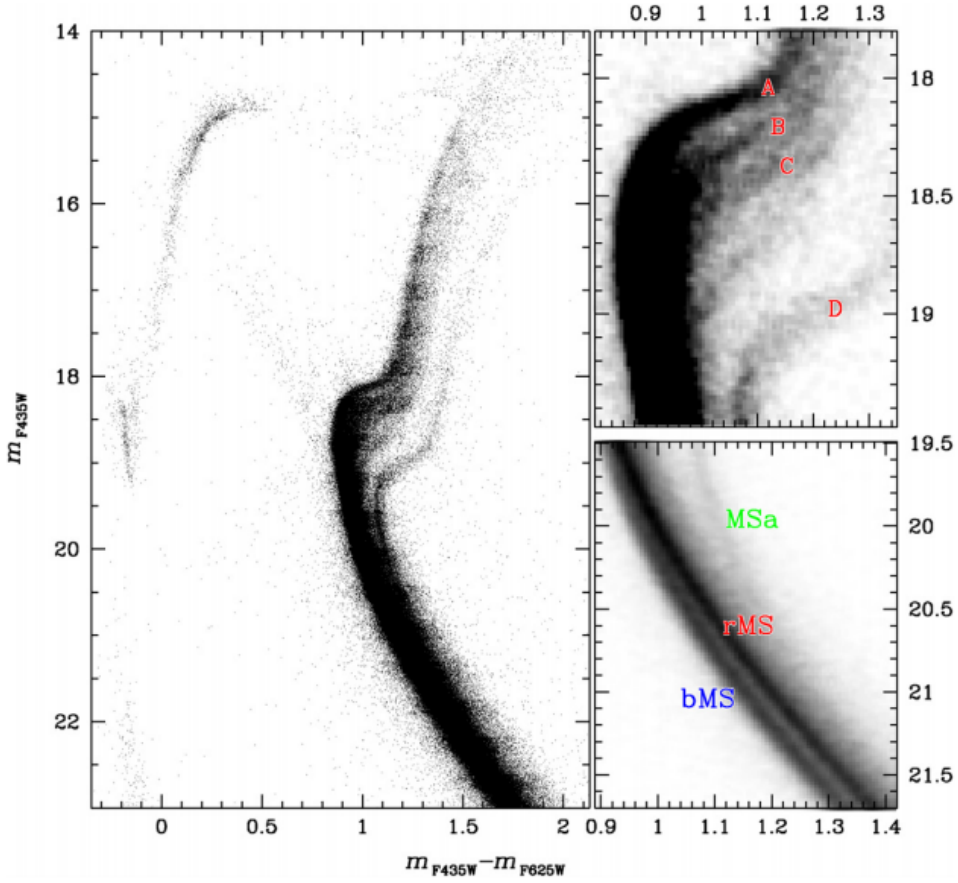


Figure 1.6:  $\omega$  Cen CMD resulting from the  $10 \times 10$  arcmin $^2$  mosaic of ACS images centered on the cluster center. On the right upper panel the four sub-giant sequences can be distinguished. In the lower right panel the three MSs are shown. The labels bMS and rMS indicate the blue and red main sequences, respectively, and MSa stands for a fainter red MS which is clearly separated from the bMS and rMS. Figure from [Bellini et al. \(2010\)](#).

Table 1.1: Fraction of stars and summary of the main properties of the seven stellar populations of M2 reported by [Milone et al. \(2015\)](#).

| POP       | Population ratio  | [Fe/H] (dex) | [Na/Fe] (dex) | $[\alpha/\text{Fe}]$ | Y (dex) | Age (Gyr)       |
|-----------|-------------------|--------------|---------------|----------------------|---------|-----------------|
| $A_I$     | $0.076 \pm 0.028$ | -1.7         | -             | 0.4                  | -       | $13.0 \pm 0.75$ |
| $A_{II}$  | $0.222 \pm 0.039$ | -1.7         | -0.16         | 0.4                  | 0.246   | $13.0 \pm 0.75$ |
| $A_{III}$ | $0.490 \pm 0.048$ | -1.7         | 0.18          | 0.4                  | -       | $13.0 \pm 0.75$ |
| $A_{IV}$  | $0.173 \pm 0.036$ | -1.7         | 0.35          | 0.4                  | 0.315   | $13.0 \pm 0.75$ |
| $B_I$     | $0.014 \pm 0.003$ | -1.5         | 0.15          | -                    | -       | -               |
| $B_{II}$  | $0.015 \pm 0.003$ | -1.5         | 0.55          | -                    | -       | -               |
| $C$       | $0.010 \pm 0.002$ | -1.0         | -0.15         | 0.2                  | 0.248   | $12.0 \pm 0.75$ |

## 1.4 The chemical composition and the origin of multiple stellar populations in GCs.

Currently, it is well known that GCs show star-to-star abundance variations often called “abundance anomalies” for certain chemical light elements such as He, Li, C, N, O, F, Na, Mg and Al ([Kayser et al. 2008](#); [Carretta et al. 2009](#); [Pancino et al. 2010](#); [Gratton et al. 2012](#)), while other elements such as Si, Ca and Fe the chemical composition remains homogeneous ([Bastian et al. 2015](#); [Sbordone et al. 2011](#)). However, the origin of the multiplicity of stellar populations is still unclear and remains a matter of debate.

Several scenarios have been proposed to explain the origin of multiplicity of GC (e.g. [Kayser et al. 2008](#); [Gratton et al. 2012](#)). These mechanisms include:

- Original inhomogeneities in the material from which GCs were formed. Because GCs are very massive objects, it is probable that their elements were formed in many compact star-forming regions along the giant progenitor molecular cloud; every region with some differences in its chemical composition with respect to the others. Due to the old age, the currently observed chemical inhomogeneities of CGs may have been caused by an inadequate mixing of interstellar primordial material at the time in which stars were formed ([Gratton et al. 2012](#)).
- Peculiar evolution of individual stars. Several factors that can change the evolution of a star within a cluster, for example the interaction of binary stars, the high mass stars that evolve faster than those of low mass because they burn their hydrogen quicker.
- Mixing. Once a massive star leaves the MS, the envelope expands outward beginning a mixing process where surface material penetrates into a region that had already experienced partial CN processing through the CNO cycle and whose abundance of light elements has been altered by proton-capture, so the polluted material is dredged up to upper layers where hydrogen is burned by the proton–proton chain. Because CNO cycle tends to produce N at the expense of C and O, a CN-CH anticorrelation would be expected. However, the so-called first dredge-up is not able to explain the observational evidences about the abundance patterns of light elements in RGB stars ([Kayser et al. 2008](#); [Lardo 2013](#)). This point is of particular importance since it motivated the spectroscopic analysis of MS stars that have not yet developed deep convective envelopes and, therefore, it is expected that they preserve the chemical composition of the parent star forming cloud.

- Self-enrichment. In this scenario, the variations in chemical composition are caused by successive generations of stars formed within the same GC (Catelan et al. 2009; Gratton et al. 2012; Bastian et al. 2015). The massive stars collaborate in the enrichment of the interstellar medium either by expulsion of stellar winds or through the explosion as supernova. First Generation stars process material enriching it through nucleosynthesis that pollutes the forming gas or the other stars within the same cluster producing the now observed chemical anomalies, inferred to be Second Generation stars (D'Antona & Caloi 2008; Bastian & Lardo 2015). First Generation stars are considered as those stars that present primordial abundances, that is, having similar chemical composition to that shown in halo field stars whereas stars that are enriched in some light elements (i.e. Na, Al, He) and depleted in others (C, O, Mg) are interpreted as Second Generation stars (Bastian & Lardo 2015; García-Hernández et al. 2015).
- Asymptotic Giant Branch (AGB) scenario. It is a particular version of the self-enrichment scenario. These stars, formed in a First Generation, loss enriched material which, when mixed with primordial material just after the formation of the First Generation, form the following generations of stars that shows the observed abundance variations today. Due to AGB star lifetimes, this is expected to operate over 30 - 200 Myr time-scales (D'Ercole et al. 2008).
- Fast rotating massive star scenario (e.g. Decressin et al. 2007; Krause et al. 2013). It is another form of self-enrichment where the enriched material ejected by rapidly rotating massive stars is mixed with primordial material to form the subsequent generations of stars. The time-scale associated with this scenario is  $< 10$  Myr (D'Ercole et al. 2008). In fact, whatever the scenario of self-enrichment, the ejected material must be enriched in helium with respect to the primordial material (D'Antona & Caloi 2008).
- Merging of GCs. Although it is unlikely that this scenario may take place in the Milky Way, because of very large relative velocities of GCs and that there are only 157 GCs, the merging of GCs is another reason that can cause multiple stellar populations (Gratton et al. 2012).
- Capture of material. During the movement of GCs around of their host galaxy, these systems can find and go through of material of interstellar medium with different chemical composition, capturing it gravitationally and giving rise to new episodes of stellar formation (Gratton et al. 2012).
- Helium enhancement. It has been suggested that the GCs showing a wide difference in the abundance of helium are not an exception but the rule, i.e., it is the most common result of the GC formation process (D'Antona & Caloi 2008).

## 1.5 Chemical partitions of multiple stellar populations in Galactic GCs

We have already mentioned the chemical inhomogeneities that better represent the different photometrically distinguished populations of M2. In this section, we describe a seminal work by [Sbordone et al. \(2011\)](#), that stands as the basis of the proposed analysis for the GC M3. These authors calculated synthetic spectra for typical chemical element mixtures observed in stellar population harbored in galactic GCs, and determined bolometric corrections to the standard Johnson-Cousins and Strömgren filters for estimating colours that, joined to theoretical isochrones, provide theoretical predictions for the effect of abundance variations on the observed CMD of GCs.

For this, [Sbordone et al. \(2011\)](#) considered a reference isochrone (see Figure 1.7) from the BaSTI data base<sup>3</sup>, ([Pietrinferni et al. 2006](#)), with the following characteristics: He mass fraction of  $Y = 0.246$ , mass fraction of metals of  $Z = 0.001$  and an age of 12 Gyr. The metallicity  $Z$  corresponds to an iron abundance of  $[Fe/H] = -1.62$ , which is compatible to that reported for M3 of -1.5 in [Harris \(1996\)](#). Also, the metallicity considers an alpha element enhancement of  $[\alpha/Fe] = +0.4$ . This composition will hereafter be considered as typical for a stellar population of First Generation in GCs, and will be labeled as “Reference” as in [Sbordone et al. \(2011\)](#).

Two more metal mixtures representative of Second Generation stars in GCs were proposed by [Sbordone et al. \(2011\)](#) using coeval isochrones calculated for the same reference parameters ( $Y = 0.246$ ,  $[Fe/H] = -1.62$  and an age of 12 Gyr) but with different mixtures of C, N, O and Na that are characteristic of extreme values of the anticorrelations observed in galactic GCs ([Carretta et al. 2010](#)). The first mixture is representative of Second Generation stars, that from now on will be labeled as “CNONa1Y2”, and include N and Na enhancements of 1.8 dex and 0.8 dex by mass, respectively, and depletions of C and O by 0.6 dex and 0.8 dex, by mass, respectively, with respect to the Reference mixture. These conditions result in a  $Z \simeq 0.00183$ . This modification to the Reference mixture had already been proposed by [Salaris et al. \(2006\)](#). The second mixture representative of Second Generation stars, subsequently labeled as “CNONa2Y2”, is the same as the Reference mixture except that the enhancement of N is 1.44 dex by mass with respect to the Reference abundance. In this case, the metal distribution was constructed to keep  $Z = 0.001$ .

---

<sup>3</sup><http://basti.oa-teramo.inaf.it/index.html>

Similar to CNONa1Y2, a fourth metal mixture was considered but with an enhancement in the helium mass fraction of  $Y = 0.400$ . The iron abundance and the age remain invariant in this mixture, while the global metallicity is  $Z \simeq 0.00146$ . This last elemental mixture is labeled as “CNONa1Y4”. The Reference, CNONa1Y2 and CNONa2Y2 chemical compositions were derived from the stellar interior calculations and included only those elements that appear relevant for constructing theoretical CMDs that display pronounced photometric differences. Although only a subset of elements is necessary for the stellar interior modeling without significantly altering the results, in the computation of synthetic spectra, the abundances for all remaining elements should be included.

For the calculation of theoretical spectral, [Sbordone et al. \(2011\)](#) produced a grid of model atmospheres using the codes ATLAS12 and, subsequently, they implemented the code SYNTHE ([Castelli 2005a,b](#)) to produce a set of high spectral resolution ( $\lambda/\Delta\lambda = 300,000$ ) spectra in the wavelength interval 300–1,000 nm. Since their goal was to build theoretical photometric points, the spectra were later on degraded to a Full Width at Half Maximum (FWHM) of 1,700 km s<sup>-1</sup>. The stellar model parameters considered in their calculations ( $T_{\text{eff}}$ ,  $\log g$ ,  $V_{\text{turb}}$ ) are listed in Table [1.2](#) and are representative of stars from the lower MS to the bright end of the RGB.

Table 1.2: Parameters used by [Sbordone et al. \(2011\)](#) to generate the model atmospheres for the four mixtures.

| $T_{\text{eff}}$ [K] | $\log g$ | $V_{\text{turb}}$ [km s <sup>-1</sup> ] |
|----------------------|----------|---|
| 4100                 | 0.50     | 2.0                                     |
| 4476                 | 1.20     | 2.0                                     |
| 4892                 | 2.06     | 2.0                                     |
| 5312                 | 3.21     | 2.0                                     |
| 5854                 | 3.78     | 2.0                                     |
| 6490                 | 4.22     | 2.0                                     |
| 6131                 | 4.50     | 2.0                                     |
| 4621                 | 4.77     | 2.0                                     |

In Figure [1.7](#) we reproduce the Fig. 1 of [Sbordone et al. \(2011\)](#) to show the effects of the four different chemical combinations in theoretical isochrones. As indicated by these authors, the First Generation population and a Second Generation mixture with  $Y = 0.246$  are virtually at the same location (solid line). The black dots are the theoretical point derived from synthetic spectra. As a final note, we want to indicate that [Sbordone et al. \(2011\)](#) provided a complete and self-consistent theoretical

predictions of the effect of abundance variations on observed CMDs. With the results of that work, it will be possible to investigate GCs with known or suspected abundance variations and several subpopulations through the information derived from their CMDs. At this point, it is important to remark that this thesis is aimed at complementing the [Sbordone et al. \(2011\)](#) work by analyzing specific spectral features that allow the investigation of the presence of multiple populations through intermediate resolution spectra of stars on the MS.

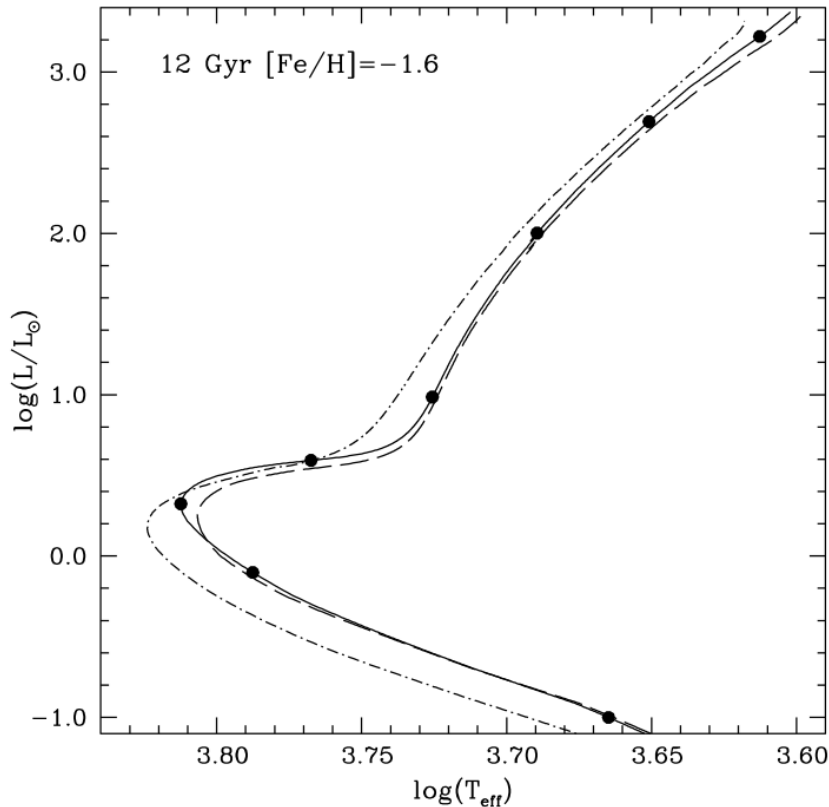


Figure 1.7: Theoretical isochrones from the MS to the tip of the RGB for the four different chemical compositions proposed by [Sbordone et al. \(2011\)](#). The solid line corresponds to both the Reference and CNONa2Y2, because they are virtually identical. The black dots along this isochrone denote the points where the model atmosphere and synthetic spectra were calculated (see Table 1.2). The dashed line corresponds to the CNONa1Y2, while the dash-dotted line is for the CNONa1Y4. Figure adapted from [Sbordone et al. \(2011\)](#).

Table 1.3 (Table 2 of [Sbordone et al. \(2011\)](#)) shows abundances of selected elements for the computing of model atmospheres. In this Table [El] is given as  $\log N(\text{El}) - \log N(\text{H}) + 12$ , and each modified chemical composition was labeled with the subscripts 1, 2 and 3 for CNONa1Y2, CNONa1Y4 and CNONa2Y2, respectively. The full table is available in Appendix A.

Table 1.3: Abundances for selected elements in the four chemical compositions used for computing model atmospheres.

| No. | El | Reference $Y = 0.246$   |        | CNONa1 $Y = 0.246$      |                         | CNONa1 $Y = 0.400$ |                         | CNONa2 $Y = 0.246$ |                         |
|-----|----|-------------------------|--------|-------------------------|-------------------------|--------------------|-------------------------|--------------------|-------------------------|
|     |    | Mass frac.              | [El]   | Mass frac.              | [El] <sub>1</sub> -[El] | Mass frac.         | [El] <sub>2</sub>       | Mass frac.         | [El] <sub>3</sub> -[El] |
| 1   | H  | 0.7530                  | 12.000 | 0.7522                  | 12.000                  | 0.0000             | 0.5985                  | 12.000             | 0.0000                  |
| 2   | He | 0.2460                  | 10.915 | 0.2460                  | 10.916                  | 0.0005             | 0.4000                  | 11.226             | 0.3108                  |
| ... |    |                         |        |                         |                         |                    |                         |                    |                         |
| 6   | C  | $7.6386 \times 10^{-5}$ | 6.930  | $1.9172 \times 10^{-5}$ | 6.330                   | -0.5999            | $1.5256 \times 10^{-5}$ | 6.330              | -0.5999                 |
| 7   | N  | $2.3430 \times 10^{-5}$ | 6.350  | $1.4768 \times 10^{-3}$ | 8.150                   | 1.8000             | $1.1752 \times 10^{-3}$ | 8.150              | 1.8000                  |
| 8   | O  | $6.7226 \times 10^{-4}$ | 7.750  | $1.0642 \times 10^{-4}$ | 6.950                   | -0.8000            | $8.4687 \times 10^{-5}$ | 6.950              | -0.8000                 |
| ... |    |                         |        |                         |                         |                    |                         |                    |                         |
| 11  | Na | $8.8125 \times 10^{-7}$ | 4.710  | $5.5531 \times 10^{-6}$ | 5.510                   | 0.7999             | $4.4189 \times 10^{-6}$ | 5.510              | 0.7999                  |
| 12  | Mg | $4.1603 \times 10^{-5}$ | 6.360  | $4.1558 \times 10^{-5}$ | 6.360                   | 0.0000             | $3.3070 \times 10^{-5}$ | 6.360              | 0.0000                  |
| 13  | Al | $1.4268 \times 10^{-6}$ | 4.850  | $1.4249 \times 10^{-6}$ | 4.850                   | -0.0001            | $1.1339 \times 10^{-6}$ | 4.850              | -0.0001                 |
| 14  | Si | $3.5638 \times 10^{-5}$ | 6.230  | $3.5600 \times 10^{-5}$ | 6.230                   | 0.0000             | $2.8329 \times 10^{-5}$ | 6.230              | 0.0000                  |
| ... |    |                         |        |                         |                         |                    |                         |                    |                         |
| 20  | Ca | $5.2045 \times 10^{-6}$ | 5.240  | $5.2009 \times 10^{-6}$ | 5.240                   | 0.0002             | $4.1387 \times 10^{-6}$ | 5.240              | 0.0002                  |
| ... |    |                         |        |                         |                         |                    |                         |                    |                         |
| 22  | Ti | $3.8667 \times 10^{-7}$ | 4.034  | $3.8512 \times 10^{-7}$ | 4.033                   | -0.0013            | $3.0646 \times 10^{-7}$ | 4.033              | -0.0013                 |
| ... |    |                         |        |                         |                         |                    |                         |                    |                         |
| 26  | Fe | $3.1648 \times 10^{-5}$ | 5.880  | $3.1613 \times 10^{-5}$ | 5.880                   | 0.0000             | $2.5156 \times 10^{-5}$ | 5.880              | 0.0000                  |
| ... |    |                         |        |                         |                         |                    |                         |                    |                         |
| 28  | Ni | $2.0542 \times 10^{-6}$ | 4.671  | $2.0503 \times 10^{-6}$ | 4.670                   | -0.0003            | $1.6315 \times 10^{-6}$ | 4.670              | -0.0003                 |
| Z   |    | $9.9937 \times 10^{-4}$ |        | $1.8343 \times 10^{-3}$ |                         |                    | $1.4597 \times 10^{-3}$ |                    | $9.9937 \times 10^{-4}$ |

## 1.6 Description of this dissertation

The goal of this thesis is to provide the theoretical and empirical framework to investigate the nature of multiple stellar populations in the Globular Cluster M3, whose global properties are described in Chapter 2, through the spectroscopic analysis of stars on the main sequence. The work is composed of two main parts that include (i)- The calculation of new Opacity Distribution Functions (ODFs) appropriate for the chemical mix observed in evolved stars of globular clusters, and their use in the creation of a new grid of theoretical spectra at very high resolution- (ii)- The computation of a set of theoretical absorption line spectroscopic indices and their correlation with the three leading atmospheric parameters: effective temperature, surface gravity and global metallicity ( $T_{\text{eff}}/\log g/[{\text{Fe}}/{\text{H}}]$ ).

For the first part (Chapter 3) we implemented a series of numerical routines within the code DFSYNTH to calculate the distribution of opacities in agreement with the chemical partitions used by [Sbordone et al. \(2011\)](#) which represent, to some extent, the prototypical elemental abundance combinations of globular clusters with multiple stellar populations. Namely, these partitions were a solar scaled Reference abundance of  $[{\text{Fe}}/{\text{H}}] = -1.62$  dex ( $Z = 0.001$ ), compatible with the metallicity of M3 of -1.5 ([Harris 1996](#)) and a Helium fraction of  $Y = 0.246$  and three other combinations that are labeled CNONa1Y2, CNONa2Y2 and CNONa1Y4 and incorporate an abundance enhancement of N and Na and depletion of C and O, as well as, for the latter, an enhancement of Helium ( $Y = 0.400$ ).

The newly created ODFs were subsequently implemented as input in the ATLAS9 code to build a grid of 3,472 stellar atmosphere models in a range of effective temperature from 4,300 to 7,000 K, at steps of 100 K, surface gravity  $\log g$  from 2.0 to 5.0, at steps of 0.1 dex, and the four different chemical compositions from [Sbordone et al. \(2011\)](#). Finally, the set of model atmospheres were used in the code SYNTHE to calculate synthetic spectra at a resolution of  $R = \lambda/\Delta\lambda = 500,000$  and subsequently broadened to a resolution of  $R = 2,500$  compatible with the multi-object spectroscopic mode of the instrument OSIRIS on the Gran Telescopio Canarias (GTC). The numerical codes used in this work were developed by R. L. Kurucz of the Harvard-Smithsonian Center for Astrophysics (CfA).

The second part is devoted to the calculation of spectroscopic indices, either as defined in the literature as part of the Lick/IDS system ([Trager et al. 1998](#)) or those reported by [Pancino et al. \(2010\)](#), and additionally, a set of new 10 indices introduced in this thesis. The later set was assembled by identifying features that vary the most among the four different chemical compositions for cases with surface gravities compatible with dwarf stars. We explore the effects of atmospheric parameters on the index values and identified the optimal spectral diagnostics that allow to trace the signatures of two stellar populations (Chapter 5). We specifically found that the indices involving molecular bands (in particular CN and CH, but also NH, OH and NO) and hydrogen features are very promising for separating stellar populations in globular clusters.

Preliminary results of the observation is given in the last part (Chapter 6). Spectroscopic data of relatively low luminosity stars of M3 has been obtained for the first time. Observations were carried out with the MOS mode of OSIRIS on the GTC. We have used two grisms: R2500U and R2500V to observe a sample of 71 stars members of M3 that included 44 Main Sequence stars, 24 objects at the Turn-off (TO) and 3 stars of the RGB. The sample was selected by matching the catalogs from [Ferraro et al. \(1997\)](#) and Gaia ([Gaia-Collaboration et al. 2016](#)) in a region of  $1 \times 7.5$  arcmin<sup>2</sup> placed as close as possible to center of M3 but avoiding the most crowded part of the cluster. We present preliminary results on this observations and briefly discuss the comparison between theoretical and empirical indices.

In Chapter 7, we present a summary of our results and discuss the conclusions obtained of this work.



# Chapter 2

## The Globular Cluster M3

### 2.1 General Properties

Messier 3, M3 or NGC 5272, is a Globular Cluster discovered in 1764 by Charles Messier in the constellation of Canes Venatici centered at R.A. (J2000): 13h 42m 11.62s and DEC (J2000): 28°22'38.2". It is located at a distance of  $10.48 \pm 0.21$  kpc ([Jurcsik et al. 2017](#)) from the Sun,  $\sim 12$  kpc from the galactic center, and  $\sim 10$  kpc above the galactic plane ([Harris 1996](#)). It has an angular diameter of  $\sim 16$  arcmin and contains an estimated half a million stars. It has an approximate mass of  $6.3 \times 10^5 M_\odot$  ([Pryor & Georges 1993](#)). Table 2.1 shows some basic M3 properties.

### 2.2 Multiple population in M3

M3 is one of the most important GC of the northern hemisphere. It is usually considered as the class I (Oo I) prototype ([Oosterhoff 1939](#)) and, for many years, it was regarded as the canonical GC par excellence. The first work in which chemical anomalies were detected in M3 was conducted by [Cohen \(1978a\)](#). In this study, a scatter in Na and Ca abundances was observed on three RGB stars, while abundances determined for other 18 elements remained constant in each star. These chemical anomalies exceeded the observational errors; therefore, they were unable to explain either by convective mixing or by errors in the data analysis. A possible explanation was that the primordial gas of M3 was chemically inhomogeneous when stellar formation took place ([Cohen 1978a](#)). Other studies showed variations in O, Na, Mg and Al ([Cohen & Meléndez 2005](#); [Johnson et al. 2005](#); [Mészáros et al. 2015](#)).

An important characteristic in the multiple stellar population in GCs is that stars showing chemical anomalies also present helium enrichment ([Piotto et al. 2007](#); [Caloi & D'Antona 2008](#); [D'Antona & Caloi 2008](#)). Because the higher helium content has a strong effect on HB morphology, several studies have been focused in searching multiple stellar populations in HB stars of M3 considering helium variations (e.g.

([Castellani et al. 2005](#); [Caloi & D’Antona 2008](#); [D’Antona & Caloi 2008](#); [Catelan et al. 2009](#); [Dalessandro et al. 2013](#); [Valcarce et al. 2016](#)). An explication is that, while a star losses mass, it increases its helium content and therefore helium enriched objects populate bluer regions of the HB ([D’Antona & Caloi 2008](#)). The blue HB stars with helium enhancement ought to be brighter than the red HB stars without helium enhancement ([Catelan et al. 2009](#)).

Table 2.1: Some important properties of M3 (Data obtained from [Harris \(1996\)](#)).

| Integrated color indices (uncorrected for reddening):                              |              |
|--|--------------|
| U - B  | 0.09         |
| B - V  | 0.69         |
| V - I  | 0.93         |
| Metallicity, [Fe/H]  |              |
| Metallicity, [Fe/H]  | -1.50        |
| Foreground reddening, E(B-V)   | 0.01         |
| Apparent visual distance modulus, (m-M) <sub>V</sub>                               | 15.07        |
| Integrated V magnitude, V <sub>t</sub>   | 6.19         |
| Integrated absolute V magnitude, M <sub>V,t</sub>                                  | -8.88        |
| Spectral type of the integrated cluster light                                      | F6           |
| Projected ellipticity of isophotes, e = 1-(b/a)                                    | 0.04         |
| Kinematical and structural parameters  |              |
| Heliocentric radial velocity, km/s   | -147.6 ± 0.2 |
| Central velocity dispersion, km/s  | 1.89         |
| Core radius, arcmin  | 0.37         |
| Half-light radius, arcmin  | 2.31         |
| Central surface brightness, Vmag/arcsec <sup>2</sup>                               | 16.64        |
| Central luminosity density (log <sub>10</sub> ), L <sub>⊙</sub> /pc <sup>3</sup> ) | 3.57         |
| Median relaxation time, Gyr  | 6.17         |

Regarding the photometric identification of multiple stellar populations, [Piotto et al. \(2015\)](#), as part of HST UV Legacy Survey of Galactic GCs showed the first evidence of a double RGB. In a more recent work [Massari et al. \(2016\)](#) studied the multiple generations phenomenon in M3, using different CMDs constructed with combinations of colors in the Strömgren photometric system. They also detected two equally populated RGBs, as depicted in Figure 2.1. Because photometry can not directly show the effects of specific elemental abundances, these later authors carried out a spectroscopic analysis of a sample of 17 giant stars with the multi-object spectrograph Fiber Large Array Multi Element Spectrograph (FLAMES) at the

European Southern Observatory (ESO)-Very Large Telescope. They demonstrated that both RGBs harbor chemically distinct populations with the left branch corresponding to First Generation stars and the right to Second Generation.

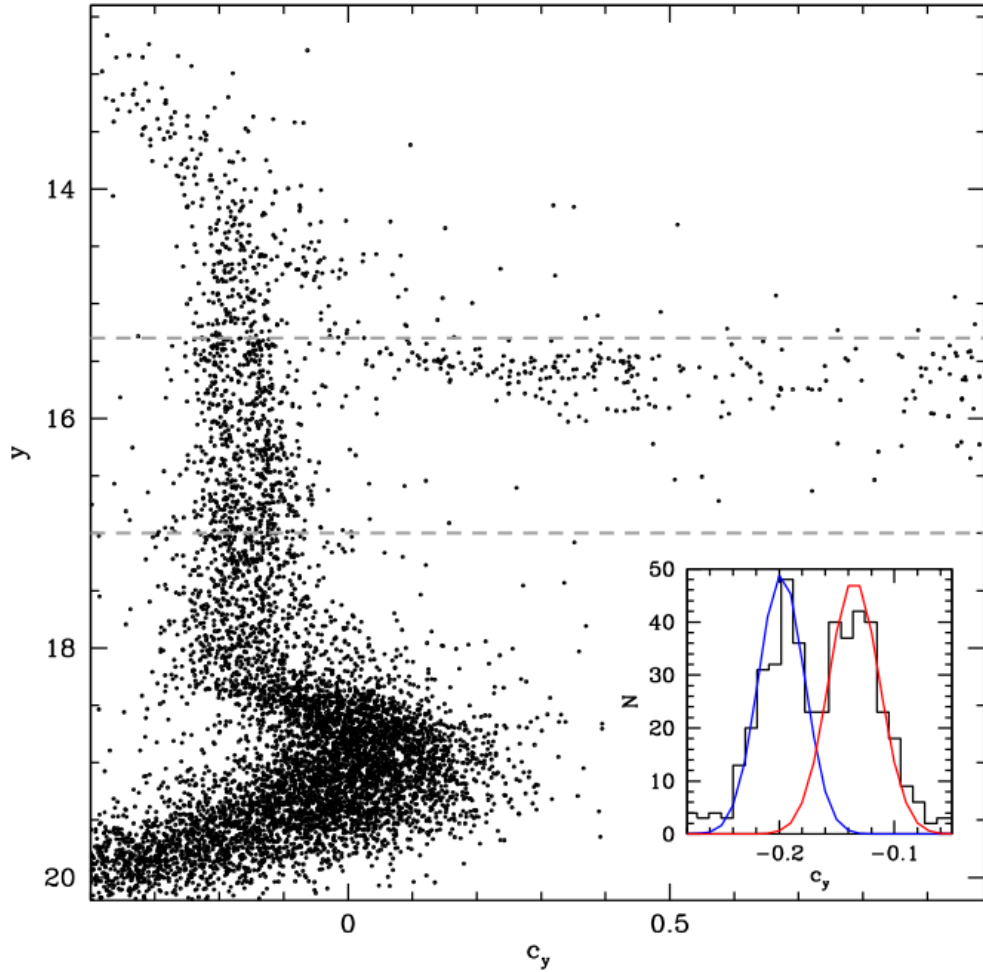


Figure 2.1:  $(c_y, y)$  CMD for M3. The index  $c_y$  is defined as  $c_y = (u - v) - (v - y)$  according to the values of the  $uvby$  filters from the Strömgren photometry. Inset: histogram of the colour distribution of stars in the RGB magnitude interval  $15.3 < y < 17$ . Figure from [Massari et al. \(2016\)](#).

Since GCs are rich in RR Lyrae stars, many works have been directed to this type of objects. RR Lyrae variables stars provide fundamental information to estimate ages and distances to GCs. The advantage of these stars is they are easy to identify through their light curves and, because of their brightness, can be detected at large distances. Some studies have been done in M3 using these variables. For example, [Bakos et al. \(2000\)](#) cataloged 274 variable stars in M3, being one of the CGs with the largest number of RR Lyrae variables. [Cacciari et al. \(2005\)](#) carried out a study of the

pulsational and evolutionary characteristics of 133 RR Lyrae stars of M3 from which about 14 % turned out to be overluminous, this probably means the stars are in more advanced evolutionary stage off the zero-age horizontal branch. On the other hand, ([Corwin & Carney 2001](#)) presented BV CCD (Charge-Coupled Device) photometry, light curves, and ephemerids for 207 RR Lyrae variables. [Jurcsik et al. \(2017\)](#) reported the first simultaneous photometric and spectroscopic study of a large set of RR Lyrae variables in M3.

The asymptotic giant branch (AGB) has been little investigated in the context of multiple stellar populations. [Gruyters et al. \(2017\)](#) studied for the first time the AGB of five GCs: In addition to M3, they obtained photometric data in the Strömgren system of M92, NGC 362, NGC 1851, and NGC 6752 and that revealed the presence of multiple populations in the RGB and AGB. Figure 2.2 show the CMD reported by [Gruyters et al. \(2017\)](#).

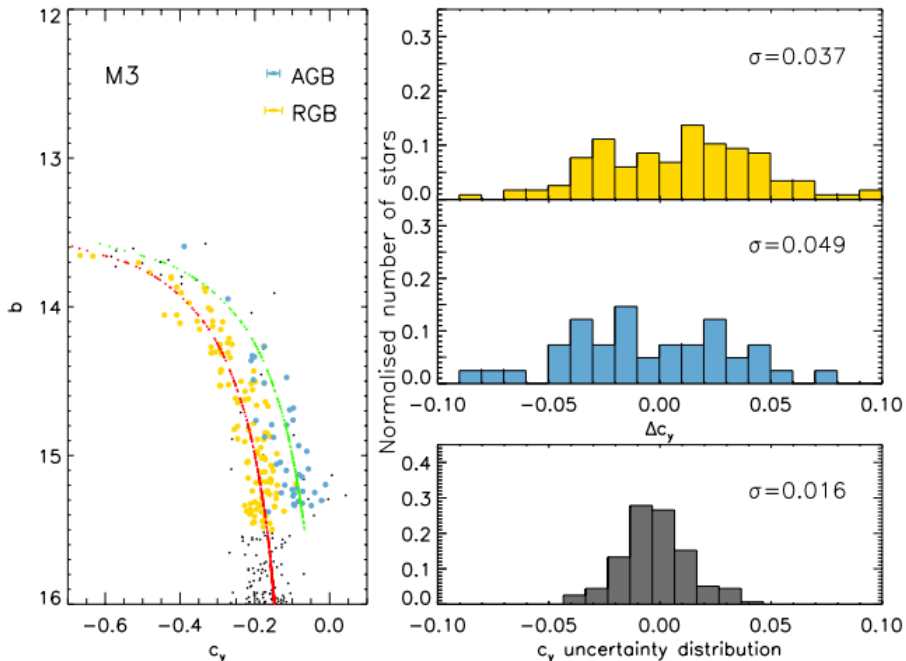


Figure 2.2:  $(c_y, y)$  CMD and  $c_y$  spread for M3. The RGB stars are indicated by the yellow bullets while the blue bullets represent the AGB stars. The upper and medium right panel give the photometric error of the RGB and AGB, respectively, and the right lower panel shows the distribution of the photometric uncertainties in  $c_y$ . Figure from [Gruyters et al. \(2017\)](#).

The fact that the dispersion of  $c_y$  of the RGB and AGB is significantly greater than the photometric errors provides sufficient evidence to confirm the presence of multiple populations where the First Generation stars are located on the left side of the RGB and AGB distributions, and a Second Generation on the right hand side. The results of this study are in agreement with those of [García-Hernández](#)

[et al. \(2015\)](#) who provided spectroscopic evidence of the presence of a second stellar generation with enhanced Al abundance, based on observations with the Apache Point Observatory Galactic Evolution Experiment (APOGEE).

The spectroscopic studies have so far concentrated on members of M3 in advanced evolutionary phases, that have gone through a series of structural changes that involve chemical mixing due to convection. In all phases evidence on the presence of First and Second Generation populations has been found. However, to our knowledge, there has been no study demonstrating the existence of different populations on the Main Sequence, this is, in star members which have not yet been subject to atmospheric chemical pollution due to mixing with the chemical contents of inner stellar layers.



# Chapter 3

## Model atmospheres and synthetic spectra

In previous pages, we have already mentioned that one of the goals of this work is to theoretically explore the sensitivity of spectral features measured in the form of spectroscopic indices to effects of the chemical mixtures present in GCs with multiple stellar populations. With that aim in mind, we have to construct the theoretical framework, a process that is presented in this chapter. Globally, the actions taken to achieve the goal are: calculation of the distribution functions of opacity appropriate for the typical chemical mix in GCs, construction of a grid of model atmospheres based on the new functions, and implementation of the newly built model grid into the computations of synthetic spectra at high resolution.

A stellar atmosphere is the part of a star that can be defined as the layer from which the radiation comes out, that is, it is a means of transport through which energy generated in the inner layers flows outward and eventually into the space.

A very useful way of to study the structure of the outer stellar layers is through model atmospheres that provide a mathematical description of the physical structure of a stellar atmosphere and of its emergent spectrum ([Bertone 2001](#)). The essential physical parameters that determine a stellar model atmosphere are the effective temperature  $T_{\text{eff}}$ , the surface gravity  $\log g$ , and the elemental abundances. For this reason, grids of model atmospheres span over a volume in this three dimensional space.

In the following, we describe the codes and procedures used to generate our grid of stellar models and synthetic spectra. We will then use the synthetic spectra to compute a set of spectroscopic indices for the different chemical compositions that [Sbordone et al. \(2011\)](#) considered to be characteristics of different stellar populations in GCs (see Section [1.5](#)). These chemical compositions adopt, as a reference, a metal-poor ( $[\text{Fe}/\text{H}] = -1.62$ )  $\alpha$ -enhanced ( $[\alpha/\text{H}] = +0.4$ ) mixture based on the solar

composition of [Grevesse & Noels \(1993\)](#); furthermore, the other three chemical compositions (called CNONa1Y2, CNONa1Y4 and CNONa2Y2) present changes in several elements. Therefore, we need to first compute the line opacity in the form of distribution functions (see next sections for details), before calculating the photospheric models and the respective spectra.

### 3.1 The library of Kurucz's codes

We made use of several Fortran codes written by Robert L. Kurucz (Harvard-Smithsonian Center of Astrophysics) in order to compute line opacity, stellar model atmospheres and their synthetic spectra.

The main one is called ATLAS and it computes theoretical stellar model atmospheres ([Kurucz 1970](#)). Even though its first version was written in the late 1960s, it is still very widely used for reproducing real stars over a large range in stellar parameters (e.g. [Bertone et al. 2004, 2008; Husser et al. 2013](#)).

The ATLAS code has been continuously modified over the following years to obtain new versions to reflect improved treatments of the physical processes that take place in a stellar atmosphere, which include changes in the temperature correction, radiation pressure, convection, and opacity distribution functions, and correction of some minor numerical instabilities and bugs ([Kurucz 1979](#)). The upgrades also include the adoption of better and larger sets of input data, such as the physical parameters of atomic and molecular electronic transitions.

One of the more important versions is ATLAS6, described in details in [Kurucz \(1979\)](#), with which a very large library of models was computed for effective temperatures ranging from 5,500 to 50,000 K, surface gravities from the main sequence down to the radiation pressure limit, and a set solar-scaled abundances, from the solar values to  $[M/H]=-2.0$ . The calculation of this extensive grid was based on the statistical distribution functions of the opacity of almost  $10^6$  atomic lines ([Kurucz 1979](#)) and diatomic molecules.

ATLAS9, the improved version of ATLAS6, is the present version of the Kurucz's code and is based on the following basic assumptions:

- The atmosphere is in a steady state.
- The flux of energy (radiative and convective) is constant with depth in the atmosphere. The flux  $F$  is specified by an effective temperature  $T_{\text{eff}}$  such that  $F = \sigma T_{\text{eff}}$ , where  $\sigma = 5.6704 \times 10^{-5} \text{ erg cm}^{-2} \text{ s}^{-2} \text{ K}^{-4}$ .

- The atmosphere is thin relative to the radius of the star, i.e. a plane-parallel geometry is considered.
- The atmosphere is homogeneous, except obviously in the normal direction to the plane-parallel geometry.
- The hydrostatic equilibrium holds.
- The local thermodynamic equilibrium is adopted.
- The atomic abundances are specified and constant throughout the atmosphere.
- The opacity is computed by means of pre-computed distribution function (see section [3.2](#) for more details over opacity distribution function).

ATLAS9 use 72 plane parallel layers where the Rosseland optical depth ranges from  $\log \tau_{\text{Ross}} = -6.875$  at the surface, to  $\log \tau_{\text{Ross}} = 2$  at the bottom of the atmosphere at steps of  $\Delta \log \tau_{\text{Ross}} = 0.125$ . The calculations of ATLAS9 are based on an absorption line list including around 58 million lines, both atomic and molecular ([Kurucz 1992](#)).

Although a more recent version of the ATLAS code exists, called ATLAS12, this work is based on ATLAS9. ATLAS12 uses the method of Opacity Sampling (OS) to compute the line opacity and, unlike ATLAS9 that uses pre-tabulated opacities, among its main characteristics is that it allows calculation of models with arbitrary chemical abundances, which can also vary with depth. Nevertheless, the big disadvantage of ATLAS12 is the very long time required to computing a single model ([Castelli 2005a](#)). Since the main difference between ATLAS9 and ATLAS12 is the treatment of the line opacity, ATLAS9 is a much more efficient choice for computing a large grid of models as required in this work.

In order to generate tables of line opacity distribution functions, we made use of another Kurucz's code, called DFSYNTH. A detailed description on how to use DFSYNTH and an example of its use can be found in [Castelli \(2005b\)](#). Another code, also part of the library of Fortran procedures written by R.L. Kurucz, is SYNTH and serves to compute synthetic spectra, at any arbitrary spectral resolution from model atmospheres. SYNTH requires as input a stellar atmosphere model computed with ATLAS9 (see Figure [3.1](#)). Both codes are consistent, they require the same input data and use the same numerical approaches for the calculations. The main difference is in the computation of the line opacity: ATLAS9 uses opacity distribution functions, while SYNTH requires to take into account the contribution of each individual line at each wavelength point.

## 3.2 ODF computation

The Opacity Distribution Functions (ODFs) are a statistical method developed to compute the line opacity ([Strom & Kurucz 1966](#); [Kurucz 1970, 1979](#); [Saxner & Gustafsson 1984](#)). Introduced to reduce the computing time due to the very large number of lines, it consists in dividing the spectrum into a number of narrow wavelength intervals  $w_i$  where the profile of the absorption coefficient  $l_\nu$  is reordered in the form of an ascending function. Although the order in the wavelength changes, the integral of total flux remains constant. Then, the length of the narrow interval is normalized to unity obtaining a distribution function that determines what fraction of the interval contains a certain value of the absorption coefficient. The ODF method provides a fast solution to the problem of the treatment of line blanketing for computing model atmosphere.

For any given chemical composition, DFSYNTHE computes ODFs for given pairs of  $T$  and  $P_{\text{gas}}$  at  $N_\nu$  intervals of frequency. Once calculated, the ODF is rearranged as a function of  $\nu$  and averaged over 12 subintervals. Thus, DFSYNTHE computes a table of  $12 \times N_\nu$  ODFs for resolving power  $R = 500,000$  at 3,507,859 frequency points from  $\lambda_1 = 8.97666$  nm to  $\lambda_f = 10,000$  nm ([Castelli 2005b](#)).

DFSYNTHE (and, consequently, ATLAS9) has two options to choose the number of intervals of frequency to use: BIG and LITTLE. The so-called BIG intervals divide the entire frequency range in 328 intervals, while the LITTLE intervals divide it in 1,212. In this work, the BIG intervals were used. The ODFs are computed for 57 values of temperature (ranging from  $\log T = 3.30$  (1,995 K) to  $\log T = 5.30$  (199,526 K) at steps of 0.02 dex) and 25 values of gas pressure  $P_{\text{gas}}$  (ranging from  $\log P_{\text{gas}} = -4.0$  to  $\log P_{\text{gas}} = 8.0$  at steps of 0.5 dex) ([Castelli & Kurucz 2003](#)), thus each BIG ODF table has a total of  $12 \times 328 \times 57 \times 25 = 5,608,800$  entries, while the LITTLE ODF table has 20,725,200 data. The ODFs tables generated with DFSYNTHE are used as input data for ATLAS9 to compute the model atmospheres and the low-resolution emergent fluxes.

We computed the ODFs for the four chemical compositions given by [Sbordone et al. \(2011\)](#): the Reference one and the other three mixtures called CNONa1Y2, CNONa1Y4 and CNONa2Y2.

## 3.3 ATLAS9 model computation

In addition to ODFs tables as input data, ATLAS9 also requires some other parameters such as: the chemical abundance (see Table A.1), a list of molecular bands, a microturbulent velocity ( $\xi = 2$  km s $^{-1}$ ) and a mixing-length-to-scale-height ratio (usually, the adopted value in Kurucz's approach is  $l/H_p = 1.25$ ). All the models were

computed by considering LTE, the convection option switched on and with the overshooting option switched off.

We computed a total of 3,472 models with  $T_{\text{eff}}$  from 4300 K to 7000 K, at step of 100 K, with  $\log g$  from 2.0 to 5.0, with step of 0.1 dex, for the four chemical composition of [Sbordone et al. \(2011\)](#).

Figure 3.1 shows an example of the output file describing the structure of a stellar atmosphere for  $T_{\text{eff}} = 6,000$  K,  $\log g = 4.5$  and the Reference chemical composition (see Table A.1). For all examples shown here, we chose  $T_{\text{eff}} = 6,000$  K because it is a representative temperature of MS stars of M3 (see Figure 6.2 or 6.6).

ATLAS9 iteratively modifies the temperature profile of the atmosphere until the radiative+convective equilibrium is achieved at all depths within chosen thresholds for the flux value (1%) and for the flux derivative with respect to depth (1%). Note that the value of these thresholds is more stringent than those adopted by Kurucz for its libraries (2% and 10%, respectively). The calculations in ATLAS9 usually converge with 15 iterations for most of the models, however, we chose to carry out 60 iterations in order to ensure the convergence for most of the models. Even so, a few models did not converge below the expected precision thresholds.

A detailed report is given in Table 3.1, where we indicate the number of models that converged to thresholds from the target one (1.0%) up to 5.0%. It is important to note that 98.36% of models converged to flux errors  $\leq 1.0\%$ , while 95.05% of them attained the chosen threshold for the flux derivative.

Table 3.1: Number of models that converged within different threshold values.

|                 | $\leq 1.0\%$ | $\leq 2.0\%$ | $\leq 3.0\%$ | $\leq 4.0\%$ | $\leq 5.0\%$ |
|-----------------|--------------|--------------|--------------|--------------|--------------|
| Flux value      | 3,415        | 3,444        | 3,444        | 3,445        | 3,445        |
| Flux derivative | 3,300        | 3,463        | 3,464        | 3,465        | 3,466        |

Furthermore, all model atmospheres reached a derivative error  $< 8.30\%$ . In Table 3.2 we report the maximum percentage flux error for those few models that exceeded a value of 15%. It is important to mention that all these models have high  $T_{\text{eff}}$  and low  $\log g$ , which makes them not relevant for the analysis of MS stars in M3. We tried to make these models converging, for example, by varying the number of iterations, but it was not possible to achieve it. A part from the fact that the combination of high temperatures and low gravities makes more difficult to achieve a hydrostatic equilibrium, it is difficult to understand the cause of this convergence problem, a task far beyond the goal of this thesis.

Figure 3.1: Example of the output file of an atmosphere model computed with ATLAS9 at  $T_{\text{eff}} = 6,000$  K,  $\log g = 4.5$  and the reference mixture. First line:  $T_{\text{eff}}$ ,  $\log g$  and the indication that the model was computed in Local Thermodynamic Equilibrium (LTE). Second: Title assigned to the model for reference, microturbulent velocity (VTURB), mixing-length-to-scale-height ratio (L/H), no convective overshooting (NOVER) and the newer set of ODFs. Third: it indicates which opacity sources were taken into account during the calculation. Fourth: convective transport used being 1.25 the mixing length parameter and without turbulence. Fifth line: ratio between the input and the solar metallicity, abundance in numeric density of hydrogen and the helium. From line 6 to 22, the abundance for the rest of the elements expressed as  $\log(N_{\text{element}}) - \log(N_{\text{H+He}})$ , where each element is represented by its atomic number to the left of its abundance. The second part shows the values of seven parameters computed with respect to depth of the atmosphere divided into 72 layers: From the left to right column: Mass per square centimeter  $\text{RHOX} = \int_0^x \rho(x) dx$  [ $\text{g cm}^{-2}$ ] at the depth  $x$ , temperature T [K], gas pressure P [ $\text{dyne cm}^{-2}$ ], electron number density XNE [ $\text{cm}^{-3}$ ], Rosseland mass absorption coefficient ABROSS  $\kappa_{\text{Ross}}$  [ $\text{cm}^2 \text{ g}^{-1}$ ], acceleration due to the absorption of radiation ACCRAD [ $\text{cm s}^{-2}$ ], microturbulent velocity VTURB [ $\text{km s}^{-1}$ ], energy flux that bear a convection FLXCNV [ $\text{erg cm}^2 \text{ s}^{-1}$ ], convective velocity VCONV [ $\text{km s}^{-1}$ ] and sound velocity VELSND [ $\text{cm s}^{-1}$ ]. Only values for the first 14 layers at the bottom and last 14 layers at the top of the atmosphere are shown. The second last line, PRADK indicates the radiation pressure at the surface.

Table 3.2: Not converged models and their associated flux error.

| Chemical composition | $T$ [K] | $\log g$ : | Flux error (%) |        |        |        |        |        |        |        |
|----------------------|---------|------------|----------------|--------|--------|--------|--------|--------|--------|--------|
|                      |         |            | 2.0            | 2.2    | 2.3    | 2.4    | 2.6    | 2.7    | 2.8    | 2.9    |
| Reference            | 6,500   |            | 22.046         |        |        |        |        |        |        |        |
|                      | 6,600   |            |                | 20.844 |        |        |        |        |        |        |
|                      | 6,700   |            |                |        | 21.453 |        |        |        |        |        |
|                      | 6,800   |            |                |        |        | 15.628 |        |        |        |        |
|                      | 6,900   |            |                |        |        |        | 20.970 |        |        |        |
|                      | 7,000   |            |                |        |        |        |        | 20.138 |        |        |
| CNONa1Y2             | 6,500   |            | 20.761         |        |        |        |        |        |        |        |
|                      | 6,600   |            |                | 21.240 | 12.368 |        |        |        |        |        |
|                      | 6,700   |            |                |        | 21.629 |        |        |        |        |        |
|                      | 6,800   |            |                |        |        | 15.220 |        |        |        |        |
|                      | 6,900   |            |                |        |        |        | 21.210 |        |        |        |
|                      | 7,000   |            |                |        |        |        |        | 20.434 |        |        |
| CNONa1Y4             | 6,500   |            | 17.526         |        |        |        |        |        |        |        |
|                      | 6,600   |            |                | 16.368 |        |        |        |        |        |        |
|                      | 6,700   |            |                |        | 17.568 |        |        |        |        |        |
|                      | 6,800   |            |                |        |        | 20.417 |        |        |        |        |
|                      | 6,900   |            |                |        |        |        | 20.516 | 15.728 |        |        |
|                      | 7,000   |            |                |        |        |        |        |        | 20.590 | 15.446 |
| CNONa2Y2             | 6,500   |            | 22.000         |        |        |        |        |        |        |        |
|                      | 6,600   |            |                | 21.829 |        |        |        |        |        |        |
|                      | 6,700   |            |                |        | 21.885 |        |        |        |        |        |
|                      | 6,800   |            |                |        |        | 15.463 |        |        |        |        |
|                      | 6,900   |            |                |        |        |        | 21.263 |        |        |        |
|                      | 7,000   |            |                |        |        |        |        |        | 20.398 |        |

Figures 3.2, 3.3, 3.4 and 3.5 show some results of the computed models. In Figure 3.2 we present all temperature profiles for a surface gravity  $\log g = 4.2$  plotted for each of the four chemical composition in the full range of temperatures (4,300 - 7,000 K). No significant changes can be easily noted among these temperature profiles as due to the different chemical mixtures, however these differences can be observed with more detail in the Figure 3.3 where an example comparing the temperature profiles of the three modified chemical compositions (CNONa1Y2, CNONa1Y4 and CNONa2Y2) with respect to the Reference composition is shown for a model with  $T_{\text{eff}} = 6,000$  K and  $\log g = 4.2$ . At these conditions, the biggest difference was only  $\Delta T \simeq 25$  K between the chemical compositions CNONa1Y4 and Reference, at the bottom of the photosphere.

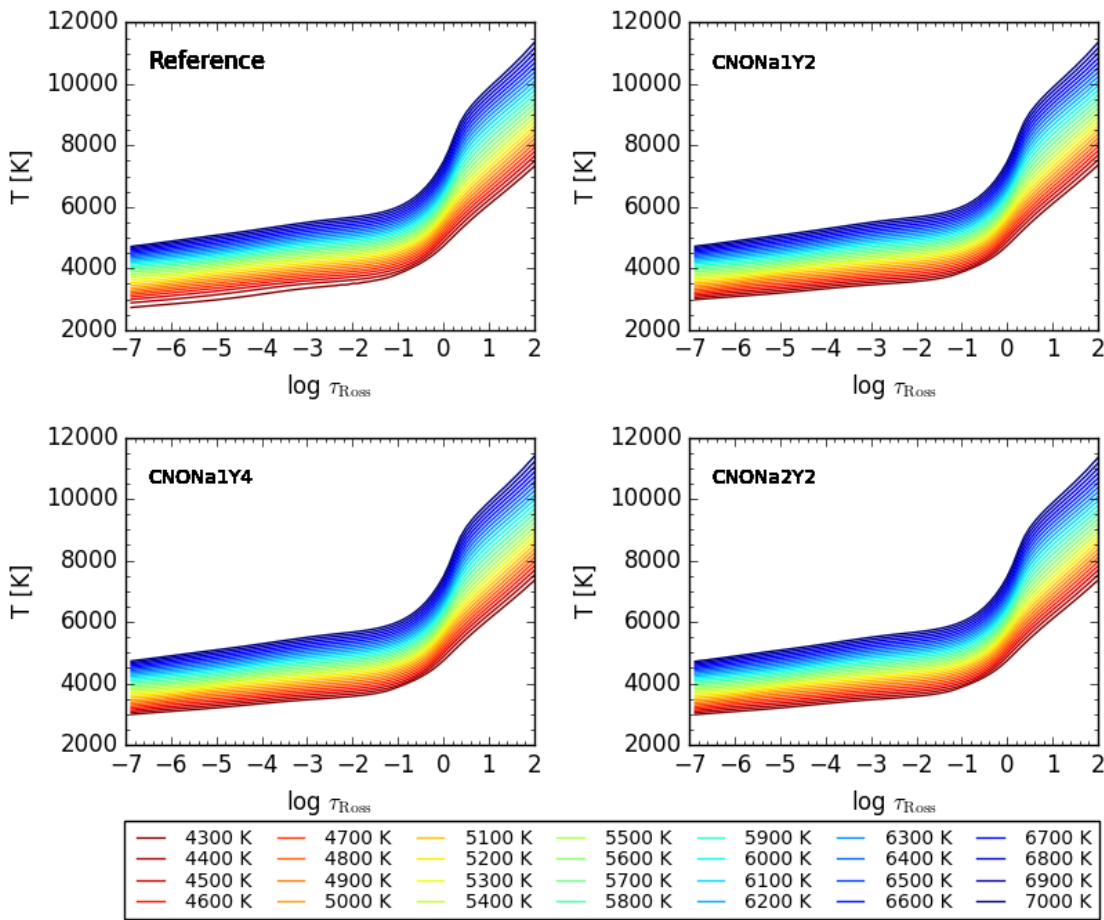


Figure 3.2: Effect of the effective temperature on the temperature profile as function of  $\log \tau$  for each of the four chemical compositions with a surface gravity  $\log g = 4.2$ .

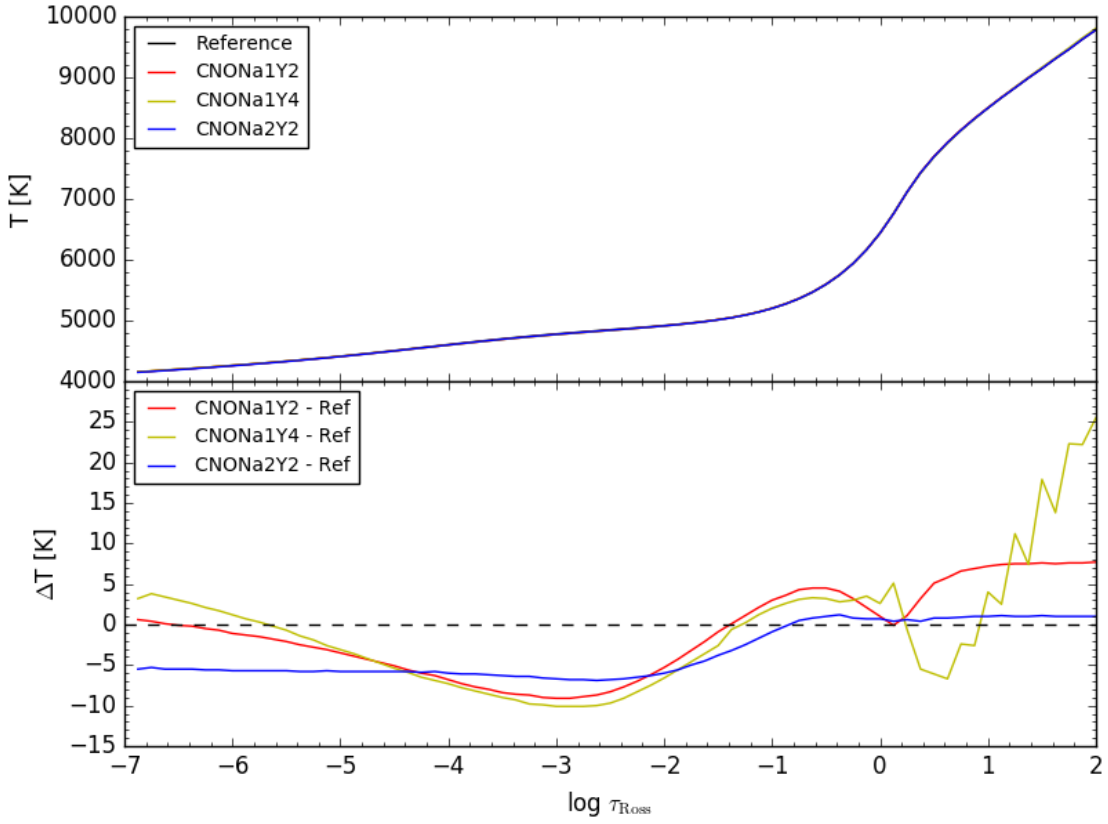


Figure 3.3: Upper panel: Temperature profile of models with  $T_{\text{eff}} = 6,000$  K and  $\log g = 4.2$  and with the four different chemical compositions of Sbordone et al. (2011). Lower panel: Temperature difference of the CNONa1Y2, CNONa1Y4 and CNONa2Y2 with respect to the Reference one.

Similar to lower panel of Figure 3.3, in Figure 3.4 we show examples of the difference of temperature profiles for other effective temperatures. The largest difference with respect to the Reference chemical composition takes place in the outer photosphere at the lower  $T_{\text{eff}}$ , while for the warmer models, the strongest discrepancy is located in the optical thick zone and for the He-enhanced mixture CNONa1Y4.

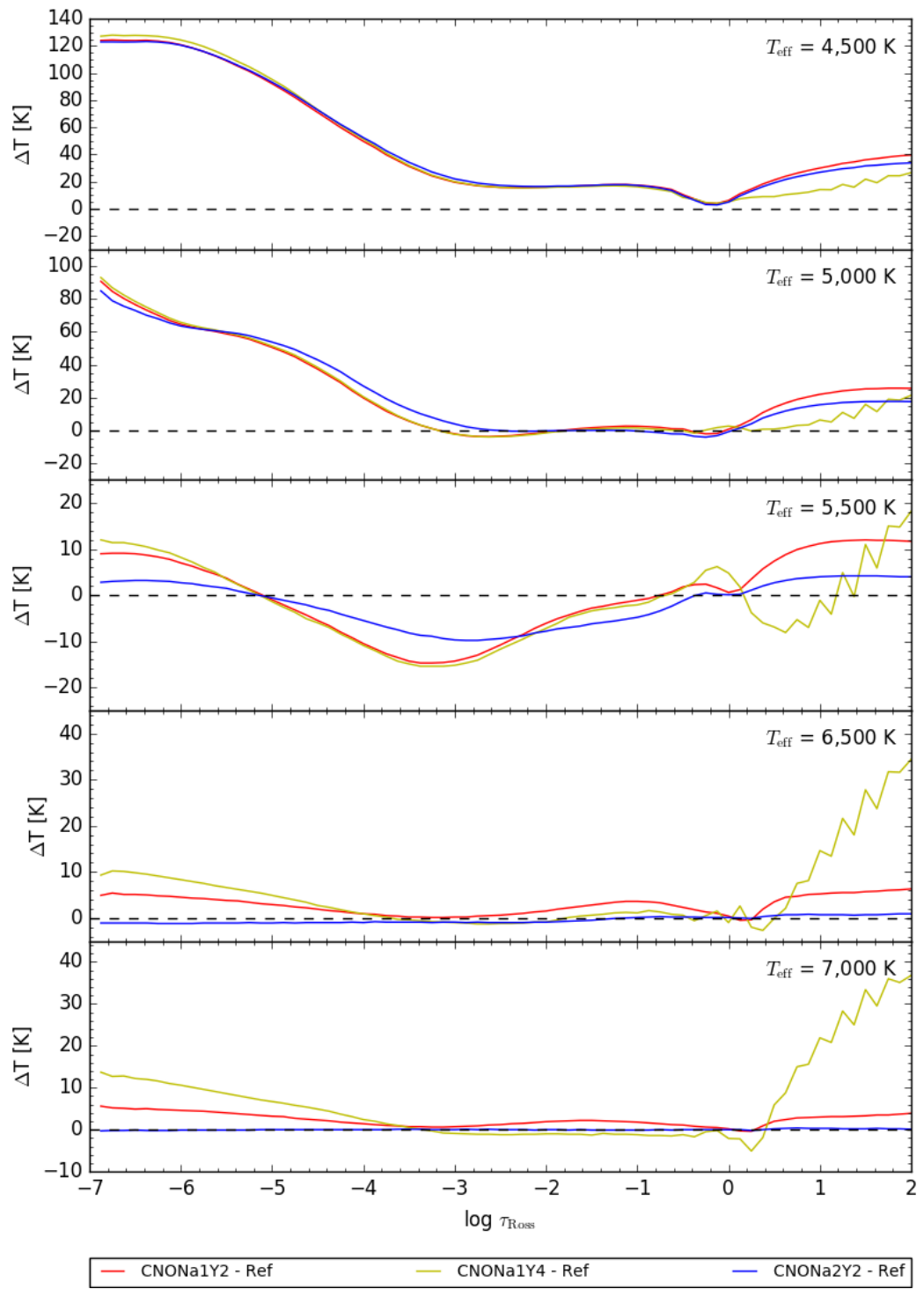


Figure 3.4: As lower panel of Figure 3.3: Temperature difference of the CNONa1Y2, CNONa1Y4 and CNONa2Y2 with respect to Reference for the temperatures indicated in each panel.

In Figure 3.5, we show the effect of surface gravity on the temperature profile for models with fixed  $T_{\text{eff}} = 6,000$  K.

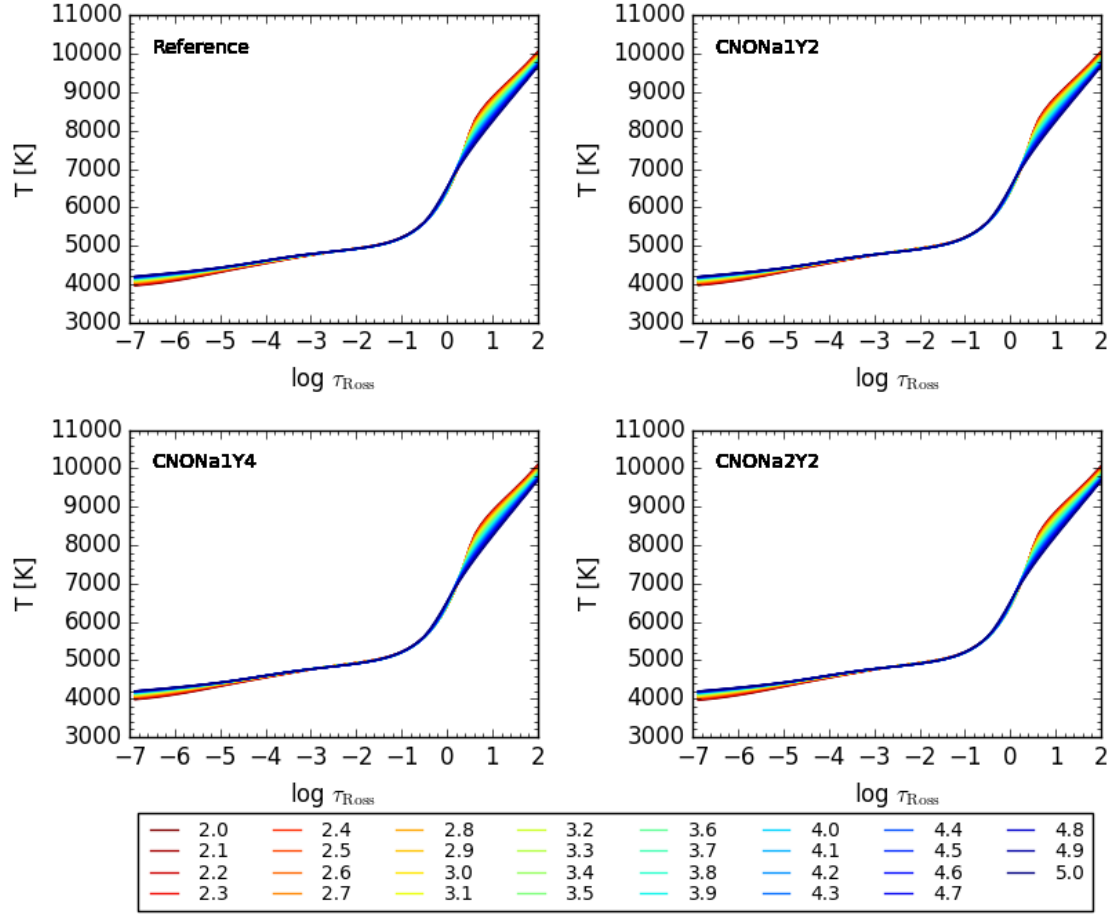


Figure 3.5: Effect of the surface gravity on the temperature profile as function of  $\log \tau_{\text{Ross}}$  for each of the four chemical compositions for models with  $T_{\text{eff}} = 6,000$  K. The different colors indicate  $\log g$  from 2.0 to 5.0.

### 3.4 SYNTHE theoretical spectra

For each stellar model atmosphere, a synthetic spectra was computed with the SYNTHE code at high-resolution,  $R = \lambda/\Delta\lambda = 500,000$ . The wavelength interval goes from 3,300 to 6,140 Å. An example of a synthetic spectrum at high resolution is shown in the upper panel of Figure 3.6. Once calculated these spectra, they were broadened to the spectral resolution of the OSIRIS’ MOS ( $R = 2,500$ ) by convolution with a Gaussian kernel. In the lower panel of the Figure 3.6, we present the same spectrum of the upper panel but broadened to  $R = \lambda/\Delta\lambda = 2,500$ . Henceforth, all the work is based on spectra at resolution  $R = 2,500$ .

In order to show the flux difference among the chemical compositions explored in this work, the spectra of the three modified chemical mixtures were compared with the Reference spectrum. These differences are shown in Figure 3.7 and are crucial for our work because we aim at identifying multiple stellar population through the analysis of spectroscopic indices. The definition of spectral indices for the analysis of these differences is presented in next Chapter.

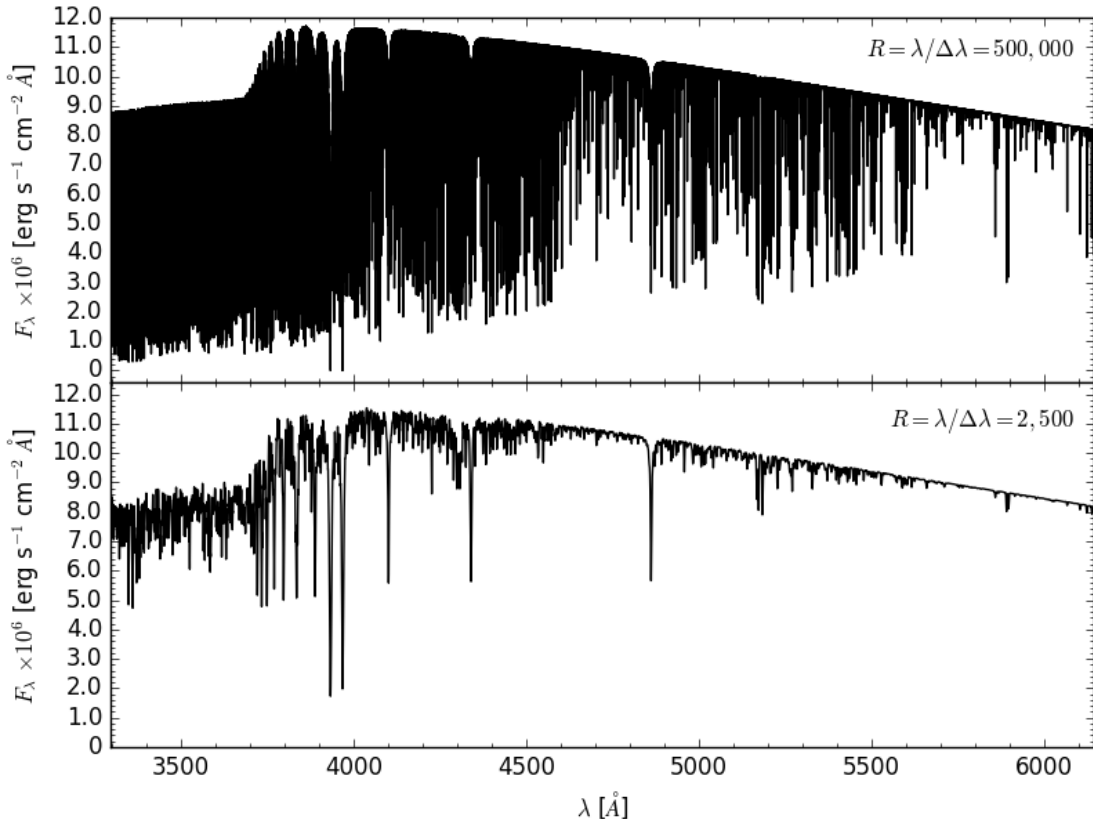


Figure 3.6: Upper panel: Synthetic spectrum of a model atmosphere of  $T_{\text{eff}} = 6,000$  K and  $\log g = 4.2$  for the Reference chemical composition at  $R = 500,000$ . Lower panel: The same spectrum broadened to  $R = 2,500$ .

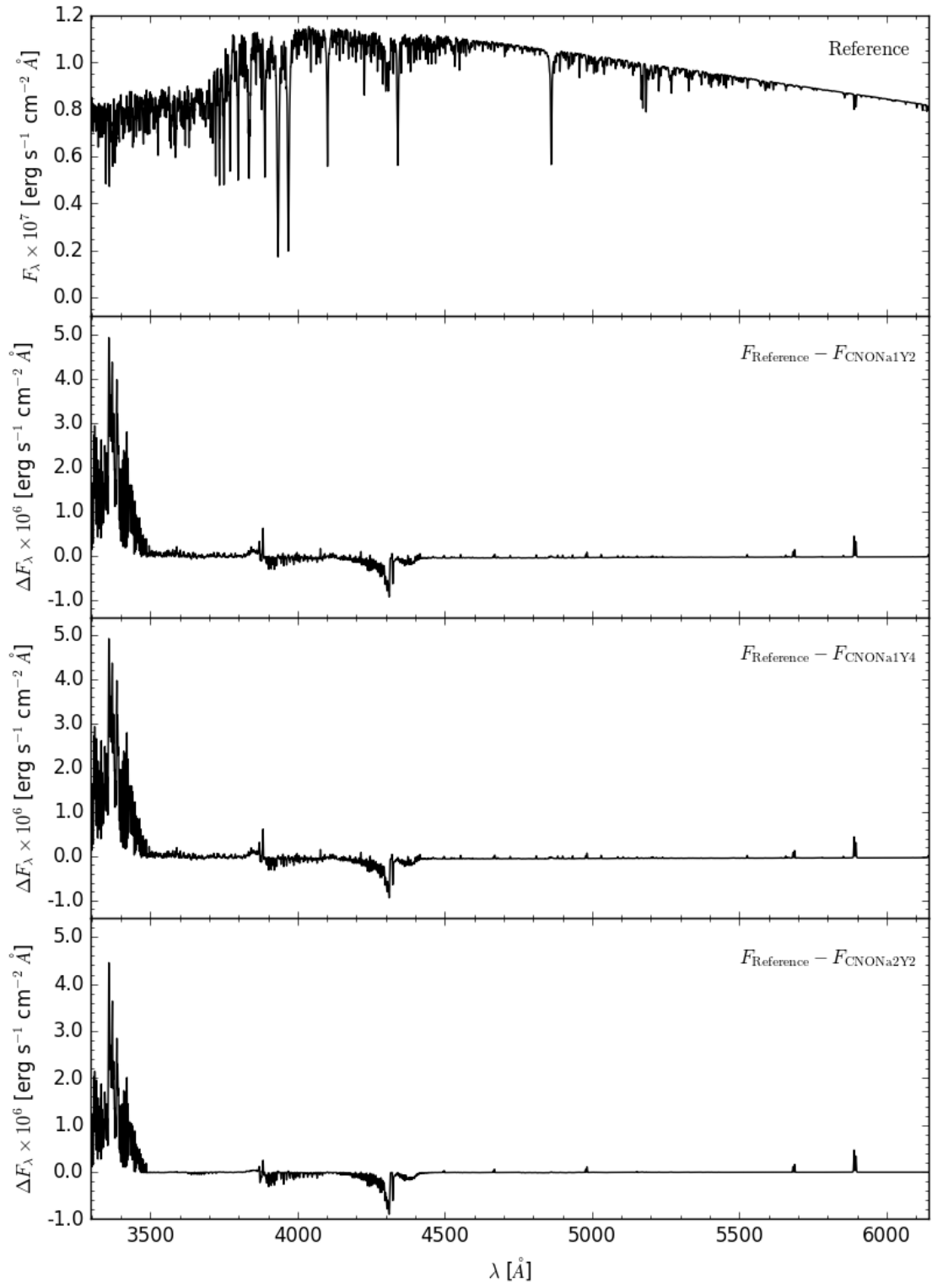


Figure 3.7: Reference spectrum (upper panel) and the difference with each of the corresponding spectra of the three modified chemical compositions, as indicated in each panel, for a model atmosphere of  $T_{\text{eff}} = 6,000$  K and  $\log g = 4.2$ .

The residual fluxes in Figure 3.7 show that the main differences are present in the blue edge of the spectra and in some particular regions such as the CH feature at 4300 Å that gives rise to the so called G band, some molecular bands at  $< 3,500$  Å and the Na lines in the red at 5,890 and 5,896 Å , for example. Blueward from the G band there are also some relatively large residuals from CN and atomic hydrogen. The identification of the bandpass for the lines with the biggest differences are shown in Figure 4.1 in the next Chapter.

# Chapter 4

## Spectroscopic indices

A spectroscopic index is a measure of the strength of a spectral feature relative to an adjacent continuum or pseudocontinuum. It is defined through one bandpass centered on the atomic line or molecular band to be evaluated, and one or two bandpasses around it to define the continuum level. Spectroscopic indices are used to extract information over the physical and chemical properties of galactic and extragalactic astronomical objects through their observed spectra.

### 4.1 Lick/IDS system

Many spectroscopic indices have been defined to measure spectral features of astronomical objects. One of the most used is the LICK/IDS system, whose development began in the 1970's by [Faber et al. \(1977\)](#) who defined three indices (Na D, MgH + Mgb and the G band (CH)) for studying the cD galaxy in Abell 401. Later, the system was used for other objects as GCs and for the synthesis of stellar populations. [Burstein et al. \(1984\)](#) added eight new indices (CN, Mg<sub>1</sub> (only MgH), TiO<sub>1</sub>, TiO<sub>2</sub>, Mg *b*, Fe5272 (Fe I and Ca I), Fe5335 (Fe I, Cr I, Ca I and Ti II) and H <sub>$\beta$</sub> ) to the LICK/IDS system and were applied to spectroscopic comparison of GCs of the Milky Way and M31 and of elliptical galaxies nuclei. Those 11 spectral indices were defined in [Faber et al. \(1985\)](#), who also used them to analyze the spectra of a sample of 110 K-giant stars. [Worthey et al. \(1994\)](#) included ten more spectroscopic indices to the LICK/IDS system to form a total of 21 with which they measured the optical absorption features of a sample 460 stars with the purpose of predicting index strengths in the integrated light of stellar populations of different ages and metallicities; in that work they found the most promising index metallicity for old stellar populations, the Mg<sub>2</sub> index. The bandpasses of these 21 spectroscopic indices were refined by [Trager et al. \(1998\)](#). Finally, [Worthey & Ottaviani \(1997\)](#) added four more indices for H <sub>$\delta$</sub>  and H <sub>$\gamma$</sub>  reaching a total of 25 spectroscopic indices whose characteristics are listed in Table 4.1.

Table 4.1: Lick/IDS index definitions. Indices 1 - 21 are from Table 2 of Trager et al. (1998) whereas indices 22 - 25 are from Table 1 of Worthey & Ottaviani (1997).

| <i>j</i> | Name                        | Index Bandpass [Å] | Pseudocontinua [Å]                     | Units | Measures <sup>a</sup>                      | Error <sup>b</sup> |
|----------|-----------------------------|--------------------|--|-------|--|--------------------|
| 1        | CN <sub>1</sub>             | 4143.375-4178.375  | 4081.375-4118.875<br>4245.375-4285.375 | mag   | CN, FeI                                    | 0.021              |
| 2        | CN <sub>2</sub>             | 4143.375-4178.375  | 4085.125-4097.625<br>4245.375-4285.375 | mag   | CN, FeI                                    | 0.023              |
| 3        | Ca4227                      | 4223.500-4236.000  | 4212.250-4221.000<br>4242.250-4252.250 | Å     | CaI, FeI, FeII                             | 0.27               |
| 4        | G4300                       | 4282.625-4317.625  | 4267.625-4283.875<br>4320.125-4336.375 | Å     | CH, FeI                                    | 0.39               |
| 5        | Fe4383                      | 4370.375-4421.625  | 4360.375-4371.625<br>4444.125-4456.625 | Å     | FeI, TiII                                  | 0.53               |
| 6        | Ca4455                      | 4453.375-4475.875  | 4447.125-4455.875<br>4478.375-4493.375 | Å     | CaI, FeI, NiI,<br>TiIII, MnI, VI           | 0.25               |
| 7        | Fe4531                      | 4515.500-4560.500  | 4505.500-4515.500<br>4561.750-4580.500 | Å     | FeI, TiI, FeII,<br>TiIII                   | 0.42               |
| 8        | Fe4668                      | 4635.250-4721.500  | 4612.750-4631.500<br>4744.000-4757.750 | Å     | FeI, TiI, CrI,<br>MgI, NiI, C <sub>2</sub> | 0.64               |
| 9        | H <sub>β</sub>              | 4847.875-4876.625  | 4827.875-4847.875<br>4876.625-4891.625 | Å     | H <sub>β</sub> , FeI                       | 0.22               |
| 10       | Fe5015                      | 4977.750-5054.000  | 4946.500-4977.750<br>5054.000-5065.250 | Å     | FeI, NiI, TiI                              | 0.46               |
| 11       | Mg <sub>1</sub>             | 5069.125-5134.125  | 4895.125-4957.625<br>5301.125-5366.125 | mag   | MgH, FeI, NiI                              | 0.007              |
| 12       | Mg <sub>2</sub>             | 5154.125-5196.625  | 4895.125-4957.625<br>5301.125-5366.125 | mag   | MgH, Mgb, FeI                              | 0.008              |
| 13       | Mgb                         | 5160.125-5192.625  | 5142.625-5161.375<br>5191.375-5206.375 | Å     | Mgb  | 0.23               |
| 14       | Fe5270                      | 5245.650-5285.650  | 5233.150-5248.150<br>5285.650-5318.150 | Å     | FeI, CaI                                   | 0.28               |
| 15       | Fe5335                      | 5312.125-5352.125  | 5304.625-5315.875<br>5353.375-5363.375 | Å     | FeI  | 0.26               |
| 16       | Fe5406                      | 5387.500-5415.000  | 5376.250-5387.500<br>5415.000-5425.000 | Å     | FeI, CrI                                   | 0.2                |
| 17       | Fe5709                      | 5698.375-5722.125  | 5674.625-5698.375<br>5724.625-5738.375 | Å     | FeI, NiI, MgI,<br>CrI, VI                  | 0.18               |
| 18       | Fe5782                      | 5778.375-5798.375  | 5767.125-5777.125<br>5799.625-5813.375 | Å     | FeI, CrI, CuI,<br>MgI                      | 0.2                |
| 19       | Na D                        | 5878.625-5911.125  | 5862.375-5877.375<br>5923.875-5949.875 | Å     | NaI  | 0.24               |
| 20       | TiO <sub>1</sub>            | 5938.375-5995.875  | 5818.375-5850.875<br>6040.375-6105.375 | mag   | TiO  | 0.007              |
| 21       | TiO <sub>2</sub>            | 6191.375-6273.875  | 6069.375-6143.375<br>6374.375-6416.875 | mag   | TiO  | 0.006              |
| 22       | H <sub>δ</sub> <sub>A</sub> | 4083.500-4122.250  | 4041.600-4079.750<br>4128.500-4161.000 | Å     |  | 0.64               |
| 23       | H <sub>γ</sub> <sub>A</sub> | 4319.750-4363.500  | 4283.500-4319.750<br>4367.250-4419.750 | Å     |  | 0.48               |
| 24       | H <sub>δ</sub> <sub>F</sub> | 4091.000-4112.250  | 4057.250-4088.500<br>4114.750-4137.250 | Å     |  | 0.4                |
| 25       | H <sub>γ</sub> <sub>F</sub> | 4331.250-4352.250  | 4283.500-4319.750<br>4354.750-4384.750 | Å     |  | 0.33               |

<sup>a</sup> Dominant species.

<sup>b</sup> Typical rms error per observation for stars.

From Lick/IDS system, only the index  $\text{TiO}_2$  was not included in our calculations because the definition of red pseudocontinua region is out of the spectral range of our stellar spectra library. The measurement procedure is described by [Worley et al. \(1994\)](#). The mean height of both the blue and red pseudocontinua are determined on either side of the feature bandpass, and a straight line is traced through the midpoint of each region. Then, the spectral index is determined by the integral of the difference in flux between this line and the observed flux within the feature bandpass. The average pseudocontinuum flux  $F_p$  is therefore calculated by:

$$F_p = \int_{\lambda_1}^{\lambda_2} F_\lambda d\lambda / (\lambda_2 - \lambda_1) \quad (4.1)$$

where  $\lambda_1$  and  $\lambda_2$  are the wavelength limits of the pseudocontinua sidebands.

For atomic features, the indices are expressed in angstroms of equivalent width as follows:

$$\text{E.W.} = \int_{\lambda_1}^{\lambda_2} \left( 1 - \frac{F_{I\lambda}}{F_{C\lambda}} \right) d\lambda \quad (4.2)$$

where  $F_{I\lambda}$  is the observed flux per unit wavelength,  $F_{C\lambda}$  is the continuum flux, and  $\lambda_1$  and  $\lambda_2$  are the wavelength limits of the feature bandpass.

The measurement of molecular bands is expressed in magnitudes, that is:

$$I_{\text{mag}} = -2.5 \log \left[ \left( \frac{1}{\lambda_2 - \lambda_1} \right) \int_{\lambda_1}^{\lambda_2} \frac{F_{I\lambda}}{F_{C\lambda}} d\lambda \right] \quad (4.3)$$

## 4.2 CN and CH indices

In order to specifically study the anticorrelations between the strength of CN and CH bands observed in galactic GCs, suitable spectroscopic indices have been defined. For example, [Norris & Freeman \(1979\)](#) defined the cyanogen index  $S(4142)$  to measure the strength of the CN band, at about 4,150 Å of 142 RGB stars of 47 Tucanae and they found a bimodal distribution of the index values, with the stars being more CN-rich toward to center of the GC. Similarly, [Norris \(1981\)](#) defined the cyanogen index  $S(3839)$  which measures an even stronger CN band to study giant stars of M4 and concluded that RGB stars showed a bimodal CN abundance distribution. Basically, these indices quantify the CN content in stellar atmospheres of red giants; in fact, the index  $S(3839)$  is not suitable for warmer MS stars because, in the same wavelength interval, there are strong hydrogen lines. Later, [Harbeck et al. \(2003\)](#) modified these indices to exclude the hydrogen lines (equations 4.4 and 4.5). On the other hand, [Cohen \(1978b\)](#) defined the methylidyne index  $CH(4300)$  to quantify the molecular absorption at 4300 Å in MS stars of M13, however they did not find

evidence of chemical anomalies with respect to field stars. Later, this index was modified by [Pancino et al. \(2010\)](#) (equation 4.6). Additionally, [Harbeck et al. \(2003\)](#) defined an index to measure the absorption strength of the CaII H and K lines, expressed in magnitudes. This index was used by [Pancino et al. \(2010\)](#) but defined as an equivalent width (EW) in Å (Equation 4.7). They also included the  $H_{\beta}$  index using the bands defined in the LICK/IDS system but in the form of Equation 4.8, i.e., integrating the continuum, not using a pseudocontinuum. For this work, we used the form of the indices reported by [Pancino et al. \(2010\)](#), which are:

$$S(3839) = -2.5 \log \frac{F_{3861-3884}}{F_{3894-3910}} \quad (4.4)$$

$$S(4142) = -2.5 \log \frac{F_{4120-4216}}{0.5F_{4055-4080} + 0.5F_{4240-4280}} \quad (4.5)$$

$$CH(4300) = -2.5 \log \frac{F_{4285-4315}}{0.5F_{4240-4280} + 0.5F_{4390-4460}} \quad (4.6)$$

$$HK = 1 - \frac{F_{3910-4020}}{F_{4020-4130}} \quad (4.7)$$

$$H_{\beta} = 1 - \frac{F_{4847.875-4876.625}}{0.5F_{4827.875-4847.875} + 0.5F_{4876.625-4891.625}} \quad (4.8)$$

### 4.3 New indices

The previous indices were defined for the study of low resolution spectra and their bands stretch out, in some cases, to about 100 Å. The theoretical work presented here is preparatory for the analysis of spectra collected with the spectrographs at the GTC, currently OSIRIS, but in the future also MEGARA will be available. These instruments reach a high spectral resolution ( $R = 2,500$  for OSIRIS, even higher for MEGARA) and, attached to the largest optical telescope available, can produce high S/N spectra of low luminosity stars in galactic GCs.

In order to fully take advantage of the high quality data that these facilities can provide, we define a new set of spectroscopic indices. Based on the results illustrated, for example, in Figure 3.7, we were able to identify lines and short spectral intervals, over the full spectral range, that show significant strength difference among the chemical compositions used in this work and we defined suitable wavelength bands to create indices that maximize the difference between the chemical mixtures.

We defined 10 new indices: their bandpasses are listed in Table 4.2. Some indices measure the same spectral features as those in previous works, like the Lick/IDS system and [Pancino et al. \(2010\)](#), but as we found significant differences

between the spectra of the four different chemical compositions, we defined different limits of the wavelength bands with the intention of maximizing the differences between chemical composition, so to ease the detection of multiple stellar populations in GCs. For molecular bands our indices  $I_{MB}$  were calculated in the following form:

$$I_{MB} = -2.5 \log \frac{F_{\lambda_{I1}-\lambda_{I2}}}{0.5F_{\lambda_{B1}-\lambda_{B2}} + 0.5F_{\lambda_{R1}-\lambda_{R2}}} \quad (4.9)$$

while, where the absorption is dominated by atomic lines, the index definition is:

$$I_i = 1 - \frac{F_{\lambda_{I1}-\lambda_{I2}}}{0.5F_{\lambda_{B1}-\lambda_{B2}} + 0.5F_{\lambda_{R1}-\lambda_{R2}}} \quad (4.10)$$

where  $F$  is the flux integrated in the range from  $\lambda_1$  to  $\lambda_2$ , the subscripts  $I$ ,  $B$  and  $R$  indicate the bandpass of the index, blue and red continuum regions, respectively.

Table 4.2: Bandpass definition of the new spectroscopic indices defined in this work.

| No. | Name       | Index Bandpass [Å] | Continuum [Å]   |
|-----|------------|--------------------|-----------------|
| 1   | NH         | 3340.0 - 3390.0    | 3310.0 - 3340.0 |
|     |            |                    | 3390.0 - 3420.0 |
| 2   | NO         | 3394.0 - 3428.0    | 3310.0 - 3340.0 |
|     |            |                    | 3450.0 - 3470.0 |
| 3   | OH         | 3434.5 - 3490.0    | 3404.5 - 3440.5 |
|     |            |                    | 3490.0 - 3520.0 |
| 4   | $H_\eta$   | 3822.5 - 3848.0    | 3803.0 - 3822.5 |
|     |            |                    | 3848.0 - 3868.0 |
| 5   | $H_\zeta$  | 3880.0 - 3896.5    | 3860.0 - 3880.0 |
|     |            |                    | 3896.5 - 3920.0 |
| 6   | HK         | 3910.0 - 3990.0    | 3845.0 - 3880.0 |
|     |            |                    | 3990.0 - 4030.0 |
| 7   | $H_\delta$ | 4090.0 - 4115.0    | 4070.0 - 4090.0 |
|     |            |                    | 4115.0 - 4130.0 |
| 8   | $H_\gamma$ | 4315.0 - 4350.0    | 4240.0 - 4270.0 |
|     |            |                    | 4350.0 - 4380.0 |
| 9   | Na         | 5677.0 - 5693.0    | 5660.0 - 5677.0 |
|     |            |                    | 5693.0 - 5710.0 |
| 10  | Na D       | 5840.0 - 5920.0    | 5817.0 - 5840.0 |
|     |            |                    | 5920.0 - 5970.0 |

The names of the molecular bands, NH, NO and OH, in Table 4.2, are given because of the more prominent spectral lines in the corresponding bandpass.

Figure 4.1 shows the central bandpasses of all indices used in this work over the difference between a Reference and CNONa1Y2 spectra at  $T_{\text{eff}} = 6,000$  K and  $\log g = 4.2$ . We computed all spectroscopic indices described above for each of the 3,472 synthetic spectra calculated in Section 3.4.

### 4.3.1 Index error and sensitivity

In order to quantitatively establish the sensitivity to chemical composition and the capability of each theoretical index to distinguish among different mixtures, we estimated a typical index error. We carried out this task by using a Monte Carlo technique, similar to the one presented in Bertone et al. (2013): at each  $i$ -th wavelength point in the bandpasses of an index, we added, to the flux of a synthetic spectrum, a flux error randomly extracted from a Gaussian distribution centered in zero and with a standard deviation  $\sigma_i = f_i / (\text{S/N})$ , assuming  $\text{S/N} = 30$ , which is the requested value for the OSIRIS/MOS observations (see Chapter 6). We then computed the spectroscopic index value on this noisy spectrum and we repeated the procedure 100 times, obtaining a distribution of index values, whose standard deviation is considered as the typical error of the spectroscopic index. The error of each index for the four chemical compositions are reported in Table 4.3 for a spectra at  $T = 6,000$  K and  $\log g = 4.2$ .

Once calculated the errors for each index, we quantify its sensitivity to difference in chemical mixtures by means of the ratio between the index value for two chemical compositions and the quadratic sum of the errors, which we called “*Throw*” (Worley et al. 1994). The definition is the following:

$$\text{Throw} = \frac{I_{\text{ref}} - I_{\text{m}}}{\sqrt{\sigma_{\text{ref}}^2 + \sigma_{\text{m}}^2}} \quad (4.11)$$

where  $I_{\text{ref}}$  is the Reference index,  $I_{\text{m}}$  is the same index but for one of the three modified chemical compositions,  $\sigma_{\text{ref}}$  and  $\sigma_{\text{m}}$  are its respective errors.

A high value of the *Throw* means that the index is a good tracer of the difference in chemical composition and therefore is suitable to identify the presence of multiple stellar populations in GCs. Using this quantity, we intent to identify the best set of spectroscopic indices, with the highest values of *Throw*, that will allow to detect different stellar populations in GCs.

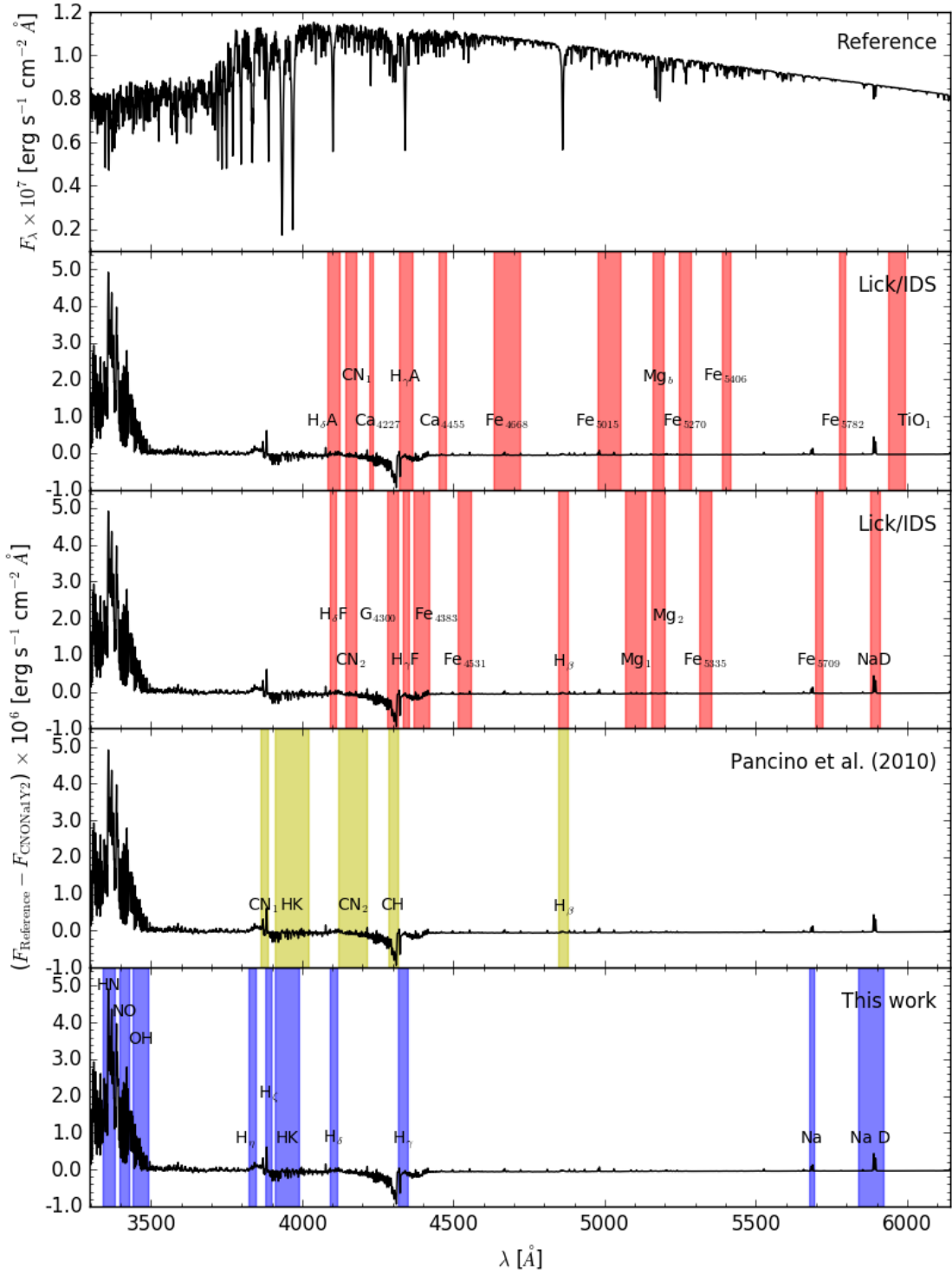


Figure 4.1: Bandpasses of all spectral indices used in this work over the difference in flux from a CNONa1Y2 spectrum with respect to one of Reference at  $T_{\text{eff}} = 6,000$  K and  $\log g = 4.2$ . Upper panel shows only the Reference spectra. The rest of the panels show the bandpasses of each index. The origin of the definition is indicated in each panel. The indices of the Lick/IDS system are shown in two panels for more clarity.

Table 4.3: Errors calculated by using a Monte Carlo technique for a spectra at  $T = 6,000$  K and  $\log g = 4.2$ .

| Indices   | Name                            | Error, $\sigma$         |                         |                         |                         |
|-----------|---------------------------------|-------------------------|-------------------------|-------------------------|-------------------------|
|           |                                 | Reference               | CNONa1Y2                | CNONa1Y4                | CNONa2Y2                |
| Lick/IDS  | CN <sub>1</sub>                 | $7.9723 \times 10^{-5}$ | $8.9713 \times 10^{-5}$ | $8.1100 \times 10^{-5}$ | $8.2707 \times 10^{-5}$ |
|           | CN <sub>2</sub>                 | $8.1413 \times 10^{-5}$ | $7.8626 \times 10^{-5}$ | $7.3383 \times 10^{-5}$ | $7.8616 \times 10^{-5}$ |
|           | Ca4227                          | $1.4742 \times 10^{-3}$ | $1.3309 \times 10^{-3}$ | $1.5066 \times 10^{-3}$ | $1.6612 \times 10^{-3}$ |
|           | G4300                           | $2.3036 \times 10^{-3}$ | $2.4152 \times 10^{-3}$ | $2.7074 \times 10^{-3}$ | $2.8049 \times 10^{-3}$ |
|           | Fe4383                          | $3.2638 \times 10^{-3}$ | $2.8271 \times 10^{-3}$ | $3.0330 \times 10^{-3}$ | $3.1781 \times 10^{-3}$ |
|           | Ca4455                          | $2.1776 \times 10^{-3}$ | $2.0091 \times 10^{-3}$ | $2.0738 \times 10^{-3}$ | $2.1122 \times 10^{-3}$ |
|           | Fe4531                          | $3.0794 \times 10^{-3}$ | $2.5013 \times 10^{-3}$ | $2.7180 \times 10^{-3}$ | $2.9759 \times 10^{-3}$ |
|           | Fe4668                          | $4.2344 \times 10^{-3}$ | $4.5752 \times 10^{-3}$ | $4.4150 \times 10^{-3}$ | $4.8870 \times 10^{-3}$ |
|           | H <sub><math>\beta</math></sub> | $2.3090 \times 10^{-3}$ | $2.5721 \times 10^{-3}$ | $2.0454 \times 10^{-3}$ | $1.8914 \times 10^{-3}$ |
|           | Fe5015                          | $4.3093 \times 10^{-3}$ | $4.2872 \times 10^{-3}$ | $3.8886 \times 10^{-3}$ | $4.3841 \times 10^{-3}$ |
|           | Mg <sub>1</sub>                 | $6.9959 \times 10^{-5}$ | $6.7869 \times 10^{-5}$ | $6.2557 \times 10^{-5}$ | $6.7108 \times 10^{-5}$ |
|           | Mg <sub>2</sub>                 | $7.6102 \times 10^{-5}$ | $7.6915 \times 10^{-5}$ | $8.5274 \times 10^{-5}$ | $8.0629 \times 10^{-5}$ |
|           | Mg <sub>b</sub>                 | $2.7058 \times 10^{-3}$ | $2.3174 \times 10^{-3}$ | $2.5618 \times 10^{-3}$ | $2.5611 \times 10^{-3}$ |
|           | Fe5270                          | $3.0959 \times 10^{-3}$ | $2.9845 \times 10^{-3}$ | $3.0983 \times 10^{-3}$ | $2.8621 \times 10^{-3}$ |
|           | Fe5335                          | $3.0851 \times 10^{-3}$ | $3.2904 \times 10^{-3}$ | $3.0752 \times 10^{-3}$ | $3.2750 \times 10^{-3}$ |
|           | Fe5406                          | $2.4098 \times 10^{-3}$ | $2.5108 \times 10^{-3}$ | $2.3543 \times 10^{-3}$ | $2.4750 \times 10^{-3}$ |
|           | Fe5709                          | $2.3438 \times 10^{-3}$ | $2.6867 \times 10^{-3}$ | $2.3882 \times 10^{-3}$ | $2.4760 \times 10^{-3}$ |
|           | Fe5782                          | $2.1928 \times 10^{-3}$ | $2.0722 \times 10^{-3}$ | $2.0761 \times 10^{-3}$ | $2.0982 \times 10^{-3}$ |
|           | Na D                            | $2.6875 \times 10^{-3}$ | $2.8683 \times 10^{-3}$ | $3.0379 \times 10^{-3}$ | $2.8872 \times 10^{-3}$ |
| CH/CN     | TiO <sub>1</sub>                | $7.8133 \times 10^{-5}$ | $7.4367 \times 10^{-5}$ | $8.2370 \times 10^{-5}$ | $7.7413 \times 10^{-5}$ |
|           | H $\delta_A$                    | $2.3470 \times 10^{-3}$ | $2.6211 \times 10^{-3}$ | $2.4240 \times 10^{-3}$ | $2.3811 \times 10^{-3}$ |
|           | H $\gamma_A$                    | $3.0218 \times 10^{-3}$ | $2.8148 \times 10^{-3}$ | $3.3783 \times 10^{-3}$ | $3.2327 \times 10^{-3}$ |
|           | H $\delta_F$                    | $1.9030 \times 10^{-3}$ | $2.0013 \times 10^{-3}$ | $2.0437 \times 10^{-3}$ | $2.1012 \times 10^{-3}$ |
|           | H $\gamma_F$                    | $2.1107 \times 10^{-3}$ | $1.7637 \times 10^{-3}$ | $1.8812 \times 10^{-3}$ | $1.7225 \times 10^{-3}$ |
|           | CN3839                          | $1.0982 \times 10^{-4}$ | $1.2109 \times 10^{-4}$ | $1.0097 \times 10^{-4}$ | $1.0950 \times 10^{-4}$ |
|           | CN4142                          | $5.7277 \times 10^{-5}$ | $5.5162 \times 10^{-5}$ | $5.6452 \times 10^{-5}$ | $5.6902 \times 10^{-5}$ |
|           | CH4300                          | $7.6479 \times 10^{-5}$ | $6.8813 \times 10^{-5}$ | $8.1769 \times 10^{-5}$ | $7.4036 \times 10^{-5}$ |
|           | HK <sub>1</sub>                 | $4.1308 \times 10^{-5}$ | $3.8062 \times 10^{-5}$ | $3.6680 \times 10^{-5}$ | $3.8161 \times 10^{-5}$ |
|           | H <sub><math>\beta</math></sub> | $1.2438 \times 10^{-4}$ | $1.1822 \times 10^{-4}$ | $1.1650 \times 10^{-4}$ | $1.3340 \times 10^{-4}$ |
| This work | NH                              | $5.9458 \times 10^{-5}$ | $6.2270 \times 10^{-5}$ | $6.1807 \times 10^{-5}$ | $5.8023 \times 10^{-5}$ |
|           | NO                              | $7.1290 \times 10^{-5}$ | $6.6552 \times 10^{-5}$ | $6.4180 \times 10^{-5}$ | $6.3968 \times 10^{-5}$ |
|           | OH                              | $5.7059 \times 10^{-5}$ | $5.9965 \times 10^{-5}$ | $5.6625 \times 10^{-5}$ | $6.0675 \times 10^{-5}$ |
|           | H $_{\eta}$                     | $7.7215 \times 10^{-5}$ | $7.8727 \times 10^{-5}$ | $8.6556 \times 10^{-5}$ | $7.7052 \times 10^{-5}$ |
|           | H $_{\zeta}$                    | $5.7195 \times 10^{-5}$ | $5.6736 \times 10^{-5}$ | $5.4077 \times 10^{-5}$ | $4.8632 \times 10^{-5}$ |
|           | HK <sub>2</sub>                 | $7.4173 \times 10^{-5}$ | $8.7431 \times 10^{-5}$ | $9.2496 \times 10^{-5}$ | $8.8014 \times 10^{-5}$ |
|           | H $_{\delta}$                   | $1.1291 \times 10^{-4}$ | $9.0598 \times 10^{-5}$ | $1.1602 \times 10^{-4}$ | $1.1371 \times 10^{-4}$ |
|           | H $_{\gamma}$                   | $6.9576 \times 10^{-5}$ | $7.2392 \times 10^{-5}$ | $6.4923 \times 10^{-5}$ | $7.4744 \times 10^{-5}$ |
|           | Na                              | $1.0043 \times 10^{-4}$ | $9.9510 \times 10^{-5}$ | $1.1583 \times 10^{-4}$ | $1.0158 \times 10^{-4}$ |
|           | Na D                            | $1.4083 \times 10^{-4}$ | $1.2014 \times 10^{-4}$ | $1.3347 \times 10^{-4}$ | $1.4550 \times 10^{-4}$ |

Up to this point, we have a set of 39 spectral indices calculated for each of the 3,742 theoretical spectra that we can analyze under the combination of certain physical parameters such as the effective temperature, surface gravity and chemical composition in order to select what indices or combination of them are the best in the identification of multiple stellar populations in GCs. In Section 5.1 of the next Chapter, we present an analysis of the effect of the effective temperature of each index for a typical surface gravity of MS stars, and in Section 5.2, we show a selection of the more promising indices for the detection of different stellar populations on three different evolutionary stages of M3.



# Chapter 5

## Results

In the previous Chapter, we computed 39 spectroscopic indices: 24 from the Lick/IDS system, 5 from [Pancino et al. \(2010\)](#) and 10 defined in this thesis, for all the synthetic spectra that compose the large library on which this work is based. In this Chapter, we describe the properties of these indices and pick out the most promising combinations of indices for distinguishing among the different stellar populations in distinct stellar evolutionary phases found in GCs. In our theoretical approach, this means to single out the indices that better disentangle the four chemical mixtures defined by [Sbordone et al. \(2011\)](#). The authors consider the Reference metal-poor  $\alpha$ -enhanced metal mixture as representative of the First Generation of stars in a GC, while the other three chemical compositions (CNONa1Y2, CNONa1Y4 and CNONa2Y2) are possible cases for a Second Generation of stars.

### 5.1 Global properties of the spectroscopic indices.

In order to illustrate the behavior of the spectroscopic indices as a function of the main atmospheric parameters, we first present the results for models with fixed surface gravity  $\log g = 4.2$ , a typical value for solar-like MS stars. Figures 5.1 and 5.2 show the indices of Lick/IDS system calculated for the four chemical mixtures; this set of indices is divided in two parts for a better appreciation according to the Table 4.1: Part A includes indices 1 to 12 while Part B includes the remaining indices, 13 to 25, but excluding the index 21, that corresponds to the  $\text{TiO}_2$ , as it lies out of the wavelength range used in this study.

Except for the hydrogen lines, the indices values show a decrement with  $T_{\text{eff}}$ , because either these chemical species tend to be destroyed as the temperature increases or the lower level of the electronic transition becomes less populated. Conversely, the values of the indices of hydrogen follow their natural trend of the Balmer lines that steadily increase in strength up to a maximum attained at temperatures of about 10,000 K (spectral type A).

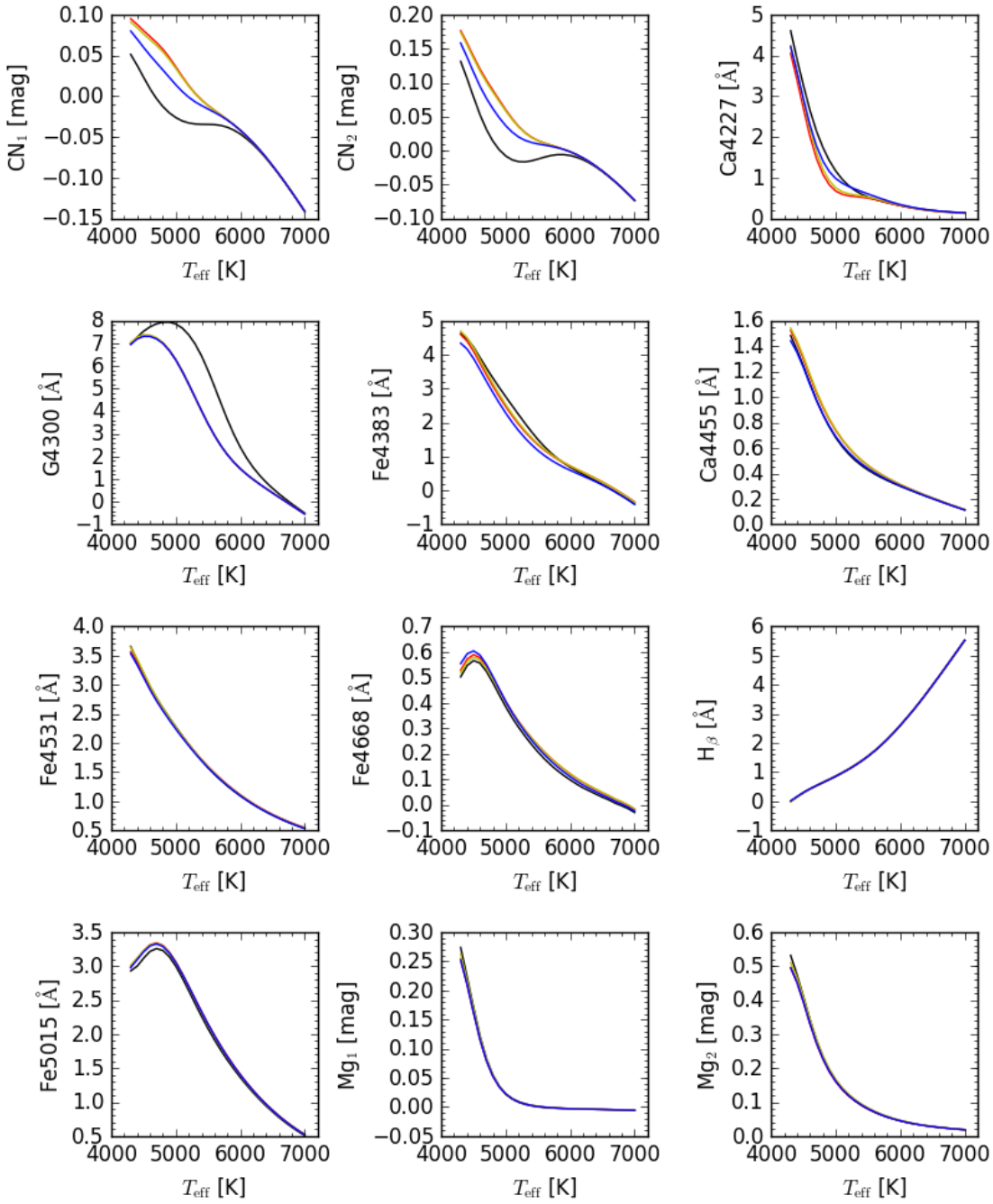


Figure 5.1: Indices from Lick/IDS system (Part A) for the four chemical compositions: Reference (black line), CNONa1Y2 (red line), CNONa1Y4 (yellow line) and CNONa2Y2 (blue line) as a function of effective temperature for a fixed surface gravity  $\log g = 4.2$ .

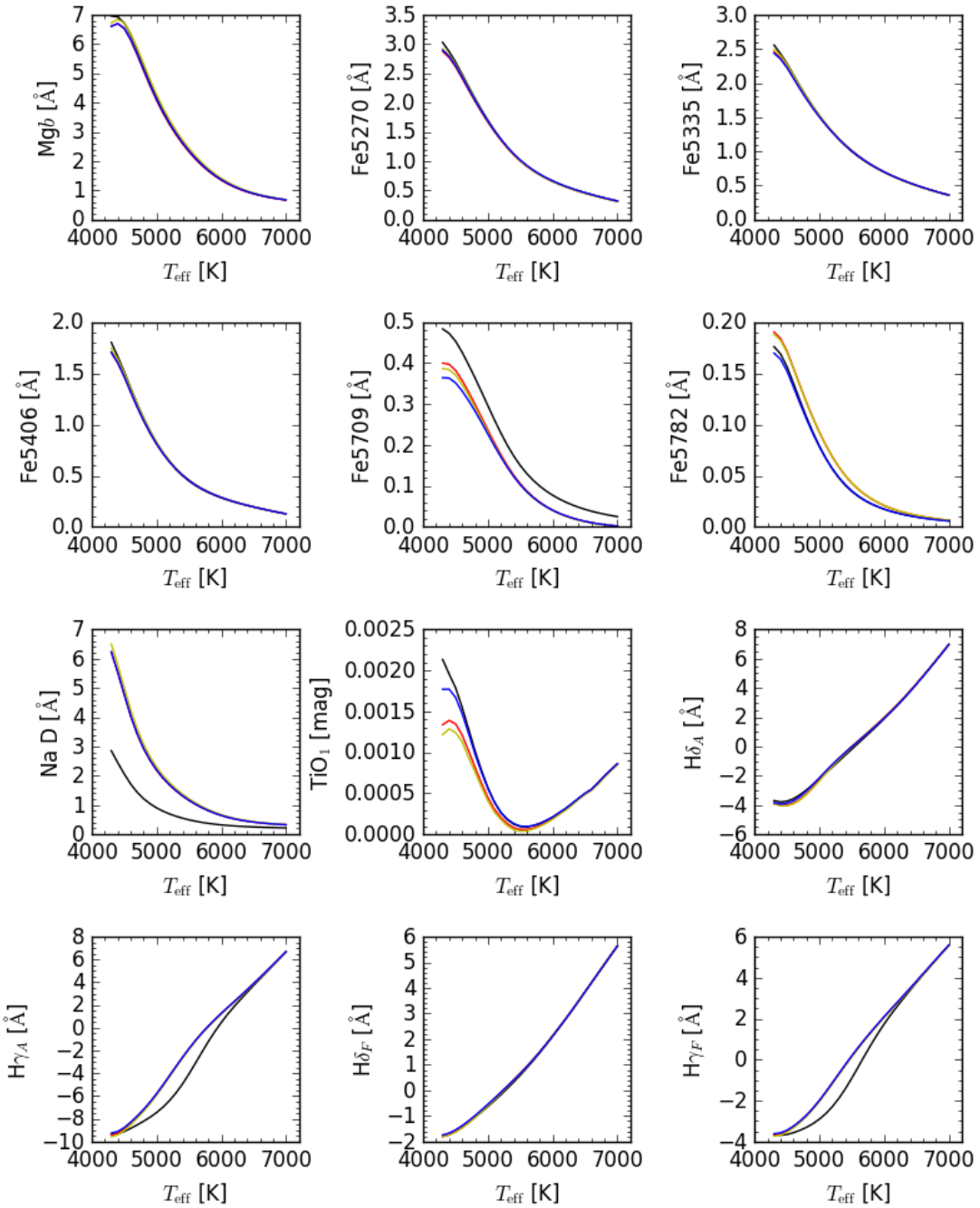


Figure 5.2: As in Figure 5.1 but the Part B of the Lick/IDS indices.

We can see, by a direct visual inspection of Figures 5.1 and 5.2, that the value of many indices is quite different between the Reference chemical composition and the other mixtures, at least over a  $T_{\text{eff}}$  interval. In some cases, it is only evident the separation between the First (black line) and the Second (all other colors) Generation of stars; however, in a few cases, the indices are able to separate among the chemical mixtures of the Second Generation. In order to emphasize the dependence of the indices

with the chemical composition, Figures 5.3 and 5.4 show the differences between the three modified chemical compositions with respect to the Reference abundance.

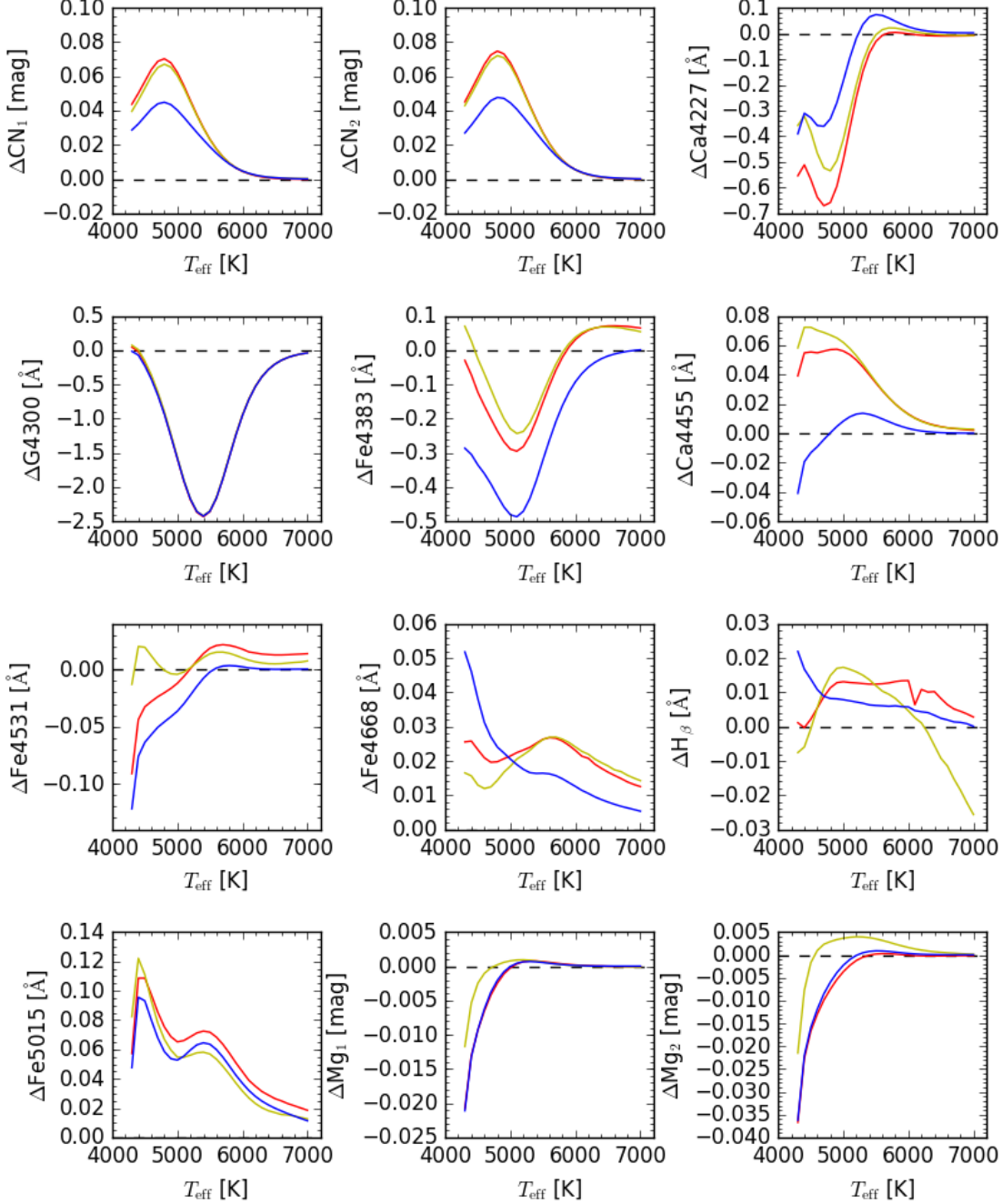


Figure 5.3: Difference between the Lick/IDS indices (Part A) of the chemical composition CNONa1Y2 (red line), CNONa1Y4 (yellow line) and CNONa2Y2 (blue line) with respect to the Reference abundance as a function of effective temperature for a fixed surface gravity  $\log g = 4.2$ .

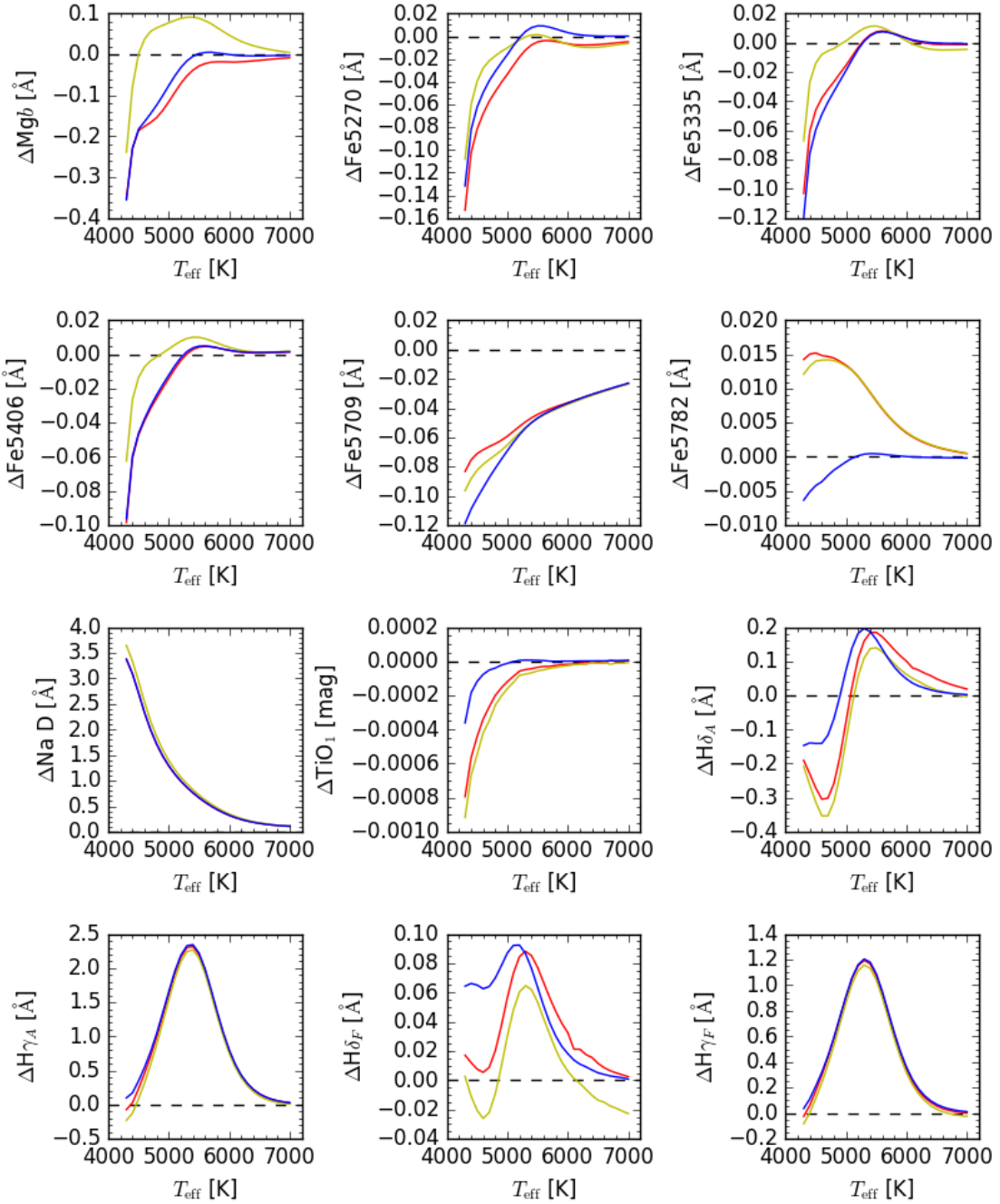


Figure 5.4: As in Figure 5.3 but the Part B of the Lick/IDS indices.

Similar to Figures 5.1 and 5.2, Figure 5.5 presents the indices calculated from Pancino et al. (2010) (first 5 panels from the upper left) along with the defined in this work (the remaining 10 panels) for the four different chemical abundances as a function of  $T_{\text{eff}}$  for a fixed surface gravity  $\log g = 4.2$ , while Figure 5.6 shows the differences between the indices of the three modified chemical compositions with respect to the Reference abundance.

The Lick indices  $\text{CN}_1$  and  $\text{CN}_2$  in Figure 5.3 have larger values in Second Generation stars, such as  $\text{CNO}\text{Na}1\text{Y}2$  ( $Y = 0.246$ ) and  $\text{CNO}\text{Na}1\text{Y}4$  ( $Y = 0.400$ ), due to N enrichment. The main difference between these two mixtures is the He content, but, as we can note, for these indices it is not relevant, since they display a very similar behavior.  $\text{CNO}\text{Na}2\text{Y}2$  ( $Y = 0.246$ ) exhibits a similar pattern but its difference with respect to the Reference abundance is lower because the N content is lower than in  $\text{CNO}\text{Na}1\text{Y}2$  ( $Y = 0.246$ ) and  $\text{CNO}\text{Na}1\text{Y}4$  ( $Y = 0.400$ ). A similar behavior is shown by  $\text{CN}3839$  and  $\text{CN}4142$ , from [Pancino et al. \(2010\)](#) (Figure 5.6). However, these indices (all measuring the CN molecule) can only differentiate between stars with  $T_{\text{eff}} \lesssim 6,200$  K, as for hotter stars the cyanogen disappears. The differences are stronger at  $T_{\text{eff}}$  around 4,800 K.

In this work, we define two indices containing nitrogen: NH (imidogen) and NO (nitric oxide). They exhibit a similar behavior like  $\text{CN}_1$ ,  $\text{CN}_2$ ,  $\text{CN}3839$  and  $\text{CN}4142$ , i.e. a good separation between First and Second Generation populations at  $T_{\text{eff}} \lesssim 6,200$  K is displayed (Figure 5.5). However, the NH index shows a better separation between populations over practically the whole range of effective temperature ( $4,300 \leq T_{\text{eff}} \leq 6,800$  K). Again, the He content has not relevant effect on the nitrogen indices: the  $\text{CNO}\text{Na}1\text{Y}2$  ( $Y = 0.246$ ) and  $\text{CNO}\text{Na}1\text{Y}4$  ( $Y = 0.400$ ) curves are practically identical. The small difference of the NO index between populations is due to combination of N-enrichment and O-depletion in the input chemical compositions, but N dominates over O because N has an enrichment of 1.8 dex while O has a depletion of -0.8 dex with respect to the Reference mixture.

Other interesting indices are those that measure the G band, produced by CH, as this molecular band has been used to identify multiple stellar populations ([Kayser et al. 2008](#); [Pancino et al. 2010](#)). In the Lick/IDS system the index is called G4300, while its name is CH4300 in [Pancino et al. \(2010\)](#), being the bandpass slightly narrower for the CH4300 index (see Table 4.1 and Equation 4.6). They are shown in Figures 5.1 and 5.5, respectively, and they obviously display a similar behavior. The difference between these indices for First and Second Generation stars can be observed in Figures 5.3 and 5.6, respectively. The CH indices distinguish very well between stellar populations of First and Second Generation in practically all range of effective temperature used in this work, with a maximum separation around 5,150 K, however, it can not differentiate among populations of Second Generation. The value of the CH index for the Reference abundance is larger than those of Second Generation stars due to the depletion of C (-0.6 dex), and it is easy to identify, specially at  $T_{\text{eff}} \sim 5,150$  K.

Another anticorrelation that exists among multiple stellar population in GCs is the Na-O one (e.g. [Carretta et al. 2006, 2009](#); [Lee 2010](#); [Gratton et al. 2015](#)). We computed indices that are sensitive to the Na content. For the case of the Na D index

(Figure 5.2), we can observe a clear differentiation between populations of First and Second Generation at low temperature ( $T_{\text{eff}} \lesssim 6,000$  K); nevertheless, this index is quite similar for mixtures of the Second Generation. In this work, we defined two indices for Na: one similar to Na D and a new one, Na (see Figure 5.5). The behavior of our Na D index with respect to effective temperature is similar to that defined in the Lick/IDS system. On the other hand, our Na index presents a good separation between stellar populations of First and Second Generation throughout the effective temperature range as can be observed in Figure 5.6. However, these Na lines are quite weak and, in an observed spectra, could not be well detected unless for a high S/N. With respect to oxygen, we defined the index OH to evaluate the possibility to identify stellar populations. We can not use the NO index for this purpose because the N-enrichment (1.8 dex) dominates over the O-depletion (-0.6 dex). The O depletion is evident in Figure 5.5 at  $T_{\text{eff}} \lesssim 6,500$  but the difference among populations of Second Generation is not clear.

As can be observed in Figures 5.1 and 5.2, the hydrogen lines are very sensitive to change in effective temperature, and some indices appear to be good candidates for identifying multiple stellar populations in GCs. For instance, the  $H\gamma$  indices of the Lick/IDS system display significant differences in the effective temperature interval  $4,800 \text{ K} < T_{\text{eff}} < 6,200 \text{ K}$  (Figure 5.4) between First and Second Generation stars with a maximum separation around 5,300 K; however, it is not possible to distinguish between enriched/depleted stellar populations, similarly to what happens with the CH indices. In the case of the hydrogen indices that we defined and the  $H_\beta$  from [Pancino et al. \(2010\)](#) (Figure 5.5), the sensitivity is less pronounced.

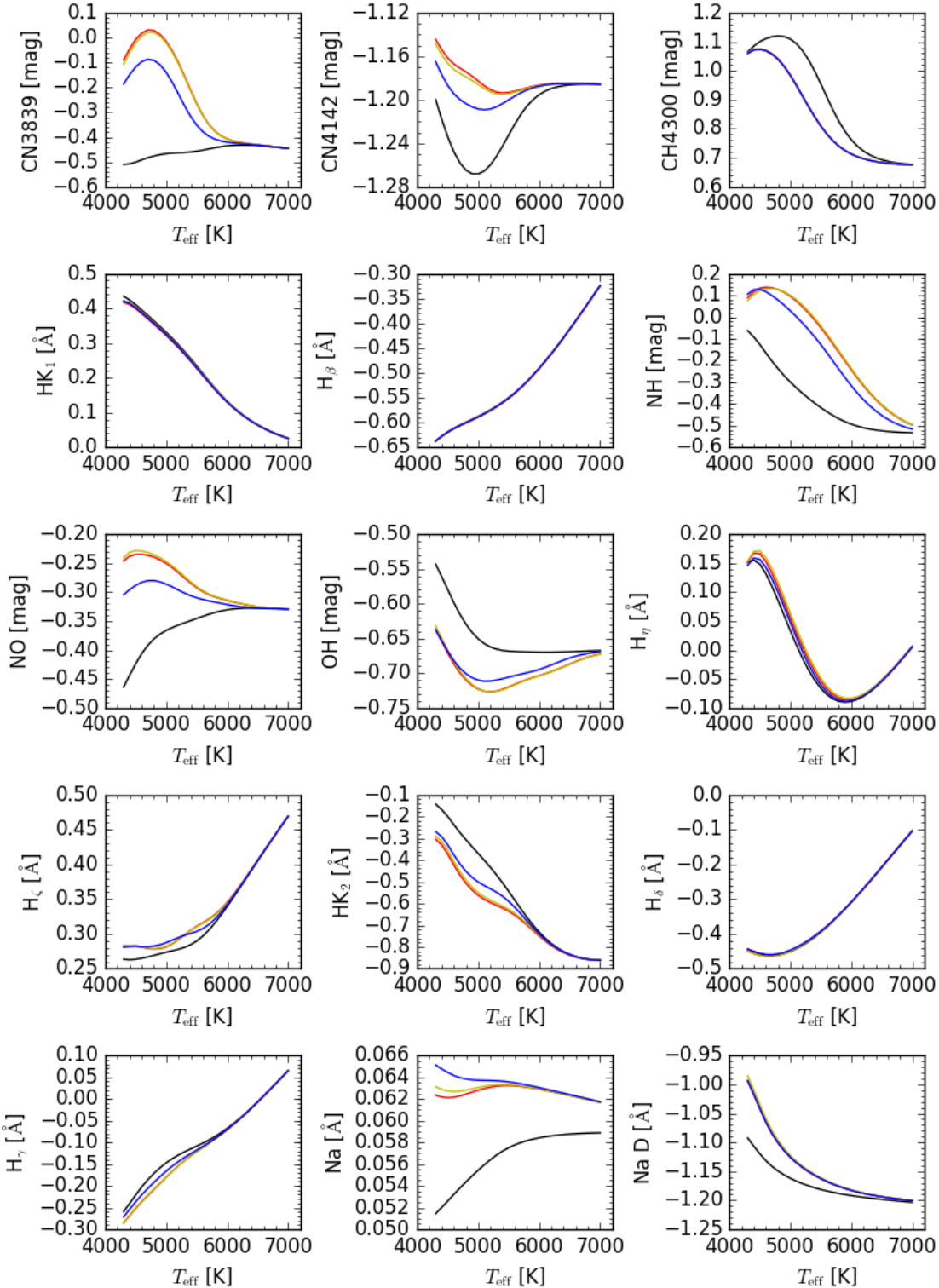


Figure 5.5: Indices from Pancino et al. (2010) and the defined in this work for the four chemical compositions: Reference (black line), CNONa1Y2 (red line), CNONa1Y4 (yellow line) and CNONa2Y2 (blue line) as a function of effective temperature for a fixed surface gravity  $\log g = 4.2$ .

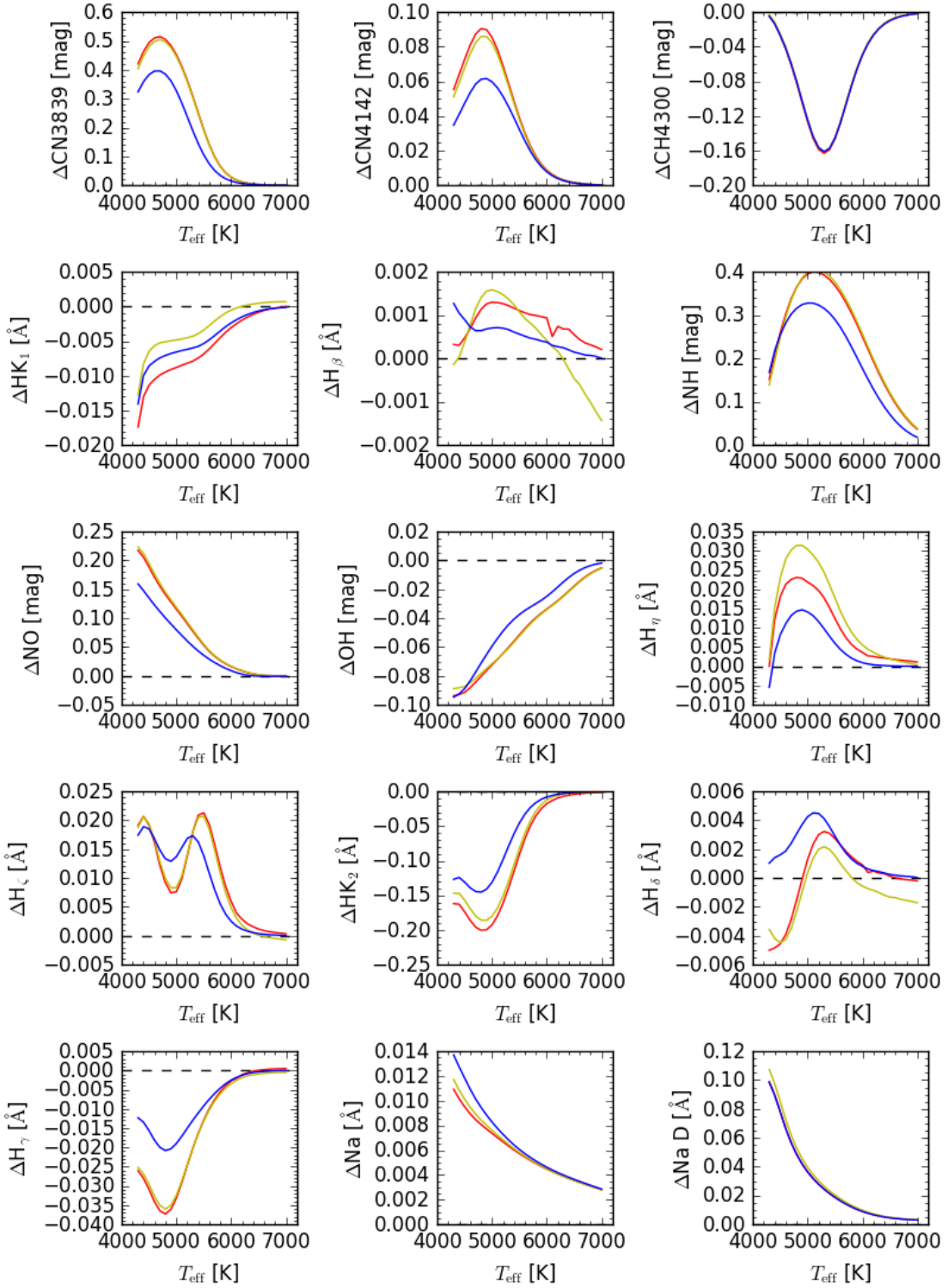


Figure 5.6: Difference between the indices from Pancino et al. (2010) and the defined in this work of the chemical composition CNONa1Y2 (red line), CNONa1Y4 (yellow line) and CNONa2Y2 (blue line) with respect to the Reference abundance as a function of effective temperature for a fixed surface gravity  $\log g = 4.2$ .

## 5.2 Suitable indices for identifying multiple population in M3

The analysis of the spectral indices that we illustrated in the previous section provides qualitative indications on which indices are the most promising for identifying and separating among different stellar populations. However, a more quantitative study can be carried out by considering the *Throw* (see Equation 4.11) of each index, since it gives the difference between the values of one index for two different chemical compositions in units of the typical errors.

We consider here the indices computed for atmospheric parameters appropriate for three evolutionary stages of M3: MS-TO, RGB and HB. These parameters are reported in Table 5.1 and highlighted in the CMD of M3 of the Figure 5.7. These regions were used to define a stellar sample for observing with The Gran Telescopio CANARIAS from [Ferraro et al. \(1997\)](#) catalog and corroborated with the Gaia catalog ([Gaia-Collaboration et al. 2016](#)) (for more details see Chapter 6.)

Table 5.1: Adopted parameters of different evolutionary stages defined in the CMD of M3.

| Region            | Range in V-mag | Range (B-V) | Range in $T_{\text{eff}}$ | $\log g$ (average) |
|-------------------|----------------|-------------|---------------------------|--------------------|
| Main Sequence     | 19.2 - 19.8    | 0.35 - 0.60 | 5,400 - 6,500             | 4.2                |
| Turn off          | 18.5 - 19.2    | 0.36 - 0.61 | 5,400 - 6,500             | 4.2                |
| Red Giant Branch  | 15.5 - 17.0    | 0.69 - 0.82 | 4,800 - 5,300             | 2.4 <sup>1</sup>   |
| Horizontal Branch | 15.5 - 16.1    | 0.30 - 0.61 | 5,400 - 6,800             | 2.8 <sup>2</sup>   |

<sup>1</sup>[Massari et al. \(2016\)](#), <sup>2</sup>[Valcarce et al. \(2016\)](#)

In Appendix B, we include all indices calculated for the three evolutionary stages of M3 described above for all range of effective temperature (4,300 - 7,000 K).

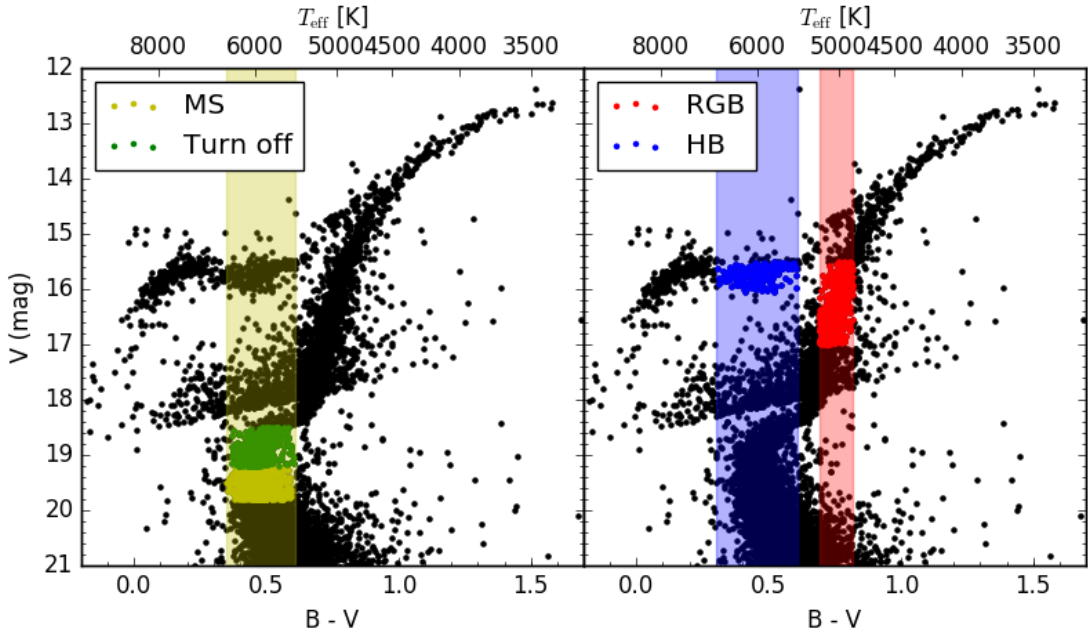


Figure 5.7: Color-magnitude diagram of M3 highlighting the regions defined in Table 5.1. Data extracted from [Ferraro et al. \(1997\)](#) catalog.

Due to its similarity, both Main Sequence and Turn-off regions are joined in one for our purpose. The conversion from  $B - V$  to  $T_{\text{eff}}$  was done using the relation of [Sekiguchi & Fukugita \(2000\)](#) with  $[\text{Fe}/\text{H}] = -1.5$  and surface gravities ( $\log g$ ) of 4.2, 2.4 and 2.8 for the MS-TO, RGB and HB, respectively. We chose an average surface gravity  $\log g = 4.2$  for the MS-TO since it is a typical value for solar-like MS stars, while for the RGB we adopted  $\log g = 2.4$  according to [Massari et al. \(2016\)](#) and, for the HB we used  $\log g = 2.8$  from [Valcarce et al. \(2016\)](#).

We show, in Figures 5.8, 5.9 and 5.10, the *Throw* of all indices, for the three mixtures representing the Second Generation of stars with respect to the Reference chemical composition, as a function of effective temperature. The indices that have the higher *Throw* are, in theory, more suitable for distinguishing multiple populations in M3.

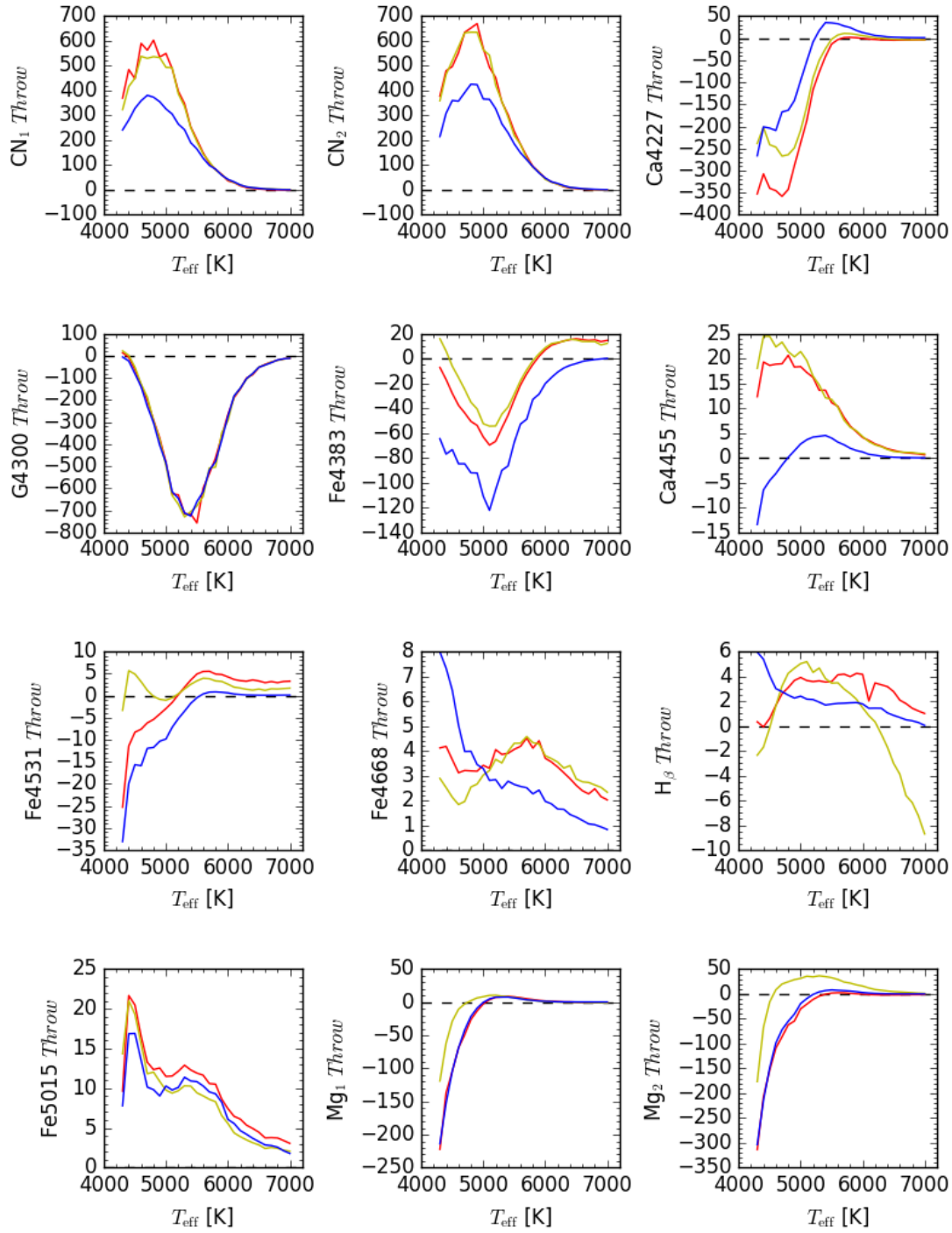


Figure 5.8: *Throw* for Lick/IDS indices (Part A) of the chemical composition CNONa1Y2 (red line), CNONa1Y4 (yellow line) and CNONa2Y2 (blue line) with respect to the Reference abundance as a function of effective temperature for a fixed surface gravity  $\log g = 4.2$ .

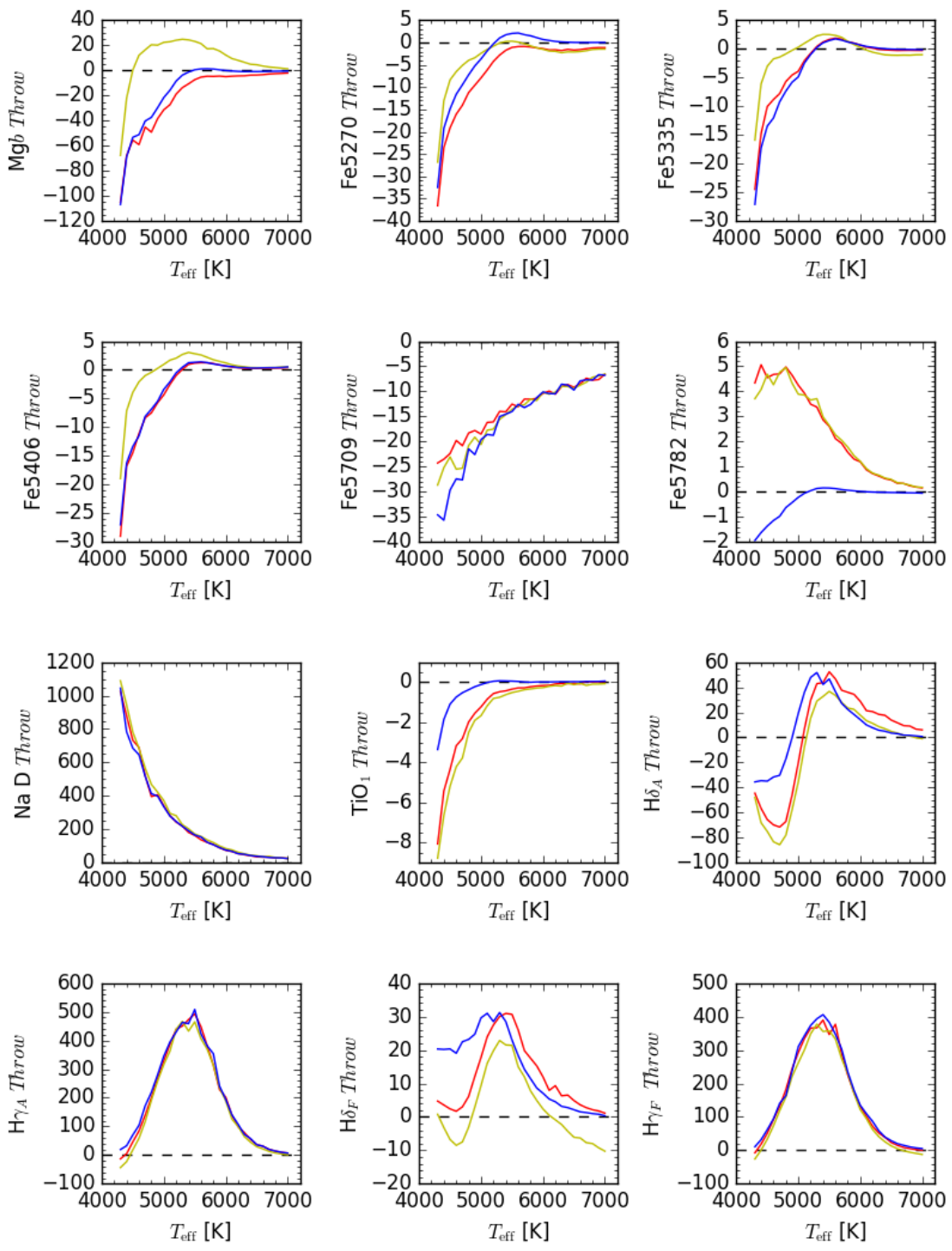


Figure 5.9: As in Figure 5.8 but the Part B of the Lick/IDS indices.

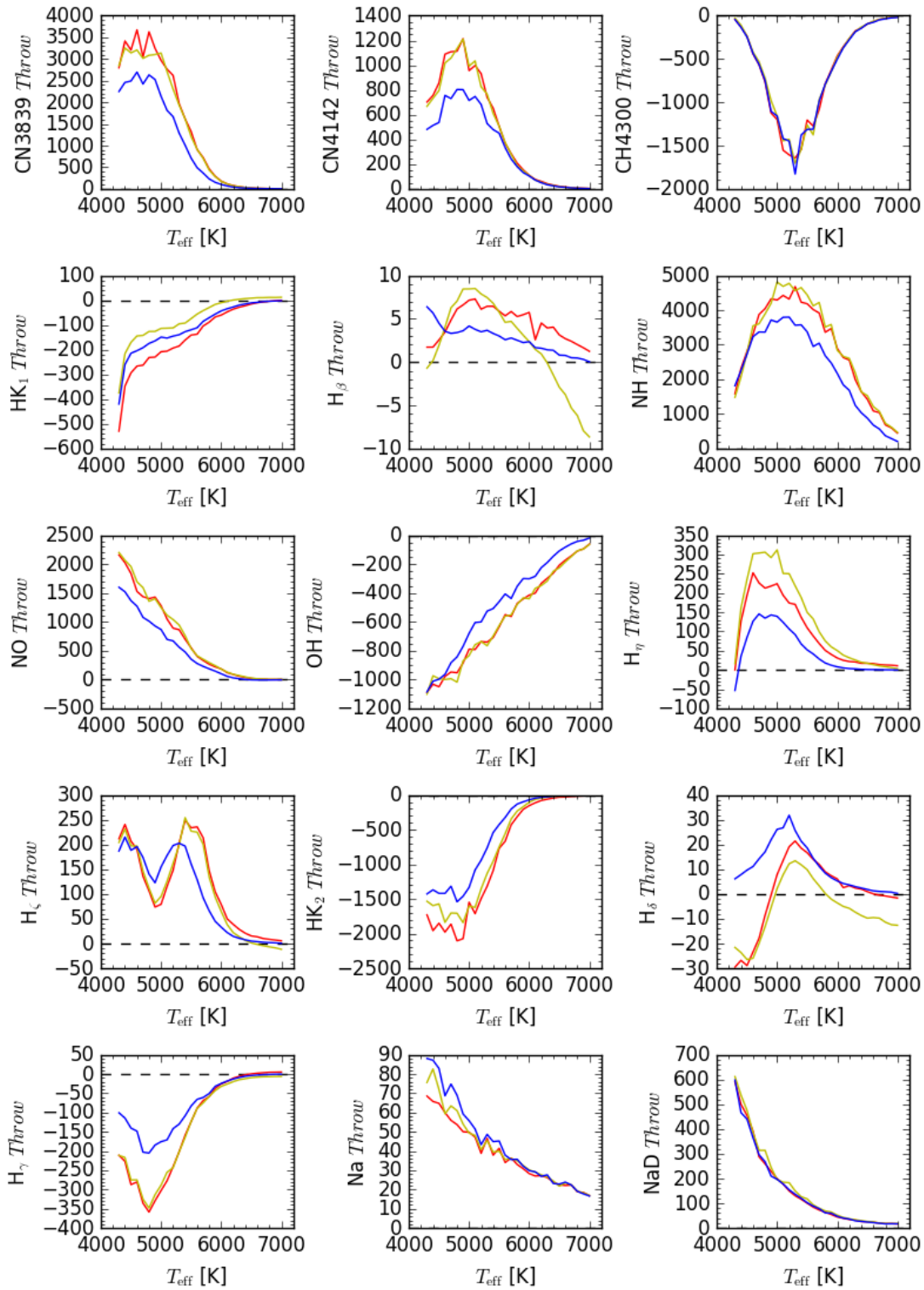


Figure 5.10: *Throw* for Pancino et al. (2010) indices and the defined in this work of the chemical composition CNONa1Y2 (red line), CNONa1Y4 (yellow line) and CNONa2Y2 (blue line) with respect to the Reference abundance as a function of effective temperature for a fixed surface gravity  $\log g = 4.2$ .

### 5.2.1 The Main Sequence

In this section, we apply our set of indices to the MS of M3, according to the definition shown in Table 5.1. In Figure 5.11, we selected and showed the Lick/IDS indices that present the larger differences among the four chemical abundances. CN<sub>1</sub>, CN<sub>2</sub>, NaD, G4300, H $\gamma_A$  and H $\gamma_F$  provide a very large separation between First and Second Generation stars being better at low temperature ( $5,400 < T_{\text{eff}} < 6,200$  K). The last three indices reach  $\text{Throw} \gtrsim 400$ . Nevertheless, their  $\text{Throw}$  is much lower among the three modified chemical compositions, so these indices are the best to differentiate between First and Second Generation stars.

The indices Ca4227, Mg<sub>2</sub>, Mgb, H $\delta_A$  and H $\delta_F$  display an interesting behavior (Figure 5.11), since they allow to distinguish among the three modified abundances of the Second Generation; however, their problem is the much lower  $\text{Throw}$  over the whole range of  $T_{\text{eff}}$  (5,400 - 6,500 K) and the little difference between them. They could be useful for discerning among different stellar populations of Second Generation after having distinguished from those of the First Generation. The index Fe4383 is not as good as the others because it has the disadvantage of not being able to differentiate between the CNONa1Y2 and CNONa1Y4 abundances.

Figure 5.12 shows the most suitable indices among those defined by [Pancino et al. \(2010\)](#) and in this work. As can be observed, the indices CN3839, CN4142, CH4300, NH, NO, OH, H $_\zeta$  and HK<sub>2</sub> have the highest  $\text{Throw}$ , particularly at low effective temperature ( $5,400 < T_{\text{eff}} \lesssim 6,200$  K), but in all of them it is difficult to distinguish between the helium-rich mixture (CNONa1Y4) and the other with the primordial He content (CNONa1Y2). Similarly, but to a lesser extent, are the indices H $_\gamma$ , Na and NaD, that can be considered as alternative indices.

Other interesting indices, in Figure 5.12, are the HK<sub>1</sub>, H $_\eta$  and H $_\delta$  that, unlike the others in this same Figure, show a good separation between the He-enriched abundances and those with  $Y = 0.246$ . Therefore, using an appropriate combination of spectral indices, it is possible to identify MS or TO stars belonging to different stellar populations.

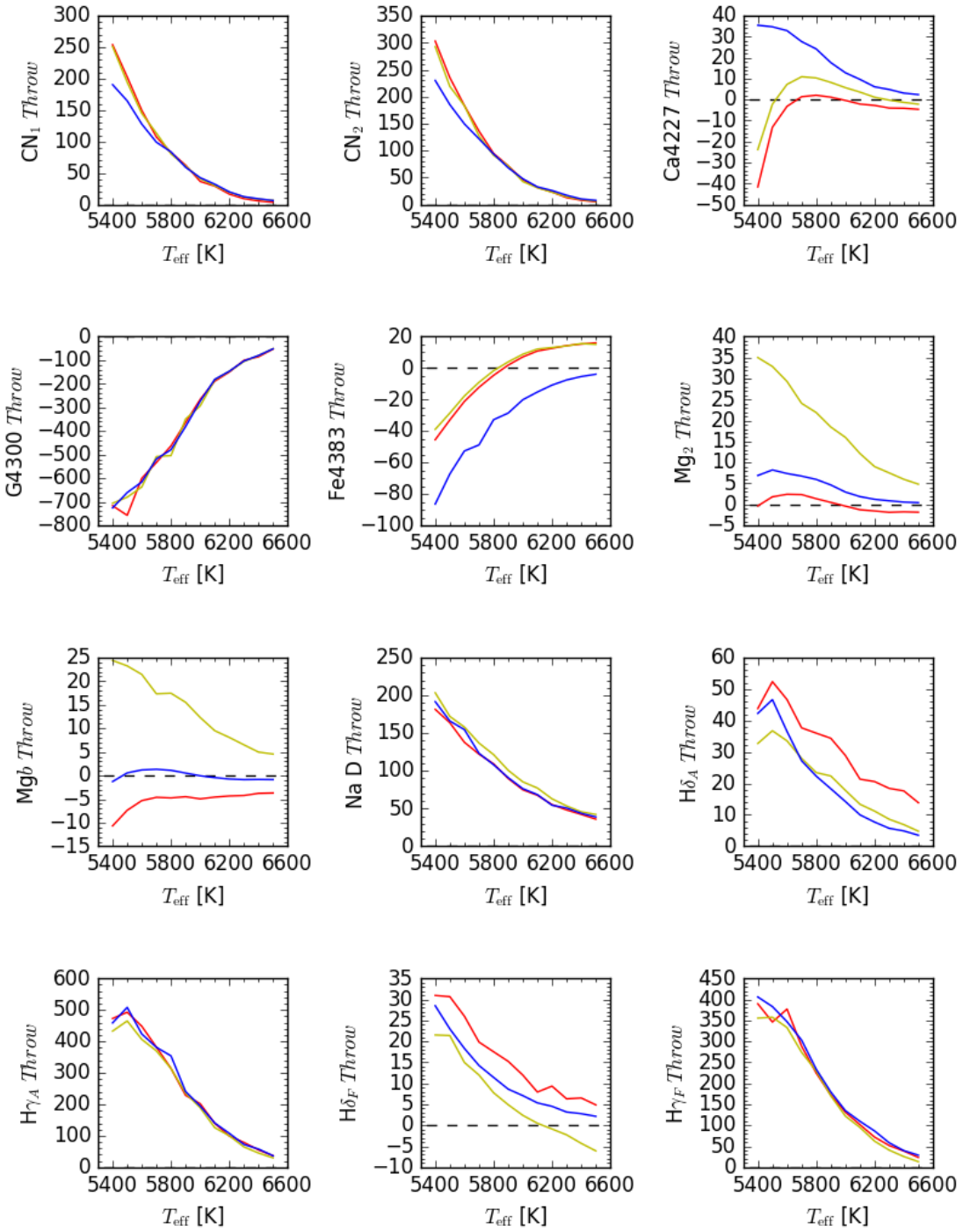


Figure 5.11: *Throw* of the chemical composition: CNONa1Y2 (red line), CNONa1Y4 (yellow line) and CNONa2Y2 (blue line) with respect to the Reference as a function of effective temperature for MS stars considering  $\log g = 4.2$ , calculated with the Lick/IDS system.

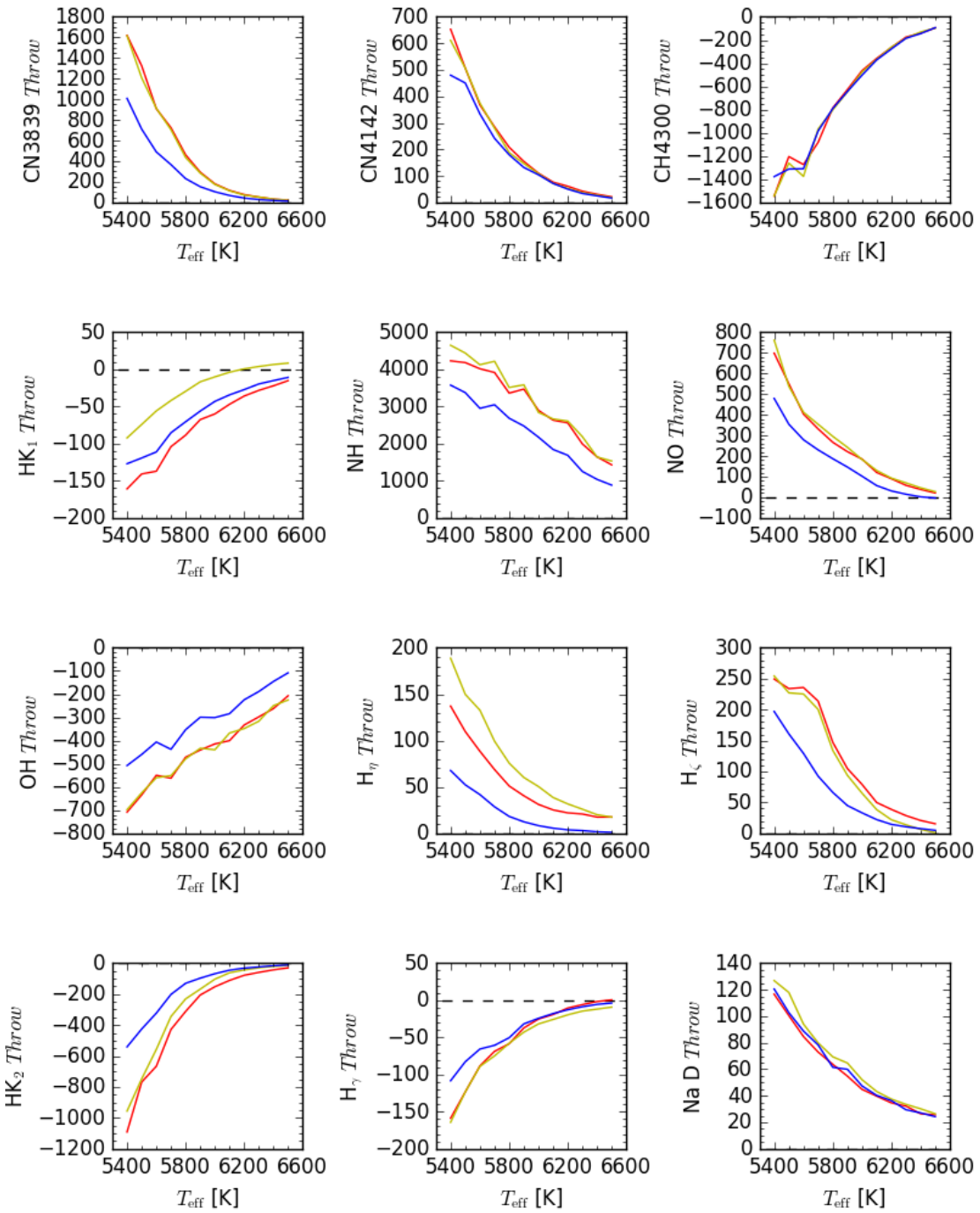


Figure 5.12: *Throw* of the chemical composition: CNONa1Y2 (red line), CNONa1Y4 (yellow line) and CNONa2Y2 (blue line) with respect to the Reference as a function of effective temperature for MS stars considering  $\log g = 4.2$ , calculated with the indices from [Pancino et al. \(2010\)](#) and the defined in this work.

We saw that the chemical mixtures CNONa1Y2 and CNONa1Y4 are only different in the helium content ( $Y = 0.246$  vs.  $Y = 0.400$ , respectively). Most indices have very similar values for these two cases. In order to make clearer which indices are the most sensitive ones for separating between these two chemical compositions, we computed the *Throw* between them and we plotted it in Figures 5.13 and 5.14.

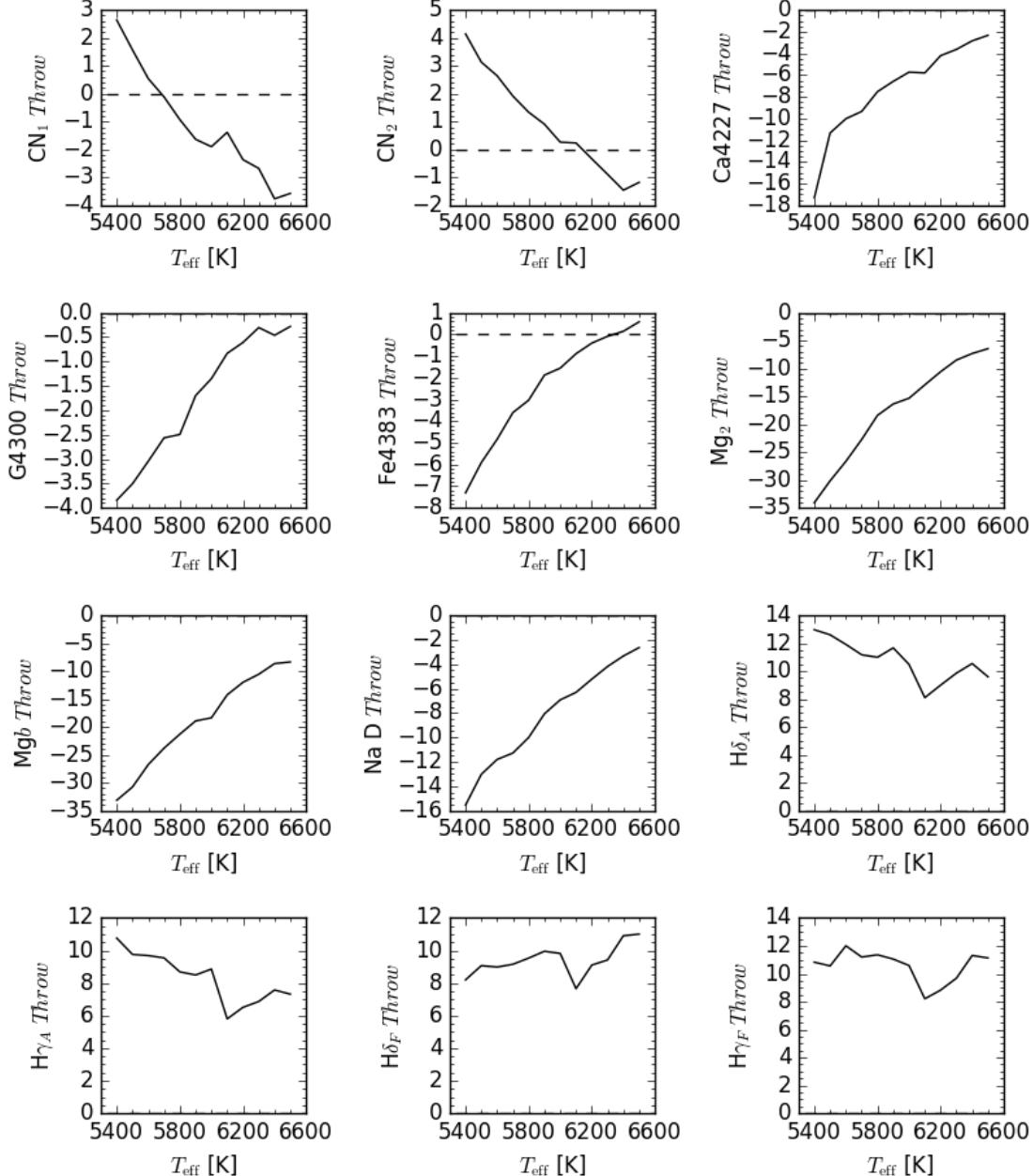


Figure 5.13: *Throw* of the chemical composition CNONa1Y2 with respect to CNONa1Y4 as a function of effective temperature for MS stars considering  $\log g = 4.2$ , calculated with the Lick/IDS system.

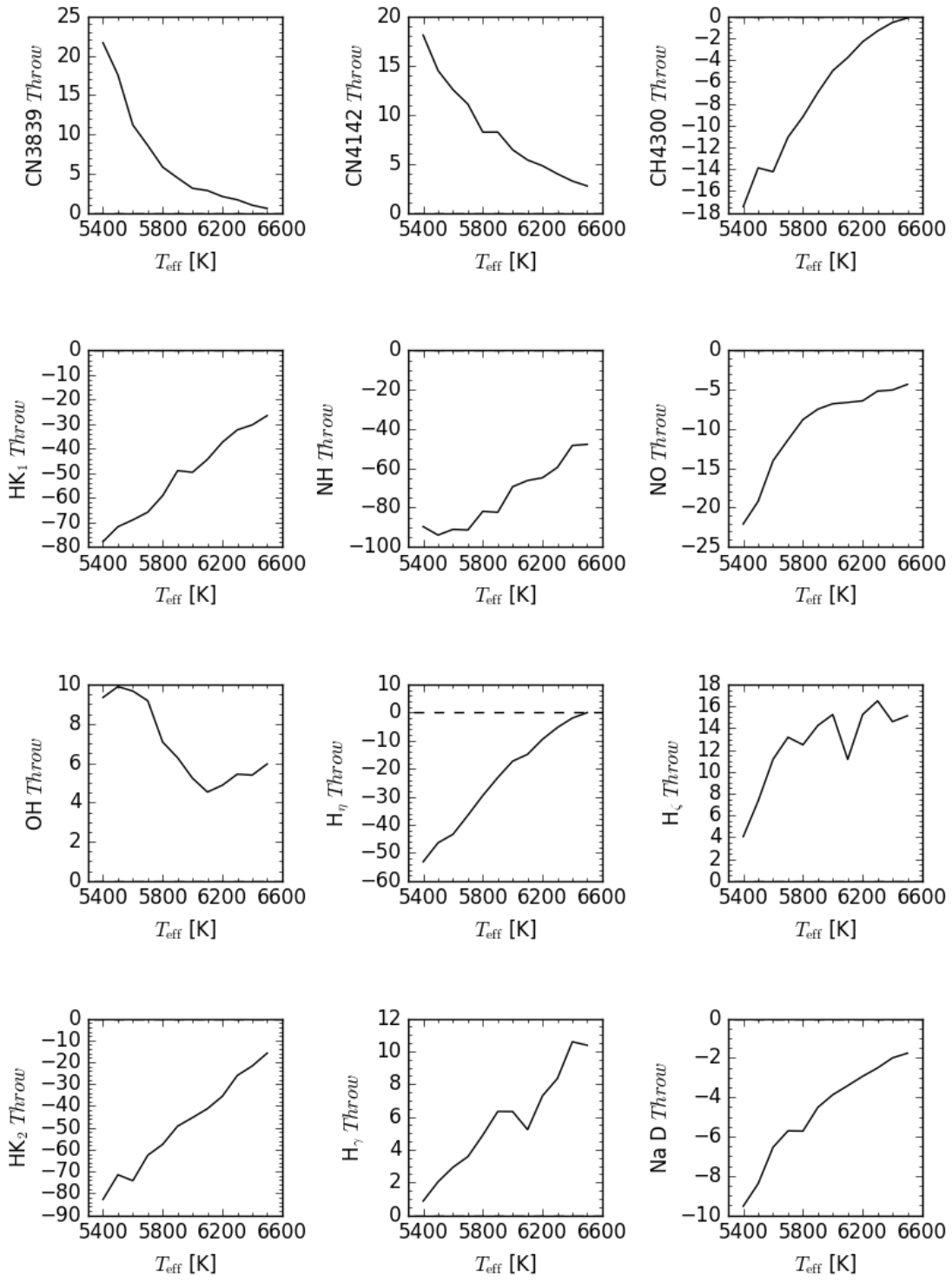


Figure 5.14: *Throw* of the chemical composition CNONa1Y2 with respect to CNONa1Y4 as a function of effective temperature for MS stars considering  $\log g = 4.2$  for the indices from Pancino et al. (2010) and the defined in this work.

As can be observed in Figure 5.13, practically all indices have a very low *Throw*, except for the magnesium indices, as they display the biggest difference at low temperatures ( $T_{\text{eff}} \lesssim 5,800$  K). In Figure 5.14, the indices HK<sub>1</sub>, HK<sub>2</sub> and NH are the most sensitive to the helium content at low temperature.

Although this work is aimed at analyzing the MS of M3, we included two more sections to apply and explore the usefulness of our set of models, theoretical spectra and spectroscopic indices to the RGB and HB [taking also into account that in the GTC observations we obtained the spectra of 3 RGB stars (see Chapter 6)].

## 5.2.2 The Red Giant Branch

For this evolutionary stage, we selected the spectral indices that exhibited the highest *Throw* among chemical abundances, they are displayed in the Figures 5.15 and 5.16. Although the range of effective temperature of the RGB of M3 (see Table 5.1) goes from 4,800 to 5,300 K, in the plots we considered up to the lower limit (4,300 K) to have a more general vision of the index behavior. For stars in the RGB, we assumed a surface gravity  $\log g = 2.4$  (Massari et al. 2016). Figure 5.15 shows the *Throw* of Lick/IDS indices. We observe that the indices of  $\text{CN}_1$  and  $\text{CN}_2$  provide a higher *Throw* than for the MS case because the molecules are more stable at low temperature; this happens for the whole range of effective temperature (4,300 - 5,400 K). However, these indices remain independent of the helium content. The discrepancy of the  $\text{CNO}_{\text{Na}2Y2}$  is due to the content of nitrogen, since it has a different abundance than in the other three mixtures (Reference,  $\text{CNO}_{\text{Na}1Y2}$  and  $\text{CNO}_{\text{Na}1Y4}$ ). The effect of the  $T_{\text{eff}}$  is relevant, therefore these indices are more effective for cooler stars, with a maximum at  $T_{\text{eff}} \sim 4,500$  K, typical effective temperature of a K-type star. The index  $\text{Ca}4227$  exhibits a similar behavior than in case of MS stars (Figure 5.11), but with a negative difference and is more sensitive to the surface gravity.

The index  $\text{G}4300$  in Figure 5.15 or  $\text{CH}4300$  in Figure 5.16 have one of the highest *Throw*, nevertheless, it is only effective to distinguish stars of Second Generation from stars of First Generation, especially at  $T_{\text{eff}} \gtrsim 4,600$  K. The *Throw* of the indices  $\text{Na D}$ ,  $\text{H}\delta_A$  and  $\text{H}\delta_F$  have a similar behavior to the  $\text{G}4300$ , i.e., they do not allow differentiate among stars of Second Generation, also their *Throw* are lower. The indices  $\text{Fe}4383$ ,  $\text{Ca}4455$ ,  $\text{Fe}5431$ ,  $\text{TiO}_1$  and  $\text{H}\gamma_A$  also display some sensitivity to the helium content, but they have a lower *Throw* with respect to other indices (e.g.  $\text{CN}_1$ ,  $\text{CN}_2$ ,  $\text{Ca}4227$ ,  $\text{G}4300$ ). The indices of magnesium ( $\text{Mg}_1$ ,  $\text{Mg}_2$  and  $\text{Mg}_b$ ) present an interesting behavior, they can distinguish between the  $\text{CNO}_{\text{Na}1Y2}$  and  $\text{CNO}_{\text{Na}1Y4}$ , i.e. they are sensitive to the helium content although their *Throw* is not so high. This means that a highly sensitive telescope will be necessary to be able to detect them.

Figure 5.16 shows the indices from (Pancino et al. 2010) and those defined in this work for synthetic spectra representative of RGB stars of M3. Since they measure the same spectral feature, the indices  $\text{CN}3839$  and  $\text{CN}4142$  have a similar behavior than  $\text{CN}_1$  and  $\text{CN}_2$  of the Lick/IDS system (Figure 5.15) and the  $\text{CH}4300$  is similar to  $\text{G}4300$ . All indices in Figure 5.16 are suitable for distinguishing between stellar populations of First and Second Generation, most of them being more effective at the lower temperature. However, they are not very sensitive to helium content, that is, the  $\text{CNO}_{\text{Na}1Y2}$  and  $\text{CNO}_{\text{Na}1Y4}$  mixtures continue to exhibit similar behavior. The best index is the  $\text{NH}$  that we defined, it has a *Throw* higher than 2,500, i.e., it would be easy to detect stellar populations but the problem is that it is defined in the near ultraviolet (bandpass: 3,340 - 3,390 nm), difficult to achieve with optical telescopes.

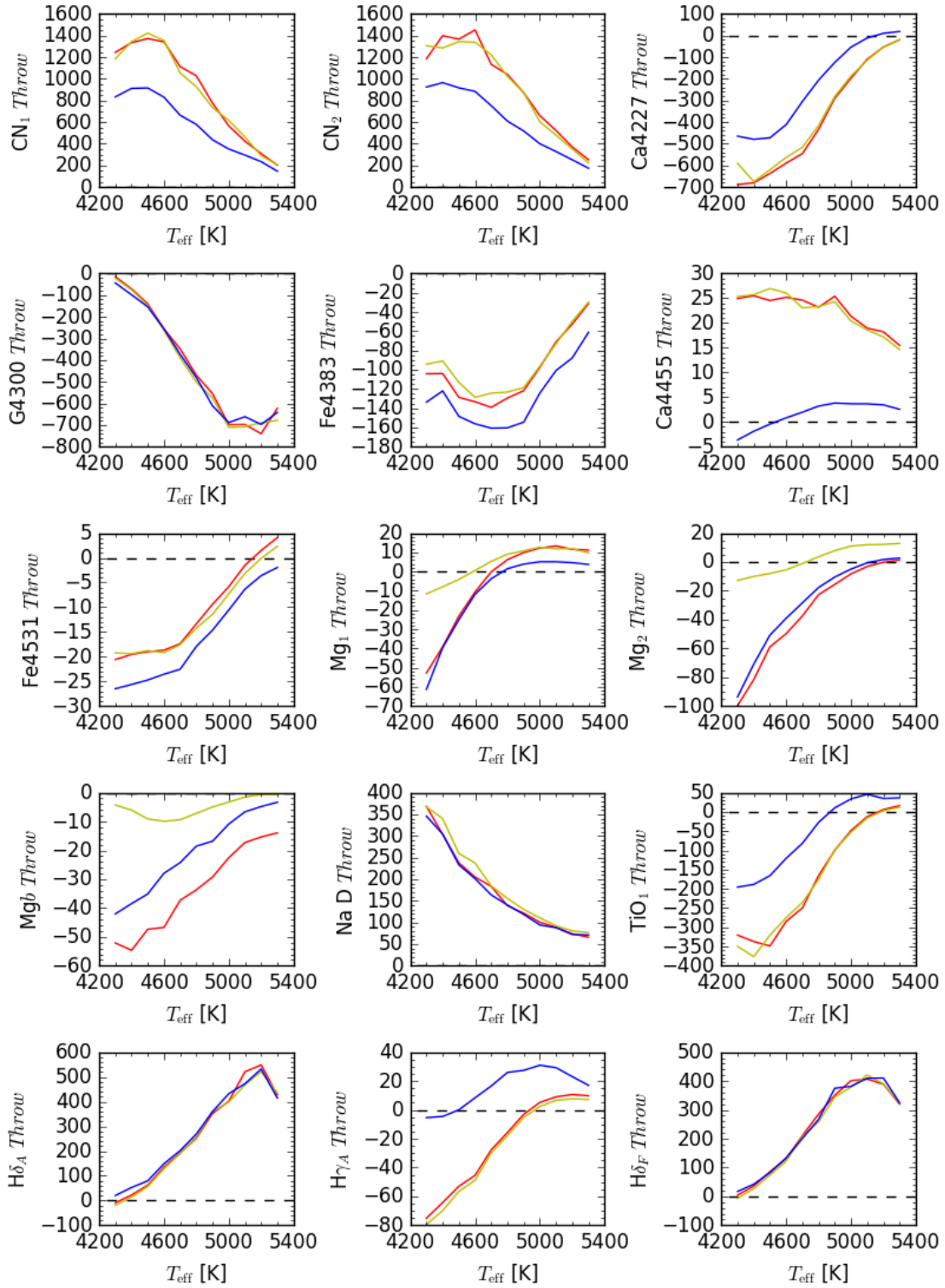


Figure 5.15: *Throw* of the chemical composition: CNONa1Y2 (red line), CNONa1Y4 (yellow line) and CNONa2Y2 (blue line) with respect to the Reference as a function of effective temperature for RGB stars considering  $\log g = 2.4$ , calculated with the Lick/IDS system.

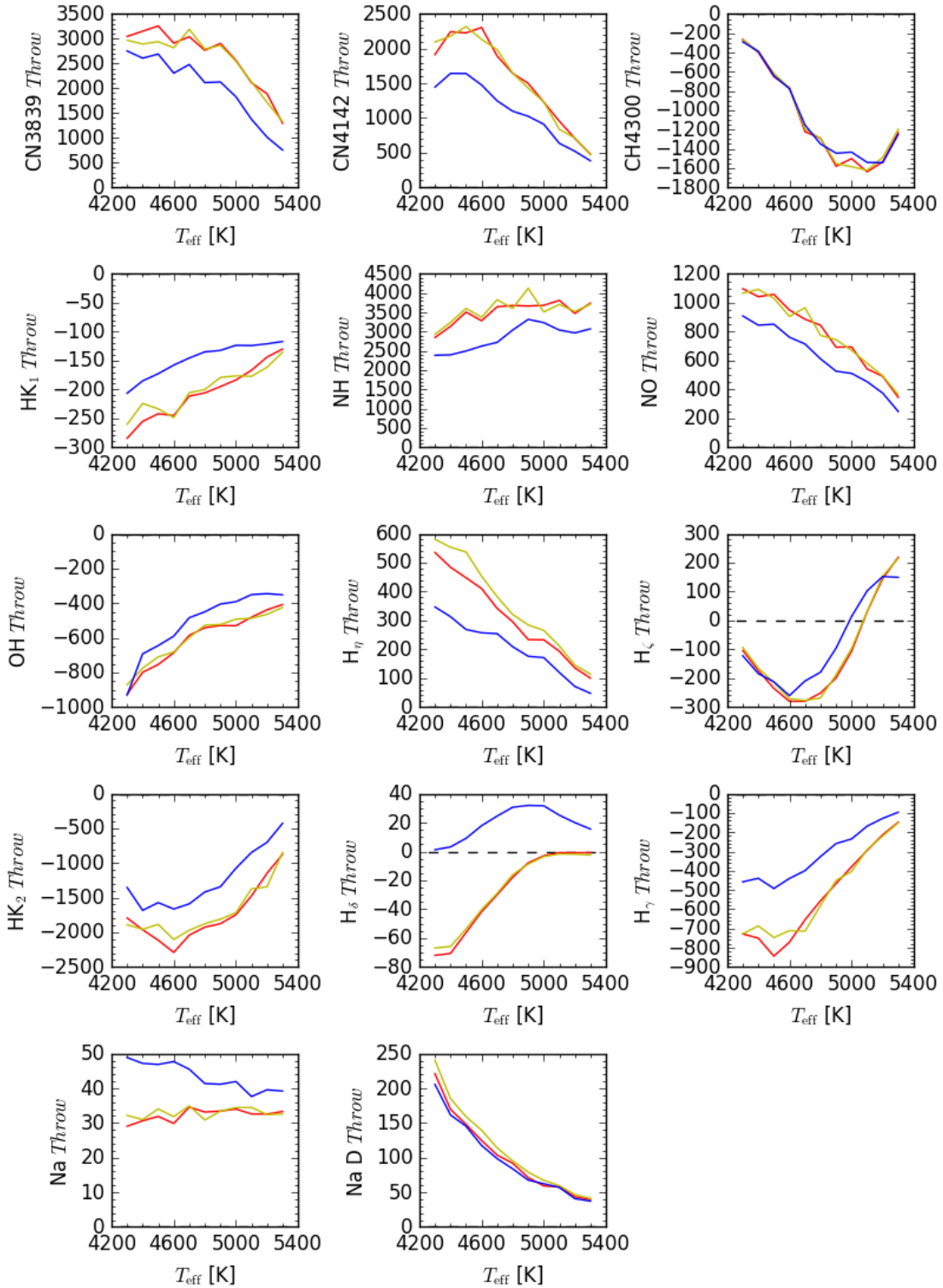


Figure 5.16: *Throw* of the chemical composition: CNONa1Y2 (red line), CNONa1Y4 (yellow line) and CNONa2Y2 (blue line) with respect to the Reference as a function of effective temperature for RGB stars considering  $\log g = 2.4$ , calculated with the indices from [Pancino et al. \(2010\)](#) and the defined in this work.

### 5.2.3 The Horizontal Branch

Figures 5.17 and 5.18 show the selected indices for the identification of multiple populations in the HB of M3. As we previously discussed, the indices are more effective at low temperatures, therefore, in this evolutionary stage there are few indices that can be useful. We assumed in this case a  $\log g = 2.8$  (Valcarce et al. 2016) and extended the range of  $T_{\text{eff}}$  from 5,400 to 7,000 K. In Figures 5.17 and 5.18 it can be observed that for  $T_{\text{eff}} \gtrsim 6,000$  K, the indices do not show significant differences between the four chemical compositions, i.e., they are not useful for our purpose. At low temperature,  $T_{\text{eff}} \lesssim 5,800$  K it is possible distinguish between stars of First and Second Generation, nevertheless, it results difficult to determine at which subpopulation of Second Generation they belong. Again, the index NH defined in this thesis is the best. The horizontal branch is not a good evolutionary stage to search for multiple stellar populations in GCs.

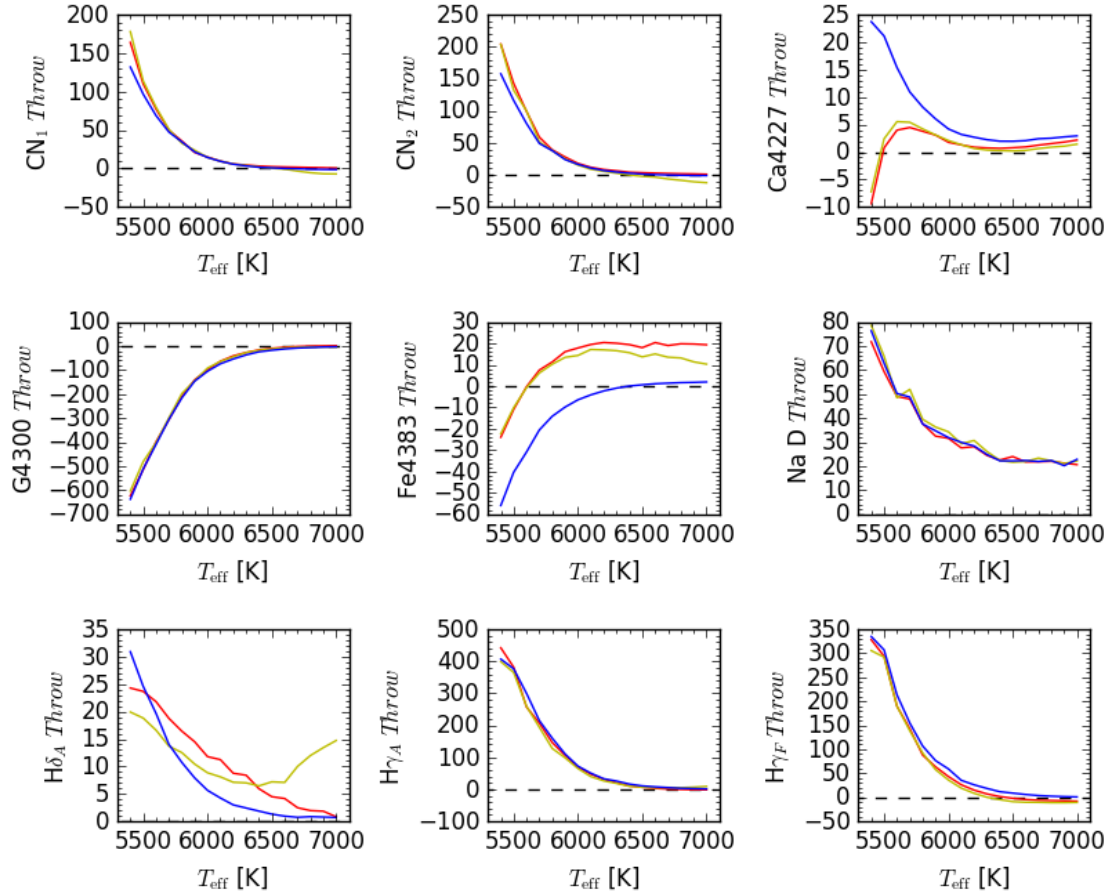


Figure 5.17: *Throw* of the chemical composition: CNONa1Y2 (red line), CNONa1Y4 (yellow line) and CNONa2Y2 (blue line) with respect to the Reference as a function of effective temperature for HB stars considering  $\log g = 2.8$ , calculated with the Lick/IDS system.

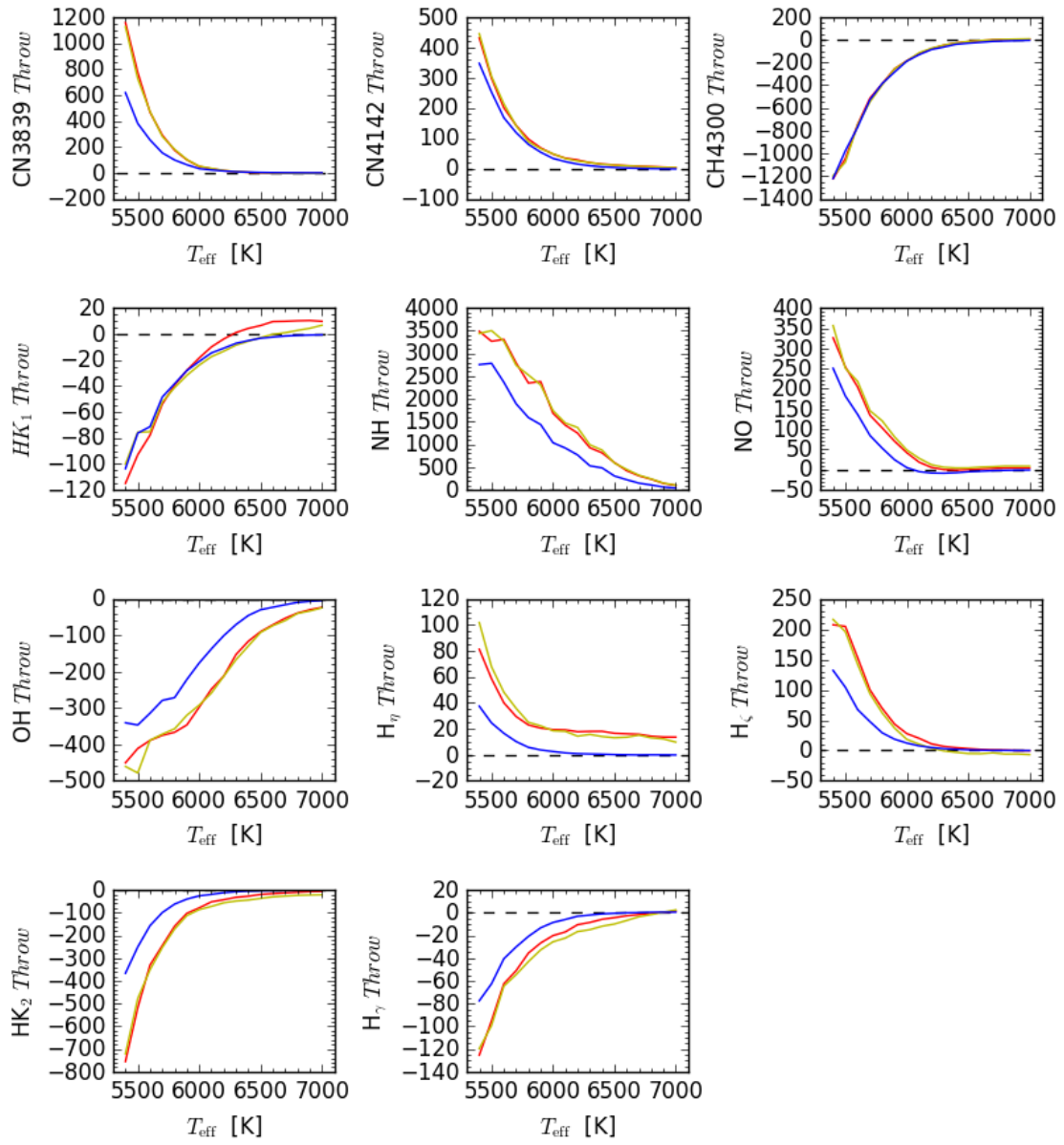


Figure 5.18: *Throw* of the chemical composition: CNONa1Y2 (red line), CNONa1Y4 (yellow line) and CNONa2Y2 (blue line) with respect to the Reference as a function of effective temperature for HB stars considering  $\log g = 2.8$ , calculated with the indices from [Pancino et al. \(2010\)](#) and the defined in this work.



# Chapter 6

## GTC Observations of M3

### 6.1 GTC and the MOS of OSIRIS

The Gran Telescopio CANARIAS (GTC) is the largest and one of the most advanced optical and infrared telescopes in the world. Led by the Instituto de Astrofísica de Canarias (IAC), the GTC is located at the Observatorio del Roque de Los Muchachos, La Palma. Its First Light ceremony took place on July 14th, 2007 but it was not until March of 2009 that it began its scientific operations.

The GTC has a primary mirror consisting of 36 individual hexagonal segments that together act as a single mirror. The collecting area of the primary mirror is comparable to that of a single mirror telescope with a 10.4 m diameter. In addition to the primary mirror, this telescope has a secondary and a tertiary mirror which, working together, produce the telescope focal plane. The scientific instruments which are used to detect are placed in the Nasmyth focal station.

OSIRIS is the acronym for Optical System for Imaging and low-intermediate Resolution Integrated Spectroscopy. Located in the Nasmyth-B focus of GTC, OSIRIS is an imager and spectrograph for the optical wavelength range providing standard broad-band imaging and long-slit spectroscopy, in addition to the narrow-band tunable filters imaging, charge-shuffling and multi-object spectroscopy (MOS). It covers the wavelength range between 365 and 1,050 nm with a total field of view of  $7.8 \times 8.5$  arcmin<sup>2</sup> for direct imaging, and  $7.5 \times 6.0$  arcmin for multi-object spectroscopy (Cabrera-Lavers 2014).

## 6.2 Definition of the stellar sample

An observing proposal (GTC9-16BMEX, P.I. Miguel Chávez) was submitted to the GTC for collecting OSIRIS MOS spectra of M3 stars, especially MS objects, with the goal of identifying spectroscopic signatures of the sub-populations present in this stellar system. The proposal requested the use of two grisms: R2500U and R2500V. The first one was needed in order to have access to the blue spectral region, densely populated by absorption lines, and the second for the region that includes the Na D doublet at  $\sim 5890 \text{ \AA}$ . A sample of 71 stars was selected: 44 stars of Main Sequence, 24 at the Turn-off and 3 of the Red Giant Branch. In what follows, we describe the quite complicated procedure that we followed in order to select a proper sample of stars in M3 and to prepare the MOS observations.

First, it was necessary to search for a suitable photometric catalog of M3 stars, according to the following characteristics:

- It should include stars far enough from the central region of the cluster in order to decrease as much as possible the source crowding, considering a typical seeing of 1 arcsec; this means a few arcmin from the cluster center.
- To be photometrically deep enough in order to include MS stars.
- To include a suitable color for selecting stars in the different evolutionary states (e.g.  $B - V$ ), which means that a proper color-magnitude diagram (CMD) can be built.

The catalog that satisfied all these criteria was the one published by Ferraro ([Ferraro et al. 1997](#)). It mainly includes astrometry data (right ascension RA, and declination DEC) and photometry: the Johnson V magnitude and color index  $B - V$  for 12,504 stars. Figure [6.1](#) shows the position of the stars in RA and DEC.

The CCD B and V photometry of M3, carried out at the 3.6 m Canada France Hawaii Telescope (CFHT) by [Ferraro et al. \(1997\)](#), covered the inner region of the cluster, up to a radius  $r$  of about  $4'$ , but avoiding the very central  $0.3'$ . This catalog was complemented with the previously published data by [Buonanno et al. \(1994\)](#), who reported the photographic photometry for more than 10,000 stars in  $r > 2.0'$  and to a size of  $14' \times 14'$  (the size of photographic plates, taken in the early 1950s at Mt. Palomar and Mt. Wilson Observatories), resulting in a catalog with about 20,000 stars with  $V \leq 18.6$  mag in  $0.3' < r < 7.0'$ . The low density of stars shown in the map of M3 of the Figure [6.1](#) in  $2.5' < r \lesssim 4'$  is caused by: 1) the [Buonanno et al. \(1994\)](#) survey was not able to resolve stars in the photographic plates due to crowding and; 2) in the [Ferraro et al. \(1997\)](#) survey, is due to the low efficiency in the blue band of the CFHT CCD-camera.

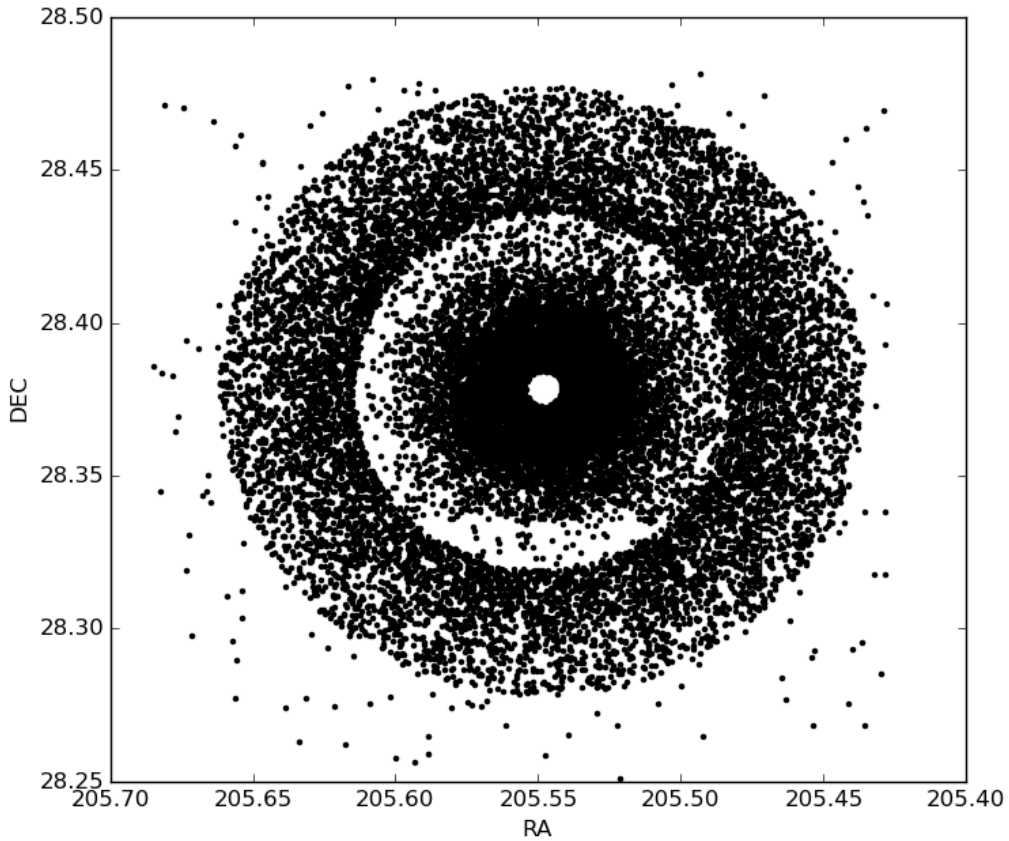


Figure 6.1: RA and DEC position of the M3 stars included in the [Ferraro et al. \(1997\)](#) catalog.

As it was discussed earlier, we were mostly interested in studying MS stars, but to take advantage of the MOS mode observation it was necessary to maximize as much as possible the number of objects to be simultaneously observed; we therefore included stars from Turn-off (TO), Red Giant Branch (RGB) and Horizontal Branch (HB). With this objective, four regions in the CMD of M3 were delimited according to the following criteria and are summarized in Table 6.1:

- Main Sequence and Turn-off: We required to observe stars in this branch with a good S/N in a reasonable time; spectra of stars with  $V \gtrsim 20$  mag may not be obtained with the necessary quality.
- Turn-off: Stars about to leave or leaving the MS were included in order to investigate possible differences in chemical composition with respect to MS

stars and discard or establish if the chemical anomalies are attributed to evolutionary changes or not.

- Red Giant Branch: Stars far enough from the blue limit of the CFHT CCD-camera ( $B > 18.6$  from data of [Ferraro et al. \(1997\)](#) catalog) and up to  $V = 15.5$  mag to avoid the saturation of the OSIRIS MOS.
- Horizontal Branch: Stars as faint as possible ( $V > 15.5$  mag), to avoid the saturation of the OSIRIS MOS, and located in a central range of the HB.

Table 6.1: Color criteria for extracting a preliminary sample of stars to observe.

| Region            | Range in V-mag | Range (B-V) | Range in $T_{\text{eff}}$ |
|-------------------|----------------|-------------|---------------------------|
| Main Sequence     | 19.2 - 19.8    | 0.35 - 0.60 | 5,400 - 6,500             |
| Turn off          | 18.5 - 19.2    | 0.36 - 0.61 | 5,400 - 6,500             |
| Red Giant Branch  | 15.5 - 17.0    | 0.69 - 0.82 | 4,800 - 5,300             |
| Horizontal Branch | 15.5 - 16.1    | 0.30 - 0.61 | 5,400 - 6,800             |

In Figure 6.2 we present the color magnitude diagram of the Ferraro stellar sample, where we indicate with different colors the regions defined (Table 6.1) to identify the targets.

Although the catalog of [Ferraro et al. \(1997\)](#) contains the information required for selecting a suitable stellar sample, the astrometry is not precise enough for the aim of our proposal; in order to reach the needed accuracy in the position of the stars, we compared the catalog's coordinates with the recent data from the Gaia astrometric satellite (Vizier catalog I/337 [Gaia-Collaboration et al. 2016](#)). Because the Gaia's catalog only include photometric data in its own system, it was necessary to convert the V magnitude of the Ferraro's catalog to the G magnitude of the Gaia's catalog by using the polynomial expression reported by [Jordi et al. \(2010\)](#). The difference was smaller than 0.31 mag between both catalogs.

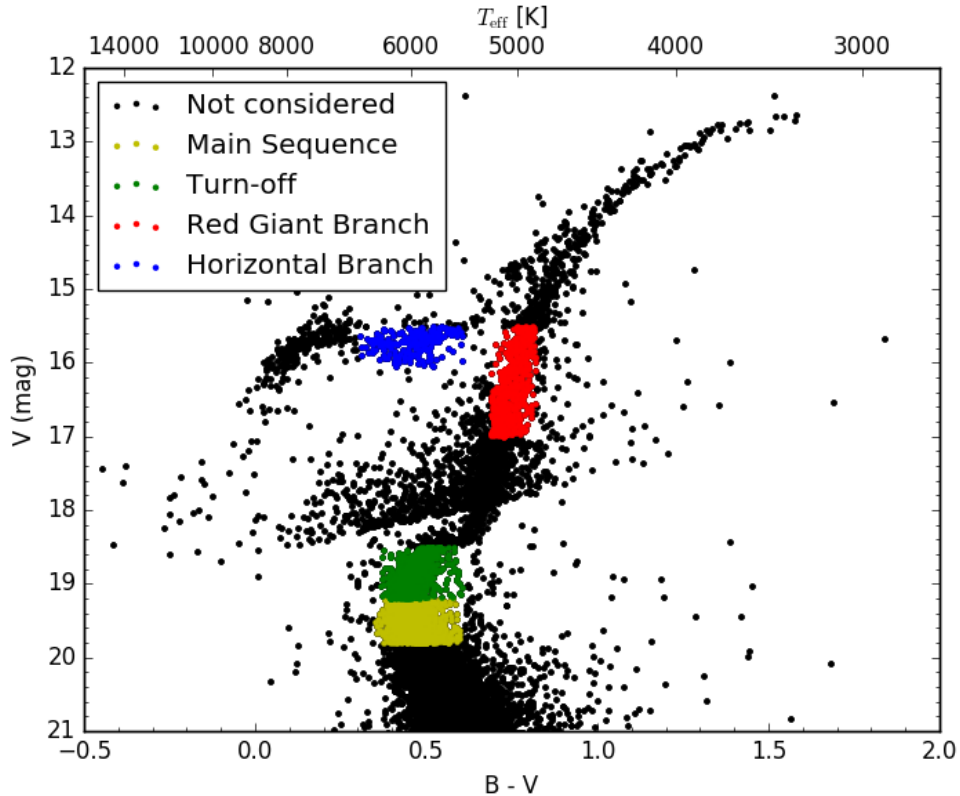


Figure 6.2: Color-magnitude diagram of the [Ferraro et al. \(1997\)](#) catalog of the globular cluster M3 highlighting the four regions used to extract a preliminary sample of stars. The conversion from  $B - V$  to  $T_{\text{eff}}$  was done using relation of [Sekiguchi & Fukugita \(2000\)](#).

For each star in the Ferraro catalog, we searched for a Gaia counterpart. For this comparison, as first step we wrote a code (using Python 2.7.13) which for each star in the regions defined in Table 6.1 (Ferraro catalog) searches for a counterpart around a circle of radius of 2 arcsec in the Gaia catalog. In order to verify if a star is the same in both catalogs, we established that the difference in magnitude G between two stars with similar coordinates (RA, DEC) were less than 0.5 mag. After the matching, only astrometric data of Gaia catalog were used because they are much more accurate, recent and precise. Even though the difference in time between the Ferraro and the Gaia observations is around 10 years, no large difference in the position of the stars was detected, since the proper motion of M3 is very small [ $-0.06 \pm 0.30 \text{ mas yr}^{-1}$  in RA and  $-2.6 \pm 0.30 \text{ mas yr}^{-1}$  in DEC ([Wu et al. 2002](#))].

The second step for selecting the targets for the observations with OSIRIS was to establish a rectangular region on an image of the cluster (from Sloan Digital Sky Survey) to place the slit. In order to maximize the number of objects without losing spectral range, we considered a rectangular of  $1 \times 7.5$  arcmin. To find its best location, a scan through the whole cluster was carried out. At the beginning of the

scan, the center of the rectangular region was placed at  $\text{DEC} = 28.37727778^\circ$  and  $\text{RA} = 205.45^\circ$  (at the edge of the image of M3). In this position, all stars, within the selected region, that matched the color criteria in Table 6.1, were counted; then the slit was moved 5 arcsec in the +RA direction and the suitable stars were counted again. This procedure continued through the +RA direction, up to the opposite edge of the cluster at  $\text{RA} = 205.65^\circ$ . The result of this scan is shown in the histogram of Figure 6.3, where it is possible to see the distribution of stars of interest through M3.

With these considerations and due to higher priority on MS objects, we decided that the best position to place the slit was in  $\text{RA} = 205.62^\circ$  ( $13h\ 42m\ 28.8s$ ) and  $\text{DEC} = 28.37727778^\circ$  ( $28^\circ\ 22'\ 38.2''$ ).

Another criterion taken in account to select the stars to observe was to choose regions as close as possible to the center of the GC but far enough away to avoid the light pollution from neighboring stars. Moreover, we used a RGB image of the Sloan Digital Sky Survey (SDSS) of M3 was for visually confirming the position and the brightness of the possible targets obtained from the match of both Ferraro's and Gaia's catalogs. The SDSS image is shown in the Figure 6.4, where the selected rectangular region is also highlighted.

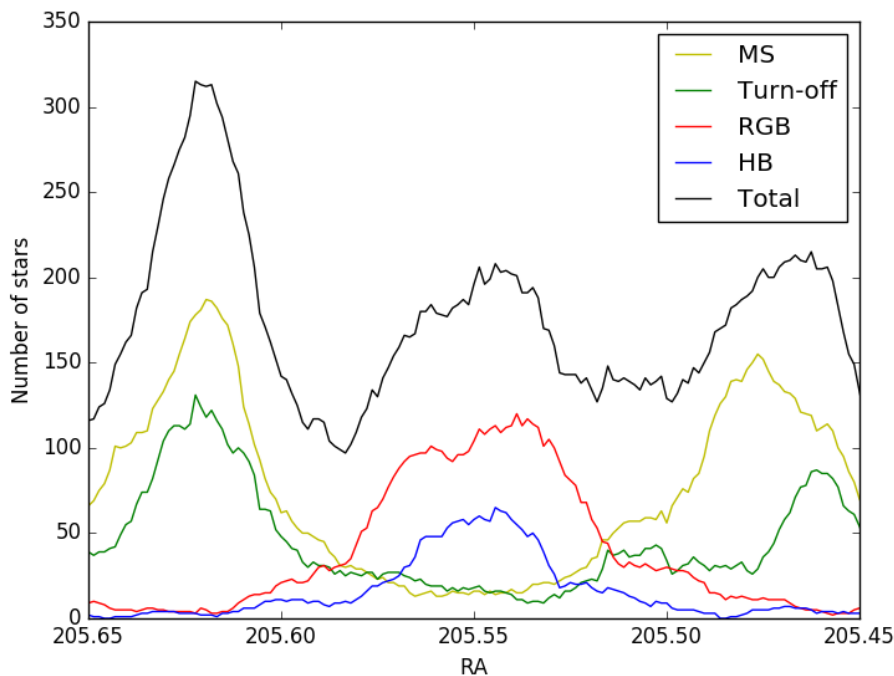


Figure 6.3: Histogram of the number of stars matched in both of Ferraro and Gaia catalogs according to the regions established in Figure 6.2 for a slit of  $\text{RA}: 1 \text{ arcmin} \times \text{DEC}: 7.5 \text{ arcmin}$ .

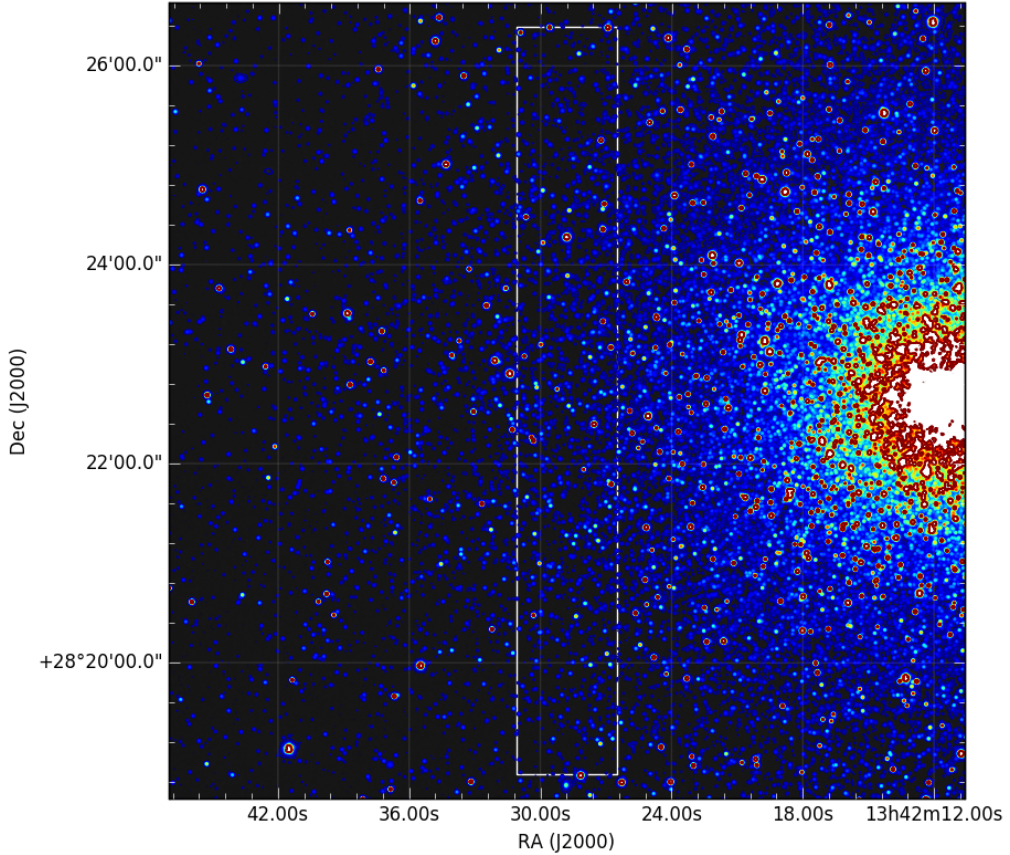


Figure 6.4: SDSS image of the eastern region of M3, centered in the  $1 \times 7.5$  arcmin rectangular region where the OSIRIS targets were identified.

Inside of this slit there were a total of 315 stars: 187 of Main Sequence, 121 of Turn-off, 5 of Red Giant Branch and 2 of Horizontal Branch. We carried out a procedure to remove the stars that could cause observational conflicts. It consisted in analyzing each star according to the next criteria:

- Stars polluted by the light of a neighboring star were not considered.
- Stars near the center of the rectangular region had priority over the stars near the edges, in order not to loose spectral coverage.
- For each star, we considered a slitlet length of 3 arcsec (in DEC direction; see Figure 6.5 for final result) and we avoid targets that had overlapping slitlets.

This procedure reduced the sample of stars to 71: 44 of Main Sequence, 24 of Turn-off and 3 of Red Giant Branch. The three stars of RGB were located where no MS or TO objects were present. No HB stars could be included. We also included five reference stars with V 17 that are needed for the field positioning.

These 71 selected target stars, along with the five reference stars, were uploaded to the OSIRIS Mask Designer tool v3.25, a Java plug-in to the JSky application, as a requirement to prepare the mask for the observation. The Figure 6.5 shows the image generated by OSIRIS Mask Designer while the Table 6.2 show the coordinates in RA and DEC as well as the G magnitude for each of the these stars.

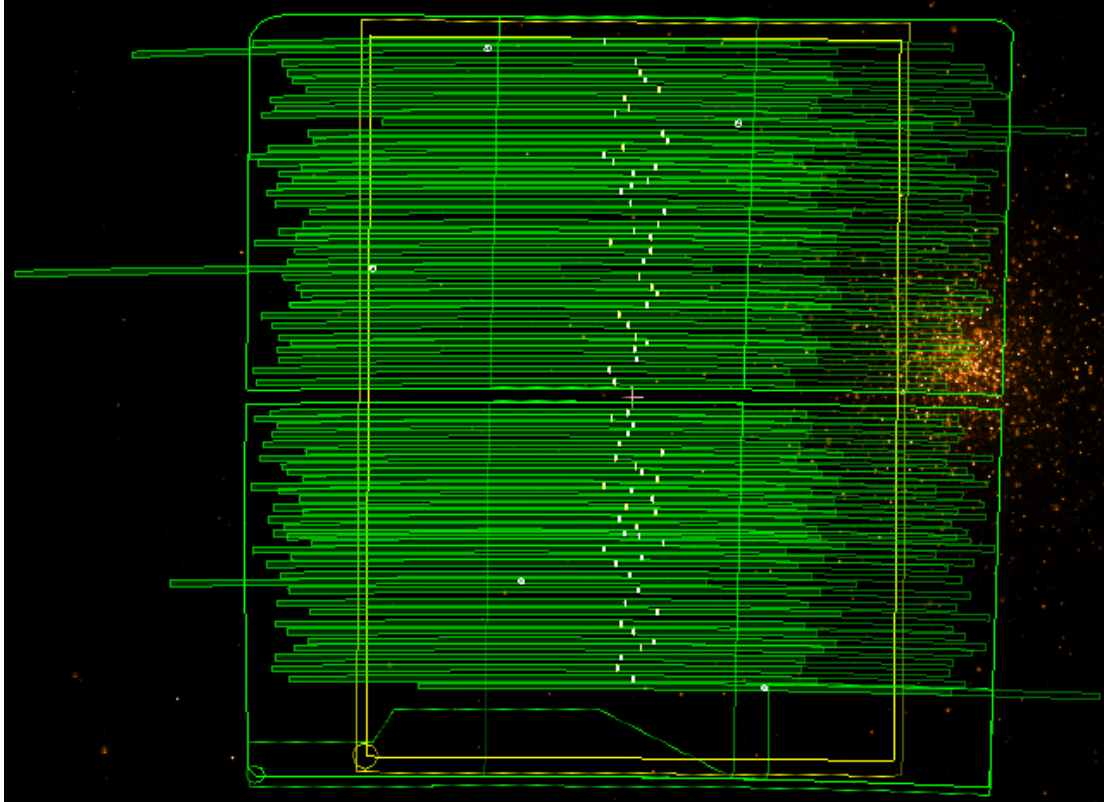


Figure 6.5: Generated image by OSIRIS Mask Designer over the U band SDSS image of M3. Every target star is indicated by a white rectangle, while the reference stars are shown in white circle.

Table 6.2: Gaia coordinates and G-band magnitudes of the 71 selected targets + 5 reference stars. The label in the second column means, MS: Main Sequence, TO: Turn-off and RG: Red Giant Branch. The error is mili-second of arc (mas).

| No. | id   | RA [deg]       | Error RA<br>[mas] | DEC [deg]     | Error DEC<br>[mas] | mag G  |
|-----|------|----------------|-------------------|---------------|--------------------|--------|
| 1   | MS01 | 205.6197844701 | 0.468             | 28.3164732700 | 0.253              | 19.269 |
| 2   | MS02 | 205.6233589296 | 0.455             | 28.3185101388 | 0.249              | 19.270 |
| 3   | MS03 | 205.6182324343 | 0.525             | 28.3224536149 | 0.286              | 19.475 |
| 4   | MS04 | 205.6154408498 | 0.451             | 28.3235482289 | 0.245              | 19.075 |
| 5   | MS05 | 205.6198004432 | 0.491             | 28.3254921107 | 0.269              | 19.232 |
| 6   | MS06 | 205.6224095324 | 0.444             | 28.3270003563 | 0.242              | 19.209 |
| 7   | MS07 | 205.6216242329 | 0.545             | 28.3310404256 | 0.298              | 19.408 |
| 8   | MS08 | 205.6206125976 | 0.485             | 28.3363383872 | 0.269              | 19.433 |
| 9   | MS09 | 205.6235375416 | 0.497             | 28.3385316709 | 0.278              | 19.218 |
| 10  | MS10 | 205.6179899470 | 0.601             | 28.3396883867 | 0.337              | 19.430 |
| 11  | MS11 | 205.6133858728 | 0.540             | 28.3424369692 | 0.293              | 19.578 |
| 12  | MS12 | 205.6192018524 | 0.418             | 28.3455366901 | 0.232              | 19.083 |
| 13  | MS13 | 205.6150676446 | 0.563             | 28.3483773495 | 0.301              | 19.521 |
| 14  | MS14 | 205.6156578949 | 0.921             | 28.3509002086 | 0.508              | 19.667 |
| 15  | MS15 | 205.6202634713 | 0.476             | 28.3525351101 | 0.262              | 19.466 |
| 16  | MS16 | 205.6146256800 | 0.456             | 28.3547774777 | 0.246              | 19.270 |
| 17  | MS17 | 205.6179378634 | 0.414             | 28.3560396913 | 0.234              | 19.061 |
| 18  | MS18 | 205.6192929608 | 0.443             | 28.3571836312 | 0.246              | 19.236 |
| 19  | MS19 | 205.6237363438 | 0.625             | 28.3588768162 | 0.342              | 19.322 |
| 20  | MS20 | 205.6229241322 | 0.567             | 28.3615539195 | 0.308              | 19.523 |
| 21  | MS21 | 205.6199377486 | 0.813             | 28.3650602107 | 0.414              | 19.476 |
| 22  | MS22 | 205.6211560125 | 0.565             | 28.3674780164 | 0.309              | 19.486 |
| 23  | MS23 | 205.6239519009 | 0.590             | 28.3733980961 | 0.317              | 19.641 |
| 24  | MS24 | 205.6250638948 | 0.435             | 28.3756922815 | 0.234              | 19.212 |
| 25  | MS25 | 205.6191811348 | 0.835             | 28.3776403640 | 0.450              | 19.788 |
| 26  | MS26 | 205.6168775498 | 0.876             | 28.3807838725 | 0.438              | 19.597 |
| 27  | MS27 | 205.6209437489 | 0.647             | 28.3841968074 | 0.358              | 19.623 |
| 28  | MS28 | 205.6230550019 | 0.564             | 28.3860886050 | 0.324              | 19.644 |
| 29  | MS29 | 205.6168962260 | 0.573             | 28.3881673888 | 0.313              | 19.337 |
| 30  | MS30 | 205.6146618867 | 0.695             | 28.3902684730 | 0.375              | 19.566 |
| 31  | MS31 | 205.6186153073 | 0.568             | 28.3934157345 | 0.307              | 19.473 |
| 32  | MS32 | 205.6176549480 | 0.839             | 28.3963836253 | 0.437              | 19.565 |
| 33  | MS33 | 205.6160793434 | 0.608             | 28.3983774463 | 0.339              | 19.367 |
| 34  | MS34 | 205.6160970810 | 0.581             | 28.4011527096 | 0.315              | 19.460 |
| 35  | MS35 | 205.6144495396 | 0.790             | 28.4034567247 | 0.429              | 19.500 |
| 36  | MS36 | 205.6202830222 | 0.598             | 28.4109900591 | 0.321              | 19.340 |
| 37  | MS37 | 205.6198874643 | 0.742             | 28.4132461214 | 0.408              | 19.581 |

Table 6.2: Continued.

| No. | id    | RA [deg]       | Error RA<br>[mas] | DEC [deg]     | Error DEC<br>[mas] | mag G  |
|-----|-------|----------------|-------------------|---------------|--------------------|--------|
| 38  | MS38  | 205.6242671818 | 0.795             | 28.4153710196 | 0.424              | 19.626 |
| 39  | MS39  | 205.6220721682 | 0.804             | 28.4183711184 | 0.431              | 19.277 |
| 40  | MS40  | 205.6218435698 | 0.476             | 28.4276051383 | 0.268              | 19.324 |
| 41  | MS41  | 205.6141992347 | 0.633             | 28.4292894790 | 0.353              | 19.529 |
| 42  | MS42  | 205.6184474234 | 0.533             | 28.4325937068 | 0.302              | 19.430 |
| 43  | MS43  | 205.6193687095 | 0.727             | 28.4346329212 | 0.397              | 19.612 |
| 44  | MS44  | 205.6261379665 | 0.460             | 28.4384414713 | 0.246              | 19.300 |
| 45  | TO01  | 205.6225314189 | 0.233             | 28.3205990574 | 0.131              | 18.345 |
| 46  | TO02  | 205.6145309300 | 1.168             | 28.3292831668 | 0.503              | 18.974 |
| 47  | TO03  | 205.6187879307 | 0.458             | 28.3334115687 | 0.254              | 18.705 |
| 48  | TO04  | 205.6186379672 | 0.332             | 28.3438505347 | 0.184              | 18.708 |
| 49  | TO05  | 205.6228091045 | 1.624             | 28.3471052552 | 0.847              | 18.884 |
| 50  | TO06  | 205.6214120914 | 0.306             | 28.3493454086 | 0.171              | 18.411 |
| 51  | TO07  | 205.6261504340 | 0.352             | 28.3533602915 | 0.222              | 19.120 |
| 52  | TO08  | 205.6136147100 | 0.344             | 28.3597257500 | 0.191              | 18.834 |
| 53  | TO09  | 205.6210693003 | 53.280            | 28.3633812894 | 47.714             | 19.143 |
| 54  | TO10  | 205.6245794927 | 0.715             | 28.3664117653 | 0.325              | 18.996 |
| 55  | TO11  | 205.6196302319 | 0.370             | 28.3795492747 | 0.198              | 18.750 |
| 56  | TO12  | 205.6193553820 | 0.284             | 28.3818615938 | 0.156              | 18.448 |
| 57  | TO13  | 205.6159317546 | 0.300             | 28.3914845078 | 0.169              | 18.719 |
| 58  | TO14  | 205.6249441523 | 0.334             | 28.4000601020 | 0.191              | 18.620 |
| 59  | TO15  | 205.6197239778 | 0.816             | 28.4021414220 | 0.433              | 18.719 |
| 60  | TO16  | 205.6205518156 | 0.379             | 28.4075709623 | 0.205              | 18.900 |
| 61  | TO17  | 205.6224937959 | 0.317             | 28.4097331971 | 0.193              | 18.793 |
| 62  | TO18  | 205.6167373643 | 0.455             | 28.4117514649 | 0.247              | 18.919 |
| 63  | TO19  | 205.6151690532 | 0.470             | 28.4144817510 | 0.253              | 18.896 |
| 64  | TO20  | 205.6262517489 | 0.422             | 28.4167490121 | 0.256              | 18.622 |
| 65  | TO21  | 205.6125117575 | 0.408             | 28.4194764900 | 0.227              | 18.897 |
| 66  | TO22  | 205.6238626888 | 0.306             | 28.4246762107 | 0.194              | 18.534 |
| 67  | TO23  | 205.6208371640 | 0.304             | 28.4258011831 | 0.210              | 18.737 |
| 68  | TO24  | 205.6173083720 | 0.510             | 28.4311198385 | 0.304              | 18.706 |
| 69  | RG01  | 205.6263105083 | 0.123             | 28.3412838013 | 0.065              | 16.350 |
| 70  | RG02  | 205.6131096892 | 0.090             | 28.4059352464 | 0.056              | 15.282 |
| 71  | RG03  | 205.6135046451 | 0.086             | 28.4208399304 | 0.060              | 15.410 |
| 72  | REF01 | 205.6441475309 | 0.270             | 28.3351282212 | 0.151              | 18.272 |
| 73  | REF02 | 205.6766416076 | 0.250             | 28.3950116100 | 0.145              | 18.393 |
| 74  | REF03 | 205.6516118763 | 0.279             | 28.4371160292 | 0.161              | 18.379 |
| 75  | REF04 | 205.5969907842 | 0.447             | 28.4228367823 | 0.247              | 18.336 |
| 76  | REF05 | 205.5912768151 | 0.265             | 28.3146835910 | 0.154              | 18.460 |

Figure 6.6 shows the position of the selected targets stars on the CMD from Ferraro et al. (1997).

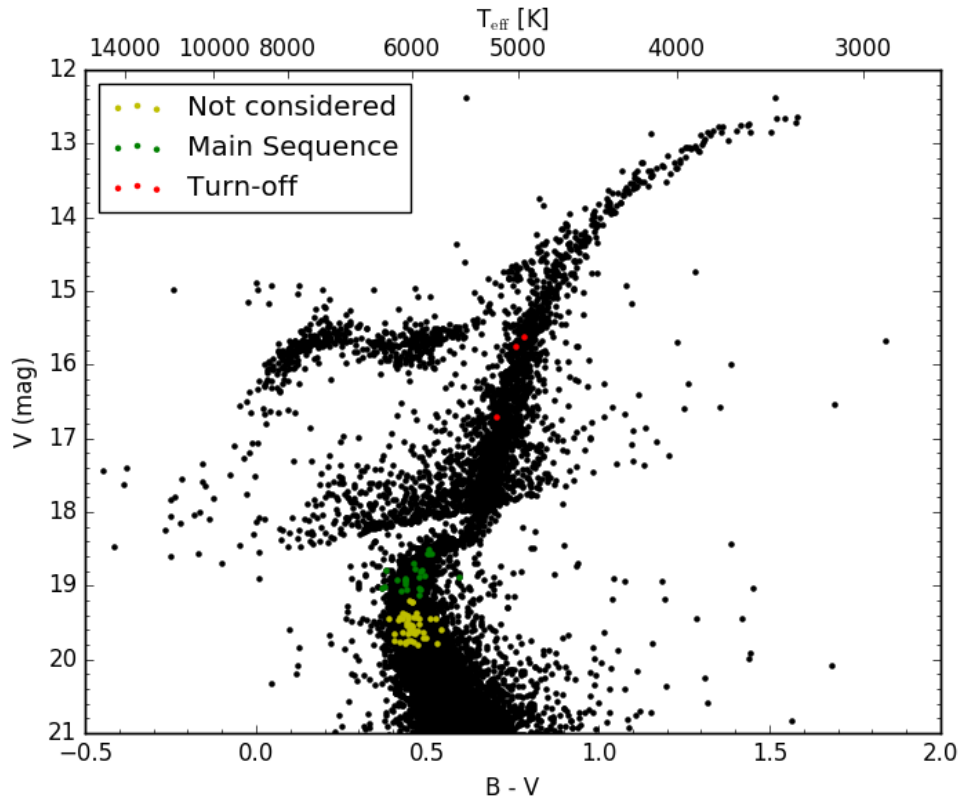


Figure 6.6: Color-magnitude diagram of the Ferraro et al. (1997) catalog of the globular cluster M3 with the 71 selected targets stars. The conversion from  $B - V$  to  $T_{\text{eff}}$  was done using relation of Sekiguchi & Fukugita (2000).

## 6.3 Preliminary observation data

The observation proposal described in the previous section was accepted satisfactory and the observations were carried out on February 2017 but, due to problems with the routine of reduction of spectra, we only present here preliminary data. These problems are caused by the subtraction of the sky because the size of the slit of 3 arcsec, chosen in the process of selection of targets, was not big enough to do this process and the flux calibration as well as the wavelength calibration have no satisfactorily performed. Now, we need to readjust the routine in order to get spectra well reduced and calibrated.

With a fast reduction process using the GTCMOS pipeline ([Gomez-González et al. 2016](#)), we were able to obtain six complete preliminary spectra (i.e. in both R2500U and R2500V grisms): four MS stars and two of the Turn off of M3. These spectra were normalized by using a spline curve, avoiding the wavelength region most affected by line blanketing. The resulting spectra are shown in Figure [6.7](#). The wavelength calibration is barely acceptable. By way of comparison, a normalized theoretical spectra, corrected by the heliocentric radial velocity of M3:  $-147.6 \text{ km s}^{-1}$  ([Harris 1996](#)), with the Reference chemical composition at  $T = 6,000 \text{ K}$  and  $\log g = 4.2$  is included in this Figure. Also, we added the bandpasses of the spectroscopic indices that fit in the spectra range (3,440 - 6,000 Å).

As can be observed in Figure [6.7](#), the spectra present some lines of emission, i.e. sky lines that must be subtracted. This fast reduction was applied to all observed spectra, however most of them presented a deficient calibration in wavelength: eight spectra (seven of MS and one of TO) in the grism R2500U resulted with an acceptable calibration while 26 (15 of MS and 11 or TO) were in the R2500V. None of these 34 spectra was “well calibrated” in both grism.

A comparison between the observed and theoretical indices would not be valid with these preliminary data, we need to do a good reduction and calibration of all spectra in order to calculate and compare spectroscopic indices and then verifying if the GC M3 has multiple stellar populations in the MS.

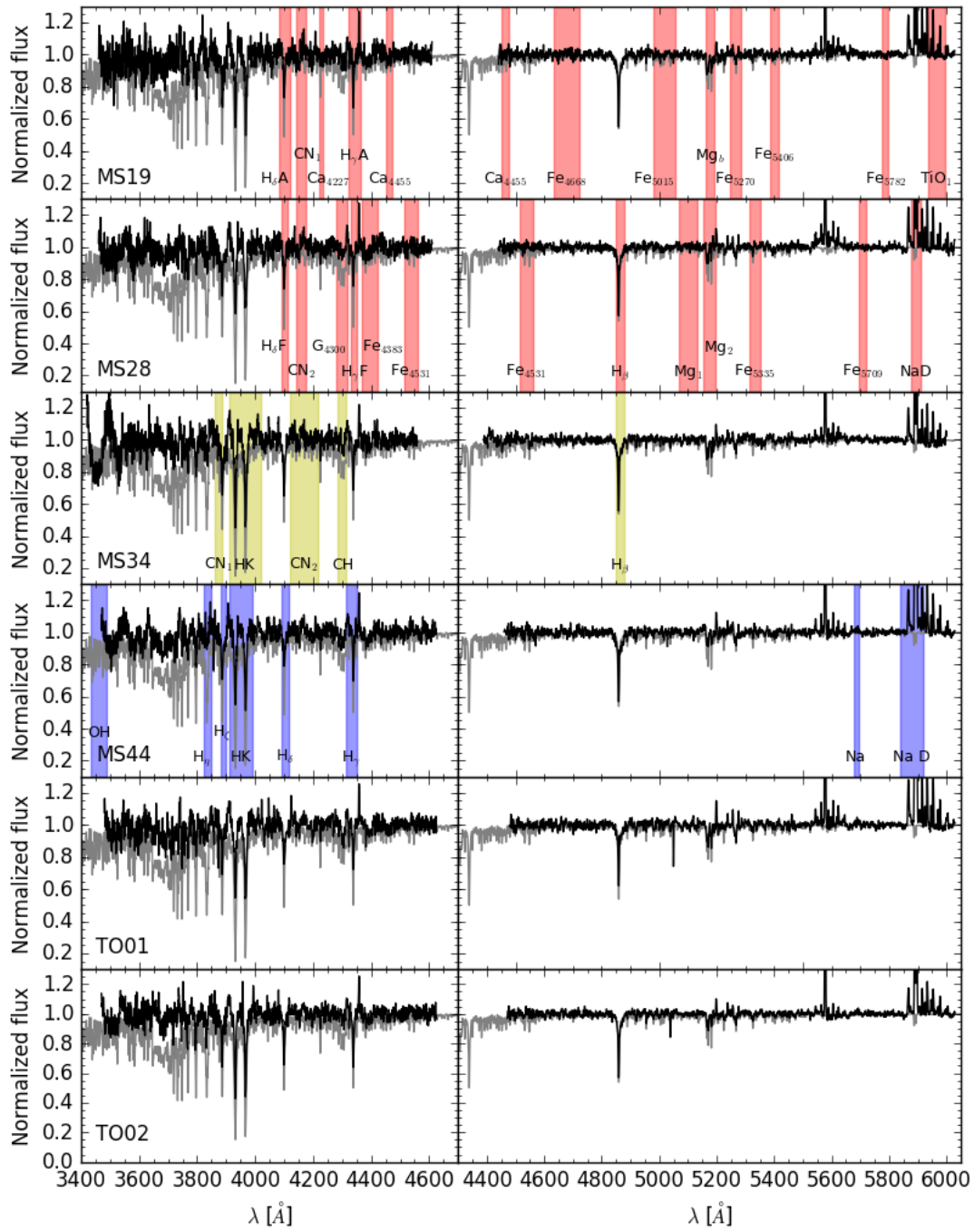


Figure 6.7: Preliminary spectra of six observed stars of MS with the GTC (in black color) and their comparison with a theoretical normalized spectra at  $T = 6,000$  K,  $\log g = 4.2$  and the Reference abundance (in gray color). Left panels show the part corresponding to grism R2500U while right panels display that of the R2500V. Each panel is labeled with the identification of the star according to Table 6.2 in the blue part of the spectra (R2500U). On the spectra of the stars MS19 and MS28 are drawn the bandpasses central of the Lick/IDS indices, on the MS34 that reported by [Pancino et al. \(2010\)](#) and on the MS44 the indices defined in this work.



# Chapter 7

## Conclusions

We carried out a theoretical study with the aim of developing suitable tools for the identification of multiple stellar population in MS stars of the Globular Cluster M3 (NGC 5272), through the analysis of spectroscopic indices.

The study of multiple stellar populations in galactic GCs, once considered the observational equivalent of single stellar population, is a hot topic in the current astrophysical research and this work represents a step further in the theoretical studies on this issue as it focuses on the spectroscopic analysis of unevolved MS star, which in the past have been mainly studied with photometric techniques. This work will therefore provide a framework for the interpretation of observations of a sample of M3 stars, carried out with the OSIRIS spectrograph, coupled to the Gran Canarias Telescope.

For this goal, we computed a large grid of 3,472 model atmospheres and high-resolution synthetic spectra using the collection of Fortran codes (DFSYNTHE, ATLAS9 and SYNTHE) developed by R. L. Kurucz. The library includes four different chemical compositions, that are found in Globular Clusters with multiple stellar populations, published by [Sbordone et al. \(2011\)](#): one of them (labeled as Reference) is typical of stars of a First Generation, while the other, with abundance variations of several light elements such as He, C, N, O, and Na, are recognized as mixtures of Second Generation stars. The grid of models and theoretical spectra covers a range of effective temperature from 4,300 to 7,000 K and surface gravity from 2.0 to 5.0 dex, suitable for the analysis not only of MS stars, but also of objects of the RGB and HB evolutionary stages.

For each synthetic spectrum, we calculated a total of 39 spectral indices: 24 defined in the Lick/IDS system, 5 reported by [Pancino et al. \(2010\)](#) and 10 defined in this work. We defined new indices in order to fully take advantage of the high-quality data that can be provided by OSIRIS/GTC. With the addition of these new indices, we considered to have entirely covered the spectral features that present the largest

differences among the chemical compositions included in this work.

In order to quantitatively establish the sensitivity to chemical composition and the capability of each theoretical index to distinguish among different mixtures, we estimated the error of each index by using a Monte Carlo technique and we used this uncertainty estimation to define a quantity, that we called *Throw*, that measures the difference between two indices in units of the corresponding error.

We considered three combinations of atmospheric parameters, representative of stars at different evolutionary stages in M3 (Main Sequence-Turn off, Red Giant Branch and Horizontal Branch), and we analyzed the behavior, in term of the *Throw*, of the all set of spectroscopic indices in order to find which of them are good candidates for separating among different possible stellar populations.

For the MS case, which is the main focus of this work we found that the indices that measure the strength of molecular bands, such as the cyanogen ( $\text{CN}_1$ ,  $\text{CN}_2$ , CN3839 and CN4142), methylidyne (G4300 and CH4300), NH, NO and OH, are the best for distinguishing Second Generation stars from objects belonging to the First Generation, in particular at  $T_{\text{eff}} < 6,200$  K); however, they do not show any relevant dependence to the helium content. In order to differentiate between stars with different content of He, the indices  $\text{Mg}_2$ ,  $\text{Mgb}$ ,  $\text{HK}_1$ ,  $\text{H}_\eta$  and  $\text{H}_\delta$  are more adequate. The index NH (imidogen) that we defined, turned out to have the biggest *Throw*, i.e. it is the best index to distinguish between First and Second Generation stars, however this index is defined in the near ultraviolet, a zone of the electromagnetic spectrum that is complicated for optical telescopes.

Finally, as an extension of the theoretical work, we were able to present here some of the spectra of MS and TO stars in M3 that were observed by the OSIRIS spectrograph in February 2017 in GTC. The spectra cover the same wavelength region as the theoretical library computed in this work with a spectral resolving power  $R \sim 2,500$ . However, the data reduction process is not yet completed for the whole observed data set, so that the search for a double (or multiple) stellar population in M3 MS stars will be carried out in the future.

# Appendix A

## Abundances of the four chemical compositions

Tabla A.1 displays the abundances of all elements considered in the four different chemical mixtures for computing model atmospheres reported by Sbordone et al. (2011). Here, [El] is given as  $\log N(\text{El}) - \log N(\text{H}) + 12$ , and each modified chemical composition CNONa1Y2, CNONa1Y4 and CNONa2Y2 is labeled with the subscripts 1, 2 and 3, respectively.

Table A.1: Abundances for all elements in the considered mixtures.

| No. | El | Reference $Y = 0.246$    |        | CNONa1 $Y = 0.246$       |                   | CNONa1 $Y = 0.400$ |                          | CNONa2 $Y = 0.246$ |                   |
|-----|----|--------------------------|--------|--------------------------|-------------------|--------------------|--------------------------|--------------------|-------------------|
|     |    | Mass frac.               | [El]   | Mass frac.               | [El] <sub>1</sub> | Mass frac.         | [El] <sub>2</sub>        | Mass frac.         | [El] <sub>3</sub> |
| 1   | H  | 0.7530                   | 12.000 | 0.7522                   | 12.000            | 0.0000             | 0.5985                   | 12.000             | 0.0000            |
| 2   | He | 0.2460                   | 10.915 | 0.2460                   | 10.916            | 0.0005             | 0.4000                   | 11.226             | 0.3108            |
| 3   | Li | $1.8376 \times 10^{-12}$ | -0.451 | $3.3729 \times 10^{-12}$ | -0.186            | 0.2642             | $2.6840 \times 10^{-12}$ | -0.186             | 0.2642            |
| 4   | Be | $4.7607 \times 10^{-12}$ | -0.151 | $8.7380 \times 10^{-12}$ | 0.114             | 0.2642             | $6.9534 \times 10^{-12}$ | 0.114              | 0.2642            |
| 5   | B  | $8.0668 \times 10^{-11}$ | 0.999  | $1.4806 \times 10^{-10}$ | 1.264             | 0.2642             | $1.1782 \times 10^{-10}$ | 1.264              | 0.2642            |
| 6   | C  | $7.6386 \times 10^{-5}$  | 6.930  | $1.9172 \times 10^{-5}$  | 6.330             | -0.5999            | $1.5256 \times 10^{-5}$  | 6.330              | -0.5999           |
| 7   | N  | $2.3430 \times 10^{-5}$  | 6.350  | $1.4768 \times 10^{-3}$  | 8.150             | 1.8000             | $1.1752 \times 10^{-3}$  | 8.150              | 1.8000            |
| 8   | O  | $6.7226 \times 10^{-4}$  | 7.750  | $1.0642 \times 10^{-4}$  | 6.950             | -0.8000            | $8.4687 \times 10^{-5}$  | 6.950              | -0.8000           |
| 9   | F  | $1.4506 \times 10^{-8}$  | 3.009  | $2.6626 \times 10^{-8}$  | 3.274             | 0.2642             | $2.1188 \times 10^{-8}$  | 3.274              | 0.2642            |
| 10  | Ne | $8.4796 \times 10^{-5}$  | 6.750  | $8.4706 \times 10^{-5}$  | 6.750             | 0.0000             | $6.7405 \times 10^{-5}$  | 6.750              | 0.0000            |
| 11  | Na | $8.8125 \times 10^{-7}$  | 4.710  | $5.5531 \times 10^{-6}$  | 5.510             | 0.7999             | $4.4189 \times 10^{-6}$  | 5.510              | 0.7999            |
| 12  | Mg | $4.1603 \times 10^{-5}$  | 6.360  | $4.1558 \times 10^{-5}$  | 6.360             | 0.0000             | $3.3070 \times 10^{-5}$  | 6.360              | 0.0000            |
| 13  | Al | $1.4268 \times 10^{-6}$  | 4.850  | $1.4249 \times 10^{-6}$  | 4.850             | -0.0001            | $1.1339 \times 10^{-6}$  | 4.850              | -0.0001           |
| 14  | Si | $3.5638 \times 10^{-5}$  | 6.230  | $3.5600 \times 10^{-5}$  | 6.230             | 0.0000             | $2.8329 \times 10^{-5}$  | 6.230              | 0.0000            |
| 15  | P  | $1.5687 \times 10^{-7}$  | 3.831  | $1.5588 \times 10^{-7}$  | 3.829             | -0.0023            | $1.2404 \times 10^{-7}$  | 3.829              | -0.0023           |
| 16  | S  | $1.9925 \times 10^{-5}$  | 5.920  | $1.9903 \times 10^{-5}$  | 5.920             | 0.0000             | $1.5838 \times 10^{-5}$  | 5.920              | 0.0000            |
| 17  | Cl | $2.0083 \times 10^{-7}$  | 3.880  | $1.9990 \times 10^{-7}$  | 3.878             | -0.0015            | $1.5907 \times 10^{-7}$  | 3.878              | -0.0015           |
| 18  | Ar | $2.3710 \times 10^{-6}$  | 4.900  | $2.3694 \times 10^{-6}$  | 4.900             | 0.0002             | $1.8855 \times 10^{-6}$  | 4.900              | 0.0002            |
| 19  | K  | $9.1921 \times 10^{-8}$  | 3.498  | $9.1695 \times 10^{-8}$  | 3.497             | -0.0006            | $7.2967 \times 10^{-8}$  | 3.497              | -0.0006           |
| 20  | Ca | $5.2045 \times 10^{-6}$  | 5.240  | $5.2009 \times 10^{-6}$  | 5.240             | 0.0002             | $4.1387 \times 10^{-6}$  | 5.240              | 0.0002            |

Table A.1: Continued.

| No. | El | Reference $Y = 0.246$    |        | CNONa1 $Y = 0.246$       |          | CNONa1 $Y = 0.400$ |                          | CNONa2 $Y = 0.246$ |          | $[El]_{3-[El]}$          |
|-----|----|--------------------------|--------|--------------------------|----------|--------------------|--------------------------|--------------------|----------|--------------------------|
|     |    | Mass frac.               | $[El]$ | Mass frac.               | $[El]_1$ | Mass frac.         | $[El]_2$                 | Mass frac.         | $[El]_3$ |                          |
| 21  | Sc | $1.3984 \times 10^{-9}$  | 1.619  | $2.5667 \times 10^{-9}$  | 1.884    | 0.2642             | $2.0425 \times 10^{-9}$  | 1.884              | 0.2642   | $1.3984 \times 10^{-9}$  |
| 22  | Ti | $3.8667 \times 10^{-7}$  | 4.034  | $3.8512 \times 10^{-7}$  | 4.033    | -0.0013            | $3.0646 \times 10^{-7}$  | 4.033              | -0.0013  | $3.8667 \times 10^{-7}$  |
| 23  | V  | $1.0713 \times 10^{-8}$  | 2.449  | $1.9663 \times 10^{-8}$  | 2.714    | 0.2642             | $1.5647 \times 10^{-8}$  | 2.714              | 0.2642   | $1.0713 \times 10^{-8}$  |
| 24  | Cr | $4.4262 \times 10^{-7}$  | 4.057  | $4.4197 \times 10^{-7}$  | 4.057    | -0.0002            | $3.5170 \times 10^{-7}$  | 4.057              | -0.0002  | $4.4262 \times 10^{-7}$  |
| 25  | Mn | $2.4179 \times 10^{-7}$  | 3.770  | $2.4208 \times 10^{-7}$  | 3.771    | 0.0010             | $1.9263 \times 10^{-7}$  | 3.771              | 0.0010   | $2.4179 \times 10^{-7}$  |
| 26  | Fe | $3.1648 \times 10^{-5}$  | 5.880  | $3.1613 \times 10^{-5}$  | 5.880    | 0.0000             | $2.5156 \times 10^{-5}$  | 5.880              | 0.0000   | $3.1648 \times 10^{-5}$  |
| 27  | Co | $1.0309 \times 10^{-7}$  | 3.369  | $1.8921 \times 10^{-7}$  | 3.634    | 0.2642             | $1.5057 \times 10^{-7}$  | 3.634              | 0.2642   | $1.0309 \times 10^{-7}$  |
| 28  | Ni | $2.0542 \times 10^{-6}$  | 4.671  | $2.0503 \times 10^{-6}$  | 4.670    | -0.0003            | $1.6315 \times 10^{-6}$  | 4.670              | -0.0003  | $2.0542 \times 10^{-6}$  |
| 29  | Cu | $2.1673 \times 10^{-8}$  | 2.659  | $3.9781 \times 10^{-8}$  | 2.924    | 0.2642             | $3.1656 \times 10^{-8}$  | 2.924              | 0.2642   | $2.1673 \times 10^{-8}$  |
| 30  | Zn | $5.4737 \times 10^{-8}$  | 3.049  | $1.0047 \times 10^{-7}$  | 3.314    | 0.2642             | $7.9948 \times 10^{-8}$  | 3.314              | 0.2642   | $5.4737 \times 10^{-8}$  |
| 31  | Ga | $1.1123 \times 10^{-9}$  | 1.329  | $2.0416 \times 10^{-9}$  | 1.594    | 0.2642             | $1.6246 \times 10^{-9}$  | 1.594              | 0.2642   | $1.1123 \times 10^{-9}$  |
| 32  | Ge | $3.9266 \times 10^{-9}$  | 1.859  | $7.2071 \times 10^{-9}$  | 2.124    | 0.2642             | $5.7351 \times 10^{-9}$  | 2.124              | 0.2642   | $3.9266 \times 10^{-9}$  |
| 33  | As | $3.6935 \times 10^{-10}$ | 0.819  | $6.7794 \times 10^{-10}$ | 1.084    | 0.2642             | $5.3948 \times 10^{-10}$ | 1.084              | 0.2642   | $3.6935 \times 10^{-10}$ |
| 34  | Se | $4.2682 \times 10^{-9}$  | 1.859  | $7.8341 \times 10^{-9}$  | 2.124    | 0.2642             | $6.2341 \times 10^{-9}$  | 2.124              | 0.2642   | $4.2682 \times 10^{-9}$  |
| 35  | Br | $7.1681 \times 10^{-10}$ | 1.079  | $1.3157 \times 10^{-9}$  | 1.344    | 0.2642             | $1.0470 \times 10^{-9}$  | 1.344              | 0.2642   | $7.1681 \times 10^{-10}$ |
| 36  | Kr | $3.5981 \times 10^{-9}$  | 1.759  | $6.6042 \times 10^{-9}$  | 2.024    | 0.2642             | $5.2553 \times 10^{-9}$  | 2.024              | 0.2642   | $3.5981 \times 10^{-9}$  |
| 37  | Rb | $7.1555 \times 10^{-10}$ | 1.049  | $1.3134 \times 10^{-9}$  | 1.314    | 0.2642             | $1.0451 \times 10^{-9}$  | 1.314              | 0.2642   | $7.1555 \times 10^{-10}$ |
| 38  | Sr | $1.7197 \times 10^{-9}$  | 1.419  | $3.1564 \times 10^{-9}$  | 1.684    | 0.2642             | $2.5117 \times 10^{-9}$  | 1.684              | 0.2642   | $1.7197 \times 10^{-9}$  |
| 39  | Y  | $3.2491 \times 10^{-10}$ | 0.689  | $5.9637 \times 10^{-10}$ | 0.954    | 0.2642             | $4.7456 \times 10^{-10}$ | 0.954              | 0.2642   | $3.2491 \times 10^{-10}$ |
| 40  | Zr | $7.6374 \times 10^{-10}$ | 1.049  | $1.4018 \times 10^{-9}$  | 1.314    | 0.2642             | $1.1155 \times 10^{-9}$  | 1.314              | 0.2642   | $7.6374 \times 10^{-10}$ |
| 41  | Nb | $5.1390 \times 10^{-11}$ | -0.131 | $9.4326 \times 10^{-11}$ | 0.134    | 0.2642             | $7.5060 \times 10^{-11}$ | 0.134              | 0.2642   | $5.1390 \times 10^{-11}$ |
| 42  | Mo | $1.6785 \times 10^{-10}$ | 0.369  | $3.0809 \times 10^{-10}$ | 0.634    | 0.2642             | $2.4516 \times 10^{-10}$ | 0.634              | 0.2642   | $1.6785 \times 10^{-10}$ |
| 43  | Tc | $2.2598 \times 10^{-20}$ | -9.511 | $4.1477 \times 10^{-20}$ | -9.246   | 0.2642             | $3.3006 \times 10^{-20}$ | -9.246             | 0.2642   | $2.2598 \times 10^{-20}$ |
| 44  | Ru | $1.4705 \times 10^{-10}$ | 0.289  | $2.6990 \times 10^{-10}$ | 0.554    | 0.2642             | $2.1478 \times 10^{-10}$ | 0.554              | 0.2642   | $1.4705 \times 10^{-10}$ |
| 45  | Rh | $2.8528 \times 10^{-11}$ | -0.431 | $5.2363 \times 10^{-11}$ | -0.166   | 0.2642             | $4.1668 \times 10^{-11}$ | -0.166             | 0.2642   | $2.8528 \times 10^{-11}$ |
| 46  | Pd | $1.0961 \times 10^{-10}$ | 0.139  | $2.0119 \times 10^{-10}$ | 0.404    | 0.2642             | $1.6010 \times 10^{-10}$ | 0.404              | 0.2642   | $1.0961 \times 10^{-10}$ |
| 47  | Ag | $1.9757 \times 10^{-11}$ | -0.611 | $3.6264 \times 10^{-11}$ | -0.346   | 0.2642             | $2.8857 \times 10^{-11}$ | -0.346             | 0.2642   | $1.9757 \times 10^{-11}$ |
| 48  | Cd | $1.3920 \times 10^{-10}$ | 0.219  | $2.5550 \times 10^{-10}$ | 0.484    | 0.2642             | $2.0332 \times 10^{-10}$ | 0.484              | 0.2642   | $1.3920 \times 10^{-10}$ |
| 49  | In | $1.1037 \times 10^{-10}$ | 0.109  | $2.0258 \times 10^{-10}$ | 0.374    | 0.2642             | $1.6120 \times 10^{-10}$ | 0.374              | 0.2642   | $1.1037 \times 10^{-10}$ |
| 50  | Sn | $2.4965 \times 10^{-10}$ | 0.449  | $4.5822 \times 10^{-10}$ | 0.714    | 0.2642             | $3.6463 \times 10^{-10}$ | 0.714              | 0.2642   | $2.4965 \times 10^{-10}$ |
| 51  | Sb | $2.5606 \times 10^{-11}$ | -0.551 | $4.6999 \times 10^{-11}$ | -0.286   | 0.2642             | $3.7400 \times 10^{-11}$ | -0.286             | 0.2642   | $2.5606 \times 10^{-11}$ |
| 52  | Te | $4.6632 \times 10^{-10}$ | 0.689  | $8.5592 \times 10^{-10}$ | 0.954    | 0.2642             | $6.8111 \times 10^{-10}$ | 0.954              | 0.2642   | $4.6632 \times 10^{-10}$ |
| 53  | I  | $8.6360 \times 10^{-11}$ | -0.041 | $1.5851 \times 10^{-10}$ | 0.224    | 0.2642             | $1.2614 \times 10^{-10}$ | 0.224              | 0.2642   | $8.6360 \times 10^{-11}$ |
| 54  | Xe | $4.0839 \times 10^{-10}$ | 0.619  | $7.4959 \times 10^{-10}$ | 0.884    | 0.2642             | $5.9649 \times 10^{-10}$ | 0.884              | 0.2642   | $4.0839 \times 10^{-10}$ |
| 55  | Cs | $3.7703 \times 10^{-11}$ | -0.421 | $6.9203 \times 10^{-11}$ | -0.156   | 0.2642             | $5.5069 \times 10^{-11}$ | -0.156             | 0.2642   | $3.7703 \times 10^{-11}$ |
| 56  | Ba | $3.8958 \times 10^{-10}$ | 0.579  | $7.1506 \times 10^{-10}$ | 0.844    | 0.2642             | $5.6901 \times 10^{-10}$ | 0.844              | 0.2642   | $3.8958 \times 10^{-10}$ |
| 57  | La | $4.3207 \times 10^{-11}$ | -0.381 | $7.9306 \times 10^{-11}$ | -0.116   | 0.2642             | $6.3108 \times 10^{-11}$ | -0.116             | 0.2642   | $4.3207 \times 10^{-11}$ |
| 58  | Ce | $1.1203 \times 10^{-10}$ | 0.029  | $2.0562 \times 10^{-10}$ | 0.294    | 0.2642             | $1.6363 \times 10^{-10}$ | 0.294              | 0.2642   | $1.1203 \times 10^{-10}$ |
| 59  | Pr | $1.5197 \times 10^{-11}$ | -0.841 | $2.7895 \times 10^{-11}$ | -0.576   | 0.2642             | $2.2197 \times 10^{-11}$ | -0.576             | 0.2642   | $1.5197 \times 10^{-11}$ |
| 60  | Nd | $9.5924 \times 10^{-11}$ | -0.051 | $1.7607 \times 10^{-10}$ | 0.214    | 0.2642             | $1.4011 \times 10^{-10}$ | 0.214              | 0.2642   | $9.5924 \times 10^{-11}$ |
| 61  | Pm | $3.3435 \times 10^{-20}$ | -9.511 | $6.1369 \times 10^{-20}$ | -9.246   | 0.2642             | $4.8835 \times 10^{-20}$ | -9.246             | 0.2642   | $3.3435 \times 10^{-20}$ |
| 62  | Sm | $3.2357 \times 10^{-11}$ | -0.541 | $5.9391 \times 10^{-11}$ | -0.276   | 0.2642             | $4.7260 \times 10^{-11}$ | -0.276             | 0.2642   | $3.2357 \times 10^{-11}$ |
| 63  | Eu | $1.0341 \times 10^{-11}$ | -1.041 | $1.8981 \times 10^{-11}$ | -0.776   | 0.2642             | $1.5104 \times 10^{-11}$ | -0.776             | 0.2642   | $1.0341 \times 10^{-11}$ |
| 64  | Gd | $4.3594 \times 10^{-11}$ | -0.431 | $8.0016 \times 10^{-11}$ | -0.166   | 0.2642             | $6.3673 \times 10^{-11}$ | -0.166             | 0.2642   | $4.3594 \times 10^{-11}$ |
| 65  | Tb | $7.4822 \times 10^{-12}$ | -1.201 | $1.3733 \times 10^{-11}$ | -0.936   | 0.2642             | $1.0928 \times 10^{-11}$ | -0.936             | 0.2642   | $7.4822 \times 10^{-12}$ |
| 66  | Dy | $4.7173 \times 10^{-11}$ | -0.411 | $8.6584 \times 10^{-11}$ | -0.146   | 0.2642             | $6.8900 \times 10^{-11}$ | -0.146             | 0.2642   | $4.7173 \times 10^{-11}$ |
| 67  | Ho | $6.3116 \times 10^{-12}$ | -1.291 | $1.1585 \times 10^{-11}$ | -1.026   | 0.2642             | $9.2186 \times 10^{-12}$ | -1.026             | 0.2642   | $6.3116 \times 10^{-12}$ |
| 68  | Er | $2.9938 \times 10^{-11}$ | -0.621 | $5.4951 \times 10^{-11}$ | -0.356   | 0.2642             | $4.3727 \times 10^{-11}$ | -0.356             | 0.2642   | $2.9938 \times 10^{-11}$ |
| 69  | Tm | $3.5527 \times 10^{-12}$ | -1.551 | $6.5208 \times 10^{-12}$ | -1.286   | 0.2642             | $5.1890 \times 10^{-12}$ | -1.286             | 0.2642   | $3.5527 \times 10^{-12}$ |
| 70  | Yb | $4.3754 \times 10^{-11}$ | -0.471 | $8.0309 \times 10^{-11}$ | -0.206   | 0.2642             | $6.3907 \times 10^{-11}$ | -0.206             | 0.2642   | $4.3754 \times 10^{-11}$ |

Table A.1: Continued.

| No. | El | Reference $Y = 0.246$    |        | CNO $Na_1$ $Y = 0.246$   |                   | CNO $Na_1$ $Y = 0.400$ |                          | CNO $Na_2$ $Y = 0.246$ |                         |
|-----|----|--------------------------|--------|--------------------------|-------------------|------------------------|--------------------------|------------------------|-------------------------|
|     |    | Mass frac.               | [El]   | Mass frac.               | [El] <sub>1</sub> | Mass frac.             | [El] <sub>2</sub>        | Mass frac.             | [El] <sub>3</sub>       |
| 71  | Lu | $4.2247 \times 10^{-12}$ | -1.491 | $7.7543 \times 10^{-12}$ | -1.226            | 0.2642                 | $6.1705 \times 10^{-12}$ | -1.226                 | 0.2642                  |
| 72  | Hf | $2.8474 \times 10^{-11}$ | -0.671 | $5.2264 \times 10^{-11}$ | -0.406            | 0.2642                 | $4.1589 \times 10^{-11}$ | -0.406                 | 0.2642                  |
| 73  | Ta | $2.8209 \times 10^{-12}$ | -1.681 | $5.1777 \times 10^{-12}$ | -1.416            | 0.2642                 | $4.1202 \times 10^{-12}$ | -1.416                 | 0.2642                  |
| 74  | W  | $4.9805 \times 10^{-11}$ | -0.441 | $9.1416 \times 10^{-11}$ | -0.176            | 0.2642                 | $7.2745 \times 10^{-11}$ | -0.176                 | 0.2642                  |
| 75  | Re | $7.4616 \times 10^{-12}$ | -1.271 | $1.3696 \times 10^{-11}$ | -1.006            | 0.2642                 | $1.0898 \times 10^{-11}$ | -1.006                 | 0.2642                  |
| 76  | Os | $1.1275 \times 10^{-10}$ | -0.101 | $2.0695 \times 10^{-10}$ | 0.164             | 0.2642                 | $1.6468 \times 10^{-10}$ | 0.164                  | 0.2642                  |
| 77  | Ir | $9.0496 \times 10^{-11}$ | -0.201 | $1.6610 \times 10^{-10}$ | 0.064             | 0.2642                 | $1.3218 \times 10^{-10}$ | 0.064                  | 0.2642                  |
| 78  | Pt | $2.5886 \times 10^{-10}$ | 0.249  | $4.7512 \times 10^{-10}$ | 0.514             | 0.2642                 | $3.7808 \times 10^{-10}$ | 0.514                  | 0.2642                  |
| 79  | Au | $4.2387 \times 10^{-11}$ | -0.541 | $7.7800 \times 10^{-11}$ | -0.276            | 0.2642                 | $6.1909 \times 10^{-11}$ | -0.276                 | 0.2642                  |
| 80  | Hg | $5.6904 \times 10^{-11}$ | -0.421 | $1.0445 \times 10^{-10}$ | -0.156            | 0.2642                 | $8.3114 \times 10^{-11}$ | -0.156                 | 0.2642                  |
| 81  | Tl | $3.4141 \times 10^{-11}$ | -0.651 | $6.2666 \times 10^{-11}$ | -0.386            | 0.2642                 | $4.9867 \times 10^{-11}$ | -0.386                 | 0.2642                  |
| 82  | Pb | $3.8835 \times 10^{-10}$ | 0.399  | $7.1281 \times 10^{-10}$ | 0.664             | 0.2642                 | $5.6722 \times 10^{-10}$ | 0.664                  | 0.2642                  |
| 83  | Bi | $2.2539 \times 10^{-11}$ | -0.841 | $4.1370 \times 10^{-11}$ | -0.576            | 0.2642                 | $3.2921 \times 10^{-11}$ | -0.576                 | 0.2642                  |
| 84  | Po | $4.8193 \times 10^{-20}$ | -9.511 | $8.8457 \times 10^{-20}$ | -9.246            | 0.2642                 | $7.0390 \times 10^{-20}$ | -9.246                 | 0.2642                  |
| 85  | At | $4.8423 \times 10^{-20}$ | -9.511 | $8.8880 \times 10^{-20}$ | -9.246            | 0.2642                 | $7.0727 \times 10^{-20}$ | -9.246                 | 0.2642                  |
| 86  | Rn | $5.1191 \times 10^{-20}$ | -9.511 | $9.3959 \times 10^{-20}$ | -9.246            | 0.2642                 | $7.4768 \times 10^{-20}$ | -9.246                 | 0.2642                  |
| 87  | Fr | $5.1421 \times 10^{-20}$ | -9.511 | $9.4382 \times 10^{-20}$ | -9.246            | 0.2642                 | $7.5105 \times 10^{-20}$ | -9.246                 | 0.2642                  |
| 88  | Ra | $5.2113 \times 10^{-20}$ | -9.511 | $9.5652 \times 10^{-20}$ | -9.246            | 0.2642                 | $7.6115 \times 10^{-20}$ | -9.246                 | 0.2642                  |
| 89  | Ac | $5.2343 \times 10^{-20}$ | -9.511 | $9.6075 \times 10^{-20}$ | -9.246            | 0.2642                 | $7.6452 \times 10^{-20}$ | -9.246                 | 0.2642                  |
| 90  | Th | $6.0034 \times 10^{-12}$ | -1.461 | $1.1019 \times 10^{-11}$ | -1.196            | 0.2642                 | $8.7685 \times 10^{-12}$ | -1.196                 | 0.2642                  |
| 91  | Pa | $5.3274 \times 10^{-20}$ | -9.511 | $9.7783 \times 10^{-20}$ | -9.246            | 0.2642                 | $7.7812 \times 10^{-20}$ | -9.246                 | 0.2642                  |
| 92  | U  | $1.5829 \times 10^{-12}$ | -2.051 | $2.9055 \times 10^{-12}$ | -1.786            | 0.2642                 | $2.3120 \times 10^{-12}$ | -1.786                 | 0.2642                  |
| 93  | Np | $5.4649 \times 10^{-20}$ | -9.511 | $1.0031 \times 10^{-19}$ | -9.246            | 0.2642                 | $7.9820 \times 10^{-20}$ | -9.246                 | 0.2642                  |
| 94  | Pu | $5.6263 \times 10^{-20}$ | -9.511 | $1.0327 \times 10^{-19}$ | -9.246            | 0.2642                 | $8.2178 \times 10^{-20}$ | -9.246                 | 0.2642                  |
| 95  | Am | $5.6033 \times 10^{-20}$ | -9.511 | $1.0285 \times 10^{-19}$ | -9.246            | 0.2642                 | $8.1841 \times 10^{-20}$ | -9.246                 | 0.2642                  |
| 96  | Cm | $5.6955 \times 10^{-20}$ | -9.511 | $1.0454 \times 10^{-19}$ | -9.246            | 0.2642                 | $8.3188 \times 10^{-20}$ | -9.246                 | 0.2642                  |
| 97  | Bk | $5.6955 \times 10^{-20}$ | -9.511 | $1.0454 \times 10^{-19}$ | -9.246            | 0.2642                 | $8.3188 \times 10^{-20}$ | -9.246                 | 0.2642                  |
| 98  | Cf | $5.7878 \times 10^{-20}$ | -9.511 | $1.0623 \times 10^{-19}$ | -9.246            | 0.2642                 | $8.4535 \times 10^{-20}$ | -9.246                 | 0.2642                  |
| 99  | Es | $5.8108 \times 10^{-20}$ | -9.511 | $1.0666 \times 10^{-19}$ | -9.246            | 0.2642                 | $8.4872 \times 10^{-20}$ | -9.246                 | 0.2642                  |
| Z   |    | $9.9937 \times 10^{-4}$  |        | $1.8343 \times 10^{-3}$  |                   |                        | $1.4597 \times 10^{-3}$  |                        | $9.9937 \times 10^{-4}$ |



## Appendix B

# Theoretical indices calculated for the case of M3

Table B.1 shows all spectral indices calculated for the MS-TO, RGB and HB for the four chemical compositions over all range of effective temperature (4,300 - 7,000 K). The label of the chemical mixtures are abbreviated as Ref, 1Y2, 1Y4 and 2Y2 for the Reference, CNONa1Y2, CNONa1Y4 and CNONa2Y2, respectively.

Table B.1: All of the spectroscopic indices calculated for the three different set of physical conditions representing at the evolutionary stages MS-TO, RGB and HB of M3, extended over the entire range of effective temperature.

| Index           | T[K] | MS-TO ( $\log g = 4.2$ ) |         |         | RGB ( $\log g = 2.4$ ) |         |         | HB ( $\log g = 2.8$ ) |         |         |         |         |
|-----------------|------|--------------------------|---------|---------|------------------------|---------|---------|-----------------------|---------|---------|---------|---------|
|                 |      | Ref                      | 1Y2     | 1Y4     | 2Y2                    | Ref     | 1Y2     | 1Y4                   | 2Y2     | Ref     | 1Y2     | 1Y4     |
|                 | 4300 | 0.0514                   | 0.0951  | 0.0910  | 0.0800                 | 0.0331  | 0.1832  | 0.1784                | 0.1346  | 0.0401  | 0.1636  | 0.1587  |
|                 | 4400 | 0.0380                   | 0.0881  | 0.0840  | 0.0702                 | 0.0153  | 0.1727  | 0.1682                | 0.1207  | 0.0216  | 0.1541  | 0.1494  |
|                 | 4500 | 0.0234                   | 0.0805  | 0.0764  | 0.0600                 | 0.0005  | 0.1585  | 0.1545                | 0.1040  | 0.0061  | 0.1430  | 0.1386  |
|                 | 4600 | 0.0093                   | 0.0733  | 0.0694  | 0.0503                 | -0.0115 | 0.1386  | 0.1354                | 0.0837  | -0.0067 | 0.1281  | 0.1243  |
|                 | 4700 | -0.0028                  | 0.0660  | 0.0624  | 0.0412                 | -0.0207 | 0.1132  | 0.1109                | 0.0611  | -0.0168 | 0.1082  | 0.1054  |
|                 | 4800 | -0.0126                  | 0.0577  | 0.0545  | 0.0322                 | -0.0270 | 0.0849  | 0.0835                | 0.0396  | -0.0243 | 0.0848  | 0.0829  |
|                 | 4900 | -0.0203                  | 0.0476  | 0.0450  | 0.0231                 | -0.0308 | 0.0577  | 0.0570                | 0.0220  | -0.0293 | 0.0606  | 0.0594  |
|                 | 5000 | -0.0261                  | 0.0361  | 0.0343  | 0.0141                 | -0.0322 | 0.0347  | 0.0344                | 0.0090  | -0.0320 | 0.0386  | 0.0380  |
|                 | 5100 | -0.0302                  | 0.0243  | 0.0230  | 0.0059                 | -0.0321 | 0.0170  | 0.0168                | -0.0001 | -0.0328 | 0.0207  | 0.0204  |
|                 | 5200 | -0.0327                  | 0.0132  | 0.0124  | -0.0011                | -0.0310 | 0.0039  | 0.0038                | -0.0065 | -0.0325 | 0.0071  | 0.0069  |
|                 | 5300 | -0.0340                  | 0.0036  | 0.0031  | -0.0068                | -0.0299 | -0.0058 | -0.0058               | -0.0117 | -0.0316 | -0.0031 | -0.0032 |
|                 | 5400 | -0.0344                  | -0.0044 | -0.0048 | -0.0114                | -0.0297 | -0.0133 | -0.0134               | -0.0165 | -0.0310 | -0.0110 | -0.0111 |
|                 | 5500 | -0.0345                  | -0.0112 | -0.0114 | -0.0156                | -0.0307 | -0.0199 | -0.0199               | -0.0215 | -0.0315 | -0.0178 | -0.0200 |
| CN <sub>1</sub> | 5600 | -0.0348                  | -0.0172 | -0.0173 | -0.0197                | -0.0335 | -0.0264 | -0.0264               | -0.0272 | -0.0334 | -0.0242 | -0.0242 |
|                 | 5700 | -0.0358                  | -0.0229 | -0.0229 | -0.0241                | -0.0378 | -0.0333 | -0.0333               | -0.0336 | -0.0369 | -0.0308 | -0.0308 |
|                 | 5800 | -0.0380                  | -0.0287 | -0.0286 | -0.0292                | -0.0435 | -0.0406 | -0.0407               | -0.0408 | -0.0418 | -0.0379 | -0.0378 |
|                 | 5900 | -0.0414                  | -0.0350 | -0.0348 | -0.0350                | -0.0505 | -0.0486 | -0.0486               | -0.0487 | -0.0482 | -0.0456 | -0.0457 |
|                 | 6000 | -0.0462                  | -0.0417 | -0.0415 | -0.0415                | -0.0584 | -0.0572 | -0.0573               | -0.0573 | -0.0556 | -0.0540 | -0.0539 |
|                 | 6100 | -0.0521                  | -0.0491 | -0.0489 | -0.0488                | -0.0672 | -0.0663 | -0.0665               | -0.0666 | -0.0640 | -0.0629 | -0.0629 |
|                 | 6200 | -0.0590                  | -0.0571 | -0.0568 | -0.0567                | -0.0766 | -0.0760 | -0.0762               | -0.0763 | -0.0732 | -0.0724 | -0.0724 |
|                 | 6300 | -0.0670                  | -0.0658 | -0.0655 | -0.0654                | -0.0864 | -0.0859 | -0.0863               | -0.0862 | -0.0829 | -0.0824 | -0.0824 |
|                 | 6400 | -0.0759                  | -0.0752 | -0.0748 | -0.0748                | -0.0965 | -0.0961 | -0.0965               | -0.0964 | -0.0932 | -0.0928 | -0.0930 |
|                 | 6500 | -0.0856                  | -0.0852 | -0.0848 | -0.0848                | -0.1071 | -0.1067 | -0.1073               | -0.1071 | -0.1037 | -0.1034 | -0.1036 |
|                 | 6600 | -0.0957                  | -0.0956 | -0.0952 | -0.0952                | -0.1177 | -0.1174 | -0.1181               | -0.1178 | -0.1147 | -0.1145 | -0.1148 |
|                 | 6700 | -0.1065                  | -0.1065 | -0.1061 | -0.1062                | -0.1281 | -0.1279 | -0.1289               | -0.1283 | -0.1258 | -0.1256 | -0.1262 |
|                 | 6800 | -0.1177                  | -0.1177 | -0.1174 | -0.1175                | -0.1387 | -0.1384 | -0.1395               | -0.1388 | -0.1367 | -0.1366 | -0.1373 |
|                 | 6900 | -0.1292                  | -0.1293 | -0.1289 | -0.1290                | -0.1495 | -0.1493 | -0.1506               | -0.1496 | -0.1477 | -0.1476 | -0.1485 |
|                 | 7000 | -0.1411                  | -0.1412 | -0.1409 | -0.1410                | -0.1605 | -0.1603 | -0.1618               | -0.1607 | -0.1589 | -0.1589 | -0.1591 |

Table B.1: Continued.

| Index           | T[K] | MS-TO ( $\log g = 4.2$ ) |         |         |         | RGB ( $\log g = 2.4$ ) |         |         |         | HB ( $\log g = 2.8$ ) |         |         |         |
|-----------------|------|--------------------------|---------|---------|---------|------------------------|---------|---------|---------|-----------------------|---------|---------|---------|
|                 |      | Ref                      | IY2     | IY4     | 2Y2     | Ref                    | IY2     | IY4     | 2Y2     | Ref                   | IY2     | IY4     | 2Y2     |
| CN <sub>2</sub> | 4300 | 0.1314                   | 0.1766  | 0.1743  | 0.1583  | 0.0838                 | 0.2403  | 0.2362  | 0.1875  | 0.0974                | 0.2259  | 0.2218  | 0.1798  |
|                 | 4400 | 0.1060                   | 0.1582  | 0.1556  | 0.1375  | 0.0543                 | 0.2188  | 0.2148  | 0.1628  | 0.0662                | 0.2045  | 0.2004  | 0.1553  |
|                 | 4500 | 0.0789                   | 0.1385  | 0.1357  | 0.1155  | 0.0300                 | 0.1959  | 0.1923  | 0.1377  | 0.0404                | 0.1838  | 0.1798  | 0.1324  |
|                 | 4600 | 0.0530                   | 0.1199  | 0.1170  | 0.0947  | 0.0112                 | 0.1696  | 0.1667  | 0.1115  | 0.0197                | 0.1615  | 0.1581  | 0.1095  |
|                 | 4700 | 0.0311                   | 0.1036  | 0.1007  | 0.0769  | -0.0023                | 0.1400  | 0.1380  | 0.0852  | 0.0040                | 0.1366  | 0.1340  | 0.0863  |
|                 | 4800 | 0.0140                   | 0.0888  | 0.0861  | 0.0617  | -0.0108                | 0.1095  | 0.1082  | 0.0619  | -0.0068               | 0.1100  | 0.1082  | 0.0647  |
|                 | 4900 | 0.0011                   | 0.0743  | 0.0720  | 0.0483  | -0.0147                | 0.0816  | 0.0808  | 0.0439  | -0.0131               | 0.0843  | 0.0832  | 0.0467  |
|                 | 5000 | -0.0079                  | 0.0601  | 0.0584  | 0.0367  | -0.0149                | 0.0589  | 0.0585  | 0.0317  | -0.0154               | 0.0622  | 0.0616  | 0.0334  |
|                 | 5100 | -0.0136                  | 0.0469  | 0.0457  | 0.0272  | -0.0125                | 0.0424  | 0.0421  | 0.0241  | -0.0147               | 0.0451  | 0.0447  | 0.0248  |
|                 | 5200 | -0.0163                  | 0.0355  | 0.0347  | 0.0201  | -0.0084                | 0.0311  | 0.0309  | 0.0197  | -0.0119               | 0.0329  | 0.0326  | 0.0195  |
|                 | 5300 | -0.0165                  | 0.0265  | 0.0259  | 0.0152  | -0.0040                | 0.0237  | 0.0235  | 0.0170  | -0.0079               | 0.0247  | 0.0245  | 0.0164  |
|                 | 5400 | -0.0150                  | 0.0197  | 0.0193  | 0.0120  | -0.0003                | 0.0187  | 0.0185  | 0.0149  | -0.0041               | 0.0191  | 0.0189  | 0.0142  |
|                 | 5500 | -0.0124                  | 0.0148  | 0.0145  | 0.0098  | 0.0020                 | 0.0148  | 0.0145  | 0.0127  | -0.0011               | 0.0149  | 0.0147  | 0.0122  |
|                 | 5600 | -0.0095                  | 0.0112  | 0.0109  | 0.0082  | 0.0027                 | 0.0111  | 0.0109  | 0.0100  | 0.0004                | 0.0112  | 0.0111  | 0.0098  |
|                 | 5700 | -0.0072                  | 0.0081  | 0.0079  | 0.0065  | 0.0017                 | 0.0072  | 0.0069  | 0.0066  | 0.0003                | 0.0075  | 0.0073  | 0.0068  |
|                 | 5800 | -0.0059                  | 0.0052  | 0.0050  | 0.0044  | -0.0007                | 0.0028  | 0.0026  | 0.0025  | -0.0013               | 0.0035  | 0.0033  | 0.0031  |
|                 | 5900 | -0.0058                  | 0.0020  | 0.0019  | 0.0017  | -0.0043                | 0.0020  | -0.0023 | -0.0022 | -0.0043               | -0.0012 | -0.0014 | -0.0014 |
|                 | 6000 | -0.0071                  | -0.0017 | -0.0018 | -0.0017 | -0.0090                | -0.0074 | -0.0078 | -0.0077 | -0.0085               | -0.0065 | -0.0067 | -0.0066 |
|                 | 6100 | -0.0097                  | -0.0060 | -0.0060 | -0.0058 | -0.0145                | -0.0134 | -0.0138 | -0.0137 | -0.0137               | -0.0123 | -0.0126 | -0.0124 |
|                 | 6200 | -0.0134                  | -0.0110 | -0.0110 | -0.0107 | -0.0206                | -0.0198 | -0.0203 | -0.0202 | -0.0197               | -0.0187 | -0.0190 | -0.0189 |
|                 | 6300 | -0.0183                  | -0.0167 | -0.0166 | -0.0164 | -0.0272                | -0.0265 | -0.0273 | -0.0269 | -0.0262               | -0.0256 | -0.0259 | -0.0257 |
|                 | 6400 | -0.0242                  | -0.0232 | -0.0230 | -0.0229 | -0.0341                | -0.0336 | -0.0343 | -0.0339 | -0.0334               | -0.0329 | -0.0334 | -0.0331 |
|                 | 6500 | -0.0309                  | -0.0303 | -0.0302 | -0.0300 | -0.0415                | -0.0411 | -0.0420 | -0.0415 | -0.0408               | -0.0405 | -0.0411 | -0.0407 |
|                 | 6600 | -0.0382                  | -0.0379 | -0.0378 | -0.0376 | -0.0491                | -0.0487 | -0.0499 | -0.0491 | -0.0489               | -0.0486 | -0.0493 | -0.0489 |
|                 | 6700 | -0.0463                  | -0.0461 | -0.0460 | -0.0459 | -0.0566                | -0.0562 | -0.0576 | -0.0567 | -0.0571               | -0.0568 | -0.0579 | -0.0571 |
|                 | 6800 | -0.0548                  | -0.0548 | -0.0548 | -0.0546 | -0.0642                | -0.0639 | -0.0655 | -0.0643 | -0.0652               | -0.0650 | -0.0662 | -0.0653 |
|                 | 6900 | -0.0638                  | -0.0639 | -0.0639 | -0.0637 | -0.0723                | -0.0720 | -0.0738 | -0.0724 | -0.0735               | -0.0733 | -0.0747 | -0.0736 |
|                 | 7000 | -0.0733                  | -0.0734 | -0.0734 | -0.0732 | -0.0807                | -0.0805 | -0.0825 | -0.0809 | -0.0821               | -0.0820 | -0.0834 | -0.0822 |
| Ca4227          | 4300 | 4.6070                   | 4.0529  | 4.2490  | 4.2161  | 1.8763                 | 4.4834  | 0.5880  | 0.8804  | 2.3048                | 1.1318  | 1.2701  | 1.5011  |
|                 | 4400 | 3.8998                   | 3.3885  | 3.5789  | 3.5895  | 1.4558                 | -0.0074 | 0.0807  | 0.4281  | 1.7921                | 0.5271  | 0.6448  | 0.9385  |
|                 | 4500 | 3.2530                   | 2.6845  | 2.8710  | 2.9252  | 1.1357                 | -0.3201 | -0.2478 | 0.1510  | 1.4045                | 0.1033  | 0.2022  | 0.5495  |
|                 | 4600 | 2.6509                   | 2.0131  | 2.1844  | 2.2926  | 0.8893                 | -0.4637 | -0.4072 | 0.0339  | 1.1058                | -0.1516 | -0.0710 | 0.3202  |
|                 | 4700 | 2.1475                   | 1.4767  | 1.6245  | 1.7861  | 0.7021                 | -0.4554 | -0.4147 | 0.0437  | 0.8738                | -0.2513 | -0.1892 | 0.2279  |
|                 | 4800 | 1.7445                   | 1.0863  | 1.2098  | 1.4124  | 0.5651                 | -0.3380 | -0.3108 | 0.1239  | 0.6972                | -0.2254 | -0.1802 | 0.2319  |
|                 | 4900 | 1.4225                   | 0.8275  | 0.9279  | 1.1532  | 0.4705                 | -0.1688 | -0.1525 | 0.2193  | 0.5667                | -0.1214 | -0.0903 | 0.2814  |
|                 | 5000 | 1.1662                   | 0.6749  | 0.7547  | 0.9823  | 0.4082                 | 0.0004  | 0.0092  | 0.2969  | 0.4747                | 0.0099  | 0.0304  | 0.3356  |
|                 | 5100 | 0.9641                   | 0.5963  | 0.6592  | 0.8699  | 0.3677                 | 0.1377  | 0.1419  | 0.3445  | 0.4124                | 0.1308  | 0.1439  | 0.3735  |
|                 | 5200 | 0.8076                   | 0.5599  | 0.6091  | 0.7898  | 0.3406                 | 0.2309  | 0.2326  | 0.3633  | 0.3705                | 0.2212  | 0.2300  | 0.3894  |
|                 | 5300 | 0.6884                   | 0.5405  | 0.5795  | 0.7238  | 0.3204                 | 0.2810  | 0.2816  | 0.3596  | 0.3414                | 0.2759  | 0.2821  | 0.3853  |
|                 | 5400 | 0.5989                   | 0.5231  | 0.5546  | 0.6635  | 0.3022                 | 0.2984  | 0.2986  | 0.3417  | 0.3185                | 0.2988  | 0.3037  | 0.3668  |
|                 | 5500 | 0.5308                   | 0.5002  | 0.5262  | 0.6050  | 0.2838                 | 0.2943  | 0.2944  | 0.3165  | 0.2978                | 0.2993  | 0.3030  | 0.3403  |
|                 | 5600 | 0.4769                   | 0.4702  | 0.4922  | 0.5474  | 0.2648                 | 0.2792  | 0.2791  | 0.2895  | 0.2774                | 0.2863  | 0.2892  | 0.3108  |
|                 | 5700 | 0.4313                   | 0.4343  | 0.4533  | 0.4915  | 0.2459                 | 0.2599  | 0.2595  | 0.2638  | 0.2573                | 0.2669  | 0.2691  | 0.2819  |
|                 | 5800 | 0.3909                   | 0.3954  | 0.4120  | 0.4386  | 0.2283                 | 0.2403  | 0.2396  | 0.2410  | 0.2381                | 0.2461  | 0.2476  | 0.2556  |
|                 | 5900 | 0.3537                   | 0.3562  | 0.3706  | 0.3898  | 0.2123                 | 0.2223  | 0.2214  | 0.2215  | 0.2205                | 0.2263  | 0.2273  | 0.2329  |
|                 | 6000 | 0.3195                   | 0.3187  | 0.3312  | 0.3459  | 0.1983                 | 0.2066  | 0.2055  | 0.2053  | 0.2049                | 0.2088  | 0.2093  | 0.2138  |
|                 | 6100 | 0.2886                   | 0.2845  | 0.2954  | 0.3074  | 0.1865                 | 0.1936  | 0.1923  | 0.1922  | 0.1914                | 0.1940  | 0.1940  | 0.1981  |
|                 | 6200 | 0.2607                   | 0.2544  | 0.2634  | 0.2741  | 0.1763                 | 0.1829  | 0.1815  | 0.1814  | 0.1800                | 0.1819  | 0.1814  | 0.1854  |
|                 | 6300 | 0.2365                   | 0.2286  | 0.2360  | 0.2460  | 0.1674                 | 0.1738  | 0.1724  | 0.1724  | 0.1702                | 0.1717  | 0.1710  | 0.1748  |
|                 | 6400 | 0.2158                   | 0.2070  | 0.2129  | 0.2226  | 0.1598                 | 0.1660  | 0.1644  | 0.1649  | 0.1618                | 0.1632  | 0.1623  | 0.1662  |
|                 | 6500 | 0.1981                   | 0.1888  | 0.1935  | 0.2032  | 0.1535                 | 0.1599  | 0.1582  | 0.1589  | 0.1544                | 0.1560  | 0.1549  | 0.1588  |
|                 | 6600 | 0.1828                   | 0.1734  | 0.1770  | 0.1867  | 0.1471                 | 0.1541  | 0.1523  | 0.1530  | 0.1479                | 0.1499  | 0.1485  | 0.1525  |
|                 | 6700 | 0.1699                   | 0.1605  | 0.1632  | 0.1731  | 0.1408                 | 0.1484  | 0.1468  | 0.1474  | 0.1417                | 0.1444  | 0.1430  | 0.1468  |
|                 | 6800 | 0.1586                   | 0.1496  | 0.1516  | 0.1615  | 0.1350                 | 0.1431  | 0.1414  | 0.1421  | 0.1355                | 0.1388  | 0.1374  | 0.1411  |
|                 | 6900 | 0.1489                   | 0.1403  | 0.1415  | 0.1516  | 0.1292                 | 0.1380  | 0.1362  | 0.1370  | 0.1296                | 0.1335  | 0.1321  | 0.1357  |
|                 | 7000 | 0.1404                   | 0.1323  | 0.1330  | 0.1432  | 0.1235                 | 0.1333  | 0.1315  | 0.1320  | 0.1239                | 0.1287  | 0.1271  | 0.1305  |
| G4300           | 4300 | 6.9578                   | 7.0022  | 7.0302  | 6.9419  | 8.0586                 | 8.0135  | 7.9898  | 7.9219  | 7.8330                | 7.7965  | 7.7835  | 7.7043  |
|                 | 4400 | 7.2600                   | 7.2403  | 7.2674  | 7.1876  | 8.2275                 | 8.0210  | 7.9996  | 7.9463  | 8.0046                | 7.8336  | 7.8175  | 7.7564  |
|                 | 4500 | 7.5291                   | 7.3418  | 7.3692  | 7.2999  | 8.3558                 | 7.9226  | 7.9077  | 7.8683  | 8.1514                | 7.7876  | 7.7740  | 7.7290  |
|                 | 4600 | 7.7212                   | 7.3295  | 7.3575  | 7.2978  | 8.4255                 | 7.7000  | 7.6935  | 7.6668  | 8.2518                | 7.6346  | 7.6260  | 7.5943  |
|                 | 4700 | 7.8546                   | 7.2158  | 7.2426  | 7.1946  | 8.4196                 | 7.3456  | 7.3488  | 7.3346  | 8.2863                | 7.3590  | 7.3577  | 7.3353  |
|                 | 4800 | 7.9282                   | 7.0057  | 7.0297  | 6.9926  | 8.3196                 | 6.8701  | 6.8812  | 6.8767  | 8.2405                | 6.9588  | 6.9652  | 6.9522  |
|                 | 4900 | 7.9322                   | 6.6844  | 6.7073  | 6.6780  | 8.1119                 | 6.2967  | 6.3155  | 6.3162  | 8.0934                | 6.4526  | 6.4674  | 6.4598  |
|                 | 5000 | 7.8482                   | 6.2649  | 6.2854  | 6.2656  | 7.7757                 | 5.6514  | 5.6758  | 5.6755  | 7.8327                | 5.8632  | 5.8825  | 5.8768  |
|                 | 5100 | 7.6703                   | 5.7565  | 5.7751  | 5.7626  | 7.2900                 | 4.9686  | 4.9963  | 4.9905  | 7.4401                | 5.2180  | 5.2418  | 5.2328  |
|                 | 5200 | 7.3763                   | 5.1904  | 5.2073  | 5.2008  | 6.6412                 | 4.2904  | 4.3198  | 4.3043  | 6.8983                | 4.5542  | 4.5807  | 4.5652  |
|                 | 5300 | 6.9675                   | 4.5985  | 4.6130  | 4.6094  | 5.8527                 | 3.6625  | 3.6897  | 3.6641  | 6.2092                | 3.9131  | 3.9394  | 3.9151  |
|                 | 5400 | 6.4393                   | 4.0069  | 4.0205  | 4.0160  | 4.9953                 | 3.1162  | 3.1388  | 3.1052  | 5.4118                | 3.3306  | 3.3539  | 3.3217  |
|                 | 5500 | 5.8017                   | 3.4429  | 3.4545  | 3.4487  | 4.1569                 | 2.6596  | 2.6762  | 2.6381  | 4.5805                | 2.8287  | 2.8465  | 2.8100  |
|                 | 5600 | 5.0904                   | 2.9281  |         |         |                        |         |         |         |                       |         |         |         |

Table B.1: Continued.

| Index  | T[K] | MS-TO ( $\log g = 4.2$ ) |         |         |         | RGB ( $\log g = 2.4$ ) |        |        |         | HB ( $\log g = 2.8$ ) |         |         |         |
|--------|------|--------------------------|---------|---------|---------|------------------------|--------|--------|---------|-----------------------|---------|---------|---------|
|        |      | Ref                      | IY2     | IY4     | 2Y2     | Ref                    | IY2    | IY4    | 2Y2     | Ref                   | IY2     | IY4     | 2Y2     |
| Fe4383 | 4300 | 4.6200                   | 4.5902  | 4.6899  | 4.3336  | 4.1740                 | 3.7623 | 3.8175 | 3.6602  | 4.2869                | 3.9602  | 4.0305  | 3.8303  |
|        | 4400 | 4.4657                   | 4.3938  | 4.4924  | 4.1612  | 3.9008                 | 3.4156 | 3.4652 | 3.3214  | 3.9919                | 3.6016  | 3.6639  | 3.4827  |
|        | 4500 | 4.2198                   | 4.0967  | 4.1947  | 3.8846  | 3.6373                 | 3.0876 | 3.1320 | 2.9948  | 3.7134                | 3.2632  | 3.3187  | 3.1487  |
|        | 4600 | 3.9124                   | 3.7500  | 3.8437  | 3.5521  | 3.3812                 | 2.7834 | 2.8229 | 2.6872  | 3.4479                | 2.9468  | 2.9964  | 2.8307  |
|        | 4700 | 3.6027                   | 3.4029  | 3.4887  | 3.2121  | 3.1286                 | 2.5110 | 2.5453 | 2.4072  | 3.1917                | 2.6564  | 2.7002  | 2.5345  |
|        | 4800 | 3.3088                   | 3.0732  | 3.1495  | 2.8835  | 2.8685                 | 2.2714 | 2.2993 | 2.1568  | 2.9387                | 2.3948  | 2.4321  | 2.2647  |
|        | 4900 | 3.0276                   | 2.7604  | 2.8281  | 2.5699  | 2.5988                 | 2.0620 | 2.0844 | 1.9370  | 2.6763                | 2.1617  | 2.1933  | 2.0233  |
|        | 5000 | 2.7571                   | 2.4680  | 2.5274  | 2.2764  | 2.3229                 | 1.8787 | 1.8957 | 1.7453  | 2.4056                | 1.9548  | 1.9797  | 1.8079  |
|        | 5100 | 2.4916                   | 2.1965  | 2.2482  | 2.0050  | 2.0546                 | 1.7169 | 1.7290 | 1.5785  | 2.1347                | 1.7701  | 1.7893  | 1.6182  |
|        | 5200 | 2.2299                   | 1.9483  | 1.9927  | 1.7596  | 1.8102                 | 1.5753 | 1.5832 | 1.4350  | 1.8779                | 1.6062  | 1.6205  | 1.4532  |
|        | 5300 | 1.9728                   | 1.7236  | 1.7611  | 1.5398  | 1.5983                 | 1.4531 | 1.4570 | 1.3133  | 1.6460                | 1.4623  | 1.4719  | 1.3107  |
|        | 5400 | 1.7262                   | 1.5226  | 1.5539  | 1.3455  | 1.4220                 | 1.3485 | 1.3489 | 1.2114  | 1.4458                | 1.3381  | 1.3433  | 1.1899  |
|        | 5500 | 1.4964                   | 1.3439  | 1.3700  | 1.1752  | 1.2772                 | 1.2585 | 1.2558 | 1.1258  | 1.2785                | 1.2312  | 1.2325  | 1.0881  |
|        | 5600 | 1.2894                   | 1.1861  | 1.2074  | 1.0263  | 1.1588                 | 1.1802 | 1.1748 | 1.0529  | 1.1392                | 1.1379  | 1.1359  | 1.0010  |
|        | 5700 | 1.1056                   | 1.0475  | 1.0645  | 0.8970  | 1.0597                 | 1.1086 | 1.1008 | 0.9876  | 1.0230                | 1.0552  | 1.0504  | 0.9252  |
|        | 5800 | 0.9455                   | 0.9248  | 0.9381  | 0.7836  | 0.9731                 | 1.0403 | 1.0305 | 0.9255  | 0.9233                | 0.9787  | 0.9719  | 0.8557  |
|        | 5900 | 0.8066                   | 0.8156  | 0.8253  | 0.6834  | 0.8941                 | 0.9724 | 0.9609 | 0.8639  | 0.8339                | 0.9045  | 0.8956  | 0.7884  |
|        | 6000 | 0.6847                   | 0.7158  | 0.7227  | 0.5924  | 0.8192                 | 0.9045 | 0.8907 | 0.8014  | 0.7503                | 0.8303  | 0.8197  | 0.7207  |
|        | 6100 | 0.5753                   | 0.6223  | 0.6265  | 0.5071  | 0.7484                 | 0.8370 | 0.8213 | 0.7392  | 0.6686                | 0.7542  | 0.7417  | 0.6504  |
|        | 6200 | 0.4738                   | 0.5319  | 0.5338  | 0.4244  | 0.6722                 | 0.7624 | 0.7451 | 0.6692  | 0.5884                | 0.6775  | 0.6622  | 0.5785  |
|        | 6300 | 0.3764                   | 0.4411  | 0.4415  | 0.3409  | 0.5947                 | 0.6856 | 0.6657 | 0.5961  | 0.5051                | 0.5955  | 0.5796  | 0.5008  |
|        | 6400 | 0.2775                   | 0.3462  | 0.3456  | 0.2526  | 0.5124                 | 0.6035 | 0.5811 | 0.5168  | 0.4165                | 0.5080  | 0.4887  | 0.4167  |
|        | 6500 | 0.1770                   | 0.2478  | 0.2452  | 0.1600  | 0.4315                 | 0.5228 | 0.4953 | 0.4382  | 0.3262                | 0.4173  | 0.3961  | 0.3292  |
|        | 6600 | 0.0720                   | 0.1430  | 0.1392  | 0.0608  | 0.3471                 | 0.4376 | 0.4087 | 0.3552  | 0.2307                | 0.3216  | 0.2972  | 0.2357  |
|        | 6700 | -0.0397                  | 0.0305  | 0.0255  | -0.0465 | 0.2529                 | 0.3446 | 0.3132 | 0.2623  | 0.1338                | 0.2243  | 0.1968  | 0.1405  |
|        | 6800 | -0.1554                  | -0.0859 | -0.0943 | -0.1586 | 0.1677                 | 0.2586 | 0.2202 | 0.1785  | 0.0308                | 0.1209  | 0.0914  | 0.0386  |
|        | 6900 | -0.2763                  | -0.2092 | -0.2182 | -0.2772 | 0.0769                 | 0.1670 | 0.1269 | 0.0879  | -0.0756               | 0.0141  | -0.0223 | -0.0671 |
|        | 7000 | -0.4056                  | -0.3409 | -0.3514 | -0.4046 | -0.0212                | 0.0688 | 0.0267 | -0.0098 | -0.1758               | -0.0872 | -0.1273 | -0.1666 |
| Ca4455 | 4300 | 1.4828                   | 1.5219  | 1.5410  | 1.4419  | 1.3829                 | 1.4556 | 1.4614 | 1.3726  | 1.4076                | 1.4756  | 1.4841  | 1.3925  |
|        | 4400 | 1.3677                   | 1.4226  | 1.4400  | 1.3484  | 1.2430                 | 1.3145 | 1.3187 | 1.2378  | 1.2614                | 1.3297  | 1.3361  | 1.2534  |
|        | 4500 | 1.2421                   | 1.2975  | 1.3143  | 1.2288  | 1.1146                 | 1.1853 | 1.1883 | 1.1133  | 1.1282                | 1.1962  | 1.2011  | 1.1249  |
|        | 4600 | 1.1063                   | 1.1612  | 1.1764  | 1.0972  | 0.9984                 | 1.0690 | 1.0709 | 1.0007  | 1.0077                | 1.0758  | 1.0795  | 1.0082  |
|        | 4700 | 0.9776                   | 1.0336  | 1.0463  | 0.9734  | 0.8957                 | 0.9671 | 0.9681 | 0.9017  | 0.9005                | 0.9696  | 0.9721  | 0.9049  |
|        | 4800 | 0.8637                   | 0.9208  | 0.9307  | 0.8641  | 0.8068                 | 0.8790 | 0.8789 | 0.8163  | 0.8077                | 0.8772  | 0.8787  | 0.8156  |
|        | 4900 | 0.7650                   | 0.8223  | 0.8299  | 0.7696  | 0.7317                 | 0.8025 | 0.8017 | 0.7432  | 0.7282                | 0.7972  | 0.7980  | 0.7394  |
|        | 5000 | 0.6812                   | 0.7373  | 0.7431  | 0.6895  | 0.6687                 | 0.7360 | 0.7345 | 0.6809  | 0.6616                | 0.7279  | 0.7277  | 0.6745  |
|        | 5100 | 0.6109                   | 0.6645  | 0.6687  | 0.6222  | 0.6156                 | 0.6775 | 0.6754 | 0.6273  | 0.6058                | 0.6672  | 0.6665  | 0.6190  |
|        | 5200 | 0.5524                   | 0.6024  | 0.6053  | 0.5656  | 0.5705                 | 0.6256 | 0.6233 | 0.5807  | 0.5589                | 0.6138  | 0.6126  | 0.5710  |
|        | 5300 | 0.5035                   | 0.5487  | 0.5507  | 0.5172  | 0.5311                 | 0.5795 | 0.5769 | 0.5394  | 0.5187                | 0.5666  | 0.5651  | 0.5289  |
|        | 5400 | 0.4624                   | 0.5023  | 0.5035  | 0.4754  | 0.4963                 | 0.5380 | 0.5354 | 0.5028  | 0.4834                | 0.5246  | 0.5228  | 0.4916  |
|        | 5500 | 0.4273                   | 0.4616  | 0.4623  | 0.4389  | 0.4650                 | 0.5006 | 0.4979 | 0.4697  | 0.4521                | 0.4870  | 0.4850  | 0.4585  |
|        | 5600 | 0.3967                   | 0.4257  | 0.4261  | 0.4064  | 0.4363                 | 0.4665 | 0.4639 | 0.4396  | 0.4237                | 0.4530  | 0.4510  | 0.4283  |
|        | 5700 | 0.3694                   | 0.3936  | 0.3937  | 0.3773  | 0.4096                 | 0.4352 | 0.4327 | 0.4119  | 0.3975                | 0.4221  | 0.4201  | 0.4008  |
|        | 5800 | 0.3447                   | 0.3646  | 0.3646  | 0.3508  | 0.3846                 | 0.4063 | 0.4039 | 0.3862  | 0.3730                | 0.3935  | 0.3915  | 0.3752  |
|        | 5900 | 0.3219                   | 0.3381  | 0.3379  | 0.3265  | 0.3609                 | 0.3794 | 0.3770 | 0.3619  | 0.3496                | 0.3668  | 0.3649  | 0.3511  |
|        | 6000 | 0.3005                   | 0.3136  | 0.3133  | 0.3038  | 0.3380                 | 0.3538 | 0.3515 | 0.3386  | 0.3272                | 0.3416  | 0.3397  | 0.3281  |
|        | 6100 | 0.2800                   | 0.2904  | 0.2902  | 0.2823  | 0.3155                 | 0.3291 | 0.3269 | 0.3159  | 0.3051                | 0.3174  | 0.3156  | 0.3058  |
|        | 6200 | 0.2602                   | 0.2686  | 0.2682  | 0.2617  | 0.2932                 | 0.3049 | 0.3028 | 0.2934  | 0.2832                | 0.2937  | 0.2918  | 0.2836  |
|        | 6300 | 0.2408                   | 0.2476  | 0.2473  | 0.2419  | 0.2708                 | 0.2810 | 0.2790 | 0.2709  | 0.2614                | 0.2703  | 0.2687  | 0.2617  |
|        | 6400 | 0.2218                   | 0.2273  | 0.2270  | 0.2225  | 0.2481                 | 0.2571 | 0.2552 | 0.2482  | 0.2395                | 0.2472  | 0.2457  | 0.2397  |
|        | 6500 | 0.2031                   | 0.2077  | 0.2075  | 0.2036  | 0.2251                 | 0.2331 | 0.2313 | 0.2252  | 0.2172                | 0.2240  | 0.2226  | 0.2173  |
|        | 6600 | 0.1847                   | 0.1884  | 0.1884  | 0.1850  | 0.2025                 | 0.2094 | 0.2079 | 0.2026  | 0.1951                | 0.2010  | 0.1997  | 0.1951  |
|        | 6700 | 0.1664                   | 0.1696  | 0.1697  | 0.1666  | 0.1799                 | 0.1860 | 0.1846 | 0.1799  | 0.1732                | 0.1784  | 0.1773  | 0.1732  |
|        | 6800 | 0.1485                   | 0.1513  | 0.1516  | 0.1486  | 0.1574                 | 0.1629 | 0.1615 | 0.1574  | 0.1515                | 0.1562  | 0.1553  | 0.1516  |
|        | 6900 | 0.1310                   | 0.1334  | 0.1339  | 0.1311  | 0.1352                 | 0.1400 | 0.1391 | 0.1352  | 0.1304                | 0.1345  | 0.1338  | 0.1305  |
|        | 7000 | 0.1140                   | 0.1161  | 0.1168  | 0.1141  | 0.1177                 | 0.1171 | 0.1134 | 0.1097  | 0.1133                | 0.1129  | 0.1107  | 0.1097  |
| Fe4531 | 4300 | 3.6566                   | 3.5654  | 3.6437  | 3.5346  | 3.5381                 | 3.4618 | 3.4640 | 3.4376  | 3.4916                | 3.4250  | 3.4366  | 3.3965  |
|        | 4400 | 3.4175                   | 3.3737  | 3.4378  | 3.3415  | 3.3924                 | 3.3169 | 3.3163 | 3.2930  | 3.3291                | 3.2688  | 3.2739  | 3.2405  |
|        | 4500 | 3.1903                   | 3.1578  | 3.2099  | 3.1266  | 3.2491                 | 3.1743 | 3.1723 | 3.1523  | 3.1812                | 3.1229  | 3.1241  | 3.0966  |
|        | 4600 | 2.9705                   | 2.9426  | 2.9826  | 2.9136  | 3.1056                 | 3.0323 | 3.0294 | 3.0126  | 3.0389                | 2.9814  | 2.9807  | 2.9577  |
|        | 4700 | 2.7739                   | 2.7503  | 2.7787  | 2.7235  | 2.9594                 | 2.8924 | 2.8890 | 2.8743  | 2.8967                | 2.8423  | 2.8401  | 2.8201  |
|        | 4800 | 2.5979                   | 2.5777  | 2.5972  | 2.5522  | 2.8098                 | 2.7549 | 2.7505 | 2.7367  | 2.7530                | 2.7046  | 2.7014  | 2.6833  |
|        | 4900 | 2.4328                   | 2.4163  | 2.4293  | 2.3916  | 2.6590                 | 2.6197 | 2.6147 | 2.6010  | 2.6059                | 2.5689  | 2.5655  | 2.5483  |
|        | 5000 | 2.2748                   | 2.2629  | 2.2708  | 2.2384  | 2.5099                 | 2.4878 | 2.4822 | 2.4680  | 2.4583                | 2.4361  | 2.4312  | 2.4142  |
|        | 5100 | 2.1220                   | 2.1160  | 2.1199  | 2.0921  | 2.3657                 | 2.3594 | 2.3531 | 2.3387  | 2.3134                | 2.3052  | 2.2994  | 2.2831  |
|        | 5200 | 1.9750                   | 1.9758  | 1.9766  | 1.9526  | 2.2287                 | 2.2349 | 2.2282 | 2.2135  | 2.1735                | 2.1779  | 2.1716  | 2.1553  |
|        | 5300 | 1.8339                   | 1.8418  | 1.8403  | 1.8193  | 2.1005                 | 2.1164 | 2.1090 | 2.0935  | 2.0418                | 2.0556  | 2.0486  | 2.0329  |
|        | 5400 | 1.7012                   | 1.7153  | 1.7119  | 1.6937  | 1.9814                 | 2.0024 | 1.9948 | 1.9794  | 1.9186                | 1.9386  | 1.9311  | 1.9157  |
|        | 5500 | 1.5775                   | 1.5962  | 1.5914  | 1.5754  | 1.8699                 | 1.8934 | 1.8854 | 1.8701  | 1.8042                | 1.8272  | 1.8187  | 1.8046  |
|        | 5600 | 1.4639                   | 1.4851  | 1.4     |         |                        |        |        |         |                       |         |         |         |

Table B.1: Continued.

| Index       | T[K] | MS-TO ( $\log g = 4.2$ ) |         |         |         | RGB ( $\log g = 2.4$ ) |         |         |         | HB ( $\log g = 2.8$ ) |         |         |         |
|-------------|------|--------------------------|---------|---------|---------|------------------------|---------|---------|---------|-----------------------|---------|---------|---------|
|             |      | Ref                      | IY2     | IY4     | 2Y2     | Ref                    | IY2     | IY4     | 2Y2     | Ref                   | IY2     | IY4     | 2Y2     |
| Fe4668      | 4300 | 0.5020                   | 0.5276  | 0.5186  | 0.5539  | 1.1471                 | 1.1016  | 1.0849  | 1.1318  | 1.0198                | 0.9868  | 0.9695  | 1.0165  |
|             | 4400 | 0.5462                   | 0.5720  | 0.5619  | 0.5923  | 1.0822                 | 1.0410  | 1.0268  | 1.0649  | 0.9812                | 0.9544  | 0.9404  | 0.9768  |
|             | 4500 | 0.5658                   | 0.5890  | 0.5787  | 0.6039  | 0.9858                 | 0.9494  | 0.9388  | 0.9667  | 0.9085                | 0.8865  | 0.8747  | 0.9035  |
|             | 4600 | 0.5561                   | 0.5770  | 0.5680  | 0.5874  | 0.8759                 | 0.8441  | 0.8350  | 0.8568  | 0.8156                | 0.7980  | 0.7883  | 0.8098  |
|             | 4700 | 0.5233                   | 0.5429  | 0.5358  | 0.5503  | 0.7629                 | 0.7373  | 0.7297  | 0.7449  | 0.7157                | 0.7028  | 0.6952  | 0.7099  |
|             | 4800 | 0.4792                   | 0.4989  | 0.4935  | 0.5032  | 0.6563                 | 0.6389  | 0.6322  | 0.6411  | 0.6200                | 0.6120  | 0.6055  | 0.6146  |
|             | 4900 | 0.4310                   | 0.4516  | 0.4477  | 0.4533  | 0.5606                 | 0.5526  | 0.5466  | 0.5503  | 0.5323                | 0.5308  | 0.5254  | 0.5291  |
|             | 5000 | 0.3843                   | 0.4057  | 0.4028  | 0.4048  | 0.4769                 | 0.4799  | 0.4744  | 0.4734  | 0.4557                | 0.4618  | 0.4569  | 0.4558  |
|             | 5100 | 0.3415                   | 0.3640  | 0.3621  | 0.3605  | 0.4059                 | 0.4189  | 0.4140  | 0.4095  | 0.3900                | 0.4037  | 0.3993  | 0.3945  |
|             | 5200 | 0.3036                   | 0.3268  | 0.3254  | 0.3212  | 0.3466                 | 0.3676  | 0.3632  | 0.3560  | 0.3339                | 0.3546  | 0.3507  | 0.3429  |
|             | 5300 | 0.2690                   | 0.2930  | 0.2921  | 0.2856  | 0.2960                 | 0.3222  | 0.3182  | 0.3091  | 0.2861                | 0.3111  | 0.3075  | 0.2985  |
|             | 5400 | 0.2368                   | 0.2620  | 0.2617  | 0.2532  | 0.2539                 | 0.2825  | 0.2791  | 0.2686  | 0.2433                | 0.2732  | 0.2698  | 0.2577  |
|             | 5500 | 0.2070                   | 0.2334  | 0.2333  | 0.2235  | 0.2179                 | 0.2479  | 0.2448  | 0.2322  | 0.2089                | 0.2399  | 0.2372  | 0.2242  |
|             | 5600 | 0.1802                   | 0.2070  | 0.2071  | 0.1964  | 0.1835                 | 0.2134  | 0.2109  | 0.1983  | 0.1781                | 0.2090  | 0.2066  | 0.1931  |
|             | 5700 | 0.1559                   | 0.1825  | 0.1829  | 0.1716  | 0.1523                 | 0.1814  | 0.1797  | 0.1661  | 0.1485                | 0.1790  | 0.1771  | 0.1629  |
|             | 5800 | 0.1343                   | 0.1602  | 0.1607  | 0.1491  | 0.1237                 | 0.1521  | 0.1501  | 0.1365  | 0.1223                | 0.1517  | 0.1502  | 0.1356  |
|             | 5900 | 0.1151                   | 0.1397  | 0.1405  | 0.1288  | 0.0992                 | 0.1266  | 0.1251  | 0.1111  | 0.0974                | 0.1255  | 0.1250  | 0.1096  |
|             | 6000 | 0.0978                   | 0.1208  | 0.1219  | 0.1103  | 0.0751                 | 0.1017  | 0.1005  | 0.0861  | 0.0761                | 0.1033  | 0.1025  | 0.0873  |
|             | 6100 | 0.0813                   | 0.1027  | 0.1041  | 0.0927  | 0.0529                 | 0.0784  | 0.0779  | 0.0629  | 0.0541                | 0.0804  | 0.0800  | 0.0645  |
|             | 6200 | 0.0665                   | 0.0872  | 0.0884  | 0.0770  | 0.0302                 | 0.0556  | 0.0546  | 0.0393  | 0.0357                | 0.0609  | 0.0605  | 0.0451  |
|             | 6300 | 0.0542                   | 0.0732  | 0.0747  | 0.0637  | 0.0139                 | 0.0379  | 0.0377  | 0.0222  | 0.0179                | 0.0420  | 0.0421  | 0.0265  |
|             | 6400 | 0.0418                   | 0.0597  | 0.0613  | 0.0505  | -0.0043                | 0.0187  | 0.0192  | 0.0033  | 0.0019                | 0.0252  | 0.0238  | 0.0097  |
|             | 6500 | 0.0299                   | 0.0467  | 0.0485  | 0.0379  | -0.0212                | 0.0013  | 0.0004  | -0.0144 | -0.0137               | 0.0085  | 0.0088  | -0.0065 |
|             | 6600 | 0.0191                   | 0.0349  | 0.0365  | 0.0265  | -0.0347                | -0.0128 | -0.0139 | -0.0285 | -0.0333               | -0.0115 | -0.0107 | -0.0267 |
|             | 6700 | 0.0063                   | 0.0212  | 0.0232  | 0.0131  | -0.0525                | -0.0319 | -0.0309 | -0.0465 | -0.0423               | -0.0219 | -0.0216 | -0.0363 |
|             | 6800 | -0.0038                  | 0.0101  | 0.0121  | 0.0025  | -0.0620                | -0.0417 | -0.0427 | -0.0572 | -0.0530               | -0.0338 | -0.0323 | -0.0475 |
|             | 6900 | -0.0154                  | -0.0022 | -0.0004 | -0.0096 | -0.0725                | -0.0529 | -0.0534 | -0.0679 | -0.0662               | -0.0474 | -0.0479 | -0.0614 |
|             | 7000 | -0.0302                  | -0.0177 | -0.0159 | -0.0249 | -0.0906                | -0.0720 | -0.0705 | -0.0865 | -0.0754               | -0.0577 | -0.0574 | -0.0709 |
| $H_{\beta}$ | 4300 | -0.0107                  | -0.0096 | -0.0183 | 0.0113  | 0.4682                 | 0.4682  | 0.4570  | 0.4784  | 0.3635                | 0.3617  | 0.3508  | 0.3742  |
|             | 4400 | 0.1454                   | 0.1452  | 0.1395  | 0.1622  | 0.5816                 | 0.5840  | 0.5740  | 0.5909  | 0.4846                | 0.4850  | 0.4757  | 0.4943  |
|             | 4500 | 0.2895                   | 0.2918  | 0.2890  | 0.3034  | 0.6851                 | 0.6926  | 0.6838  | 0.6940  | 0.5928                | 0.5978  | 0.5897  | 0.6016  |
|             | 4600 | 0.4165                   | 0.4220  | 0.4221  | 0.4274  | 0.7838                 | 0.7971  | 0.7888  | 0.7917  | 0.6933                | 0.7040  | 0.6968  | 0.7014  |
|             | 4700 | 0.5283                   | 0.5371  | 0.5396  | 0.5372  | 0.8830                 | 0.9006  | 0.8926  | 0.8905  | 0.7913                | 0.8073  | 0.8007  | 0.7990  |
|             | 4800 | 0.6341                   | 0.6455  | 0.6491  | 0.6424  | 0.9864                 | 1.0066  | 0.9979  | 0.9931  | 0.8961                | 0.9119  | 0.9058  | 0.9010  |
|             | 4900 | 0.7402                   | 0.7531  | 0.7573  | 0.7484  | 1.0996                 | 1.1194  | 1.1112  | 1.1057  | 1.0065                | 1.0231  | 1.0189  | 1.0132  |
|             | 5000 | 0.8505                   | 0.8636  | 0.8678  | 0.8583  | 1.2244                 | 1.2432  | 1.2346  | 1.2300  | 1.1268                | 1.1454  | 1.1385  | 1.1331  |
|             | 5100 | 0.9673                   | 0.9802  | 0.9840  | 0.9748  | 1.3623                 | 1.3799  | 1.3704  | 1.3673  | 1.2592                | 1.2767  | 1.2692  | 1.2650  |
|             | 5200 | 1.0929                   | 1.1057  | 1.1090  | 1.1002  | 1.5148                 | 1.5305  | 1.5206  | 1.5193  | 1.4047                | 1.4208  | 1.4129  | 1.4101  |
|             | 5300 | 1.2280                   | 1.2406  | 1.2431  | 1.2349  | 1.6857                 | 1.7015  | 1.6896  | 1.6901  | 1.5638                | 1.5784  | 1.5705  | 1.5685  |
|             | 5400 | 1.3754                   | 1.3879  | 1.3891  | 1.3818  | 1.8731                 | 1.8868  | 1.8749  | 1.8774  | 1.7380                | 1.7516  | 1.7440  | 1.7426  |
|             | 5500 | 1.5372                   | 1.5497  | 1.5492  | 1.5434  | 2.0749                 | 2.0876  | 2.0746  | 2.0790  | 1.9319                | 1.9448  | 1.9331  | 1.9364  |
|             | 5600 | 1.7153                   | 1.7278  | 1.7257  | 1.7214  | 2.2937                 | 2.3050  | 2.2908  | 2.2971  | 2.1431                | 2.1549  | 2.1422  | 2.1473  |
|             | 5700 | 1.9100                   | 1.9228  | 1.9195  | 1.9160  | 2.5290                 | 2.5398  | 2.5240  | 2.5325  | 2.3703                | 2.3806  | 2.3668  | 2.3742  |
|             | 5800 | 2.1220                   | 2.1352  | 2.1303  | 2.1281  | 2.7823                 | 2.7914  | 2.7743  | 2.7850  | 2.6132                | 2.6234  | 2.6071  | 2.6166  |
|             | 5900 | 2.3507                   | 2.3641  | 2.3571  | 2.3565  | 3.0523                 | 3.0598  | 3.0411  | 3.0544  | 2.8734                | 2.8815  | 2.8654  | 2.8763  |
|             | 6000 | 2.5942                   | 2.6076  | 2.5988  | 2.6000  | 3.3362                 | 3.3425  | 3.3218  | 3.3379  | 3.1470                | 3.1537  | 3.1359  | 3.1492  |
|             | 6100 | 2.8517                   | 2.8581  | 2.8543  | 2.8564  | 3.6318                 | 3.6367  | 3.6155  | 3.6333  | 3.4340                | 3.4393  | 3.4195  | 3.4357  |
|             | 6200 | 3.1134                   | 3.1243  | 3.1145  | 3.1178  | 3.9373                 | 3.9410  | 3.9189  | 3.9385  | 3.7325                | 3.7371  | 3.7157  | 3.7341  |
|             | 6300 | 3.3910                   | 3.4011  | 3.3892  | 3.3951  | 4.2520                 | 4.2549  | 4.2324  | 4.2531  | 4.0437                | 4.0471  | 4.0240  | 4.0448  |
|             | 6400 | 3.6787                   | 3.6889  | 3.6732  | 3.6820  | 4.5748                 | 4.5767  | 4.5531  | 4.5754  | 4.3632                | 4.3658  | 4.3413  | 4.3644  |
|             | 6500 | 3.9765                   | 3.9847  | 3.9673  | 3.9790  | 4.9023                 | 4.9028  | 4.8796  | 4.9024  | 4.6890                | 4.6906  | 4.6654  | 4.6894  |
|             | 6600 | 4.2779                   | 4.2844  | 4.2665  | 4.2799  | 5.2316                 | 5.2312  | 5.2088  | 5.2312  | 5.0179                | 5.0190  | 4.9939  | 5.0183  |
|             | 6700 | 4.5845                   | 4.5896  | 4.5692  | 4.5859  | 5.5581                 | 5.5586  | 5.5369  | 5.5585  | 5.3466                | 5.3467  | 5.3235  | 5.3463  |
|             | 6800 | 4.8947                   | 4.8992  | 4.8762  | 4.8960  | 5.8829                 | 5.8821  | 5.8615  | 5.8832  | 5.6768                | 5.6769  | 5.6512  | 5.6768  |
|             | 6900 | 5.2076                   | 5.2114  | 5.1854  | 5.2085  | 6.2002                 | 6.1990  | 6.1831  | 6.2001  | 6.0042                | 6.0042  | 5.9791  | 6.0046  |
|             | 7000 | 5.5221                   | 5.5249  | 5.4965  | 5.5222  | 6.5103                 | 6.5091  | 6.4938  | 6.5103  | 6.3272                | 6.3265  | 6.3020  | 6.3270  |
| Fe5015      | 4300 | 2.9316                   | 2.9889  | 3.0140  | 2.9792  | 4.3772                 | 4.4039  | 4.3490  | 4.3923  | 3.9753                | 4.0142  | 3.9681  | 4.0042  |
|             | 4400 | 2.9997                   | 3.1083  | 3.1219  | 3.0954  | 4.4528                 | 4.4789  | 4.4309  | 4.4617  | 4.1108                | 4.1539  | 4.1082  | 4.1383  |
|             | 4500 | 3.1170                   | 3.2257  | 3.2280  | 3.2102  | 4.4103                 | 4.4322  | 4.3934  | 4.4127  | 4.1444                | 4.1852  | 4.1452  | 4.1665  |
|             | 4600 | 3.2185                   | 3.3159  | 3.3117  | 3.2986  | 4.2767                 | 4.2925  | 4.2618  | 4.2745  | 4.0799                | 4.1145  | 4.0818  | 4.0961  |
|             | 4700 | 3.2599                   | 3.3453  | 3.3378  | 3.3277  | 4.0834                 | 4.0988  | 4.0740  | 4.0843  | 3.9401                | 3.9703  | 3.9442  | 3.9546  |
|             | 4800 | 3.2322                   | 3.3076  | 3.2991  | 3.2908  | 3.8556                 | 3.8788  | 3.8575  | 3.8676  | 3.7525                | 3.7835  | 3.7619  | 3.7707  |
|             | 4900 | 3.1405                   | 3.2093  | 3.2001  | 3.1943  | 3.6144                 | 3.6494  | 3.6304  | 3.6408  | 3.5370                | 3.5750  | 3.5573  | 3.5662  |
|             | 5000 | 3.0013                   | 3.0665  | 3.0561  | 3.0540  | 3.3733                 | 3.4200  | 3.4024  | 3.4134  | 3.3097                | 3.3582  | 3.3412  | 3.3506  |
|             | 5100 | 2.8298                   | 2.8959  | 2.8845  | 2.8853  | 3.1402                 | 3.1957  | 3.1787  | 3.1895  | 3.0828                | 3.1397  | 3.1239  | 3.1331  |
|             | 5200 | 2.6430                   | 2.7116  | 2.6991  | 2.7026  | 2.9198                 | 2.9798  | 2.9633  | 2.9733  | 2.8639                | 2.9261  | 2.9106  | 2.9199  |
|             | 5300 | 2.4507                   | 2.5220  | 2.5084  | 2.5139  | 2.7134                 | 2.7753  | 2.7588  | 2.7674  | 2.6563                | 2.7208  | 2.7056  | 2.7135  |
|             | 5400 | 2.2625                   | 2.3350  | 2.3206  | 2.3270  | 2.5212                 | 2.5812  | 2.5652  | 2.5721  | 2.4622                | 2.5264  | 2.5113  | 2.5175  |
|             | 5500 | 2.0837                   | 2.1555  | 2.1406  | 2.1473  | 2.3403                 | 2.3967  | 2.3810  | 2.3865  | 2.2812                | 2.3424  | 2.3268  | 2.3324  |
|             | 5600 | 1.9175                   | 1.9859  |         |         |                        |         |         |         |                       |         |         |         |

Table B.1: Continued.

| Index           | T[K] | MS-TO ( $\log g = 4.2$ ) |         |         |         | RGB ( $\log g = 2.4$ ) |         |         |         | HB ( $\log g = 2.8$ ) |         |         |         |
|-----------------|------|--------------------------|---------|---------|---------|------------------------|---------|---------|---------|-----------------------|---------|---------|---------|
|                 |      | Ref                      | IY2     | IY4     | 2Y2     | Ref                    | IY2     | IY4     | 2Y2     | Ref                   | IY2     | IY4     | 2Y2     |
| Mg <sub>1</sub> | 4300 | 0.2739                   | 0.2531  | 0.2621  | 0.2528  | 0.0985                 | 0.0938  | 0.0975  | 0.0932  | 0.1307                | 0.1241  | 0.1287  | 0.1235  |
|                 | 4400 | 0.2232                   | 0.2102  | 0.2179  | 0.2100  | 0.0652                 | 0.0619  | 0.0645  | 0.0616  | 0.0891                | 0.0845  | 0.0880  | 0.0843  |
|                 | 4500 | 0.1714                   | 0.1621  | 0.1690  | 0.1622  | 0.0426                 | 0.0406  | 0.0422  | 0.0404  | 0.0589                | 0.0558  | 0.0583  | 0.0558  |
|                 | 4600 | 0.1224                   | 0.1158  | 0.1213  | 0.1161  | 0.0281                 | 0.0272  | 0.0281  | 0.0270  | 0.0384                | 0.0367  | 0.0382  | 0.0367  |
|                 | 4700 | 0.0833                   | 0.0791  | 0.0831  | 0.0795  | 0.0189                 | 0.0189  | 0.0193  | 0.0185  | 0.0251                | 0.0245  | 0.0253  | 0.0244  |
|                 | 4800 | 0.0550                   | 0.0526  | 0.0552  | 0.0530  | 0.0130                 | 0.0135  | 0.0138  | 0.0131  | 0.0166                | 0.0168  | 0.0172  | 0.0166  |
|                 | 4900 | 0.0354                   | 0.0343  | 0.0360  | 0.0346  | 0.0091                 | 0.0100  | 0.0101  | 0.0094  | 0.0111                | 0.0118  | 0.0120  | 0.0115  |
|                 | 5000 | 0.0224                   | 0.0222  | 0.0232  | 0.0224  | 0.0064                 | 0.0075  | 0.0074  | 0.0068  | 0.0075                | 0.0085  | 0.0085  | 0.0080  |
|                 | 5100 | 0.0138                   | 0.0141  | 0.0147  | 0.0142  | 0.0045                 | 0.0056  | 0.0056  | 0.0050  | 0.0051                | 0.0061  | 0.0061  | 0.0056  |
|                 | 5200 | 0.0082                   | 0.0088  | 0.0091  | 0.0088  | 0.0031                 | 0.0042  | 0.0041  | 0.0035  | 0.0034                | 0.0044  | 0.0044  | 0.0039  |
|                 | 5300 | 0.0045                   | 0.0053  | 0.0054  | 0.0052  | 0.0020                 | 0.0030  | 0.0029  | 0.0024  | 0.0021                | 0.0031  | 0.0030  | 0.0026  |
|                 | 5400 | 0.0020                   | 0.0028  | 0.0028  | 0.0027  | 0.0011                 | 0.0020  | 0.0019  | 0.0014  | 0.0011                | 0.0020  | 0.0019  | 0.0015  |
|                 | 5500 | 0.0004                   | 0.0011  | 0.0010  | 0.0010  | 0.0003                 | 0.0011  | 0.0010  | 0.0005  | 0.0003                | 0.0010  | 0.0010  | 0.0006  |
|                 | 5600 | -0.0007                  | -0.0001 | -0.0002 | -0.0003 | -0.0004                | 0.0003  | 0.0002  | -0.0002 | -0.0004               | 0.0002  | 0.0001  | -0.0002 |
|                 | 5700 | -0.0015                  | -0.0011 | -0.0012 | -0.0012 | -0.0010                | -0.0004 | -0.0005 | -0.0009 | -0.0011               | -0.0005 | -0.0006 | -0.0009 |
|                 | 5800 | -0.0021                  | -0.0018 | -0.0019 | -0.0019 | -0.0016                | -0.0010 | -0.0011 | -0.0015 | -0.0017               | -0.0012 | -0.0013 | -0.0016 |
|                 | 5900 | -0.0026                  | -0.0023 | -0.0024 | -0.0024 | -0.0020                | -0.0016 | -0.0016 | -0.0019 | -0.0022               | -0.0018 | -0.0019 | -0.0021 |
|                 | 6000 | -0.0030                  | -0.0028 | -0.0029 | -0.0028 | -0.0026                | -0.0022 | -0.0022 | -0.0025 | -0.0026               | -0.0023 | -0.0023 | -0.0025 |
|                 | 6100 | -0.0033                  | -0.0031 | -0.0032 | -0.0032 | -0.0031                | -0.0027 | -0.0027 | -0.0030 | -0.0030               | -0.0027 | -0.0028 | -0.0030 |
|                 | 6200 | -0.0035                  | -0.0034 | -0.0035 | -0.0035 | -0.0034                | -0.0030 | -0.0031 | -0.0033 | -0.0034               | -0.0032 | -0.0032 | -0.0034 |
|                 | 6300 | -0.0038                  | -0.0037 | -0.0038 | -0.0037 | -0.0036                | -0.0033 | -0.0034 | -0.0036 | -0.0037               | -0.0035 | -0.0036 | -0.0037 |
|                 | 6400 | -0.0040                  | -0.0040 | -0.0040 | -0.0040 | -0.0038                | -0.0036 | -0.0036 | -0.0038 | -0.0040               | -0.0038 | -0.0038 | -0.0039 |
|                 | 6500 | -0.0042                  | -0.0042 | -0.0043 | -0.0042 | -0.0040                | -0.0037 | -0.0038 | -0.0039 | -0.0042               | -0.0041 | -0.0041 | -0.0042 |
|                 | 6600 | -0.0045                  | -0.0045 | -0.0045 | -0.0045 | -0.0041                | -0.0039 | -0.0040 | -0.0040 | -0.0044               | -0.0042 | -0.0043 | -0.0043 |
|                 | 6700 | -0.0048                  | -0.0048 | -0.0048 | -0.0048 | -0.0041                | -0.0040 | -0.0040 | -0.0041 | -0.0045               | -0.0043 | -0.0044 | -0.0044 |
|                 | 6800 | -0.0051                  | -0.0051 | -0.0051 | -0.0050 | -0.0043                | -0.0041 | -0.0042 | -0.0042 | -0.0045               | -0.0044 | -0.0046 | -0.0045 |
|                 | 6900 | -0.0053                  | -0.0054 | -0.0054 | -0.0053 | -0.0041                | -0.0040 | -0.0042 | -0.0041 | -0.0047               | -0.0046 | -0.0047 | -0.0046 |
|                 | 7000 | -0.0057                  | -0.0057 | -0.0058 | -0.0057 | -0.0039                | -0.0038 | -0.0040 | -0.0038 | -0.0048               | -0.0047 | -0.0048 | -0.0047 |
| Mg <sub>2</sub> | 4300 | 0.5321                   | 0.4954  | 0.5106  | 0.4959  | 0.2372                 | 0.2266  | 0.2358  | 0.2274  | 0.2970                | 0.2835  | 0.2944  | 0.2842  |
|                 | 4400 | 0.4739                   | 0.4513  | 0.4662  | 0.4519  | 0.1864                 | 0.1776  | 0.1853  | 0.1786  | 0.2368                | 0.2261  | 0.2356  | 0.2272  |
|                 | 4500 | 0.4100                   | 0.3933  | 0.4083  | 0.3941  | 0.1477                 | 0.1405  | 0.1467  | 0.1417  | 0.1885                | 0.1797  | 0.1878  | 0.1811  |
|                 | 4600 | 0.3430                   | 0.3300  | 0.3440  | 0.3312  | 0.1194                 | 0.1139  | 0.1188  | 0.1150  | 0.1515                | 0.1446  | 0.1511  | 0.1460  |
|                 | 4700 | 0.2833                   | 0.2734  | 0.2856  | 0.2747  | 0.0990                 | 0.0950  | 0.0988  | 0.0959  | 0.1240                | 0.1188  | 0.1241  | 0.1201  |
|                 | 4800 | 0.2340                   | 0.2265  | 0.2369  | 0.2281  | 0.0838                 | 0.0812  | 0.0842  | 0.0819  | 0.1036                | 0.1000  | 0.1042  | 0.1011  |
|                 | 4900 | 0.1945                   | 0.1892  | 0.1979  | 0.1907  | 0.0723                 | 0.0707  | 0.0732  | 0.0712  | 0.0882                | 0.0859  | 0.0894  | 0.0868  |
|                 | 5000 | 0.1635                   | 0.1598  | 0.1672  | 0.1612  | 0.0633                 | 0.0624  | 0.0645  | 0.0628  | 0.0762                | 0.0749  | 0.0778  | 0.0756  |
|                 | 5100 | 0.1390                   | 0.1368  | 0.1429  | 0.1380  | 0.0560                 | 0.0556  | 0.0574  | 0.0559  | 0.0667                | 0.0661  | 0.0685  | 0.0666  |
|                 | 5200 | 0.1196                   | 0.1184  | 0.1235  | 0.1195  | 0.0501                 | 0.0501  | 0.0515  | 0.0503  | 0.0590                | 0.0588  | 0.0608  | 0.0592  |
|                 | 5300 | 0.1038                   | 0.1033  | 0.1077  | 0.1042  | 0.0452                 | 0.0453  | 0.0465  | 0.0455  | 0.0526                | 0.0526  | 0.0543  | 0.0530  |
|                 | 5400 | 0.0908                   | 0.0907  | 0.0945  | 0.0915  | 0.0412                 | 0.0414  | 0.0423  | 0.0415  | 0.0472                | 0.0473  | 0.0488  | 0.0476  |
|                 | 5500 | 0.0798                   | 0.0800  | 0.0834  | 0.0807  | 0.0378                 | 0.0380  | 0.0387  | 0.0381  | 0.0427                | 0.0429  | 0.0441  | 0.0431  |
|                 | 5600 | 0.0706                   | 0.0709  | 0.0738  | 0.0715  | 0.0349                 | 0.0351  | 0.0357  | 0.0352  | 0.0390                | 0.0391  | 0.0400  | 0.0393  |
|                 | 5700 | 0.0627                   | 0.0629  | 0.0655  | 0.0634  | 0.0325                 | 0.0326  | 0.0331  | 0.0327  | 0.0357                | 0.0358  | 0.0366  | 0.0360  |
|                 | 5800 | 0.0559                   | 0.0561  | 0.0583  | 0.0565  | 0.0305                 | 0.0306  | 0.0309  | 0.0307  | 0.0330                | 0.0330  | 0.0336  | 0.0332  |
|                 | 5900 | 0.0501                   | 0.0501  | 0.0520  | 0.0505  | 0.0289                 | 0.0289  | 0.0291  | 0.0290  | 0.0307                | 0.0306  | 0.0311  | 0.0308  |
|                 | 6000 | 0.0450                   | 0.0450  | 0.0466  | 0.0453  | 0.0273                 | 0.0273  | 0.0275  | 0.0274  | 0.0287                | 0.0287  | 0.0290  | 0.0288  |
|                 | 6100 | 0.0406                   | 0.0405  | 0.0420  | 0.0409  | 0.0259                 | 0.0259  | 0.0260  | 0.0260  | 0.0271                | 0.0270  | 0.0273  | 0.0271  |
|                 | 6200 | 0.0368                   | 0.0366  | 0.0379  | 0.0370  | 0.0248                 | 0.0248  | 0.0248  | 0.0249  | 0.0256                | 0.0255  | 0.0257  | 0.0256  |
|                 | 6300 | 0.0335                   | 0.0333  | 0.0344  | 0.0336  | 0.0238                 | 0.0238  | 0.0238  | 0.0239  | 0.0243                | 0.0242  | 0.0243  | 0.0243  |
|                 | 6400 | 0.0306                   | 0.0304  | 0.0313  | 0.0307  | 0.0229                 | 0.0229  | 0.0229  | 0.0230  | 0.0232                | 0.0231  | 0.0232  | 0.0232  |
|                 | 6500 | 0.0281                   | 0.0279  | 0.0287  | 0.0281  | 0.0222                 | 0.0221  | 0.0221  | 0.0222  | 0.0221                | 0.0220  | 0.0221  | 0.0222  |
|                 | 6600 | 0.0258                   | 0.0256  | 0.0263  | 0.0259  | 0.0214                 | 0.0214  | 0.0213  | 0.0215  | 0.0213                | 0.0212  | 0.0212  | 0.0213  |
|                 | 6700 | 0.0238                   | 0.0236  | 0.0242  | 0.0238  | 0.0208                 | 0.0207  | 0.0206  | 0.0208  | 0.0205                | 0.0204  | 0.0204  | 0.0205  |
|                 | 6800 | 0.0220                   | 0.0219  | 0.0223  | 0.0221  | 0.0201                 | 0.0200  | 0.0199  | 0.0201  | 0.0197                | 0.0197  | 0.0196  | 0.0198  |
|                 | 6900 | 0.0204                   | 0.0203  | 0.0206  | 0.0195  | 0.0195                 | 0.0193  | 0.0196  | 0.0190  | 0.0189                | 0.0188  | 0.0190  | 0.0190  |
|                 | 7000 | 0.0189                   | 0.0188  | 0.0190  | 0.0191  | 0.0188                 | 0.0188  | 0.0191  | 0.0183  | 0.0182                | 0.0181  | 0.0181  | 0.0183  |
| Mgb             | 4300 | 6.9616                   | 6.6099  | 6.7231  | 6.6065  | 3.8156                 | 3.6264  | 3.8005  | 3.6610  | 4.6802                | 4.4748  | 4.6614  | 4.5006  |
|                 | 4400 | 6.9284                   | 6.6992  | 6.8492  | 6.6986  | 3.2871                 | 3.0970  | 3.2643  | 3.1427  | 4.1470                | 3.9495  | 4.1363  | 3.9856  |
|                 | 4500 | 6.7200                   | 6.5337  | 6.7211  | 6.5372  | 2.7967                 | 2.6101  | 2.7637  | 2.6651  | 3.6119                | 3.4164  | 3.5959  | 3.4640  |
|                 | 4600 | 6.3190                   | 6.1430  | 6.3566  | 6.1548  | 2.3760                 | 2.2023  | 2.3383  | 2.2624  | 3.1158                | 2.9296  | 3.0948  | 2.9855  |
|                 | 4700 | 5.8028                   | 5.6367  | 5.8594  | 5.6582  | 2.0313                 | 1.8776  | 1.9958  | 1.9374  | 2.6836                | 2.5155  | 2.6633  | 2.5746  |
|                 | 4800 | 5.2488                   | 5.0946  | 5.3138  | 5.1252  | 1.7521                 | 1.6220  | 1.7236  | 1.6773  | 2.3229                | 2.1766  | 2.3070  | 2.2350  |
|                 | 4900 | 4.7011                   | 4.5642  | 4.7724  | 4.6005  | 1.5270                 | 1.4186  | 1.5064  | 1.4693  | 2.0216                | 1.9008  | 2.0159  | 1.9562  |
|                 | 5000 | 4.1904                   | 4.0750  | 4.2681  | 4.1145  | 1.3411                 | 1.2524  | 1.3283  | 1.2986  | 1.7705                | 1.6730  | 1.7732  | 1.7237  |
|                 | 5100 | 3.7294                   | 3.6366  | 3.8126  | 3.6769  | 1.1856                 | 1.1139  | 1.1794  | 1.1566  | 1.5585                | 1.4804  | 1.5680  | 1.5266  |
|                 | 5200 | 3.3188                   | 3.2481  | 3.4073  | 3.2871  | 1.0561                 | 0.9973  | 1.0535  | 1.0367  | 1.3791                | 1.3160  | 1.3924  | 1.3586  |
|                 | 5300 | 2.9540                   | 2.9017  | 3.0450  | 2.9384  | 0.9506                 | 0.9006  | 0.9483  | 0.9373  | 1.2273                | 1.1750  | 1.2413  | 1.2142  |
|                 | 5400 | 2.6317                   | 2.5935  | 2.7228  | 2.6272  | 0.8654                 | 0.8212  | 0.8614  | 0.8556  | 1.0999                | 1.0552  | 1.1122  | 1.0912  |
|                 | 5500 | 2.3462                   | 2.3180  | 2.4349  | 2.3484  | 0.7981                 | 0.7577  | 0.7911  | 0.7902  | 0.9952                | 0.9554  | 1.0035  | 0.9885  |
|                 | 5600 | 2.0947                   | 2.0723  |         |         |                        |         |         |         |                       |         |         |         |

Table B.1: Continued.

| Index  | T[K] | MS-TO ( $\log g = 4.2$ ) |        |        |        | RGB ( $\log g = 2.4$ ) |        |        |        | HB ( $\log g = 2.8$ ) |        |        |        |
|--------|------|--------------------------|--------|--------|--------|------------------------|--------|--------|--------|-----------------------|--------|--------|--------|
|        |      | Ref                      | IY2    | IY4    | 2Y2    | Ref                    | IY2    | IY4    | 2Y2    | Ref                   | IY2    | IY4    | 2Y2    |
| Fe5270 | 4300 | 3.0271                   | 2.8741 | 2.9191 | 2.8955 | 2.4865                 | 2.4139 | 2.4323 | 2.4412 | 2.5996                | 2.5110 | 2.5369 | 2.5419 |
|        | 4400 | 2.8704                   | 2.7679 | 2.8105 | 2.7883 | 2.3027                 | 2.2403 | 2.2559 | 2.2641 | 2.4036                | 2.3307 | 2.3530 | 2.3584 |
|        | 4500 | 2.6916                   | 2.6101 | 2.6521 | 2.6294 | 2.1264                 | 2.0691 | 2.0822 | 2.0905 | 2.2176                | 2.1536 | 2.1728 | 2.1788 |
|        | 4600 | 2.4843                   | 2.4163 | 2.4564 | 2.4349 | 1.9581                 | 1.9016 | 1.9124 | 1.9228 | 2.0397                | 1.9802 | 1.9965 | 2.0042 |
|        | 4700 | 2.2739                   | 2.2168 | 2.2523 | 2.2348 | 1.7977                 | 1.7423 | 1.7506 | 1.7645 | 1.8690                | 1.8127 | 1.8264 | 1.8368 |
|        | 4800 | 2.0711                   | 2.0224 | 2.0539 | 2.0402 | 1.6460                 | 1.5943 | 1.6002 | 1.6180 | 1.7082                | 1.6554 | 1.6664 | 1.6802 |
|        | 4900 | 1.8775                   | 1.8369 | 1.8642 | 1.8543 | 1.5049                 | 1.4592 | 1.4628 | 1.4843 | 1.5569                | 1.5105 | 1.5190 | 1.5365 |
|        | 5000 | 1.6961                   | 1.6627 | 1.6859 | 1.6801 | 1.3749                 | 1.3369 | 1.3385 | 1.3628 | 1.4171                | 1.3786 | 1.3845 | 1.4048 |
|        | 5100 | 1.5272                   | 1.5016 | 1.5206 | 1.5189 | 1.2577                 | 1.2273 | 1.2271 | 1.2534 | 1.2904                | 1.2594 | 1.2629 | 1.2856 |
|        | 5200 | 1.3732                   | 1.3550 | 1.3701 | 1.3720 | 1.1547                 | 1.1297 | 1.1282 | 1.1555 | 1.1780                | 1.1532 | 1.1547 | 1.1788 |
|        | 5300 | 1.2349                   | 1.2228 | 1.2345 | 1.2392 | 1.0656                 | 1.0437 | 1.0409 | 1.0687 | 1.0801                | 1.0593 | 1.0591 | 1.0840 |
|        | 5400 | 1.1134                   | 1.1058 | 1.1145 | 1.1211 | 0.9881                 | 0.9675 | 0.9639 | 0.9918 | 0.9954                | 0.9769 | 0.9753 | 1.0003 |
|        | 5500 | 1.0077                   | 1.0028 | 1.0091 | 1.0169 | 0.9195                 | 0.8992 | 0.8949 | 0.9228 | 0.9218                | 0.9041 | 0.9013 | 0.9265 |
|        | 5600 | 0.9166                   | 0.9128 | 0.9171 | 0.9257 | 0.8581                 | 0.8374 | 0.8328 | 0.8605 | 0.8570                | 0.8392 | 0.8357 | 0.8607 |
|        | 5700 | 0.8382                   | 0.8344 | 0.8369 | 0.8462 | 0.8022                 | 0.7812 | 0.7763 | 0.8039 | 0.7988                | 0.7808 | 0.7769 | 0.8015 |
|        | 5800 | 0.7702                   | 0.7657 | 0.7669 | 0.7767 | 0.7505                 | 0.7293 | 0.7242 | 0.7515 | 0.7459                | 0.7276 | 0.7234 | 0.7477 |
|        | 5900 | 0.7106                   | 0.7051 | 0.7054 | 0.7154 | 0.7026                 | 0.6814 | 0.6764 | 0.7032 | 0.6974                | 0.6790 | 0.6747 | 0.6984 |
|        | 6000 | 0.6579                   | 0.6515 | 0.6509 | 0.6612 | 0.6576                 | 0.6367 | 0.6315 | 0.6579 | 0.6517                | 0.6335 | 0.6293 | 0.6524 |
|        | 6100 | 0.6108                   | 0.6034 | 0.6024 | 0.6130 | 0.6150                 | 0.5946 | 0.5898 | 0.6153 | 0.6091                | 0.5914 | 0.5872 | 0.6095 |
|        | 6200 | 0.5678                   | 0.5602 | 0.5585 | 0.5691 | 0.5743                 | 0.5545 | 0.5500 | 0.5745 | 0.5689                | 0.5519 | 0.5478 | 0.5692 |
|        | 6300 | 0.5289                   | 0.5212 | 0.5191 | 0.5296 | 0.5352                 | 0.5162 | 0.5119 | 0.5355 | 0.5308                | 0.5145 | 0.5106 | 0.5310 |
|        | 6400 | 0.4929                   | 0.4854 | 0.4832 | 0.4933 | 0.4977                 | 0.4795 | 0.4756 | 0.4979 | 0.4940                | 0.4786 | 0.4751 | 0.4943 |
|        | 6500 | 0.4596                   | 0.4524 | 0.4501 | 0.4598 | 0.4615                 | 0.4441 | 0.4405 | 0.4617 | 0.4592                | 0.4447 | 0.4411 | 0.4594 |
|        | 6600 | 0.4282                   | 0.4214 | 0.4191 | 0.4283 | 0.4263                 | 0.4097 | 0.4065 | 0.4266 | 0.4253                | 0.4116 | 0.4082 | 0.4255 |
|        | 6700 | 0.3986                   | 0.3923 | 0.3902 | 0.3987 | 0.3922                 | 0.3765 | 0.3736 | 0.3925 | 0.3925                | 0.3796 | 0.3769 | 0.3927 |
|        | 6800 | 0.3702                   | 0.3645 | 0.3627 | 0.3703 | 0.3590                 | 0.3441 | 0.3417 | 0.3594 | 0.3608                | 0.3487 | 0.3464 | 0.3611 |
|        | 6900 | 0.3437                   | 0.3384 | 0.3367 | 0.3438 | 0.3265                 | 0.3124 | 0.3107 | 0.3269 | 0.3303                | 0.3188 | 0.3169 | 0.3306 |
|        | 7000 | 0.3183                   | 0.3134 | 0.3120 | 0.3184 | 0.2953                 | 0.2819 | 0.2804 | 0.2956 | 0.3007                | 0.2899 | 0.2885 | 0.3010 |
| Fe5335 | 4300 | 2.5563                   | 2.4532 | 2.4893 | 2.4367 | 2.3251                 | 2.2843 | 2.2948 | 2.2602 | 2.3653                | 2.3215 | 2.3375 | 2.2965 |
|        | 4400 | 2.4277                   | 2.3670 | 2.4006 | 2.3517 | 2.1665                 | 2.1252 | 2.1344 | 2.1064 | 2.2022                | 2.1627 | 2.1763 | 2.1425 |
|        | 4500 | 2.2833                   | 2.2373 | 2.2695 | 2.2239 | 2.0101                 | 1.9677 | 1.9757 | 1.9535 | 2.0443                | 2.0061 | 2.0178 | 1.9902 |
|        | 4600 | 2.1186                   | 2.0807 | 2.1106 | 2.0695 | 1.8590                 | 1.8162 | 1.8231 | 1.8065 | 1.8925                | 1.8547 | 1.8648 | 1.8430 |
|        | 4700 | 1.9555                   | 1.9236 | 1.9499 | 1.9149 | 1.7155                 | 1.6762 | 1.6817 | 1.6699 | 1.7473                | 1.7120 | 1.7207 | 1.7039 |
|        | 4800 | 1.8014                   | 1.7748 | 1.7976 | 1.7682 | 1.5818                 | 1.5497 | 1.5536 | 1.5455 | 1.6119                | 1.5816 | 1.5887 | 1.5760 |
|        | 4900 | 1.6570                   | 1.6361 | 1.6559 | 1.6310 | 1.4599                 | 1.4366 | 1.4393 | 1.4341 | 1.4863                | 1.4640 | 1.4697 | 1.4605 |
|        | 5000 | 1.5233                   | 1.5079 | 1.5246 | 1.5044 | 1.3498                 | 1.3358 | 1.3373 | 1.3343 | 1.3721                | 1.3584 | 1.3624 | 1.3559 |
|        | 5100 | 1.3988                   | 1.3896 | 1.4032 | 1.3873 | 1.2522                 | 1.2460 | 1.2465 | 1.2454 | 1.2694                | 1.2633 | 1.2660 | 1.2617 |
|        | 5200 | 1.2841                   | 1.2809 | 1.2915 | 1.2796 | 1.1667                 | 1.1659 | 1.1655 | 1.1655 | 1.1784                | 1.1780 | 1.1793 | 1.1770 |
|        | 5300 | 1.1791                   | 1.1809 | 1.1890 | 1.1801 | 1.0921                 | 1.0943 | 1.0931 | 1.0939 | 1.0984                | 1.1013 | 1.1015 | 1.1006 |
|        | 5400 | 1.0847                   | 1.0901 | 1.0960 | 1.0895 | 1.0264                 | 1.0297 | 1.0279 | 1.0294 | 1.0278                | 1.0325 | 1.0317 | 1.0316 |
|        | 5500 | 1.0001                   | 1.0077 | 1.0116 | 1.0070 | 0.9673                 | 0.9705 | 0.9682 | 0.9702 | 0.9652                | 0.9701 | 0.9682 | 0.9693 |
|        | 5600 | 0.9250                   | 0.9331 | 0.9354 | 0.9325 | 0.9134                 | 0.9159 | 0.9132 | 0.9157 | 0.9089                | 0.9130 | 0.9106 | 0.9123 |
|        | 5700 | 0.8581                   | 0.8657 | 0.8667 | 0.8652 | 0.8634                 | 0.8650 | 0.8619 | 0.8649 | 0.8572                | 0.8603 | 0.8574 | 0.8598 |
|        | 5800 | 0.7985                   | 0.8049 | 0.8047 | 0.8044 | 0.8165                 | 0.8171 | 0.8138 | 0.8173 | 0.8092                | 0.8111 | 0.8078 | 0.8109 |
|        | 5900 | 0.7448                   | 0.7496 | 0.7486 | 0.7494 | 0.7721                 | 0.7719 | 0.7684 | 0.7723 | 0.7643                | 0.7651 | 0.7616 | 0.7652 |
|        | 6000 | 0.6960                   | 0.6992 | 0.6972 | 0.6991 | 0.7296                 | 0.7288 | 0.7251 | 0.7293 | 0.7216                | 0.7215 | 0.7179 | 0.7219 |
|        | 6100 | 0.6514                   | 0.6528 | 0.6506 | 0.6534 | 0.6891                 | 0.6879 | 0.6842 | 0.6885 | 0.6809                | 0.6803 | 0.6766 | 0.6808 |
|        | 6200 | 0.6098                   | 0.6104 | 0.6074 | 0.6110 | 0.6500                 | 0.6484 | 0.6449 | 0.6491 | 0.6419                | 0.6410 | 0.6371 | 0.6416 |
|        | 6300 | 0.5715                   | 0.5713 | 0.5679 | 0.5721 | 0.6121                 | 0.6103 | 0.6070 | 0.6110 | 0.6048                | 0.6035 | 0.5996 | 0.6041 |
|        | 6400 | 0.5357                   | 0.5350 | 0.5313 | 0.5359 | 0.5759                 | 0.5740 | 0.5705 | 0.5745 | 0.5690                | 0.5675 | 0.5637 | 0.5681 |
|        | 6500 | 0.5023                   | 0.5013 | 0.4975 | 0.5022 | 0.5408                 | 0.5386 | 0.5352 | 0.5391 | 0.5345                | 0.5328 | 0.5290 | 0.5333 |
|        | 6600 | 0.4707                   | 0.4696 | 0.4658 | 0.4704 | 0.5070                 | 0.5044 | 0.5014 | 0.5050 | 0.5016                | 0.4997 | 0.4961 | 0.5002 |
|        | 6700 | 0.4407                   | 0.4395 | 0.4358 | 0.4403 | 0.4744                 | 0.4716 | 0.4687 | 0.4722 | 0.4696                | 0.4674 | 0.4642 | 0.4680 |
|        | 6800 | 0.4125                   | 0.4113 | 0.4077 | 0.4120 | 0.4432                 | 0.4399 | 0.4372 | 0.4405 | 0.4389                | 0.4364 | 0.4334 | 0.4370 |
|        | 6900 | 0.3857                   | 0.3845 | 0.3810 | 0.3852 | 0.4131                 | 0.4093 | 0.4069 | 0.4100 | 0.4095                | 0.4066 | 0.4038 | 0.4073 |
|        | 7000 | 0.3602                   | 0.3590 | 0.3558 | 0.3595 | 0.3840                 | 0.3797 | 0.3775 | 0.3805 | 0.3813                | 0.3780 | 0.3755 | 0.3787 |
| Fe5406 | 4300 | 1.8016                   | 1.7031 | 1.7391 | 1.7053 | 1.3588                 | 1.3132 | 1.3304 | 1.3130 | 1.4503                | 1.3988 | 1.4218 | 1.3995 |
|        | 4400 | 1.6627                   | 1.6018 | 1.6362 | 1.6031 | 1.2026                 | 1.1622 | 1.1766 | 1.1613 | 1.2837                | 1.2408 | 1.2603 | 1.2409 |
|        | 4500 | 1.5157                   | 1.4685 | 1.5023 | 1.4695 | 1.0621                 | 1.0254 | 1.0371 | 1.0241 | 1.1338                | 1.0963 | 1.1126 | 1.0962 |
|        | 4600 | 1.3561                   | 1.3172 | 1.3488 | 1.3184 | 0.9380                 | 0.9037 | 0.9130 | 0.9028 | 1.0005                | 0.9668 | 0.9802 | 0.9668 |
|        | 4700 | 1.2025                   | 1.1708 | 1.1988 | 1.1723 | 0.8282                 | 0.7970 | 0.8042 | 0.7966 | 0.8821                | 0.8521 | 0.8630 | 0.8525 |
|        | 4800 | 1.0621                   | 1.0365 | 1.0606 | 1.0384 | 0.7304                 | 0.7043 | 0.7097 | 0.7041 | 0.7773                | 0.7520 | 0.7606 | 0.7525 |
|        | 4900 | 0.9351                   | 0.9154 | 0.9360 | 0.9174 | 0.6432                 | 0.6241 | 0.6281 | 0.6240 | 0.6842                | 0.6653 | 0.6720 | 0.6659 |
|        | 5000 | 0.8227                   | 0.8087 | 0.8259 | 0.8107 | 0.5660                 | 0.5548 | 0.5576 | 0.5546 | 0.6021                | 0.5903 | 0.5954 | 0.5908 |
|        | 5100 | 0.7238                   | 0.7153 | 0.7295 | 0.7172 | 0.4994                 | 0.4952 | 0.4972 | 0.4949 | 0.5309                | 0.5257 | 0.5296 | 0.5259 |
|        | 5200 | 0.6381                   | 0.6346 | 0.6460 | 0.6362 | 0.4436                 | 0.4442 | 0.4456 | 0.4435 | 0.4708                | 0.4703 | 0.4733 | 0.4703 |
|        | 5300 | 0.5644                   | 0.5647 | 0.5738 | 0.5661 | 0.3975                 | 0.4005 | 0.4014 | 0.3995 | 0.4206                | 0.4229 | 0.4251 | 0.4226 |
|        | 5400 | 0.5020                   | 0.5049 | 0.5121 | 0.5059 | 0.3589                 | 0.3630 | 0.3637 | 0.3617 | 0.3789                | 0.3826 | 0.3843 | 0.3819 |
|        | 5500 | 0.4495                   | 0.4538 | 0.4595 | 0.4544 | 0.3258                 | 0.3302 | 0.3307 | 0.3287 | 0.3438                | 0.3479 | 0.3491 | 0.3469 |
|        | 5600 | 0.4054                   | 0.4101 |        |        |                        |        |        |        |                       |        |        |        |

Table B.1: Continued.

| Index  | T[K] | MS-TO ( $\log g = 4.2$ ) |        |        |        | RGB ( $\log g = 2.4$ ) |         |         |        | HB ( $\log g = 2.8$ ) |         |         |        |
|--------|------|--------------------------|--------|--------|--------|------------------------|---------|---------|--------|-----------------------|---------|---------|--------|
|        |      | Ref                      | IY2    | IY4    | 2Y2    | Ref                    | IY2     | IY4     | 2Y2    | Ref                   | IY2     | IY4     | 2Y2    |
| Fe5709 | 4300 | 0.4833                   | 0.4000 | 0.3868 | 0.3643 | 0.7331                 | 0.6825  | 0.6750  | 0.6549 | 0.6908                | 0.6399  | 0.6314  | 0.6107 |
|        | 4400 | 0.4724                   | 0.3969 | 0.3841 | 0.3632 | 0.6770                 | 0.6278  | 0.6214  | 0.6001 | 0.6416                | 0.5935  | 0.5858  | 0.5644 |
|        | 4500 | 0.4533                   | 0.3821 | 0.3708 | 0.3517 | 0.6175                 | 0.5679  | 0.5625  | 0.5424 | 0.5906                | 0.5422  | 0.5357  | 0.5156 |
|        | 4600 | 0.4265                   | 0.3580 | 0.3481 | 0.3320 | 0.5560                 | 0.5057  | 0.5014  | 0.4841 | 0.5376                | 0.4879  | 0.4824  | 0.4653 |
|        | 4700 | 0.3960                   | 0.3297 | 0.3208 | 0.3085 | 0.4939                 | 0.4445  | 0.4409  | 0.4270 | 0.4830                | 0.4328  | 0.4283  | 0.4147 |
|        | 4800 | 0.3638                   | 0.2994 | 0.2916 | 0.2826 | 0.4331                 | 0.3860  | 0.3829  | 0.3721 | 0.4282                | 0.3791  | 0.3752  | 0.3650 |
|        | 4900 | 0.3299                   | 0.2679 | 0.2610 | 0.2549 | 0.3758                 | 0.3312  | 0.3285  | 0.3204 | 0.3750                | 0.3278  | 0.3247  | 0.3172 |
|        | 5000 | 0.2954                   | 0.2362 | 0.2302 | 0.2263 | 0.3236                 | 0.2811  | 0.2789  | 0.2730 | 0.3251                | 0.2802  | 0.2775  | 0.2722 |
|        | 5100 | 0.2613                   | 0.2054 | 0.2003 | 0.1979 | 0.2776                 | 0.2365  | 0.2345  | 0.2305 | 0.2800                | 0.2370  | 0.2347  | 0.2312 |
|        | 5200 | 0.2289                   | 0.1764 | 0.1719 | 0.1707 | 0.2380                 | 0.1977  | 0.1960  | 0.1934 | 0.2405                | 0.1989  | 0.1969  | 0.1947 |
|        | 5300 | 0.1991                   | 0.1497 | 0.1458 | 0.1455 | 0.2043                 | 0.1645  | 0.1630  | 0.1615 | 0.2066                | 0.1660  | 0.1642  | 0.1630 |
|        | 5400 | 0.1726                   | 0.1260 | 0.1227 | 0.1228 | 0.1760                 | 0.1363  | 0.1350  | 0.1345 | 0.1779                | 0.1380  | 0.1364  | 0.1359 |
|        | 5500 | 0.1498                   | 0.1054 | 0.1026 | 0.1030 | 0.1520                 | 0.1124  | 0.1113  | 0.1115 | 0.1537                | 0.1142  | 0.1129  | 0.1131 |
|        | 5600 | 0.1303                   | 0.0879 | 0.0855 | 0.0860 | 0.1316                 | 0.0923  | 0.0913  | 0.0922 | 0.1333                | 0.0942  | 0.0931  | 0.0938 |
|        | 5700 | 0.1137                   | 0.0731 | 0.0710 | 0.0717 | 0.1143                 | 0.0754  | 0.0747  | 0.0760 | 0.1159                | 0.0774  | 0.0764  | 0.0775 |
|        | 5800 | 0.0997                   | 0.0606 | 0.0588 | 0.0596 | 0.0995                 | 0.0612  | 0.0606  | 0.0623 | 0.1010                | 0.0632  | 0.0624  | 0.0638 |
|        | 5900 | 0.0877                   | 0.0500 | 0.0486 | 0.0494 | 0.0868                 | 0.0493  | 0.0488  | 0.0508 | 0.0883                | 0.0514  | 0.0507  | 0.0522 |
|        | 6000 | 0.0774                   | 0.0411 | 0.0399 | 0.0407 | 0.0758                 | 0.0393  | 0.0389  | 0.0410 | 0.0774                | 0.0414  | 0.0409  | 0.0425 |
|        | 6100 | 0.0685                   | 0.0336 | 0.0326 | 0.0334 | 0.0664                 | 0.0310  | 0.0307  | 0.0329 | 0.0680                | 0.0331  | 0.0327  | 0.0344 |
|        | 6200 | 0.0607                   | 0.0273 | 0.0265 | 0.0272 | 0.0582                 | 0.0239  | 0.0238  | 0.0260 | 0.0599                | 0.0261  | 0.0258  | 0.0275 |
|        | 6300 | 0.0540                   | 0.0219 | 0.0213 | 0.0220 | 0.0511                 | 0.0181  | 0.0180  | 0.0202 | 0.0527                | 0.0201  | 0.0200  | 0.0216 |
|        | 6400 | 0.0481                   | 0.0174 | 0.0168 | 0.0175 | 0.0449                 | 0.0132  | 0.0132  | 0.0154 | 0.0466                | 0.0153  | 0.0152  | 0.0169 |
|        | 6500 | 0.0431                   | 0.0136 | 0.0131 | 0.0138 | 0.0395                 | 0.0091  | 0.0092  | 0.0114 | 0.0412                | 0.0112  | 0.0111  | 0.0128 |
|        | 6600 | 0.0385                   | 0.0103 | 0.0100 | 0.0106 | 0.0348                 | 0.0058  | 0.0059  | 0.0080 | 0.0364                | 0.0078  | 0.0077  | 0.0094 |
|        | 6700 | 0.0346                   | 0.0076 | 0.0074 | 0.0079 | 0.0306                 | 0.0032  | 0.0032  | 0.0054 | 0.0323                | 0.0050  | 0.0050  | 0.0066 |
|        | 6800 | 0.0311                   | 0.0054 | 0.0052 | 0.0057 | 0.0269                 | 0.0010  | 0.0012  | 0.0032 | 0.0286                | 0.0027  | 0.0027  | 0.0043 |
|        | 6900 | 0.0280                   | 0.0035 | 0.0033 | 0.0039 | 0.0236                 | -0.0007 | -0.0005 | 0.0014 | 0.0253                | 0.0009  | 0.0010  | 0.0025 |
|        | 7000 | 0.0252                   | 0.0019 | 0.0018 | 0.0023 | 0.0207                 | -0.0021 | -0.0018 | 0.0000 | 0.0224                | -0.0005 | -0.0004 | 0.0010 |
| Fe5782 | 4300 | 0.1761                   | 0.1903 | 0.1882 | 0.1697 | 0.2586                 | 0.2678  | 0.2675  | 0.2525 | 0.2485                | 0.2602  | 0.2596  | 0.2427 |
|        | 4400 | 0.1689                   | 0.1840 | 0.1822 | 0.1638 | 0.2266                 | 0.2350  | 0.2352  | 0.2208 | 0.2194                | 0.2307  | 0.2304  | 0.2143 |
|        | 4500 | 0.1564                   | 0.1716 | 0.1704 | 0.1522 | 0.1965                 | 0.2045  | 0.2050  | 0.1909 | 0.1920                | 0.2029  | 0.2030  | 0.1873 |
|        | 4600 | 0.1403                   | 0.1551 | 0.1544 | 0.1366 | 0.1683                 | 0.1766  | 0.1773  | 0.1634 | 0.1661                | 0.1770  | 0.1773  | 0.1619 |
|        | 4700 | 0.1234                   | 0.1381 | 0.1376 | 0.1207 | 0.1424                 | 0.1519  | 0.1527  | 0.1387 | 0.1420                | 0.1533  | 0.1538  | 0.1386 |
|        | 4800 | 0.1073                   | 0.1218 | 0.1215 | 0.1054 | 0.1192                 | 0.1300  | 0.1309  | 0.1169 | 0.1200                | 0.1320  | 0.1326  | 0.1176 |
|        | 4900 | 0.0925                   | 0.1065 | 0.1062 | 0.0911 | 0.1098                 | 0.1117  | 0.1117  | 0.0979 | 0.1005                | 0.1131  | 0.1138  | 0.0991 |
|        | 5000 | 0.0790                   | 0.0924 | 0.0922 | 0.0782 | 0.0821                 | 0.0942  | 0.0950  | 0.0817 | 0.0837                | 0.0965  | 0.0971  | 0.0832 |
|        | 5100 | 0.0670                   | 0.0797 | 0.0797 | 0.0668 | 0.0682                 | 0.0798  | 0.0806  | 0.0683 | 0.0696                | 0.0820  | 0.0826  | 0.0696 |
|        | 5200 | 0.0567                   | 0.0685 | 0.0685 | 0.0569 | 0.0570                 | 0.0677  | 0.0684  | 0.0572 | 0.0582                | 0.0696  | 0.0702  | 0.0584 |
|        | 5300 | 0.0480                   | 0.0586 | 0.0587 | 0.0484 | 0.0480                 | 0.0577  | 0.0583  | 0.0482 | 0.0489                | 0.0591  | 0.0597  | 0.0492 |
|        | 5400 | 0.0407                   | 0.0501 | 0.0502 | 0.0412 | 0.0408                 | 0.0493  | 0.0498  | 0.0409 | 0.0415                | 0.0504  | 0.0509  | 0.0417 |
|        | 5500 | 0.0348                   | 0.0430 | 0.0430 | 0.0352 | 0.0350                 | 0.0423  | 0.0427  | 0.0350 | 0.0354                | 0.0432  | 0.0435  | 0.0356 |
|        | 5600 | 0.0299                   | 0.0369 | 0.0370 | 0.0303 | 0.0302                 | 0.0364  | 0.0367  | 0.0301 | 0.0305                | 0.0371  | 0.0374  | 0.0306 |
|        | 5700 | 0.0259                   | 0.0318 | 0.0319 | 0.0262 | 0.0262                 | 0.0314  | 0.0318  | 0.0260 | 0.0264                | 0.0320  | 0.0323  | 0.0264 |
|        | 5800 | 0.0225                   | 0.0276 | 0.0277 | 0.0229 | 0.0273                 | 0.0275  | 0.0275  | 0.0230 | 0.0277                | 0.0279  | 0.0229  |        |
|        | 5900 | 0.0198                   | 0.0240 | 0.0241 | 0.0199 | 0.0200                 | 0.0237  | 0.0240  | 0.0198 | 0.0202                | 0.0241  | 0.0243  | 0.0200 |
|        | 6000 | 0.0174                   | 0.0209 | 0.0210 | 0.0175 | 0.0177                 | 0.0207  | 0.0210  | 0.0174 | 0.0177                | 0.0210  | 0.0212  | 0.0176 |
|        | 6100 | 0.0154                   | 0.0183 | 0.0184 | 0.0154 | 0.0157                 | 0.0182  | 0.0184  | 0.0153 | 0.0157                | 0.0184  | 0.0186  | 0.0155 |
|        | 6200 | 0.0137                   | 0.0162 | 0.0162 | 0.0137 | 0.0139                 | 0.0160  | 0.0162  | 0.0135 | 0.0140                | 0.0162  | 0.0163  | 0.0137 |
|        | 6300 | 0.0122                   | 0.0143 | 0.0144 | 0.0122 | 0.0124                 | 0.0141  | 0.0142  | 0.0120 | 0.0125                | 0.0143  | 0.0144  | 0.0122 |
|        | 6400 | 0.0110                   | 0.0127 | 0.0127 | 0.0109 | 0.0111                 | 0.0124  | 0.0126  | 0.0107 | 0.0111                | 0.0126  | 0.0127  | 0.0108 |
|        | 6500 | 0.0098                   | 0.0113 | 0.0113 | 0.0097 | 0.0100                 | 0.0110  | 0.0111  | 0.0095 | 0.0100                | 0.0111  | 0.0112  | 0.0096 |
|        | 6600 | 0.0089                   | 0.0100 | 0.0101 | 0.0087 | 0.0090                 | 0.0097  | 0.0098  | 0.0085 | 0.0090                | 0.0099  | 0.0100  | 0.0086 |
|        | 6700 | 0.0080                   | 0.0090 | 0.0090 | 0.0079 | 0.0081                 | 0.0086  | 0.0087  | 0.0076 | 0.0081                | 0.0087  | 0.0088  | 0.0077 |
|        | 6800 | 0.0073                   | 0.0081 | 0.0081 | 0.0071 | 0.0074                 | 0.0077  | 0.0077  | 0.0068 | 0.0073                | 0.0077  | 0.0078  | 0.0069 |
|        | 6900 | 0.0066                   | 0.0072 | 0.0073 | 0.0064 | 0.0067                 | 0.0068  | 0.0068  | 0.0061 | 0.0067                | 0.0069  | 0.0070  | 0.0062 |
|        | 7000 | 0.0060                   | 0.0065 | 0.0066 | 0.0059 | 0.0061                 | 0.0060  | 0.0054  | 0.0061 | 0.0061                | 0.0062  | 0.0056  |        |
| Na D   | 4300 | 2.8572                   | 6.2331 | 6.5011 | 6.2308 | 1.0514                 | 2.4687  | 2.5761  | 2.4484 | 1.3081                | 3.0789  | 3.2250  | 3.0652 |
|        | 4400 | 2.4461                   | 5.5373 | 5.7825 | 5.5346 | 0.8791                 | 2.0450  | 2.1323  | 2.0274 | 1.0764                | 2.5389  | 2.6580  | 2.5275 |
|        | 4500 | 2.0633                   | 4.7816 | 5.0110 | 4.7803 | 0.7478                 | 1.7140  | 1.7858  | 1.6996 | 0.9020                | 2.1191  | 2.2177  | 2.1108 |
|        | 4600 | 1.7166                   | 4.0443 | 4.2498 | 4.0458 | 0.6461                 | 1.4517  | 1.5117  | 1.4405 | 0.7682                | 1.7891  | 1.8715  | 1.7832 |
|        | 4700 | 1.4358                   | 3.4265 | 3.6027 | 3.4307 | 0.5660                 | 1.2414  | 1.2922  | 1.2336 | 0.6638                | 1.5262  | 1.5959  | 1.5226 |
|        | 4800 | 1.2159                   | 2.9263 | 3.0761 | 2.9330 | 0.5021                 | 1.0716  | 1.1148  | 1.0665 | 0.5813                | 1.3145  | 1.3738  | 1.3130 |
|        | 4900 | 1.0419                   | 2.5206 | 2.6483 | 2.5281 | 0.4502                 | 0.9330  | 0.9697  | 0.9302 | 0.5148                | 1.1414  | 1.1922  | 1.1412 |
|        | 5000 | 0.9027                   | 2.1885 | 2.2984 | 2.1969 | 0.4080                 | 0.8186  | 0.8499  | 0.8176 | 0.4608                | 0.9978  | 1.0416  | 0.9989 |
|        | 5100 | 0.7894                   | 1.9132 | 2.0080 | 1.9216 | 0.3738                 | 0.7234  | 0.7496  | 0.7235 | 0.4167                | 0.8768  | 0.9144  | 0.8785 |
|        | 5200 | 0.6960                   | 1.6817 | 1.7645 | 1.6897 | 0.3465                 | 0.6438  | 0.6656  | 0.6445 | 0.3808                | 0.7740  | 0.8063  | 0.7761 |
|        | 5300 | 0.6178                   | 1.4833 | 1.5559 | 1.4906 | 0.3252                 | 0.5781  | 0.5959  | 0.5789 | 0.3519                | 0.6868  | 0.7140  | 0.6888 |
|        | 5400 | 0.5516                   | 1.3107 | 1.3746 | 1.3172 | 0.3087                 | 0.5246  | 0.5389  | 0.5253 | 0.3290                | 0.6136  | 0.6360  | 0.6152 |
|        | 5500 | 0.4953                   | 1.1590 | 1.2156 | 1.1647 | 0.2959                 | 0.4817  | 0.4928  | 0.4822 | 0.3109                | 0.5530  | 0.5714  | 0.5544 |
|        | 5600 | 0.4474                   | 1.0254 | 1.0754 | 1.0303 |                        |         |         |        |                       |         |         |        |

Table B.1: Continued.

| Index            | T[K] | MS-TO ( $\log g = 4.2$ ) |         |         |         | RGB ( $\log g = 2.4$ ) |         |         |         | HB ( $\log g = 2.8$ ) |         |         |         |
|------------------|------|--------------------------|---------|---------|---------|------------------------|---------|---------|---------|-----------------------|---------|---------|---------|
|                  |      | Ref                      | 1Y2     | 1Y4     | 2Y2     | Ref                    | 1Y2     | 1Y4     | 2Y2     | Ref                   | 1Y2     | 1Y4     | 2Y2     |
| TiO <sub>1</sub> | 4300 | 0.0021                   | 0.0013  | 0.0012  | 0.0018  | 0.0038                 | 0.0035  | 0.0035  | 0.0038  | 0.0036                | 0.0033  | 0.0032  | 0.0035  |
|                  | 4400 | 0.0020                   | 0.0014  | 0.0013  | 0.0018  | 0.0034                 | 0.0032  | 0.0031  | 0.0034  | 0.0033                | 0.0030  | 0.0029  | 0.0032  |
|                  | 4500 | 0.0018                   | 0.0013  | 0.0012  | 0.0017  | 0.0030                 | 0.0027  | 0.0027  | 0.0029  | 0.0029                | 0.0026  | 0.0026  | 0.0028  |
|                  | 4600 | 0.0016                   | 0.0012  | 0.0011  | 0.0015  | 0.0025                 | 0.0023  | 0.0023  | 0.0025  | 0.0025                | 0.0022  | 0.0022  | 0.0024  |
|                  | 4700 | 0.0013                   | 0.0010  | 0.0009  | 0.0012  | 0.0021                 | 0.0018  | 0.0018  | 0.0020  | 0.0020                | 0.0018  | 0.0018  | 0.0020  |
|                  | 4800 | 0.0010                   | 0.0008  | 0.0008  | 0.0010  | 0.0017                 | 0.0015  | 0.0014  | 0.0016  | 0.0016                | 0.0014  | 0.0014  | 0.0016  |
|                  | 4900 | 0.0008                   | 0.0006  | 0.0006  | 0.0008  | 0.0013                 | 0.0011  | 0.0011  | 0.0013  | 0.0013                | 0.0011  | 0.0011  | 0.0012  |
|                  | 5000 | 0.0006                   | 0.0004  | 0.0004  | 0.0006  | 0.0010                 | 0.0008  | 0.0008  | 0.0010  | 0.0010                | 0.0008  | 0.0008  | 0.0010  |
|                  | 5100 | 0.0004                   | 0.0003  | 0.0003  | 0.0004  | 0.0007                 | 0.0006  | 0.0006  | 0.0008  | 0.0007                | 0.0006  | 0.0006  | 0.0007  |
|                  | 5200 | 0.0003                   | 0.0002  | 0.0002  | 0.0003  | 0.0006                 | 0.0005  | 0.0005  | 0.0006  | 0.0006                | 0.0005  | 0.0005  | 0.0006  |
|                  | 5300 | 0.0002                   | 0.0001  | 0.0001  | 0.0002  | 0.0005                 | 0.0004  | 0.0004  | 0.0005  | 0.0004                | 0.0004  | 0.0004  | 0.0004  |
|                  | 5400 | 0.0001                   | 0.0001  | 0.0001  | 0.0001  | 0.0004                 | 0.0003  | 0.0003  | 0.0004  | 0.0004                | 0.0003  | 0.0003  | 0.0004  |
|                  | 5500 | 0.0001                   | 0.0001  | 0.0000  | 0.0001  | 0.0004                 | 0.0003  | 0.0003  | 0.0004  | 0.0003                | 0.0003  | 0.0003  | 0.0003  |
|                  | 5600 | 0.0001                   | 0.0001  | 0.0000  | 0.0001  | 0.0003                 | 0.0003  | 0.0003  | 0.0003  | 0.0003                | 0.0003  | 0.0002  | 0.0003  |
|                  | 5700 | 0.0001                   | 0.0001  | 0.0001  | 0.0001  | 0.0003                 | 0.0003  | 0.0003  | 0.0003  | 0.0003                | 0.0003  | 0.0003  | 0.0003  |
|                  | 5800 | 0.0001                   | 0.0001  | 0.0001  | 0.0001  | 0.0004                 | 0.0004  | 0.0003  | 0.0004  | 0.0003                | 0.0003  | 0.0003  | 0.0003  |
|                  | 5900 | 0.0002                   | 0.0001  | 0.0001  | 0.0002  | 0.0004                 | 0.0004  | 0.0004  | 0.0004  | 0.0004                | 0.0003  | 0.0003  | 0.0004  |
|                  | 6000 | 0.0002                   | 0.0002  | 0.0002  | 0.0002  | 0.0005                 | 0.0005  | 0.0004  | 0.0005  | 0.0004                | 0.0004  | 0.0004  | 0.0004  |
|                  | 6100 | 0.0003                   | 0.0002  | 0.0002  | 0.0003  | 0.0005                 | 0.0005  | 0.0005  | 0.0006  | 0.0005                | 0.0005  | 0.0005  | 0.0005  |
|                  | 6200 | 0.0003                   | 0.0003  | 0.0003  | 0.0003  | 0.0006                 | 0.0006  | 0.0006  | 0.0006  | 0.0005                | 0.0005  | 0.0005  | 0.0005  |
|                  | 6300 | 0.0004                   | 0.0004  | 0.0004  | 0.0004  | 0.0007                 | 0.0007  | 0.0007  | 0.0007  | 0.0007                | 0.0007  | 0.0007  | 0.0007  |
|                  | 6400 | 0.0004                   | 0.0004  | 0.0004  | 0.0004  | 0.0007                 | 0.0007  | 0.0007  | 0.0007  | 0.0007                | 0.0007  | 0.0007  | 0.0007  |
|                  | 6500 | 0.0005                   | 0.0005  | 0.0005  | 0.0005  | 0.0008                 | 0.0008  | 0.0008  | 0.0008  | 0.0007                | 0.0007  | 0.0007  | 0.0007  |
|                  | 6600 | 0.0005                   | 0.0005  | 0.0005  | 0.0006  | 0.0009                 | 0.0009  | 0.0009  | 0.0009  | 0.0008                | 0.0008  | 0.0008  | 0.0008  |
|                  | 6700 | 0.0006                   | 0.0006  | 0.0006  | 0.0006  | 0.0011                 | 0.0011  | 0.0010  | 0.0011  | 0.0009                | 0.0009  | 0.0009  | 0.0009  |
|                  | 6800 | 0.0007                   | 0.0007  | 0.0007  | 0.0007  | 0.0011                 | 0.0012  | 0.0011  | 0.0012  | 0.0010                | 0.0010  | 0.0010  | 0.0010  |
|                  | 6900 | 0.0008                   | 0.0008  | 0.0008  | 0.0008  | 0.0013                 | 0.0013  | 0.0013  | 0.0013  | 0.0011                | 0.0011  | 0.0011  | 0.0011  |
|                  | 7000 | 0.0009                   | 0.0009  | 0.0008  | 0.0009  | 0.0014                 | 0.0014  | 0.0014  | 0.0014  | 0.0012                | 0.0012  | 0.0012  | 0.0012  |
| $H\delta_A$      | 4300 | -3.7046                  | -3.8949 | -3.9125 | -3.8514 | -3.3255                | -4.7643 | -4.7403 | -4.1496 | -3.3962               | -4.5340 | -4.5287 | -4.0244 |
|                  | 4400 | -3.7903                  | -4.0203 | -4.0528 | -3.9295 | -3.1378                | -4.5712 | -4.5503 | -3.9265 | -3.2306               | -4.3980 | -4.3927 | -3.8547 |
|                  | 4500 | -3.7382                  | -4.0096 | -4.0507 | -3.8790 | -2.8803                | -4.2287 | -4.2076 | -3.5647 | -2.9999               | -4.1291 | -4.1269 | -3.5702 |
|                  | 4600 | -3.5647                  | -3.8691 | -3.9178 | -3.7054 | -2.5645                | -3.7306 | -3.7250 | -3.0780 | -2.7083               | -3.7234 | -3.7274 | -3.1680 |
|                  | 4700 | -3.2963                  | -3.5975 | -3.6494 | -3.4130 | -2.2117                | -3.1231 | -3.1267 | -2.5160 | -2.3727               | -3.2018 | -3.2135 | -2.6744 |
|                  | 4800 | -2.9664                  | -3.2247 | -3.2776 | -3.0349 | -1.8369                | -2.4652 | -2.4760 | -1.9437 | -2.0103               | -2.6113 | -2.6300 | -2.1404 |
|                  | 4900 | -2.5976                  | -2.7764 | -2.8303 | -2.5985 | -1.4491                | -1.8185 | -1.8328 | -1.4106 | -1.6313               | -1.9981 | -2.0205 | -1.6136 |
|                  | 5000 | -2.2100                  | -2.2864 | -2.3410 | -2.1353 | -1.0520                | -1.2228 | -1.2383 | -0.9279 | -1.2411               | -1.4107 | -1.4357 | -1.1251 |
|                  | 5100 | -1.8108                  | -1.7852 | -1.8392 | -1.6713 | -0.6487                | -0.6914 | -0.7062 | -0.4945 | -0.8430               | -0.8750 | -0.8999 | -0.6828 |
|                  | 5200 | -1.4065                  | -1.2976 | -1.3500 | -1.2246 | -0.2445                | -0.2192 | -0.2323 | -0.0961 | -0.4412               | -0.3928 | -0.4162 | -0.2747 |
|                  | 5300 | -0.9993                  | -0.8395 | -0.8894 | -0.8023 | 0.1611                 | 0.2159  | 0.2028  | 0.2867  | -0.0385               | 0.0457  | 0.0236  | 0.1100  |
|                  | 5400 | -0.5921                  | -0.4079 | -0.4550 | -0.4054 | 0.5604                 | 0.6202  | 0.6103  | 0.6594  | 0.3605                | 0.4526  | 0.4350  | 0.4810  |
|                  | 5500 | -0.1852                  | -0.0001 | -0.0453 | -0.0206 | 0.9568                 | 1.0121  | 1.0033  | 1.0306  | 0.7592                | 0.8459  | 0.8285  | 0.8515  |
|                  | 5600 | 0.2210                   | 0.3929  | 0.3492  | 0.3571  | 1.3590                 | 1.4065  | 1.3990  | 1.4121  | 1.1589                | 1.2360  | 1.2201  | 1.2278  |
|                  | 5700 | 0.6276                   | 0.7808  | 0.7387  | 0.7352  | 1.7721                 | 1.8121  | 1.8059  | 1.8106  | 1.5668                | 1.6329  | 1.6183  | 1.6169  |
|                  | 5800 | 1.0393                   | 1.1728  | 1.1315  | 1.1222  | 2.1985                 | 2.2316  | 2.2271  | 2.2259  | 1.9853                | 2.0430  | 2.0278  | 2.0215  |
|                  | 5900 | 1.4579                   | 1.5738  | 1.5336  | 1.5216  | 2.6396                 | 2.6671  | 2.6647  | 2.6593  | 2.4245                | 2.4725  | 2.4607  | 2.4506  |
|                  | 6000 | 1.8868                   | 1.9872  | 1.9485  | 1.9352  | 3.0991                 | 3.1217  | 3.1203  | 3.1134  | 2.8771                | 2.9177  | 2.9081  | 2.8961  |
|                  | 6100 | 2.3304                   | 2.4113  | 2.3805  | 2.3667  | 3.5735                 | 3.5918  | 3.5939  | 3.5846  | 3.3467                | 3.3814  | 3.3731  | 3.3605  |
|                  | 6200 | 2.7810                   | 2.8554  | 2.8222  | 2.8086  | 4.0608                 | 4.0757  | 4.0815  | 4.0688  | 3.8330                | 3.8621  | 3.8565  | 3.8433  |
|                  | 6300 | 3.2552                   | 3.3206  | 3.2863  | 3.2770  | 4.5499                 | 4.5617  | 4.5747  | 4.5561  | 4.3312                | 4.3561  | 4.3528  | 4.3389  |
|                  | 6400 | 3.7494                   | 3.8074  | 3.7722  | 3.7658  | 5.0473                 | 5.0568  | 5.0725  | 5.0522  | 4.8409                | 4.8606  | 4.8626  | 4.8468  |
|                  | 6500 | 4.2607                   | 4.3091  | 4.2766  | 4.2727  | 5.5543                 | 5.5589  | 5.5823  | 5.5579  | 5.3556                | 5.3714  | 5.3780  | 5.3597  |
|                  | 6600 | 4.7823                   | 4.8234  | 4.7938  | 4.7916  | 6.0531                 | 6.0569  | 6.0892  | 6.0565  | 5.8796                | 5.8927  | 5.9041  | 5.8827  |
|                  | 6700 | 5.3168                   | 5.3513  | 5.3230  | 5.3238  | 6.5426                 | 6.5428  | 6.5482  | 6.5453  | 6.3967                | 6.4046  | 6.4284  | 6.3990  |
|                  | 6800 | 5.8600                   | 5.8886  | 5.8631  | 5.8652  | 7.0290                 | 7.0296  | 7.0768  | 7.0309  | 6.9042                | 6.9103  | 6.9402  | 6.9068  |
|                  | 6900 | 6.4100                   | 6.4336  | 6.4093  | 6.4140  | 7.5182                 | 7.5184  | 7.5751  | 7.5203  | 7.4091                | 7.4146  | 7.4494  | 7.4114  |
|                  | 7000 | 6.9680                   | 6.9868  | 6.9644  | 6.9702  | 8.0099                 | 8.0077  | 8.0688  | 8.0121  | 7.9171                | 7.9197  | 7.9614  | 7.9191  |
| $H\gamma_A$      | 4300 | -9.3466                  | -9.4198 | -9.5779 | -9.2482 | -8.3476                | -8.3948 | -8.4486 | -8.2360 | -8.5844               | -8.5964 | -8.6809 | -8.4402 |
|                  | 4400 | -9.2817                  | -9.2561 | -9.4089 | -9.1101 | -8.0917                | -7.9753 | -8.0198 | -7.8484 | -8.2804               | -8.1549 | -8.2231 | -8.0294 |
|                  | 4500 | -9.1117                  | -8.8804 | -9.0298 | -8.7655 | -7.8623                | -7.5169 | -7.5574 | -7.4254 | -8.0255               | -7.7028 | -7.7618 | -7.6117 |
|                  | 4600 | -8.8352                  | -8.3771 | -8.5173 | -8.2903 | -7.6318                | -6.9950 | -7.0348 | -6.9360 | -7.7840               | -7.2080 | -7.2615 | -7.1468 |
|                  | 4700 | -8.5294                  | -7.8188 | -7.9449 | -7.7537 | -7.3755                | -6.3927 | -6.4341 | -6.3599 | -7.5270               | -6.6456 | -6.6967 | -6.6064 |
|                  | 4800 | -8.2074                  | -7.2190 | -7.3290 | -7.1666 | -7.0667                | -5.7069 | -5.7499 | -5.6911 | -7.2294               | -6.0021 | -6.0524 | -5.9793 |
|                  | 4900 | -7.8528                  | -6.5529 | -6.6499 | -6.5078 | -6.6763                | -4.9489 | -4.9932 | -4.9414 | -6.8630               | -5.2825 | -5.3320 | -5.2678 |
|                  | 5000 | -7.4424                  | -5.8265 | -5.9114 | -5.7885 | -6.1668                | -4.1358 | -4.1807 | -4.1293 | -6.4024               | -4.4993 | -4.5493 | -4.4888 |
|                  | 5100 | -6.9643                  | -5.0445 | -5.1183 | -5.0098 | -5.5019                | -3.2961 | -3.3404 | -3.2864 | -5.8152               | -3.6785 | -3.7278 | -3.6665 |
|                  | 5200 | -6.3907                  | -4.2324 | -4.2971 | -4.2019 | -4.6641                | -2.4669 | -2.5090 | -2.4505 | -5.0751               | -2.8502 | -2.8974 | -2.8342 |
|                  | 5300 | -5.7177                  | -3.4167 | -3.4737 | -3.3885 | -3.6806                | -1.6795 | -1.7187 | -1.6564 | -4.1837               | -2.0481 | -2.0924 | -2.0260 |
|                  | 5400 | -4.9357                  | -2.6180 | -2.6693 | -2.5907 | -2.6330                | -0.9625 | -0.9949 | -0.9313 | -3.1870               | -1.3001 | -1.3372 | -1.2712 |
|                  | 5500 | -4.0519                  | -1.8547 | -1.9012 | -1.8279 | -1.6116                | -0.3155 | -0.3421 | -0.2802 | -2.1615               | -0.6156 | -0.6484 | -0.5821 |
|                  | 5600 | -3.1                     |         |         |         |                        |         |         |         |                       |         |         |         |

Table B.1: Continued.

| Index | T[K] | MS-TO ( $\log g = 4.2$ ) |         |         |         | RGB ( $\log g = 2.4$ ) |         |         |         | HB ( $\log g = 2.8$ ) |         |         |         |
|-------|------|--------------------------|---------|---------|---------|------------------------|---------|---------|---------|-----------------------|---------|---------|---------|
|       |      | Ref                      | IY2     | IY4     | 2Y2     | Ref                    | IY2     | IY4     | 2Y2     | Ref                   | IY2     | IY4     | 2Y2     |
|       | 4300 | -1.8023                  | -1.7852 | -1.7998 | -1.7380 | -1.5897                | -1.8052 | -1.8131 | -1.6055 | -1.6458               | -1.8033 | -1.8198 | -1.6325 |
|       | 4400 | -1.7318                  | -1.7198 | -1.7427 | -1.6656 | -1.3896                | -1.5924 | -1.5987 | -1.4043 | -1.4435               | -1.5971 | -1.6115 | -1.4354 |
|       | 4500 | -1.6041                  | -1.5965 | -1.6247 | -1.5389 | -1.1949                | -1.3710 | -1.3764 | -1.1947 | -1.2499               | -1.3875 | -1.4005 | -1.2361 |
|       | 4600 | -1.4382                  | -1.4328 | -1.4644 | -1.3757 | -0.9958                | -1.1326 | -1.1385 | -0.9704 | -1.0552               | -1.1656 | -1.1781 | -1.0257 |
|       | 4700 | -1.2507                  | -1.2419 | -1.2728 | -1.1865 | -0.7869                | -0.8774 | -0.8842 | -0.7326 | -0.8539               | -0.9278 | -0.9403 | -0.8021 |
|       | 4800 | -1.0507                  | -1.0305 | -1.0600 | -0.9808 | -0.5659                | -0.6111 | -0.6193 | -0.4884 | -0.6405               | -0.6764 | -0.6891 | -0.5682 |
|       | 4900 | -0.8409                  | -0.8038 | -0.8315 | -0.7626 | -0.3306                | -0.3401 | -0.3478 | -0.2409 | -0.4152               | -0.4160 | -0.4271 | -0.3269 |
|       | 5000 | -0.6239                  | -0.5673 | -0.5936 | -0.5368 | -0.0812                | -0.0669 | -0.0745 | 0.0088  | -0.1765               | -0.1498 | -0.1625 | -0.0836 |
|       | 5100 | -0.3981                  | -0.3249 | -0.3500 | -0.3059 | 0.1820                 | 0.2082  | 0.2005  | 0.2624  | 0.0752                | 0.1168  | 0.1043  | 0.1630  |
|       | 5200 | -0.1641                  | -0.0795 | -0.1037 | -0.0716 | 0.4570                 | 0.4858  | 0.4786  | 0.5230  | 0.3393                | 0.3862  | 0.3741  | 0.4153  |
|       | 5300 | 0.0796                   | 0.1678  | 0.1443  | 0.1662  | 0.7460                 | 0.7751  | 0.7662  | 0.7972  | 0.6156                | 0.6617  | 0.6487  | 0.6770  |
|       | 5400 | 0.3333                   | 0.4185  | 0.3952  | 0.4096  | 1.0434                 | 1.0680  | 1.0604  | 1.0815  | 0.9012                | 0.9424  | 0.9317  | 0.9482  |
|       | 5500 | 0.5984                   | 0.6756  | 0.6519  | 0.6620  | 1.3469                 | 1.3682  | 1.3603  | 1.3746  | 1.1985                | 1.2340  | 1.2215  | 1.2332  |
| Hδ_F  | 5600 | 0.8758                   | 0.9425  | 0.9178  | 0.9265  | 1.6611                 | 1.6787  | 1.6708  | 1.6806  | 1.5057                | 1.5358  | 1.5233  | 1.5310  |
|       | 5700 | 1.1653                   | 1.2217  | 1.1967  | 1.2046  | 1.9865                 | 2.0012  | 1.9930  | 2.0010  | 1.8230                | 1.8478  | 1.8353  | 1.8413  |
|       | 5800 | 1.4688                   | 1.5158  | 1.4896  | 1.4989  | 2.3234                 | 2.3345  | 2.3262  | 2.3335  | 2.1496                | 2.1711  | 2.1569  | 2.1631  |
|       | 5900 | 1.7844                   | 1.8234  | 1.7968  | 1.8076  | 2.6723                 | 2.6802  | 2.6720  | 2.6797  | 2.4913                | 2.5073  | 2.4947  | 2.5011  |
|       | 6000 | 2.1096                   | 2.1421  | 2.1157  | 2.1277  | 3.0301                 | 3.0351  | 3.0264  | 3.0355  | 2.8415                | 2.8535  | 2.8408  | 2.8487  |
|       | 6100 | 2.4452                   | 2.4665  | 2.4465  | 2.4590  | 3.3946                 | 3.3971  | 3.3894  | 3.3989  | 3.1999                | 3.2084  | 3.1956  | 3.2051  |
|       | 6200 | 2.7815                   | 2.8027  | 2.7793  | 2.7925  | 3.7634                 | 3.7638  | 3.7571  | 3.7665  | 3.5648                | 3.5706  | 3.5579  | 3.5687  |
|       | 6300 | 3.1298                   | 3.1474  | 3.1235  | 3.1390  | 4.1318                 | 4.1311  | 4.1264  | 4.1342  | 3.9331                | 3.9367  | 3.9243  | 3.9361  |
|       | 6400 | 3.4855                   | 3.5010  | 3.4751  | 3.4925  | 4.5018                 | 4.5006  | 4.4968  | 4.5037  | 4.3051                | 4.3071  | 4.2958  | 4.3075  |
|       | 6500 | 3.8466                   | 3.8581  | 3.8330  | 3.8517  | 4.8724                 | 4.8700  | 4.8686  | 4.8738  | 4.6773                | 4.6782  | 4.6682  | 4.6789  |
|       | 6600 | 4.2069                   | 4.2155  | 4.1918  | 4.2108  | 5.2382                 | 5.2356  | 5.2371  | 5.2393  | 5.0490                | 5.0491  | 5.0407  | 5.0502  |
|       | 6700 | 4.5680                   | 4.5745  | 4.5504  | 4.5710  | 5.5947                 | 5.5931  | 5.5976  | 5.5961  | 5.4142                | 5.4135  | 5.4096  | 5.4148  |
|       | 6800 | 4.9284                   | 4.9333  | 4.9092  | 4.9306  | 5.9446                 | 5.9431  | 5.9501  | 5.9462  | 5.7730                | 5.7727  | 5.7691  | 5.7741  |
|       | 6900 | 5.2862                   | 5.2899  | 5.2651  | 5.2879  | 6.2889                 | 6.2881  | 6.2996  | 6.2900  | 6.1247                | 6.1241  | 6.1229  | 6.1257  |
|       | 7000 | 5.6420                   | 5.6443  | 5.6191  | 5.6427  | 6.6292                 | 6.6294  | 6.6410  | 6.6305  | 6.4697                | 6.4699  | 6.4700  | 6.4706  |
|       | 4300 | -3.6497                  | -3.6755 | -3.7331 | -3.6137 | -3.0137                | -2.9999 | -3.0349 | -2.9582 | -3.1825               | -3.1647 | -3.2099 | -3.1154 |
|       | 4400 | -3.6828                  | -3.6228 | -3.6808 | -3.5722 | -2.9343                | -2.8110 | -2.8433 | -2.7863 | -3.0869               | -2.9758 | -3.0161 | -2.9424 |
|       | 4500 | -3.6508                  | -3.4765 | -3.5351 | -3.4398 | -2.8558                | -2.5871 | -2.6185 | -2.5800 | -2.9990               | -2.7625 | -2.8005 | -2.7469 |
|       | 4600 | -3.5627                  | -3.2671 | -3.3251 | -3.2434 | -2.7632                | -2.3185 | -2.3502 | -2.3251 | -2.9033               | -2.5122 | -2.5489 | -2.5107 |
|       | 4700 | -3.4456                  | -3.0134 | -3.0686 | -2.9991 | -2.6417                | -1.9991 | -2.0318 | -2.0136 | -2.7853               | -2.2156 | -2.2520 | -2.2223 |
|       | 4800 | -3.3016                  | -2.7195 | -2.7708 | -2.7100 | -2.4747                | -1.6319 | -1.6657 | -1.6484 | -2.6277               | -1.8693 | -1.9056 | -1.8794 |
|       | 4900 | -3.1243                  | -2.3777 | -2.4258 | -2.3701 | -2.2436                | -1.2272 | -1.2607 | -1.2403 | -2.4168               | -1.4799 | -1.5147 | -1.4871 |
|       | 5000 | -2.9023                  | -1.9942 | -2.0394 | -1.9875 | -1.9294                | -0.7954 | -0.8283 | -0.8022 | -2.1370               | -1.0567 | -1.0928 | -1.0617 |
|       | 5100 | -2.6291                  | -1.5768 | -1.6183 | -1.5691 | -1.5190                | -0.3513 | -0.3831 | -0.3507 | -1.7738               | -0.6168 | -0.6519 | -0.6159 |
|       | 5200 | -2.2917                  | -1.1395 | -1.1782 | -1.1306 | -1.0162                | 0.0891  | 0.0595  | 0.0979  | -1.3214               | -0.1725 | -0.2057 | -0.1651 |
|       | 5300 | -1.8907                  | -0.6967 | -0.7329 | -0.6857 | -0.4457                | 0.5166  | 0.4884  | 0.5318  | -0.7924               | 0.2620  | 0.2306  | 0.2757  |
|       | 5400 | -1.4245                  | -0.2577 | -0.2918 | -0.2443 | 0.1450                 | 0.9170  | 0.8929  | 0.9396  | -0.2189               | 0.6761  | 0.6495  | 0.6959  |
|       | 5500 | -0.9044                  | 0.1701  | 0.1373  | 0.1857  | 0.7135                 | 1.2928  | 1.2713  | 1.3195  | 0.3600                | 1.0685  | 1.0431  | 1.0926  |
| Hγ_F  | 5600 | -0.3526                  | 0.5820  | 0.5502  | 0.5994  | 1.2394                 | 1.6495  | 1.6310  | 1.6789  | 0.9123                | 1.4406  | 1.4178  | 1.4673  |
|       | 5700 | 0.2053                   | 0.9767  | 0.9464  | 0.9952  | 1.7176                 | 1.9953  | 1.9787  | 2.0262  | 1.4219                | 1.7974  | 1.7767  | 1.8255  |
|       | 5800 | 0.7477                   | 1.3567  | 1.3272  | 1.3749  | 2.1565                 | 2.3362  | 2.3210  | 2.3676  | 1.8871                | 2.1444  | 2.1240  | 2.1719  |
|       | 5900 | 1.2610                   | 1.7242  | 1.6952  | 1.7420  | 2.5688                 | 2.6802  | 2.6656  | 2.7112  | 2.3210                | 2.4897  | 2.4721  | 2.5179  |
|       | 6000 | 1.7388                   | 2.0812  | 2.0538  | 2.0980  | 2.9631                 | 3.0281  | 3.0135  | 3.0583  | 2.7286                | 2.8353  | 2.8182  | 2.8628  |
|       | 6100 | 2.1859                   | 2.4269  | 2.4070  | 2.4485  | 3.3457                 | 3.3799  | 3.3666  | 3.4095  | 3.1205                | 3.1849  | 3.1678  | 3.2113  |
|       | 6200 | 2.5997                   | 2.7733  | 2.7500  | 2.7891  | 3.7217                 | 3.7353  | 3.7228  | 3.7638  | 3.5027                | 3.5386  | 3.5220  | 3.5640  |
|       | 6300 | 2.9993                   | 3.1199  | 3.0968  | 3.1350  | 4.0916                 | 4.0921  | 4.0811  | 4.1193  | 3.8796                | 3.8963  | 3.8798  | 3.9207  |
|       | 6400 | 3.3869                   | 3.4706  | 3.4451  | 3.4833  | 4.4582                 | 4.4507  | 4.4410  | 4.4762  | 4.2535                | 4.2573  | 4.2414  | 4.2809  |
|       | 6500 | 3.7679                   | 3.8229  | 3.7979  | 3.8356  | 4.8209                 | 4.8073  | 4.8003  | 4.8323  | 4.6222                | 4.6179  | 4.6035  | 4.6401  |
|       | 6600 | 4.1397                   | 4.1747  | 4.1508  | 4.1874  | 5.1796                 | 5.1627  | 5.1577  | 5.1866  | 4.9866                | 4.9772  | 4.9647  | 4.9983  |
|       | 6700 | 4.5070                   | 4.5280  | 4.5035  | 4.5404  | 5.5326                 | 5.5148  | 5.5119  | 5.5373  | 5.3461                | 5.3331  | 5.3241  | 5.3533  |
|       | 6800 | 4.8706                   | 4.8819  | 4.8573  | 4.8939  | 5.8783                 | 5.8592  | 5.8592  | 5.8812  | 5.7028                | 5.6883  | 5.6786  | 5.7077  |
|       | 6900 | 5.2288                   | 5.2336  | 5.2082  | 5.2451  | 6.2126                 | 6.1933  | 6.1994  | 6.2138  | 6.0530                | 6.0370  | 6.0296  | 6.0560  |
|       | 7000 | 5.5836                   | 5.5837  | 5.5578  | 5.5944  | 6.5417                 | 6.5231  | 6.5293  | 6.5424  | 6.3926                | 6.3765  | 6.3719  | 6.3942  |
|       | 4300 | -0.5105                  | -0.0899 | -0.1066 | -0.1868 | -0.3077                | 0.1414  | 0.1356  | 0.0713  | -0.3547               | 0.1148  | 0.1072  | 0.0350  |
|       | 4400 | -0.5079                  | -0.0441 | -0.0598 | -0.1485 | -0.3034                | 0.1536  | 0.1484  | 0.0815  | -0.3466               | 0.1321  | 0.1255  | 0.0506  |
|       | 4500 | -0.5010                  | -0.0065 | -0.0204 | -0.1175 | -0.3048                | 0.1544  | 0.1502  | 0.0789  | -0.3435               | 0.1384  | 0.1327  | 0.0557  |
|       | 4600 | -0.4917                  | 0.0188  | 0.0068  | -0.0958 | -0.3119                | 0.1430  | 0.1393  | 0.0627  | -0.3450               | 0.1325  | 0.1279  | 0.0471  |
|       | 4700 | -0.4832                  | 0.0320  | 0.0220  | -0.0868 | -0.3257                | 0.1179  | 0.1152  | 0.0317  | -0.3514               | 0.1148  | 0.1106  | 0.0245  |
|       | 4800 | -0.4763                  | 0.0291  | 0.0207  | -0.0913 | -0.3461                | 0.0807  | 0.0789  | -0.0127 | -0.3631               | 0.0845  | 0.0813  | -0.0115 |
|       | 4900 | -0.4709                  | 0.0135  | 0.0063  | -0.1091 | -0.3710                | 0.0338  | 0.0328  | -0.0684 | -0.3794               | 0.0438  | 0.0415  | -0.0598 |
|       | 5000 | -0.4669                  | -0.0146 | -0.0207 | -0.1395 | -0.3961                | -0.0222 | -0.0225 | -0.1333 | -0.3980               | -0.0061 | -0.0078 | -0.1180 |
|       | 5100 | -0.4646                  | -0.0532 | -0.0585 | -0.1802 | -0.4168                | -0.0878 | -0.0875 | -0.2027 | -0.4153               | -0.0654 | -0.0663 | -0.1824 |
|       | 5200 | -0.4632                  | -0.1001 | -0.1050 | -0.2264 | -0.4305                | -0.1618 | -0.1605 | -0.2690 | -0.4284               | -0.1333 | -0.1335 | -0.2467 |
|       | 5300 | -0.4622                  | -0.1540 | -0.1582 | -0.2737 | -0.4370                | -0.2361 | -0.2344 | -0.3241 | -0.4358               | -0.2050 | -0.2044 | -0.3035 |
|       | 5400 | -0.4604                  | -0.2104 | -0.2138 | -0.3165 | -0.4384                | -0.3007 | -0.2989 | -0.3642 | -0.4382               | -0.2717 | -0.2708 | -0.3475 |
|       | 5500 | -0.4571                  | -0.2646 | -0.2672 | -0.3519 | -0.4369                | -0.3493 | -0.3477 | -0.3904 | -0.4373               | -0.3257 | -0.3246 | -0.3781 |
|       | 5600 | -0.4527                  | -0.3120 | -0.3138 | -0.3784 | -0.4348                | -0.3819 | -0.3807 | -0.4063 | -0.4351               | -0.3644 | -0.3635 | -0.3977 |
|       | 5700 | -0.4477                  | -0.3495 | -0.3507 | -0.3968 | -0.4330                | -0.4023 | -0.4014 | -0.4158 | -0.4329               | -0.3900 | -0.3893 | -0.4097 |
|       | 5800 | -0.4427                  | -0.3768 |         |         |                        |         |         |         |                       |         |         |         |

Table B.1: Continued.

| Index  | T[K] | MS-TO ( $\log g = 4.2$ ) |         |         |         | RGB ( $\log g = 2.4$ ) |         |         | HB ( $\log g = 2.8$ ) |         |         |         |         |
|--------|------|--------------------------|---------|---------|---------|------------------------|---------|---------|-----------------------|---------|---------|---------|---------|
|        |      | Ref                      | IY2     | IY4     | 2Y2     | Ref                    | IY2     | IY4     | 2Y2                   | Ref     | IY2     | IY4     |         |
| CN4142 | 4300 | -1.1996                  | -1.1443 | -1.1485 | -1.1648 | -1.2227                | -1.0584 | -1.0639 | -1.1075               | -1.2183 | -1.0799 | -1.0857 | -1.1238 |
|        | 4400 | -1.2178                  | -1.1539 | -1.1585 | -1.1769 | -1.2380                | -1.0652 | -1.0703 | -1.1172               | -1.2340 | -1.0856 | -1.0911 | -1.1323 |
|        | 4500 | -1.2342                  | -1.1616 | -1.1665 | -1.1869 | -1.2500                | -1.0745 | -1.0791 | -1.1287               | -1.2467 | -1.0923 | -1.0975 | -1.1412 |
|        | 4600 | -1.2479                  | -1.1670 | -1.1721 | -1.1945 | -1.2582                | -1.0878 | -1.0916 | -1.1425               | -1.2560 | -1.1016 | -1.1062 | -1.1516 |
|        | 4700 | -1.2582                  | -1.1709 | -1.1758 | -1.1998 | -1.2624                | -1.1051 | -1.1081 | -1.1577               | -1.2618 | -1.1144 | -1.1181 | -1.1633 |
|        | 4800 | -1.2648                  | -1.1744 | -1.1789 | -1.2036 | -1.2625                | -1.1246 | -1.1268 | -1.1715               | -1.2638 | -1.1298 | -1.1326 | -1.1749 |
|        | 4900 | -1.2681                  | -1.1783 | -1.1822 | -1.2065 | -1.2586                | -1.1433 | -1.1449 | -1.1816               | -1.2619 | -1.1458 | -1.1478 | -1.1843 |
|        | 5000 | -1.2683                  | -1.1828 | -1.1860 | -1.2085 | -1.2511                | -1.1586 | -1.1597 | -1.1874               | -1.2565 | -1.1598 | -1.1613 | -1.1903 |
|        | 5100 | -1.2654                  | -1.1872 | -1.1897 | -1.2092 | -1.2409                | -1.1693 | -1.1701 | -1.1896               | -1.2479 | -1.1703 | -1.1715 | -1.1927 |
|        | 5200 | -1.2598                  | -1.1907 | -1.1928 | -1.2085 | -1.2294                | -1.1758 | -1.1765 | -1.1893               | -1.2374 | -1.1771 | -1.1780 | -1.1926 |
|        | 5300 | -1.2519                  | -1.1929 | -1.1946 | -1.2064 | -1.2179                | -1.1791 | -1.1796 | -1.1878               | -1.2260 | -1.1807 | -1.1814 | -1.1910 |
|        | 5400 | -1.2425                  | -1.1937 | -1.1950 | -1.2034 | -1.2077                | -1.1804 | -1.1808 | -1.1859               | -1.2151 | -1.1822 | -1.1827 | -1.1888 |
|        | 5500 | -1.2322                  | -1.1932 | -1.1943 | -1.2000 | -1.1994                | -1.1806 | -1.1810 | -1.1842               | -1.2058 | -1.1824 | -1.1828 | -1.1867 |
|        | 5600 | -1.2222                  | -1.1920 | -1.1930 | -1.1966 | -1.1933                | -1.1804 | -1.1807 | -1.1830               | -1.1984 | -1.1821 | -1.1825 | -1.1850 |
|        | 5700 | -1.2133                  | -1.1905 | -1.1913 | -1.1935 | -1.1891                | -1.1803 | -1.1805 | -1.1822               | -1.1930 | -1.1817 | -1.1820 | -1.1838 |
|        | 5800 | -1.2057                  | -1.1889 | -1.1896 | -1.1909 | -1.1863                | -1.1802 | -1.1804 | -1.1817               | -1.1892 | -1.1813 | -1.1816 | -1.1829 |
|        | 5900 | -1.1998                  | -1.1876 | -1.1882 | -1.1890 | -1.1845                | -1.1802 | -1.1804 | -1.1816               | -1.1867 | -1.1812 | -1.1814 | -1.1825 |
|        | 6000 | -1.1952                  | -1.1865 | -1.1870 | -1.1875 | -1.1836                | -1.1805 | -1.1806 | -1.1816               | -1.1851 | -1.1812 | -1.1814 | -1.1824 |
|        | 6100 | -1.1919                  | -1.1857 | -1.1861 | -1.1864 | -1.1831                | -1.1808 | -1.1809 | -1.1819               | -1.1842 | -1.1814 | -1.1816 | -1.1824 |
|        | 6200 | -1.1896                  | -1.1852 | -1.1855 | -1.1857 | -1.1830                | -1.1812 | -1.1813 | -1.1822               | -1.1838 | -1.1817 | -1.1818 | -1.1826 |
|        | 6300 | -1.1880                  | -1.1849 | -1.1852 | -1.1853 | -1.1831                | -1.1816 | -1.1818 | -1.1826               | -1.1836 | -1.1820 | -1.1821 | -1.1829 |
|        | 6400 | -1.1870                  | -1.1847 | -1.1850 | -1.1851 | -1.1832                | -1.1821 | -1.1822 | -1.1830               | -1.1837 | -1.1825 | -1.1826 | -1.1832 |
|        | 6500 | -1.1864                  | -1.1848 | -1.1850 | -1.1850 | -1.1836                | -1.1827 | -1.1828 | -1.1835               | -1.1838 | -1.1829 | -1.1830 | -1.1836 |
|        | 6600 | -1.1859                  | -1.1848 | -1.1850 | -1.1850 | -1.1840                | -1.1833 | -1.1833 | -1.1840               | -1.1842 | -1.1834 | -1.1835 | -1.1841 |
|        | 6700 | -1.1857                  | -1.1849 | -1.1851 | -1.1851 | -1.1844                | -1.1838 | -1.1839 | -1.1845               | -1.1846 | -1.1840 | -1.1841 | -1.1846 |
|        | 6800 | -1.1857                  | -1.1851 | -1.1853 | -1.1853 | -1.1848                | -1.1843 | -1.1844 | -1.1849               | -1.1849 | -1.1844 | -1.1845 | -1.1849 |
|        | 6900 | -1.1857                  | -1.1854 | -1.1855 | -1.1855 | -1.1853                | -1.1849 | -1.1849 | -1.1854               | -1.1852 | -1.1849 | -1.1849 | -1.1853 |
|        | 7000 | -1.1858                  | -1.1856 | -1.1857 | -1.1857 | -1.1859                | -1.1856 | -1.1856 | -1.1860               | -1.1856 | -1.1854 | -1.1854 | -1.1857 |
| CH4300 | 4300 | 1.0652                   | 1.0607  | 1.0623  | 1.0605  | 1.1383                 | 1.1104  | 1.1100  | 1.1091                | 1.1246  | 1.1016  | 1.1018  | 1.0998  |
|        | 4400 | 1.0854                   | 1.0720  | 1.0737  | 1.0719  | 1.1476                 | 1.1037  | 1.1034  | 1.1032                | 1.1338  | 1.0972  | 1.0973  | 1.0962  |
|        | 4500 | 1.1010                   | 1.0741  | 1.0760  | 1.0743  | 1.1540                 | 1.0895  | 1.0897  | 1.0902                | 1.1413  | 1.0871  | 1.0874  | 1.0871  |
|        | 4600 | 1.1113                   | 1.0690  | 1.0712  | 1.0696  | 1.1557                 | 1.0671  | 1.0678  | 1.0689                | 1.1453  | 1.0697  | 1.0704  | 1.0707  |
|        | 4700 | 1.1180                   | 1.0571  | 1.0594  | 1.0582  | 1.1510                 | 1.0368  | 1.0381  | 1.0396                | 1.1442  | 1.0445  | 1.0457  | 1.0464  |
|        | 4800 | 1.1206                   | 1.0389  | 1.0412  | 1.0404  | 1.1382                 | 1.0003  | 1.0020  | 1.0037                | 1.1364  | 1.0123  | 1.0139  | 1.0149  |
|        | 4900 | 1.1183                   | 1.0137  | 1.0161  | 1.0156  | 1.1161                 | 0.9600  | 0.9620  | 0.9636                | 1.1201  | 0.9752  | 0.9772  | 0.9782  |
|        | 5000 | 1.0996                   | 0.9830  | 0.9853  | 0.9851  | 1.0841                 | 0.9180  | 0.9201  | 0.9214                | 1.0948  | 0.9353  | 0.9374  | 0.9383  |
|        | 5100 | 1.0938                   | 0.9481  | 0.9503  | 0.9503  | 1.0426                 | 0.8766  | 0.8787  | 0.8794                | 1.0600  | 0.8947  | 0.8969  | 0.8974  |
|        | 5200 | 1.0697                   | 0.9113  | 0.9134  | 0.9135  | 0.9931                 | 0.8381  | 0.8401  | 0.8401                | 1.0166  | 0.8556  | 0.8577  | 0.8577  |
|        | 5300 | 1.0379                   | 0.8748  | 0.8767  | 0.8767  | 0.9391                 | 0.8044  | 0.8062  | 0.8056                | 0.9668  | 0.8201  | 0.8220  | 0.8214  |
|        | 5400 | 0.9990                   | 0.8401  | 0.8419  | 0.8417  | 0.8860                 | 0.7769  | 0.7783  | 0.7772                | 0.9147  | 0.7897  | 0.7913  | 0.7903  |
|        | 5500 | 0.9550                   | 0.8086  | 0.8102  | 0.8097  | 0.8385                 | 0.7552  | 0.7563  | 0.7550                | 0.8651  | 0.7650  | 0.7662  | 0.7649  |
|        | 5600 | 0.9091                   | 0.7812  | 0.7825  | 0.7818  | 0.7993                 | 0.7388  | 0.7395  | 0.7380                | 0.8216  | 0.7457  | 0.7466  | 0.7451  |
|        | 5700 | 0.8647                   | 0.7581  | 0.7593  | 0.7584  | 0.7686                 | 0.7263  | 0.7267  | 0.7251                | 0.7862  | 0.7309  | 0.7316  | 0.7300  |
|        | 5800 | 0.8245                   | 0.7394  | 0.7403  | 0.7394  | 0.7455                 | 0.7167  | 0.7170  | 0.7153                | 0.7586  | 0.7196  | 0.7201  | 0.7185  |
|        | 5900 | 0.7902                   | 0.7245  | 0.7253  | 0.7243  | 0.7284                 | 0.7092  | 0.7093  | 0.7077                | 0.7377  | 0.7109  | 0.7112  | 0.7096  |
|        | 6000 | 0.7622                   | 0.7129  | 0.7135  | 0.7126  | 0.7157                 | 0.7032  | 0.7033  | 0.7016                | 0.7222  | 0.7041  | 0.7043  | 0.7027  |
|        | 6100 | 0.7401                   | 0.7039  | 0.7043  | 0.7035  | 0.7062                 | 0.6982  | 0.6983  | 0.6966                | 0.7106  | 0.6987  | 0.6988  | 0.6972  |
|        | 6200 | 0.7231                   | 0.6969  | 0.6971  | 0.6964  | 0.6989                 | 0.6941  | 0.6941  | 0.6924                | 0.7020  | 0.6942  | 0.6943  | 0.6927  |
|        | 6300 | 0.7101                   | 0.6914  | 0.6916  | 0.6909  | 0.6933                 | 0.6905  | 0.6906  | 0.6888                | 0.6954  | 0.6905  | 0.6906  | 0.6890  |
|        | 6400 | 0.7004                   | 0.6871  | 0.6872  | 0.6866  | 0.6887                 | 0.6873  | 0.6874  | 0.6857                | 0.6903  | 0.6874  | 0.6874  | 0.6860  |
|        | 6500 | 0.6931                   | 0.6838  | 0.6838  | 0.6832  | 0.6851                 | 0.6846  | 0.6847  | 0.6829                | 0.6863  | 0.6847  | 0.6848  | 0.6833  |
|        | 6600 | 0.6876                   | 0.6811  | 0.6811  | 0.6805  | 0.6819                 | 0.6820  | 0.6821  | 0.6804                | 0.6831  | 0.6823  | 0.6824  | 0.6809  |
|        | 6700 | 0.6835                   | 0.6791  | 0.6791  | 0.6785  | 0.6792                 | 0.6796  | 0.6798  | 0.6781                | 0.6804  | 0.6801  | 0.6803  | 0.6789  |
|        | 6800 | 0.6805                   | 0.6775  | 0.6775  | 0.6769  | 0.6769                 | 0.6775  | 0.6777  | 0.6761                | 0.6780  | 0.6781  | 0.6784  | 0.6770  |
|        | 6900 | 0.6784                   | 0.6764  | 0.6764  | 0.6758  | 0.6747                 | 0.6754  | 0.6757  | 0.6741                | 0.6762  | 0.6765  | 0.6768  | 0.6754  |
|        | 7000 | 0.6769                   | 0.6756  | 0.6756  | 0.6750  | 0.6727                 | 0.6734  | 0.6739  | 0.6722                | 0.6744  | 0.6748  | 0.6752  | 0.6738  |
| HK1    | 4300 | 0.4349                   | 0.4175  | 0.4221  | 0.4208  | 0.4225                 | 0.4121  | 0.4132  | 0.4149                | 0.4199  | 0.4085  | 0.4112  | 0.4114  |
|        | 4400 | 0.4237                   | 0.4107  | 0.4155  | 0.4138  | 0.4102                 | 0.4005  | 0.4013  | 0.4032                | 0.4060  | 0.3957  | 0.3980  | 0.3985  |
|        | 4500 | 0.4104                   | 0.3991  | 0.4040  | 0.4019  | 0.3977                 | 0.3884  | 0.3891  | 0.3912                | 0.3927  | 0.3831  | 0.3851  | 0.3858  |
|        | 4600 | 0.3950                   | 0.3845  | 0.3893  | 0.3871  | 0.3844                 | 0.3755  | 0.3759  | 0.3782                | 0.3791  | 0.3699  | 0.3718  | 0.3726  |
|        | 4700 | 0.3792                   | 0.3693  | 0.3740  | 0.3718  | 0.3698                 | 0.3613  | 0.3615  | 0.3640                | 0.3646  | 0.3559  | 0.3576  | 0.3585  |
|        | 4800 | 0.3635                   | 0.3540  | 0.3584  | 0.3564  | 0.3538                 | 0.3457  | 0.3458  | 0.3483                | 0.3491  | 0.3407  | 0.3422  | 0.3433  |
|        | 4900 | 0.3474                   | 0.3384  | 0.3425  | 0.3407  | 0.3364                 | 0.3287  | 0.3287  | 0.3309                | 0.3322  | 0.3242  | 0.3258  | 0.3267  |
|        | 5000 | 0.3309                   | 0.3221  | 0.3260  | 0.3243  | 0.3173                 | 0.3099  | 0.3098  | 0.3118                | 0.3139  | 0.3063  | 0.3077  | 0.3085  |
|        | 5100 | 0.3135                   | 0.3050  | 0.3088  | 0.3071  | 0.2967                 | 0.2894  | 0.2893  | 0.2911                | 0.2941  | 0.2867  | 0.2880  | 0.2886  |
|        | 5200 | 0.2952                   | 0.2870  | 0.2907  | 0.2890  | 0.2745                 | 0.2676  | 0.2674  | 0.2690                | 0.2729  | 0.2657  | 0.2670  | 0.2673  |
|        | 5300 | 0.2759                   | 0.2680  | 0.2716  | 0.2699  | 0.2513                 | 0.2452  | 0.2448  | 0.2462                | 0.2504  | 0.2438  | 0.2449  | 0.2451  |
|        | 5400 | 0.2555                   | 0.2481  | 0.2516  | 0.2498  | 0.2280                 | 0.2229  | 0.2224  | 0.2236                | 0.2275  | 0.2216  | 0.2225  | 0.2226  |
|        | 5500 | 0.2344                   | 0.2275  | 0.2310  | 0.2291  | 0.2055                 | 0.2014  | 0.2007  | 0.2018                | 0.2048  | 0.1999  | 0.2006  | 0.2006  |
|        | 5600 | 0.2128                   | 0.2067  | 0.2101  | 0.2080  | 0.184                  |         |         |                       |         |         |         |         |

Table B.1: Continued.

| Index       | T[K] | MS-TO ( $\log g = 4.2$ ) |         |         |         | RGB ( $\log g = 2.4$ ) |         |         |         | HB ( $\log g = 2.8$ ) |         |         |         |
|-------------|------|--------------------------|---------|---------|---------|------------------------|---------|---------|---------|-----------------------|---------|---------|---------|
|             |      | Ref                      | IY2     | IY4     | 2Y2     | Ref                    | IY2     | IY4     | 2Y2     | Ref                   | IY2     | IY4     | 2Y2     |
| $H_{\beta}$ | 4300 | -0.6380                  | -0.6377 | -0.6381 | -0.6367 | -0.6099                | -0.6095 | -0.6101 | -0.6091 | -0.6159               | -0.6156 | -0.6162 | -0.6151 |
|             | 4400 | -0.6284                  | -0.6281 | -0.6284 | -0.6274 | -0.6034                | -0.6028 | -0.6034 | -0.6026 | -0.6088               | -0.6084 | -0.6089 | -0.6081 |
|             | 4500 | -0.6198                  | -0.6194 | -0.6195 | -0.6189 | -0.5976                | -0.5967 | -0.5971 | -0.5968 | -0.6027               | -0.6020 | -0.6024 | -0.6020 |
|             | 4600 | -0.6125                  | -0.6118 | -0.6117 | -0.6118 | -0.5922                | -0.5908 | -0.5913 | -0.5914 | -0.5972               | -0.5960 | -0.5964 | -0.5964 |
|             | 4700 | -0.6063                  | -0.6053 | -0.6051 | -0.6056 | -0.5868                | -0.5851 | -0.5856 | -0.5860 | -0.5919               | -0.5903 | -0.5907 | -0.5911 |
|             | 4800 | -0.6005                  | -0.5994 | -0.5991 | -0.5999 | -0.5811                | -0.5793 | -0.5798 | -0.5804 | -0.5862               | -0.5846 | -0.5850 | -0.5855 |
|             | 4900 | -0.5948                  | -0.5936 | -0.5933 | -0.5942 | -0.5749                | -0.5731 | -0.5736 | -0.5742 | -0.5801               | -0.5785 | -0.5788 | -0.5794 |
|             | 5000 | -0.5889                  | -0.5876 | -0.5873 | -0.5882 | -0.5679                | -0.5663 | -0.5667 | -0.5673 | -0.5735               | -0.5718 | -0.5722 | -0.5728 |
|             | 5100 | -0.5826                  | -0.5813 | -0.5811 | -0.5819 | -0.5602                | -0.5587 | -0.5592 | -0.5597 | -0.5661               | -0.5645 | -0.5650 | -0.5655 |
|             | 5200 | -0.5757                  | -0.5745 | -0.5743 | -0.5750 | -0.5516                | -0.5502 | -0.5508 | -0.5511 | -0.5580               | -0.5565 | -0.5570 | -0.5574 |
|             | 5300 | -0.5683                  | -0.5670 | -0.5669 | -0.5676 | -0.5419                | -0.5406 | -0.5413 | -0.5413 | -0.5490               | -0.5477 | -0.5482 | -0.5485 |
|             | 5400 | -0.5600                  | -0.5589 | -0.5588 | -0.5594 | -0.5313                | -0.5302 | -0.5309 | -0.5310 | -0.5391               | -0.5380 | -0.5384 | -0.5387 |
|             | 5500 | -0.5509                  | -0.5498 | -0.5498 | -0.5504 | -0.5199                | -0.5188 | -0.5196 | -0.5195 | -0.5281               | -0.5271 | -0.5278 | -0.5278 |
|             | 5600 | -0.5409                  | -0.5398 | -0.5399 | -0.5404 | -0.5074                | -0.5065 | -0.5074 | -0.5072 | -0.5161               | -0.5152 | -0.5159 | -0.5158 |
|             | 5700 | -0.5298                  | -0.5288 | -0.5290 | -0.5294 | -0.4940                | -0.4932 | -0.4941 | -0.4938 | -0.5032               | -0.5024 | -0.5032 | -0.5030 |
|             | 5800 | -0.5178                  | -0.5168 | -0.5171 | -0.5174 | -0.4796                | -0.4789 | -0.4799 | -0.4795 | -0.4894               | -0.4886 | -0.4896 | -0.4892 |
|             | 5900 | -0.5048                  | -0.5039 | -0.5043 | -0.5044 | -0.4643                | -0.4637 | -0.4647 | -0.4641 | -0.4746               | -0.4740 | -0.4749 | -0.4744 |
|             | 6000 | -0.4910                  | -0.4901 | -0.4906 | -0.4906 | -0.4481                | -0.4476 | -0.4488 | -0.4480 | -0.4591               | -0.4585 | -0.4595 | -0.4589 |
|             | 6100 | -0.4763                  | -0.4758 | -0.4761 | -0.4760 | -0.4313                | -0.4308 | -0.4321 | -0.4312 | -0.4427               | -0.4423 | -0.4434 | -0.4426 |
|             | 6200 | -0.4615                  | -0.4607 | -0.4613 | -0.4612 | -0.4139                | -0.4135 | -0.4148 | -0.4138 | -0.4257               | -0.4253 | -0.4266 | -0.4256 |
|             | 6300 | -0.4457                  | -0.4450 | -0.4457 | -0.4454 | -0.3960                | -0.3957 | -0.3970 | -0.3959 | -0.4080               | -0.4077 | -0.4090 | -0.4079 |
|             | 6400 | -0.4293                  | -0.4286 | -0.4295 | -0.4291 | -0.3776                | -0.3773 | -0.3787 | -0.3776 | -0.3898               | -0.3895 | -0.3909 | -0.3897 |
|             | 6500 | -0.4123                  | -0.4118 | -0.4128 | -0.4122 | -0.3589                | -0.3588 | -0.3601 | -0.3589 | -0.3713               | -0.3710 | -0.3725 | -0.3712 |
|             | 6600 | -0.3951                  | -0.3947 | -0.3957 | -0.3950 | -0.3402                | -0.3401 | -0.3414 | -0.3402 | -0.3525               | -0.3523 | -0.3538 | -0.3525 |
|             | 6700 | -0.3777                  | -0.3773 | -0.3785 | -0.3776 | -0.3216                | -0.3214 | -0.3227 | -0.3216 | -0.3338               | -0.3337 | -0.3350 | -0.3338 |
|             | 6800 | -0.3600                  | -0.3597 | -0.3610 | -0.3599 | -0.3031                | -0.3030 | -0.3042 | -0.3031 | -0.3150               | -0.3148 | -0.3163 | -0.3150 |
|             | 6900 | -0.3421                  | -0.3419 | -0.3434 | -0.3421 | -0.2850                | -0.2849 | -0.2859 | -0.2850 | -0.2963               | -0.2962 | -0.2976 | -0.2963 |
|             | 7000 | -0.3242                  | -0.3240 | -0.3256 | -0.3242 | -0.2673                | -0.2673 | -0.2682 | -0.2673 | -0.2779               | -0.2778 | -0.2792 | -0.2779 |
| HN          | 4300 | -0.0625                  | 0.0888  | 0.0765  | 0.1051  | -0.1411                | 0.1273  | 0.1346  | 0.0699  | -0.1247               | 0.1585  | 0.1656  | 0.0999  |
|             | 4400 | -0.0922                  | 0.1160  | 0.1028  | 0.1257  | -0.1731                | 0.1098  | 0.1164  | 0.0494  | -0.1591               | 0.1389  | 0.1460  | 0.0759  |
|             | 4500 | -0.1268                  | 0.1326  | 0.1219  | 0.1282  | -0.2037                | 0.0916  | 0.0978  | 0.0292  | -0.1916               | 0.1190  | 0.1261  | 0.0532  |
|             | 4600 | -0.1656                  | 0.1369  | 0.1299  | 0.1164  | -0.2334                | 0.0714  | 0.0772  | 0.0082  | -0.2225               | 0.0977  | 0.1047  | 0.0305  |
|             | 4700 | -0.2039                  | 0.1344  | 0.1309  | 0.0986  | -0.2624                | 0.0486  | 0.0541  | -0.0142 | -0.2523               | 0.0744  | 0.0812  | 0.0072  |
|             | 4800 | -0.2385                  | 0.1266  | 0.1262  | 0.0775  | -0.2909                | 0.0234  | 0.0286  | -0.0379 | -0.2807               | 0.0491  | 0.0557  | -0.0168 |
|             | 4900 | -0.2706                  | 0.1135  | 0.1158  | 0.0541  | -0.3189                | -0.0035 | 0.0016  | -0.0628 | -0.3087               | 0.0224  | 0.0289  | -0.0416 |
|             | 5000 | -0.2996                  | 0.0956  | 0.1000  | 0.0285  | -0.3464                | -0.0318 | -0.0269 | -0.0896 | -0.3358               | -0.0055 | 0.0005  | -0.0679 |
|             | 5100 | -0.3265                  | 0.0735  | 0.0795  | 0.0013  | -0.3730                | -0.0617 | -0.0569 | -0.1188 | -0.3622               | -0.0351 | -0.0292 | -0.0961 |
|             | 5200 | -0.3513                  | 0.0476  | 0.0547  | -0.0278 | -0.3982                | -0.0935 | -0.0887 | -0.1510 | -0.3875               | -0.0661 | -0.0605 | -0.1268 |
|             | 5300 | -0.3746                  | 0.0183  | 0.0261  | -0.0587 | -0.4214                | -0.1273 | -0.1225 | -0.1865 | -0.4111               | -0.0990 | -0.0936 | -0.1604 |
|             | 5400 | -0.3965                  | -0.0138 | -0.0057 | -0.0917 | -0.4419                | -0.1632 | -0.1583 | -0.2245 | -0.4327               | -0.1338 | -0.1285 | -0.1967 |
|             | 5500 | -0.4171                  | -0.0486 | -0.0405 | -0.1271 | -0.4593                | -0.2009 | -0.1960 | -0.2639 | -0.4517               | -0.1702 | -0.1651 | -0.2348 |
|             | 5600 | -0.4362                  | -0.0857 | -0.0775 | -0.1645 | -0.4738                | -0.2397 | -0.2348 | -0.3032 | -0.4679               | -0.2081 | -0.2030 | -0.2738 |
|             | 5700 | -0.4536                  | -0.1243 | -0.1165 | -0.2031 | -0.4855                | -0.2788 | -0.2740 | -0.3407 | -0.4812               | -0.2467 | -0.2417 | -0.3121 |
|             | 5800 | -0.4690                  | -0.1638 | -0.1565 | -0.2419 | -0.4947                | -0.3168 | -0.3122 | -0.3751 | -0.4920               | -0.2851 | -0.2803 | -0.3483 |
|             | 5900 | -0.4822                  | -0.2036 | -0.1968 | -0.2800 | -0.5020                | -0.3525 | -0.3482 | -0.4054 | -0.5005               | -0.3223 | -0.3176 | -0.3813 |
|             | 6000 | -0.4934                  | -0.2427 | -0.2365 | -0.3162 | -0.5077                | -0.3849 | -0.3810 | -0.4316 | -0.5072               | -0.3570 | -0.3526 | -0.4105 |
|             | 6100 | -0.5025                  | -0.2806 | -0.2748 | -0.3499 | -0.5122                | -0.4136 | -0.4101 | -0.4538 | -0.5124               | -0.3884 | -0.3844 | -0.4358 |
|             | 6200 | -0.5099                  | -0.3164 | -0.3112 | -0.3807 | -0.5158                | -0.4383 | -0.4352 | -0.4721 | -0.5165               | -0.4162 | -0.4127 | -0.4572 |
|             | 6300 | -0.5158                  | -0.3495 | -0.3448 | -0.4080 | -0.5187                | -0.4592 | -0.4566 | -0.4869 | -0.5197               | -0.4403 | -0.4372 | -0.4750 |
|             | 6400 | -0.5204                  | -0.3796 | -0.3753 | -0.4321 | -0.5211                | -0.4765 | -0.4743 | -0.4984 | -0.5223               | -0.4608 | -0.4581 | -0.4894 |
|             | 6500 | -0.5241                  | -0.4065 | -0.4026 | -0.4531 | -0.5231                | -0.4904 | -0.4887 | -0.5072 | -0.5244               | -0.4778 | -0.4756 | -0.5007 |
|             | 6600 | -0.5269                  | -0.4303 | -0.4268 | -0.4711 | -0.5248                | -0.5013 | -0.5000 | -0.5139 | -0.5261               | -0.4916 | -0.4898 | -0.5093 |
|             | 6700 | -0.5292                  | -0.4512 | -0.4481 | -0.4861 | -0.5263                | -0.5096 | -0.5086 | -0.5188 | -0.5276               | -0.5025 | -0.5011 | -0.5159 |
|             | 6800 | -0.5311                  | -0.4692 | -0.4665 | -0.4984 | -0.5276                | -0.5158 | -0.5152 | -0.5225 | -0.5288               | -0.5109 | -0.5098 | -0.5207 |
|             | 6900 | -0.5325                  | -0.4844 | -0.4821 | -0.5082 | -0.5287                | -0.5205 | -0.5200 | -0.5253 | -0.5299               | -0.5172 | -0.5164 | -0.5244 |
|             | 7000 | -0.5338                  | -0.4970 | -0.4951 | -0.5159 | -0.5297                | -0.5239 | -0.5236 | -0.5275 | -0.5309               | -0.5219 | -0.5213 | -0.5271 |
| NO          | 4300 | -0.4641                  | -0.2461 | -0.2406 | -0.3045 | -0.4324                | -0.3197 | -0.3185 | -0.3394 | -0.4367               | -0.3105 | -0.3090 | -0.3345 |
|             | 4400 | -0.4433                  | -0.2377 | -0.2311 | -0.2955 | -0.4165                | -0.3096 | -0.3081 | -0.3295 | -0.4183               | -0.2992 | -0.2975 | -0.3233 |
|             | 4500 | -0.4235                  | -0.2349 | -0.2284 | -0.2883 | -0.4043                | -0.3039 | -0.3022 | -0.3237 | -0.4042               | -0.2924 | -0.2905 | -0.3162 |
|             | 4600 | -0.4058                  | -0.2347 | -0.2290 | -0.2829 | -0.3951                | -0.3019 | -0.3009 | -0.3212 | -0.3933               | -0.2894 | -0.2874 | -0.3127 |
|             | 4700 | -0.3917                  | -0.2364 | -0.2315 | -0.2802 | -0.3880                | -0.3025 | -0.3006 | -0.3211 | -0.3850               | -0.2895 | -0.2874 | -0.3120 |
|             | 4800 | -0.3805                  | -0.2396 | -0.2354 | -0.2802 | -0.3824                | -0.3049 | -0.3032 | -0.3227 | -0.3786               | -0.2920 | -0.2899 | -0.3132 |
|             | 4900 | -0.3724                  | -0.2442 | -0.2405 | -0.2823 | -0.3779                | -0.3086 | -0.3069 | -0.3252 | -0.3736               | -0.2959 | -0.2939 | -0.3155 |
|             | 5000 | -0.3659                  | -0.2504 | -0.2471 | -0.2861 | -0.3738                | -0.3131 | -0.3115 | -0.3280 | -0.3694               | -0.3008 | -0.2990 | -0.3185 |
|             | 5100 | -0.3611                  | -0.2578 | -0.2547 | -0.2910 | -0.3695                | -0.3178 | -0.3163 | -0.3307 | -0.3654               | -0.3061 | -0.3045 | -0.3216 |
|             | 5200 | -0.3568                  | -0.2665 | -0.2636 | -0.2964 | -0.3649                | -0.3223 | -0.3209 | -0.3330 | -0.3612               | -0.3113 | -0.3099 | -0.3244 |
|             | 5300 | -0.3530                  | -0.2755 | -0.2729 | -0.3015 | -0.3599                | -0.3263 | -0.3250 | -0.3348 | -0.3567               | -0.3162 | -0.3149 | -0.3267 |
|             | 5400 | -0.3493                  | -0.2843 | -0.2821 | -0.3061 | -0.3551                | -0.3295 | -0.3283 | -0.3362 | -0.3522               | -0.3202 | -0.3191 | -0.3286 |
|             | 5500 | -0.3455                  | -0.2923 | -0.2906 | -0.3097 | -0.3508                | -0.3318 | -0.3306 | -0.3373 | -0.3479               | -0.3234 | -0.3223 | -0.3301 |
|             | 5600 | -0.3417                  | -0.2990 | -0.2976 |         |                        |         |         |         |                       |         |         |         |

Table B.1: Continued.

| Index     | T[K] | MS-TO ( $\log g = 4.2$ ) |         |         |         | RGB ( $\log g = 2.4$ ) |         |         |         | HB ( $\log g = 2.8$ ) |         |         |         |
|-----------|------|--------------------------|---------|---------|---------|------------------------|---------|---------|---------|-----------------------|---------|---------|---------|
|           |      | Ref                      | IY2     | IY4     | 2Y2     | Ref                    | IY2     | IY4     | 2Y2     | Ref                   | IY2     | IY4     | 2Y2     |
| OH        | 4300 | -0.5429                  | -0.6366 | -0.6317 | -0.6376 | -0.5992                | -0.6747 | -0.6738 | -0.6680 | -0.5818               | -0.6703 | -0.6692 | -0.6618 |
|           | 4400 | -0.5611                  | -0.6539 | -0.6492 | -0.6535 | -0.6216                | -0.6899 | -0.6893 | -0.6828 | -0.6060               | -0.6866 | -0.6858 | -0.6776 |
|           | 4500 | -0.5798                  | -0.6711 | -0.6671 | -0.6685 | -0.6399                | -0.7014 | -0.7011 | -0.6939 | -0.6262               | -0.6994 | -0.6988 | -0.6897 |
|           | 4600 | -0.5985                  | -0.6867 | -0.6833 | -0.6819 | -0.6541                | -0.7095 | -0.7094 | -0.7015 | -0.6427               | -0.7087 | -0.7085 | -0.6986 |
|           | 4700 | -0.6153                  | -0.6996 | -0.6970 | -0.6927 | -0.6645                | -0.7146 | -0.7147 | -0.7060 | -0.6555               | -0.7151 | -0.7151 | -0.7044 |
|           | 4800 | -0.6297                  | -0.7099 | -0.7079 | -0.7008 | -0.6715                | -0.7173 | -0.7175 | -0.7083 | -0.6646               | -0.7187 | -0.7190 | -0.7077 |
|           | 4900 | -0.6414                  | -0.7176 | -0.7162 | -0.7065 | -0.6758                | -0.7184 | -0.7186 | -0.7090 | -0.6708               | -0.7203 | -0.7207 | -0.7090 |
|           | 5000 | -0.6507                  | -0.7229 | -0.7221 | -0.7099 | -0.6780                | -0.7182 | -0.7184 | -0.7087 | -0.6745               | -0.7204 | -0.7207 | -0.7090 |
|           | 5100 | -0.6575                  | -0.7259 | -0.7257 | -0.7115 | -0.6786                | -0.7170 | -0.7172 | -0.7078 | -0.6764               | -0.7192 | -0.7196 | -0.7083 |
|           | 5200 | -0.6623                  | -0.7266 | -0.7268 | -0.7112 | -0.6783                | -0.7150 | -0.7153 | -0.7066 | -0.6770               | -0.7173 | -0.7177 | -0.7071 |
|           | 5300 | -0.6654                  | -0.7256 | -0.7261 | -0.7099 | -0.6774                | -0.7126 | -0.7129 | -0.7050 | -0.6767               | -0.7149 | -0.7152 | -0.7057 |
|           | 5400 | -0.6672                  | -0.7231 | -0.7239 | -0.7079 | -0.6763                | -0.7101 | -0.7104 | -0.7033 | -0.6760               | -0.7123 | -0.7125 | -0.7041 |
|           | 5500 | -0.6682                  | -0.7197 | -0.7205 | -0.7056 | -0.6753                | -0.7076 | -0.7080 | -0.7011 | -0.6751               | -0.7097 | -0.7099 | -0.7024 |
|           | 5600 | -0.6688                  | -0.7159 | -0.7168 | -0.7034 | -0.6744                | -0.7051 | -0.7055 | -0.6983 | -0.6743               | -0.7071 | -0.7074 | -0.7002 |
|           | 5700 | -0.6691                  | -0.7123 | -0.7130 | -0.7014 | -0.6736                | -0.7023 | -0.7028 | -0.6949 | -0.6736               | -0.7046 | -0.7049 | -0.6974 |
|           | 5800 | -0.6694                  | -0.7090 | -0.7096 | -0.6993 | -0.6730                | -0.6992 | -0.6997 | -0.6908 | -0.6730               | -0.7018 | -0.7022 | -0.6940 |
|           | 5900 | -0.6696                  | -0.7061 | -0.7066 | -0.6971 | -0.6724                | -0.6955 | -0.6960 | -0.6866 | -0.6724               | -0.6986 | -0.6991 | -0.6900 |
|           | 6000 | -0.6697                  | -0.7033 | -0.7038 | -0.6945 | -0.6718                | -0.6914 | -0.6920 | -0.6826 | -0.6719               | -0.6949 | -0.6955 | -0.6859 |
|           | 6100 | -0.6698                  | -0.7006 | -0.7010 | -0.6915 | -0.6712                | -0.6872 | -0.6878 | -0.6791 | -0.6713               | -0.6909 | -0.6914 | -0.6820 |
|           | 6200 | -0.6698                  | -0.6976 | -0.6980 | -0.6881 | -0.6706                | -0.6832 | -0.6837 | -0.6762 | -0.6708               | -0.6867 | -0.6873 | -0.6785 |
|           | 6300 | -0.6696                  | -0.6942 | -0.6946 | -0.6845 | -0.6700                | -0.6797 | -0.6802 | -0.6738 | -0.6702               | -0.6828 | -0.6833 | -0.6757 |
|           | 6400 | -0.6694                  | -0.6905 | -0.6910 | -0.6811 | -0.6694                | -0.6767 | -0.6772 | -0.6720 | -0.6696               | -0.6793 | -0.6798 | -0.6734 |
|           | 6500 | -0.6691                  | -0.6867 | -0.6872 | -0.6781 | -0.6688                | -0.6744 | -0.6747 | -0.6705 | -0.6690               | -0.6764 | -0.6768 | -0.6716 |
|           | 6600 | -0.6688                  | -0.6831 | -0.6835 | -0.6754 | -0.6682                | -0.6724 | -0.6727 | -0.6693 | -0.6684               | -0.6741 | -0.6744 | -0.6702 |
|           | 6700 | -0.6684                  | -0.6797 | -0.6802 | -0.6733 | -0.6677                | -0.6709 | -0.6711 | -0.6684 | -0.6679               | -0.6722 | -0.6724 | -0.6691 |
|           | 6800 | -0.6680                  | -0.6768 | -0.6772 | -0.6715 | -0.6672                | -0.6697 | -0.6699 | -0.6677 | -0.6674               | -0.6706 | -0.6709 | -0.6682 |
|           | 6900 | -0.6676                  | -0.6743 | -0.6747 | -0.6701 | -0.6668                | -0.6687 | -0.6689 | -0.6671 | -0.6670               | -0.6694 | -0.6696 | -0.6675 |
|           | 7000 | -0.6673                  | -0.6723 | -0.6726 | -0.6690 | -0.6664                | -0.6680 | -0.6681 | -0.6666 | -0.6666               | -0.6685 | -0.6686 | -0.6669 |
| $H_\eta$  | 4300 | 0.1520                   | 0.1520  | 0.1537  | 0.1465  | 0.0350                 | 0.0875  | 0.0928  | 0.0697  | 0.0705                | 0.1138  | 0.1197  | 0.0980  |
|           | 4400 | 0.1553                   | 0.1674  | 0.1705  | 0.1588  | 0.0099                 | 0.0626  | 0.0680  | 0.0445  | 0.0456                | 0.0910  | 0.0974  | 0.0750  |
|           | 4500 | 0.1483                   | 0.1664  | 0.1713  | 0.1565  | -0.0152                | 0.0349  | 0.0402  | 0.0177  | 0.0198                | 0.0647  | 0.0713  | 0.0490  |
|           | 4600 | 0.1316                   | 0.1529  | 0.1595  | 0.1427  | -0.0387                | 0.0061  | 0.0114  | -0.0091 | -0.0055               | 0.0366  | 0.0430  | 0.0223  |
|           | 4700 | 0.1095                   | 0.1321  | 0.1398  | 0.1228  | -0.0599                | -0.0214 | -0.0165 | -0.0337 | -0.0292               | 0.0081  | 0.0145  | -0.0037 |
|           | 4800 | 0.0851                   | 0.1082  | 0.1165  | 0.0994  | -0.0783                | -0.0458 | -0.0415 | -0.0550 | -0.0503               | -0.0183 | -0.0124 | -0.0274 |
|           | 4900 | 0.0592                   | 0.0821  | 0.0906  | 0.0739  | -0.0937                | -0.0656 | -0.0617 | -0.0728 | -0.0690               | -0.0410 | -0.0355 | -0.0481 |
|           | 5000 | 0.0335                   | 0.0554  | 0.0639  | 0.0476  | -0.1060                | -0.0810 | -0.0776 | -0.0883 | -0.0850               | -0.0595 | -0.0549 | -0.0665 |
|           | 5100 | 0.0086                   | 0.0296  | 0.0376  | 0.0218  | -0.1153                | -0.0934 | -0.0907 | -0.1018 | -0.0979               | -0.0749 | -0.0710 | -0.0830 |
|           | 5200 | -0.0142                  | 0.0055  | 0.0128  | -0.0026 | -0.1214                | -0.1043 | -0.1020 | -0.1122 | -0.1077               | -0.0885 | -0.0851 | -0.0968 |
|           | 5300 | -0.0345                  | -0.0167 | -0.0101 | -0.0247 | -0.1243                | -0.1125 | -0.1107 | -0.1185 | -0.1143               | -0.0998 | -0.0970 | -0.1070 |
|           | 5400 | -0.0519                  | -0.0366 | -0.0307 | -0.0441 | -0.1243                | -0.1169 | -0.1155 | -0.1207 | -0.1178               | -0.1079 | -0.1055 | -0.1131 |
|           | 5500 | -0.0661                  | -0.0537 | -0.0484 | -0.0601 | -0.1218                | -0.1172 | -0.1162 | -0.1197 | -0.1183               | -0.1117 | -0.1101 | -0.1154 |
|           | 5600 | -0.0769                  | -0.0672 | -0.0626 | -0.0725 | -0.1171                | -0.1140 | -0.1134 | -0.1158 | -0.1162               | -0.1116 | -0.1105 | -0.1143 |
|           | 5700 | -0.0844                  | -0.0769 | -0.0730 | -0.0812 | -0.1105                | -0.1082 | -0.1079 | -0.1097 | -0.1117               | -0.1083 | -0.1076 | -0.1105 |
|           | 5800 | -0.0886                  | -0.0829 | -0.0797 | -0.0865 | -0.1023                | -0.1004 | -0.1003 | -0.1018 | -0.1052               | -0.1025 | -0.1021 | -0.1045 |
|           | 5900 | -0.0900                  | -0.0855 | -0.0830 | -0.0885 | -0.0926                | -0.0909 | -0.0910 | -0.0923 | -0.0970               | -0.0947 | -0.0945 | -0.0966 |
|           | 6000 | -0.0887                  | -0.0851 | -0.0831 | -0.0877 | -0.0818                | -0.0802 | -0.0804 | -0.0817 | -0.0876               | -0.0854 | -0.0855 | -0.0873 |
|           | 6100 | -0.0850                  | -0.0823 | -0.0808 | -0.0844 | -0.0702                | -0.0685 | -0.0687 | -0.0700 | -0.0770               | -0.0749 | -0.0751 | -0.0768 |
|           | 6200 | -0.0797                  | -0.0771 | -0.0761 | -0.0793 | -0.0579                | -0.0563 | -0.0565 | -0.0579 | -0.0654               | -0.0634 | -0.0637 | -0.0653 |
|           | 6300 | -0.0724                  | -0.0701 | -0.0695 | -0.0721 | -0.0452                | -0.0435 | -0.0437 | -0.0452 | -0.0532               | -0.0513 | -0.0516 | -0.0532 |
|           | 6400 | -0.0637                  | -0.0616 | -0.0613 | -0.0635 | -0.0320                | -0.0303 | -0.0305 | -0.0320 | -0.0404               | -0.0385 | -0.0389 | -0.0403 |
|           | 6500 | -0.0538                  | -0.0518 | -0.0518 | -0.0537 | -0.0187                | -0.0171 | -0.0171 | -0.0187 | -0.0271               | -0.0253 | -0.0257 | -0.0271 |
|           | 6600 | -0.0431                  | -0.0413 | -0.0414 | -0.0430 | -0.0055                | -0.0039 | -0.0038 | -0.0055 | -0.0137               | -0.0120 | -0.0123 | -0.0137 |
|           | 6700 | -0.0316                  | -0.0300 | -0.0303 | -0.0315 | 0.0079                 | 0.0095  | 0.0096  | 0.0079  | -0.0004               | 0.0013  | 0.0012  | -0.0004 |
|           | 6800 | -0.0196                  | -0.0181 | -0.0186 | -0.0196 | 0.0215                 | 0.0230  | 0.0232  | 0.0215  | 0.0131                | 0.0146  | 0.0145  | 0.0131  |
|           | 6900 | -0.0072                  | -0.0059 | -0.0065 | -0.0072 | 0.0348                 | 0.0361  | 0.0365  | 0.0348  | 0.0267                | 0.0281  | 0.0280  | 0.0267  |
|           | 7000 | 0.0055                   | 0.0066  | 0.0059  | 0.0055  | 0.0483                 | 0.0494  | 0.0498  | 0.0483  | 0.0403                | 0.0415  | 0.0413  | 0.0402  |
| $H_\zeta$ | 4300 | 0.2635                   | 0.2826  | 0.2822  | 0.2809  | 0.2748                 | 0.2648  | 0.2661  | 0.2630  | 0.2743                | 0.2725  | 0.2734  | 0.2705  |
|           | 4400 | 0.2628                   | 0.2835  | 0.2834  | 0.2817  | 0.2758                 | 0.2598  | 0.2612  | 0.2592  | 0.2755                | 0.2680  | 0.2690  | 0.2671  |
|           | 4500 | 0.2634                   | 0.2826  | 0.2828  | 0.2819  | 0.2769                 | 0.2553  | 0.2567  | 0.2566  | 0.2767                | 0.2637  | 0.2648  | 0.2642  |
|           | 4600 | 0.2649                   | 0.2810  | 0.2815  | 0.2817  | 0.2779                 | 0.2523  | 0.2538  | 0.2560  | 0.2780                | 0.2605  | 0.2615  | 0.2631  |
|           | 4700 | 0.2669                   | 0.2790  | 0.2797  | 0.2817  | 0.2791                 | 0.2521  | 0.2533  | 0.2583  | 0.2792                | 0.2590  | 0.2601  | 0.2641  |
|           | 4800 | 0.2691                   | 0.2783  | 0.2790  | 0.2824  | 0.2803                 | 0.2554  | 0.2563  | 0.2641  | 0.2804                | 0.2603  | 0.2611  | 0.2679  |
|           | 4900 | 0.2714                   | 0.2789  | 0.2797  | 0.2843  | 0.2816                 | 0.2627  | 0.2634  | 0.2733  | 0.2816                | 0.2651  | 0.2658  | 0.2749  |
|           | 5000 | 0.2737                   | 0.2813  | 0.2820  | 0.2874  | 0.2830                 | 0.2740  | 0.2743  | 0.2841  | 0.2828                | 0.2738  | 0.2741  | 0.2838  |
|           | 5100 | 0.2757                   | 0.2856  | 0.2861  | 0.2910  | 0.2852                 | 0.2880  | 0.2880  | 0.2942  | 0.2846                | 0.2854  | 0.2854  | 0.2928  |
|           | 5200 | 0.2778                   | 0.2917  | 0.2920  | 0.2947  | 0.2890                 | 0.3019  | 0.3016  | 0.3019  | 0.2876                | 0.2982  | 0.2979  | 0.3003  |
|           | 5300 | 0.2806                   | 0.2986  | 0.2986  | 0.2979  | 0.2952                 | 0.3131  | 0.3128  | 0.3078  | 0.2925                | 0.3094  | 0.3090  | 0.3060  |
|           | 5400 | 0.2844                   | 0.3053  | 0.3049  | 0.3006  | 0.3036                 | 0.3210  | 0.3208  | 0.3136  | 0.2996                | 0.3179  | 0.3175  | 0.3111  |
|           | 5500 | 0.2897                   | 0.3110  | 0.3104  | 0.3035  | 0.3136                 | 0.3276  | 0.3274  | 0.3206  | 0.3086                | 0.3245  | 0.3241  | 0.3172  |
|           | 5600 | 0.2968                   | 0.3161  | 0       |         |                        |         |         |         |                       |         |         |         |

Table B.1: Continued.

| Index           | T[K] | MS-TO ( $\log g = 4.2$ ) |             |         |         | RGB ( $\log g = 2.4$ ) |         |         |         | HB ( $\log g = 2.8$ ) |         |         |         |
|-----------------|------|--------------------------|-------------|---------|---------|------------------------|---------|---------|---------|-----------------------|---------|---------|---------|
|                 |      | Ref                      | IY2         | IY4     | 2Y2     | Ref                    | IY2     | IY4     | 2Y2     | Ref                   | IY2     | IY4     | 2Y2     |
| HK <sub>2</sub> | 4300 | -0.1426                  | -0.3046     | -0.2894 | -0.2694 | -0.2143                | -0.4055 | -0.3989 | -0.3659 | -0.2043               | -0.3939 | -0.3828 | -0.3534 |
|                 | 4400 | -0.1679                  | -0.3307     | -0.3149 | -0.2921 | -0.2456                | -0.4485 | -0.4430 | -0.4053 | -0.2419               | -0.4433 | -0.4333 | -0.3990 |
|                 | 4500 | -0.1997                  | -0.3733     | -0.3565 | -0.3306 | -0.2724                | -0.4845 | -0.4801 | -0.4369 | -0.2731               | -0.4849 | -0.4759 | -0.4368 |
|                 | 4600 | -0.2376                  | -0.4235     | -0.4066 | -0.3766 | -0.2968                | -0.5140 | -0.5104 | -0.4613 | -0.3008               | -0.5192 | -0.5112 | -0.4668 |
|                 | 4700 | -0.2740                  | -0.4697     | -0.4538 | -0.4184 | -0.3201                | -0.5365 | -0.5340 | -0.4786 | -0.3270               | -0.5467 | -0.5395 | -0.4896 |
|                 | 4800 | -0.3074                  | -0.5079     | -0.4932 | -0.4528 | -0.3433                | -0.5532 | -0.5518 | -0.4908 | -0.3520               | -0.5675 | -0.5613 | -0.5059 |
|                 | 4900 | -0.3391                  | -0.5388     | -0.5252 | -0.4802 | -0.3672                | -0.5659 | -0.5652 | -0.4997 | -0.3778               | -0.5831 | -0.5775 | -0.5173 |
|                 | 5000 | -0.3703                  | -0.5628     | -0.5504 | -0.5014 | -0.3939                | -0.5760 | -0.5761 | -0.5080 | -0.4053               | -0.5951 | -0.5906 | -0.5271 |
|                 | 5100 | -0.4017                  | -0.5813     | -0.5700 | -0.5180 | -0.4251                | -0.5848 | -0.5857 | -0.5179 | -0.4361               | -0.6054 | -0.6017 | -0.5374 |
|                 | 5200 | -0.4343                  | -0.5960     | -0.5854 | -0.5327 | -0.4614                | -0.5931 | -0.5945 | -0.5319 | -0.4710               | -0.6147 | -0.6118 | -0.5504 |
|                 | 5300 | -0.4689                  | -0.6087     | -0.5988 | -0.5483 | -0.5015                | -0.6023 | -0.6044 | -0.5516 | -0.5099               | -0.6243 | -0.6221 | -0.5685 |
|                 | 5400 | -0.5058                  | -0.6213     | -0.6121 | -0.5671 | -0.5433                | -0.6155 | -0.6180 | -0.5771 | -0.5513               | -0.6364 | -0.6349 | -0.5923 |
|                 | 5500 | -0.5449                  | -0.6358     | -0.6273 | -0.5904 | -0.5844                | -0.6335 | -0.6364 | -0.6065 | -0.5928               | -0.6527 | -0.6520 | -0.6204 |
|                 | 5600 | -0.5852                  | -0.6536     | -0.6457 | -0.6180 | -0.6226                | -0.6554 | -0.6585 | -0.6367 | -0.6325               | -0.6731 | -0.6730 | -0.6506 |
|                 | 5700 | -0.6255                  | -0.6752     | -0.6678 | -0.6486 | -0.6566                | -0.6787 | -0.6821 | -0.6658 | -0.6685               | -0.6959 | -0.6962 | -0.6804 |
|                 | 5800 | -0.6642                  | -0.6994     | -0.6927 | -0.6804 | -0.6864                | -0.7015 | -0.7052 | -0.6922 | -0.7002               | -0.7187 | -0.7196 | -0.7080 |
|                 | 5900 | -0.7001                  | -0.7249     | -0.7188 | -0.7114 | -0.7118                | -0.7226 | -0.7264 | -0.7156 | -0.7273               | -0.7403 | -0.7415 | -0.7325 |
|                 | 6000 | -0.7324                  | -0.7500     | -0.7445 | -0.7404 | -0.7332                | -0.7412 | -0.7452 | -0.7357 | -0.7504               | -0.7597 | -0.7613 | -0.7538 |
|                 | 6100 | -0.7605                  | -0.7735     | -0.7685 | -0.7662 | -0.7512                | -0.7573 | -0.7613 | -0.7529 | -0.7695               | -0.7764 | -0.7783 | -0.7718 |
|                 | 6200 | -0.7848                  | -0.7943     | -0.7901 | -0.7889 | -0.7663                | -0.7711 | -0.7749 | -0.7674 | -0.7851               | -0.7903 | -0.7924 | -0.7866 |
|                 | 6300 | -0.8049                  | -0.8120     | -0.8085 | -0.8078 | -0.7786                | -0.7824 | -0.7862 | -0.7793 | -0.7976               | -0.8017 | -0.8039 | -0.7987 |
|                 | 6400 | -0.8212                  | -0.8266     | -0.8238 | -0.8233 | -0.7885                | -0.7916 | -0.7952 | -0.7890 | -0.8076               | -0.8108 | -0.8131 | -0.8083 |
|                 | 6500 | -0.8341                  | -0.8383     | -0.8360 | -0.8356 | -0.7965                | -0.7991 | -0.8024 | -0.7969 | -0.8152               | -0.8177 | -0.8201 | -0.8156 |
|                 | 6600 | -0.8441                  | -0.8473     | -0.8455 | -0.8451 | -0.8033                | -0.8053 | -0.8083 | -0.8035 | -0.8209               | -0.8230 | -0.8252 | -0.8213 |
|                 | 6700 | -0.8515                  | -0.8540     | -0.8525 | -0.8522 | -0.8085                | -0.8101 | -0.8129 | -0.8087 | -0.8255               | -0.8271 | -0.8290 | -0.8257 |
|                 | 6800 | -0.8565                  | -0.8585     | -0.8574 | -0.8570 | -0.8122                | -0.8135 | -0.8161 | -0.8124 | -0.8286               | -0.8298 | -0.8317 | -0.8287 |
|                 | 6900 | -0.8596                  | -0.8611     | -0.8603 | -0.8599 | -0.8150                | -0.8162 | -0.8184 | -0.8151 | -0.8302               | -0.8312 | -0.8330 | -0.8304 |
|                 | 7000 | -0.8608                  | -0.8621     | -0.8614 | -0.8611 | -0.8169                | -0.8179 | -0.8198 | -0.8170 | -0.8309               | -0.8317 | -0.8335 | -0.8310 |
| H <sub>δ</sub>  | 4300 | -0.4444                  | -0.4494     | -0.4480 | -0.4434 | -0.4752                | -0.4879 | -0.4875 | -0.4750 | -0.4691               | -0.4802 | -0.4801 | -0.4684 |
|                 | 4400 | -0.4519                  | -0.4567     | -0.4561 | -0.4504 | -0.4753                | -0.4868 | -0.4864 | -0.4747 | -0.4698               | -0.4800 | -0.4799 | -0.4690 |
|                 | 4500 | -0.4574                  | -0.4620     | -0.4619 | -0.4558 | -0.4744                | -0.4841 | -0.4837 | -0.4729 | -0.4697               | -0.4784 | -0.4783 | -0.4682 |
|                 | 4600 | -0.4610                  | -0.4649     | -0.4653 | -0.4592 | -0.4717                | -0.4790 | -0.4787 | -0.4689 | -0.4680               | -0.4748 | -0.4748 | -0.4655 |
|                 | 4700 | -0.4621                  | -0.4649     | -0.4655 | -0.4596 | -0.4666                | -0.4715 | -0.4713 | -0.4625 | -0.4644               | -0.4689 | -0.4690 | -0.4607 |
|                 | 4800 | -0.4606                  | -0.4621     | -0.4629 | -0.4575 | -0.4590                | -0.4618 | -0.4618 | -0.4540 | -0.4583               | -0.4609 | -0.4611 | -0.4538 |
|                 | 4900 | -0.4568                  | -0.4568     | -0.4577 | -0.4531 | -0.4491                | -0.4504 | -0.4504 | -0.4439 | -0.4500               | -0.4511 | -0.4449 | -0.4449 |
|                 | 5000 | -0.4509                  | -0.4496     | -0.4505 | -0.4467 | -0.4372                | -0.4376 | -0.4377 | -0.4322 | -0.4396               | -0.4392 | -0.4396 | -0.4345 |
|                 | 5100 | -0.4431                  | -0.4407     | -0.4417 | -0.4385 | -0.4235                | -0.4236 | -0.4238 | -0.4193 | -0.4273               | -0.4264 | -0.4268 | -0.4227 |
|                 | 5200 | -0.4334                  | -0.4304     | -0.4314 | -0.4290 | -0.4085                | -0.4087 | -0.4088 | -0.4052 | -0.4134               | -0.4124 | -0.4128 | -0.4096 |
|                 | 5300 | -0.4222                  | -0.4189     | -0.4200 | -0.4180 | -0.3922                | -0.3924 | -0.3926 | -0.3898 | -0.3983               | -0.3973 | -0.3978 | -0.3953 |
|                 | 5400 | -0.4094                  | -0.4063     | -0.4074 | -0.4059 | -0.3751                | -0.3754 | -0.3756 | -0.3733 | -0.3821               | -0.3813 | -0.3818 | -0.3799 |
|                 | 5500 | -0.3954                  | -0.3926     | -0.3938 | -0.3925 | -0.3574                | -0.3577 | -0.3580 | -0.3561 | -0.3650               | -0.3644 | -0.3650 | -0.3634 |
|                 | 5600 | -0.3801                  | -0.3778     | -0.3791 | -0.3778 | -0.3389                | -0.3393 | -0.3396 | -0.3380 | -0.3471               | -0.3467 | -0.3472 | -0.3459 |
|                 | 5700 | -0.3638                  | -0.3619     | -0.3633 | -0.3620 | -0.3197                | -0.3201 | -0.3204 | -0.3190 | -0.3284               | -0.3282 | -0.3288 | -0.3276 |
|                 | 5800 | -0.3464                  | -0.3450     | -0.3464 | -0.3451 | -0.2997                | -0.3002 | -0.3006 | -0.2992 | -0.3092               | -0.3090 | -0.3097 | -0.3086 |
|                 | 5900 | -0.3282                  | -0.3270     | -0.3285 | -0.3272 | -0.2790                | -0.2796 | -0.2799 | -0.2786 | -0.2890               | -0.2891 | -0.2897 | -0.2886 |
|                 | 6000 | -0.3093                  | -0.3084     | -0.3099 | -0.3085 | -0.2578                | -0.2585 | -0.2589 | -0.2575 | -0.2683               | -0.2685 | -0.2692 | -0.2680 |
|                 | 6100 | -0.2898                  | -0.2894     | -0.2905 | -0.2891 | -0.2362                | -0.2370 | -0.2374 | -0.2360 | -0.2472               | -0.2475 | -0.2482 | -0.2469 |
|                 | 6200 | -0.2702                  | -0.2697     | -0.2710 | -0.2696 | -0.2144                | -0.2153 | -0.2156 | -0.2143 | -0.2257               | -0.2261 | -0.2268 | -0.2255 |
|                 | 6300 | -0.2499                  | -0.2495     | -0.2509 | -0.2494 | -0.1927                | -0.1935 | -0.1937 | -0.1925 | -0.2041               | -0.2045 | -0.2052 | -0.2039 |
|                 | 6400 | -0.2292                  | -0.2289     | -0.2303 | -0.2288 | -0.1708                | -0.1716 | -0.1718 | -0.1707 | -0.1822               | -0.1827 | -0.1833 | -0.1821 |
|                 | 6500 | -0.2081                  | -0.2080     | -0.2095 | -0.2079 | -0.1490                | -0.1498 | -0.1498 | -0.1489 | -0.1603               | -0.1609 | -0.1614 | -0.1603 |
|                 | 6600 | -0.1872                  | -0.1872     | -0.1886 | -0.1870 | -0.1274                | -0.1281 | -0.1281 | -0.1273 | -0.1385               | -0.1390 | -0.1395 | -0.1385 |
|                 | 6700 | -0.1662                  | -0.1663     | -0.1677 | -0.1661 | -0.1063                | -0.1069 | -0.1067 | -0.1062 | -0.1170               | -0.1175 | -0.1178 | -0.1170 |
|                 | 6800 | -0.1453                  | -0.1454     | -0.1468 | -0.1452 | -0.0857                | -0.0862 | -0.0858 | -0.0855 | -0.0958               | -0.0963 | -0.0965 | -0.0958 |
|                 | 6900 | -0.1245                  | -0.1246     | -0.1261 | -0.1244 | -0.0653                | -0.0658 | -0.0651 | -0.0652 | -0.0751               | -0.0755 | -0.0756 | -0.0750 |
|                 | 7000 | -0.1038                  | -0.1040     | -0.1055 | -0.1038 | -0.0452                | -0.0455 | -0.0449 | -0.0451 | -0.0548               | -0.0551 | -0.0552 | -0.0547 |
| H <sub>γ</sub>  | 4300 | -0.2594                  | -0.2854     | -0.2845 | -0.2717 | -0.2249                | -0.3120 | -0.3094 | -0.2791 | -0.2317               | -0.3029 | -0.3006 | -0.2739 |
|                 | 4400 | -0.2404                  | -0.2684     | -0.2673 | -0.2539 | -0.2035                | -0.2949 | -0.2924 | -0.2608 | -0.2099               | -0.2862 | -0.2839 | -0.2560 |
|                 | 4500 | -0.2209                  | -0.2517     | -0.2504 | -0.2365 | -0.1845                | -0.2765 | -0.2742 | -0.2417 | -0.1906               | -0.2694 | -0.2672 | -0.2385 |
|                 | 4600 | -0.2022                  | -0.2364     | -0.2350 | -0.2204 | -0.1680                | -0.2559 | -0.2540 | -0.2214 | -0.1735               | -0.2514 | -0.2495 | -0.2204 |
|                 | 4700 | -0.1856                  | -0.2222     | -0.2207 | -0.2057 | -0.1541                | -0.2330 | -0.2317 | -0.2005 | -0.1589               | -0.2316 | -0.2302 | -0.2018 |
|                 | 4800 | -0.1710                  | -0.2083     | -0.2070 | -0.1918 | -0.1429                | -0.2094 | -0.2085 | -0.1809 | -0.1465               | -0.2106 | -0.2096 | -0.1835 |
|                 | 4900 | -0.1583                  | -0.1943     | -0.1933 | -0.1786 | -0.1340                | -0.1869 | -0.1864 | -0.1639 | -0.1365               | -0.1896 | -0.1890 | -0.1667 |
|                 | 5000 | -0.1471                  | -0.1803     | -0.1795 | -0.1661 | -0.1268                | -0.1670 | -0.1667 | -0.1496 | -0.1284               | -0.1703 | -0.1700 | -0.1524 |
|                 | 5100 | -0.1374                  | -0.1665     | -0.1661 | -0.1545 | -0.1204                | -0.1501 | -0.1500 | -0.1376 | -0.1216               | -0.1536 | -0.1535 | -0.1403 |
|                 | 5200 | -0.1291                  | -0.1537     | -0.1535 | -0.1441 | -0.1142                | -0.1357 | -0.1357 | -0.1269 | -0.1155               | -0.1392 | -0.1392 | -0.1298 |
|                 | 5300 | -0.1218                  | -0.1420     | -0.1419 | -0.1347 | -0.1073                | -0.1228 | -0.1229 | -0.1167 | -0.1092               | -0.1267 | -0.1268 | -0.1200 |
|                 | 5400 | -0.1150                  | -0.1313     | -0.1314 | -0.1261 | -0.0997                | -0.1109 | -0.1110 | -0.1064 | -0.1024               | -0.1152 | -0.1153 | -0.1105 |
|                 | 5500 | -0.1086                  | -0.1214     | -0.1216 | -0.1177 | -0.0911                | -0.0992 | -0.0994 | -0.0958 | -0.0946               | -0.1040 | -0.1042 | -0.1005 |
|                 | 5600 | -0.1019                  | -0.1118</td |         |         |                        |         |         |         |                       |         |         |         |

Table B.1: Continued.

| Index | T[K] | MS-TO ( $\log g = 4.2$ ) |         |         |         | RGB ( $\log g = 2.4$ ) |         |         |         | HB ( $\log g = 2.8$ ) |         |         |         |
|-------|------|--------------------------|---------|---------|---------|------------------------|---------|---------|---------|-----------------------|---------|---------|---------|
|       |      | Ref                      | IY2     | IY4     | 2Y2     | Ref                    | IY2     | IY4     | 2Y2     | Ref                   | IY2     | IY4     | 2Y2     |
| Na    | 4300 | 0.0514                   | 0.0624  | 0.0631  | 0.0651  | 0.0461                 | 0.0507  | 0.0509  | 0.0536  | 0.0470                | 0.0522  | 0.0525  | 0.0551  |
|       | 4400 | 0.0520                   | 0.0622  | 0.0629  | 0.0648  | 0.0476                 | 0.0522  | 0.0523  | 0.0549  | 0.0483                | 0.0534  | 0.0537  | 0.0562  |
|       | 4500 | 0.0526                   | 0.0621  | 0.0627  | 0.0644  | 0.0490                 | 0.0537  | 0.0538  | 0.0562  | 0.0496                | 0.0547  | 0.0549  | 0.0572  |
|       | 4600 | 0.0532                   | 0.0622  | 0.0627  | 0.0642  | 0.0504                 | 0.0552  | 0.0553  | 0.0574  | 0.0508                | 0.0560  | 0.0562  | 0.0582  |
|       | 4700 | 0.0538                   | 0.0623  | 0.0627  | 0.0640  | 0.0516                 | 0.0566  | 0.0567  | 0.0584  | 0.0519                | 0.0572  | 0.0573  | 0.0590  |
|       | 4800 | 0.0544                   | 0.0624  | 0.0628  | 0.0638  | 0.0527                 | 0.0578  | 0.0579  | 0.0593  | 0.0529                | 0.0583  | 0.0584  | 0.0598  |
|       | 4900 | 0.0549                   | 0.0626  | 0.0629  | 0.0638  | 0.0537                 | 0.0588  | 0.0589  | 0.0601  | 0.0538                | 0.0592  | 0.0593  | 0.0604  |
|       | 5000 | 0.0554                   | 0.0628  | 0.0631  | 0.0637  | 0.0546                 | 0.0597  | 0.0597  | 0.0607  | 0.0547                | 0.0600  | 0.0601  | 0.0610  |
|       | 5100 | 0.0559                   | 0.0630  | 0.0632  | 0.0637  | 0.0553                 | 0.0604  | 0.0604  | 0.0612  | 0.0554                | 0.0606  | 0.0607  | 0.0615  |
|       | 5200 | 0.0564                   | 0.0631  | 0.0633  | 0.0637  | 0.0559                 | 0.0609  | 0.0609  | 0.0616  | 0.0560                | 0.0612  | 0.0612  | 0.0618  |
|       | 5300 | 0.0568                   | 0.0632  | 0.0633  | 0.0637  | 0.0564                 | 0.0613  | 0.0614  | 0.0619  | 0.0565                | 0.0616  | 0.0616  | 0.0621  |
|       | 5400 | 0.0572                   | 0.0632  | 0.0633  | 0.0636  | 0.0569                 | 0.0617  | 0.0617  | 0.0622  | 0.0569                | 0.0619  | 0.0619  | 0.0623  |
|       | 5500 | 0.0575                   | 0.0632  | 0.0633  | 0.0636  | 0.0572                 | 0.0619  | 0.0619  | 0.0624  | 0.0573                | 0.0621  | 0.0621  | 0.0625  |
|       | 5600 | 0.0578                   | 0.0632  | 0.0633  | 0.0635  | 0.0575                 | 0.0621  | 0.0621  | 0.0625  | 0.0575                | 0.0622  | 0.0622  | 0.0626  |
|       | 5700 | 0.0580                   | 0.0632  | 0.0632  | 0.0634  | 0.0577                 | 0.0622  | 0.0622  | 0.0625  | 0.0578                | 0.0623  | 0.0623  | 0.0626  |
|       | 5800 | 0.0582                   | 0.0631  | 0.0631  | 0.0633  | 0.0579                 | 0.0623  | 0.0623  | 0.0626  | 0.0580                | 0.0624  | 0.0624  | 0.0627  |
|       | 5900 | 0.0583                   | 0.0630  | 0.0630  | 0.0632  | 0.0581                 | 0.0623  | 0.0623  | 0.0626  | 0.0581                | 0.0624  | 0.0624  | 0.0627  |
|       | 6000 | 0.0584                   | 0.0629  | 0.0629  | 0.0630  | 0.0582                 | 0.0623  | 0.0623  | 0.0626  | 0.0583                | 0.0624  | 0.0624  | 0.0626  |
|       | 6100 | 0.0585                   | 0.0628  | 0.0628  | 0.0629  | 0.0583                 | 0.0623  | 0.0623  | 0.0625  | 0.0584                | 0.0624  | 0.0624  | 0.0626  |
|       | 6200 | 0.0586                   | 0.0627  | 0.0627  | 0.0628  | 0.0584                 | 0.0622  | 0.0622  | 0.0624  | 0.0585                | 0.0623  | 0.0623  | 0.0625  |
|       | 6300 | 0.0587                   | 0.0626  | 0.0625  | 0.0627  | 0.0585                 | 0.0622  | 0.0622  | 0.0624  | 0.0585                | 0.0623  | 0.0622  | 0.0624  |
|       | 6400 | 0.0587                   | 0.0624  | 0.0624  | 0.0625  | 0.0586                 | 0.0621  | 0.0621  | 0.0623  | 0.0586                | 0.0622  | 0.0622  | 0.0623  |
|       | 6500 | 0.0588                   | 0.0623  | 0.0623  | 0.0624  | 0.0586                 | 0.0620  | 0.0620  | 0.0621  | 0.0587                | 0.0621  | 0.0621  | 0.0622  |
|       | 6600 | 0.0588                   | 0.0622  | 0.0622  | 0.0623  | 0.0587                 | 0.0619  | 0.0618  | 0.0620  | 0.0587                | 0.0620  | 0.0619  | 0.0621  |
|       | 6700 | 0.0588                   | 0.0621  | 0.0621  | 0.0621  | 0.0587                 | 0.0617  | 0.0617  | 0.0619  | 0.0587                | 0.0618  | 0.0618  | 0.0619  |
|       | 6800 | 0.0589                   | 0.0619  | 0.0619  | 0.0620  | 0.0587                 | 0.0616  | 0.0616  | 0.0617  | 0.0588                | 0.0617  | 0.0617  | 0.0618  |
|       | 6900 | 0.0589                   | 0.0618  | 0.0618  | 0.0619  | 0.0588                 | 0.0614  | 0.0614  | 0.0615  | 0.0588                | 0.0615  | 0.0615  | 0.0616  |
|       | 7000 | 0.0589                   | 0.0617  | 0.0617  | 0.0617  | 0.0588                 | 0.0612  | 0.0612  | 0.0613  | 0.0588                | 0.0614  | 0.0614  | 0.0615  |
| Na D  | 4300 | -1.0923                  | -0.9934 | -0.9850 | -0.9939 | -1.1420                | -1.1012 | -1.0985 | -1.1027 | -1.1356               | -1.0851 | -1.0812 | -1.0862 |
|       | 4400 | -1.1066                  | -1.0168 | -1.0093 | -1.0173 | -1.1494                | -1.1155 | -1.1134 | -1.1170 | -1.1446               | -1.1027 | -1.0995 | -1.1038 |
|       | 4500 | -1.1197                  | -1.0414 | -1.0345 | -1.0418 | -1.1554                | -1.1271 | -1.1254 | -1.1285 | -1.1517               | -1.1166 | -1.1141 | -1.1177 |
|       | 4600 | -1.1316                  | -1.0649 | -1.0589 | -1.0654 | -1.1604                | -1.1368 | -1.1353 | -1.1380 | -1.1575               | -1.1280 | -1.1259 | -1.1290 |
|       | 4700 | -1.1415                  | -1.0847 | -1.0797 | -1.0851 | -1.1647                | -1.1450 | -1.1437 | -1.1460 | -1.1624               | -1.1375 | -1.1357 | -1.1383 |
|       | 4800 | -1.1496                  | -1.1009 | -1.0967 | -1.1012 | -1.1685                | -1.1520 | -1.1509 | -1.1527 | -1.1667               | -1.1455 | -1.1440 | -1.1462 |
|       | 4900 | -1.1563                  | -1.1143 | -1.1107 | -1.1145 | -1.1720                | -1.1581 | -1.1571 | -1.1586 | -1.1705               | -1.1525 | -1.1512 | -1.1530 |
|       | 5000 | -1.1620                  | -1.1256 | -1.1225 | -1.1257 | -1.1751                | -1.1633 | -1.1625 | -1.1637 | -1.1738               | -1.1585 | -1.1574 | -1.1589 |
|       | 5100 | -1.1670                  | -1.1351 | -1.1325 | -1.1352 | -1.1779                | -1.1679 | -1.1672 | -1.1682 | -1.1769               | -1.1637 | -1.1628 | -1.1641 |
|       | 5200 | -1.1713                  | -1.1433 | -1.1411 | -1.1434 | -1.1804                | -1.1719 | -1.1714 | -1.1721 | -1.1796               | -1.1684 | -1.1676 | -1.1686 |
|       | 5300 | -1.1750                  | -1.1505 | -1.1485 | -1.1506 | -1.1826                | -1.1754 | -1.1750 | -1.1756 | -1.1820               | -1.1725 | -1.1718 | -1.1727 |
|       | 5400 | -1.1784                  | -1.1569 | -1.1551 | -1.1570 | -1.1847                | -1.1785 | -1.1781 | -1.1787 | -1.1842               | -1.1760 | -1.1755 | -1.1763 |
|       | 5500 | -1.1813                  | -1.1625 | -1.1610 | -1.1626 | -1.1865                | -1.1811 | -1.1809 | -1.1814 | -1.1862               | -1.1792 | -1.1787 | -1.1795 |
|       | 5600 | -1.1839                  | -1.1676 | -1.1662 | -1.1677 | -1.1882                | -1.1835 | -1.1833 | -1.1838 | -1.1880               | -1.1819 | -1.1816 | -1.1822 |
|       | 5700 | -1.1862                  | -1.1721 | -1.1709 | -1.1722 | -1.1898                | -1.1856 | -1.1855 | -1.1859 | -1.1896               | -1.1844 | -1.1841 | -1.1847 |
|       | 5800 | -1.1883                  | -1.1761 | -1.1751 | -1.1762 | -1.1914                | -1.1875 | -1.1874 | -1.1878 | -1.1911               | -1.1865 | -1.1863 | -1.1868 |
|       | 5900 | -1.1902                  | -1.1796 | -1.1787 | -1.1798 | -1.1928                | -1.1893 | -1.1892 | -1.1896 | -1.1926               | -1.1884 | -1.1883 | -1.1887 |
|       | 6000 | -1.1918                  | -1.1828 | -1.1820 | -1.1829 | -1.1942                | -1.1909 | -1.1909 | -1.1912 | -1.1939               | -1.1902 | -1.1901 | -1.1905 |
|       | 6100 | -1.1934                  | -1.1855 | -1.1849 | -1.1857 | -1.1955                | -1.1924 | -1.1924 | -1.1927 | -1.1952               | -1.1918 | -1.1917 | -1.1921 |
|       | 6200 | -1.1947                  | -1.1880 | -1.1874 | -1.1881 | -1.1969                | -1.1939 | -1.1938 | -1.1942 | -1.1965               | -1.1933 | -1.1932 | -1.1936 |
|       | 6300 | -1.1960                  | -1.1901 | -1.1897 | -1.1902 | -1.1981                | -1.1953 | -1.1952 | -1.1956 | -1.1977               | -1.1947 | -1.1946 | -1.1950 |
|       | 6400 | -1.1972                  | -1.1920 | -1.1917 | -1.1921 | -1.1994                | -1.1966 | -1.1966 | -1.1969 | -1.1990               | -1.1961 | -1.1960 | -1.1963 |
|       | 6500 | -1.1984                  | -1.1937 | -1.1934 | -1.1938 | -2.006                 | -1.1979 | -1.1978 | -1.1981 | -2.001                | -1.1973 | -1.1973 | -1.1976 |
|       | 6600 | -1.1994                  | -1.1953 | -1.1950 | -1.1954 | -2.017                 | -1.1991 | -1.1991 | -1.1993 | -2.012                | -1.1985 | -1.1985 | -1.1987 |
|       | 6700 | -1.2005                  | -1.1967 | -1.1965 | -1.1968 | -2.029                 | -1.2004 | -1.2003 | -1.2006 | -2.023                | -1.1997 | -1.1997 | -1.1999 |
|       | 6800 | -1.2015                  | -1.1980 | -1.1978 | -1.1981 | -2.041                 | -1.2016 | -1.2016 | -1.2018 | -2.035                | -1.2009 | -1.2008 | -1.2011 |
|       | 6900 | -1.2025                  | -1.1992 | -1.1990 | -1.1993 | -2.053                 | -1.2028 | -1.2027 | -1.2029 | -2.046                | -1.2021 | -1.2020 | -1.2022 |
|       | 7000 | -1.2034                  | -1.2004 | -1.2002 | -1.2004 | -2.064                 | -1.2039 | -1.2038 | -1.2041 | -2.056                | -1.2032 | -1.2031 | -1.2033 |

# Index of Figures

|     |   |    |
|-----|---|----|
| 1.1 | Distribution of metallicity [Fe/H] of 152 globular clusters of the Milky Way. The data were extracted from the catalog of Harris (1996). . . . .  | 2  |
| 1.2 | Color-magnitude diagram of M3 which is described with an isochrone calculated for a metallicity $Z = 0.001$ and an age of 12 Gyr. Data for CMD were extracted from the Advanced Camera for Surveys (ACS) of galactic GC (Sarajedini et al. 2007) and the isochrone was calculated using the Padova and Trieste Stellar Evolution Code (PARSEC) (Bressan et al. 2012) ( <a href="http://stev.oapd.inaf.it/cmd">http://stev.oapd.inaf.it/cmd</a> ). . . . .   | 4  |
| 1.3 | Comparison of the cyanogen distribution for RGB stars in the GCs NGC 3201 (Smith & Norris 1982), M4 (Norris 1981) and NGC 6752 (Norris et al. 1981). The abscissa indicates the cyanogen excess $\delta S(3839)$ on the CN index defined in Norris (1981), while the scale on the ordinate is arbitrary. Plot adapted from Smith & Norris (1982). . . . .   | 6  |
| 1.4 | Combined histograms of the CN-excess parameter for stars on the lower RGB of the clusters sample from Kayser et al. (2008). The gray histogram includes all eight clusters (M 15, M 22, M 55, NGC 288, NGC 362, NGC 5286, Palomar 12, and Terzan 7). In the black histogram Pal 12 and Ter 7 are not included because they are believed to belong to the Sgr dSph. $\delta CN$ shows a bimodal distribution, which was fitted by two Gaussians. The minimum between the two Gaussians marks the criterion to differentiate between CN-strong and CN-weak stars. Figure from Kayser et al. (2008). . . . . | 7  |
| 1.5 | Na-O anticorrelation observed in the 19 galactic GCs studied by Carretta et al. (2009). Upper limits in O abundances are shown as arrows and detections are indicated as open circles. Figure from Carretta et al. (2009). . . . .  | 8  |
| 1.6 | $\omega$ Cen CMD resulting from the $10 \times 10$ arcmin $^2$ mosaic of ACS images centered on the cluster center. On the right upper panel the four sub-giant sequences can be distinguished. In the lower right panel the three MSs are shown. The labels bMS and rMS indicate the blue and red main sequences, respectively, and MSA stands for a fainter red MS which is clearly separated from the bMS and rMS. Figure from Bellini et al. (2010). . . . .  | 10 |

- 1.7 Theoretical isochrones from the MS to the tip of the RGB for the four different chemical compositions proposed by Sbordone et al. (2011). The solid line corresponds to both the Reference and CNONa2Y2, because they are virtually identical. The black dots along this isochrone denote the points where the model atmosphere and synthetic spectra were calculated (see Table 1.2). The dashed line corresponds to the CNONa1Y2, while the dash-dotted line is for the CNONa1Y4. Figure adapted from Sbordone et al. (2011). . . . . 15

- 2.1  $(c_y, y)$  CMD for M3. The index  $c_y$  is defined as  $c_y = (u - v) - (v - y)$  according to the values of the  $uvby$  filters from the Strömgren photometry. Inset: histogram of the colour distribution of stars in the RGB magnitude interval  $15.3 < y < 17$ . Figure from Massari et al. (2016). . . . . 21

- 2.2  $(c_y, y)$  CMD and  $c_y$  spread for M3. The RGB stars are indicated by the yellow bullets while the blue bullets represent the AGB stars. The upper and medium right panel give the photometric error of the RGB and AGB, respectively, and the right lower panel shows the distribution of the photometric uncertainties in  $c_y$ . Figure from Gruyters et al. (2017). 22

|  |    |
|--|----|
| 3.1 Example of the output file of an atmosphere model computed with ATLAS9 at $T_{\text{eff}} = 6,000$ K, $\log g = 4.5$ and the reference mixture. First line: $T_{\text{eff}}$ , $\log g$ and the indication that the model was computed in Local Thermodynamic Equilibrium (LTE). Second: Title assigned to the model for reference, microturbulent velocity (VTURB), mixing-length-to-scale-height ratio (L/H), no convective overshooting (NOVER) and the newer set of ODFs. Third: it indicates which opacity sources were taken into account during the calculation. Fourth: convective transport used being 1.25 the mixing length parameter and without turbulence. Fifth line: ratio between the input and the solar metallicity, abundance in numeric density of hydrogen and the helium. From line 6 to 22, the abundance for the rest of the elements expressed as $\log(N_{\text{element}}) - \log(N_{\text{H+He}})$ , where each element is represented by its atomic number to the left of its abundance. The second part shows the values of seven parameters computed with respect to depth of the atmosphere divided into 72 layers: From the left to right column: Mass per square centimeter $\text{RHOX} = \int_0^x \rho(x)dx$ [ $\text{g cm}^{-2}$ ] at the depth $x$ , temperature T [K], gas pressure P [dyne $\text{cm}^{-2}$ ], electron number density XNE [ $\text{cm}^{-3}$ ], Rosseland mass absorption coefficient ABROSS $\kappa_{\text{Ross}}$ [ $\text{cm}^2 \text{ g}^{-1}$ ], acceleration due to the absorption of radiation ACCRAD [ $\text{cm s}^{-2}$ ], microturbulent velocity VTURB [ $\text{km s}^{-1}$ ], energy flux that bear a convection FLXCNV [ $\text{erg cm}^2 \text{ s}^{-1}$ ], convective velocity VCONV [ $\text{km s}^{-1}$ ] and sound velocity VELSND [ $\text{cm s}^{-1}$ ]. Only values for the first 14 layers at the bottom and last 14 layers at the top of the atmosphere are shown. The second last line, PRADK indicates the radiation pressure at the surface. . . . . | 30 |
| 3.2 Effect of the effective temperature on the temperature profile as function of $\log \tau$ for each of the four chemical compositions with a surface gravity $\log g = 4.2$ . . . . .   | 32 |
| 3.3 Upper panel: Temperature profile of models with $T_{\text{eff}} = 6,000$ K and $\log g = 4.2$ and with the four different chemical compositions of Sbordone et al. (2011). Lower panel: Temperature difference of the CNONa1Y2, CNONa1Y4 and CNONa2Y2 with respect to the Reference one. . . . .   | 33 |
| 3.4 As lower panel of Figure 3.3: Temperature difference of the CNONa1Y2, CNONa1Y4 and CNONa2Y2 with respect to Reference for the temperatures indicated in each panel. . . . .  | 34 |
| 3.5 Effect of the surface gravity on the temperature profile as function of $\log \tau_{\text{Ross}}$ for each of the four chemical compositions for models with $T_{\text{eff}} = 6,000$ K. The different colors indicate $\log g$ from 2.0 to 5.0. . . . .   | 35 |

|     |   |    |
|-----|---|----|
| 3.6 | Upper panel: Synthetic spectrum of a model atmosphere of $T_{\text{eff}} = 6,000$ K and $\log g = 4.2$ for the Reference chemical composition at $R = 500,000$ . Lower panel: The same spectrum broadened to $R = 2,500$ .  | 36 |
| 3.7 | Reference spectrum (upper panel) and the difference with each of the corresponding spectra of the three modified chemical compositions, as indicated in each panel, for a model atmosphere of $T_{\text{eff}} = 6,000$ K and $\log g = 4.2$ .   | 37 |
| 4.1 | Bandpasses of all spectral indices used in this work over the difference in flux from a CNONa1Y2 spectrum with respect to one of Reference at $T_{\text{eff}} = 6,000$ K and $\log g = 4.2$ . Upper panel shows only the Reference spectra. The rest of the panels show the bandpasses of each index. The origin of the definition is indicated in each panel. The indices of the Lick/IDS system are shown in two panels for more clarity. | 45 |
| 5.1 | Indices from Lick/IDS system (Part A) for the four chemical compositions: Reference (black line), CNONa1Y2 (red line), CNONa1Y4 (yellow line) and CNONa2Y2 (blue line) as a function of effective temperature for a fixed surface gravity $\log g = 4.2$ .  | 50 |
| 5.2 | As in Figure 5.1 but the Part B of the Lick/IDS indices.  | 51 |
| 5.3 | Difference between the Lick/IDS indices (Part A) of the chemical composition CNONa1Y2 (red line), CNONa1Y4 (yellow line) and CNONa2Y2 (blue line) with respect to the Reference abundance as a function of effective temperature for a fixed surface gravity $\log g = 4.2$ .   | 52 |
| 5.4 | As in Figure 5.3 but the Part B of the Lick/IDS indices.  | 53 |
| 5.5 | Indices from Pancino et al. (2010) and the defined in this work for the four chemical compositions: Reference (black line), CNONa1Y2 (red line), CNONa1Y4 (yellow line) and CNONa2Y2 (blue line) as a function of effective temperature for a fixed surface gravity $\log g = 4.2$ .  | 56 |
| 5.6 | Difference between the indices from Pancino et al. (2010) and the defined in this work of the chemical composition CNONa1Y2 (red line), CNONa1Y4 (yellow line) and CNONa2Y2 (blue line) with respect to the Reference abundance as a function of effective temperature for a fixed surface gravity $\log g = 4.2$ .   | 57 |
| 5.7 | Color-magnitude diagram of M3 highlighting the regions defined in Table 5.1. Data extracted from Ferraro et al. (1997) catalog.   | 59 |
| 5.8 | <i>Throw</i> for Lick/IDS indices (Part A) of the chemical composition CNONa1Y2 (red line), CNONa1Y4 (yellow line) and CNONa2Y2 (blue line) with respect to the Reference abundance as a function of effective temperature for a fixed surface gravity $\log g = 4.2$ .   | 60 |
| 5.9 | As in Figure 5.8 but the Part B of the Lick/IDS indices.  | 61 |

|      |   |    |
|------|---|----|
| 5.10 | <i>Throw</i> for Pancino et al. (2010) indices and the defined in this work of the chemical composition CNONa1Y2 (red line), CNONa1Y4 (yellow line) and CNONa2Y2 (blue line) with respect to the Reference abundance as a function of effective temperature for a fixed surface gravity $\log g = 4.2$ . . . . .            | 62 |
| 5.11 | <i>Throw</i> of the chemical composition: CNONa1Y2 (red line), CNONa1Y4 (yellow line) and CNONa2Y2 (blue line) with respect to the Reference as a function of effective temperature for MS stars considering $\log g = 4.2$ , calculated with the Lick/IDS system. . . . .  | 64 |
| 5.12 | <i>Throw</i> of the chemical composition: CNONa1Y2 (red line), CNONa1Y4 (yellow line) and CNONa2Y2 (blue line) with respect to the Reference as a function of effective temperature for MS stars considering $\log g = 4.2$ , calculated with the indices from Pancino et al. (2010) and the defined in this work. . . . .  | 65 |
| 5.13 | <i>Throw</i> of the chemical composition CNONa1Y2 with respect to CNONa1Y4 as a function of effective temperature for MS stars considering $\log g = 4.2$ , calculated with the Lick/IDS system. . . . .  | 66 |
| 5.14 | <i>Throw</i> of the chemical composition CNONa1Y2 with respect to CNONa1Y4 as a function of effective temperature for MS stars considering $\log g = 4.2$ for the indices from Pancino et al. (2010) and the defined in this work. . . . .  | 67 |
| 5.15 | <i>Throw</i> of the chemical composition: CNONa1Y2 (red line), CNONa1Y4 (yellow line) and CNONa2Y2 (blue line) with respect to the Reference as a function of effective temperature for RGB stars considering $\log g = 2.4$ , calculated with the Lick/IDS system. . . . .   | 70 |
| 5.16 | <i>Throw</i> of the chemical composition: CNONa1Y2 (red line), CNONa1Y4 (yellow line) and CNONa2Y2 (blue line) with respect to the Reference as a function of effective temperature for RGB stars considering $\log g = 2.4$ , calculated with the indices from Pancino et al. (2010) and the defined in this work. . . . . | 71 |
| 5.17 | <i>Throw</i> of the chemical composition: CNONa1Y2 (red line), CNONa1Y4 (yellow line) and CNONa2Y2 (blue line) with respect to the Reference as a function of effective temperature for HB stars considering $\log g = 2.8$ , calculated with the Lick/IDS system. . . . .  | 72 |
| 5.18 | <i>Throw</i> of the chemical composition: CNONa1Y2 (red line), CNONa1Y4 (yellow line) and CNONa2Y2 (blue line) with respect to the Reference as a function of effective temperature for HB stars considering $\log g = 2.8$ , calculated with the indices from Pancino et al. (2010) and the defined in this work. . . . .  | 73 |
| 6.1  | RA and DEC position of the M3 stars included in the Ferraro et al. (1997) catalog. . . . .  | 77 |

|     |   |    |
|-----|---|----|
| 6.2 | Color-magnitude diagram of the Ferraro et al. (1997) catalog of the globular cluster M3 highlighting the four regions used to extract a preliminary sample of stars. The conversion from $B - V$ to $T_{\text{eff}}$ was done using relation of Sekiguchi & Fukugita (2000). . . . .  | 79 |
| 6.3 | Histogram of the number of stars matched in both of Ferraro and Gaia catalogs according to the regions established in Figure 6.2 for a slit of RA: 1 arcmin $\times$ DEC: 7.5 arcmin. . . . .   | 80 |
| 6.4 | SDSS image of the eastern region of M3, centered in the $1 \times 7.5$ arcmin rectangular region where the OSIRIS targets were identified. . . . .  | 81 |
| 6.5 | Generated image by OSIRIS Mask Designer over the U band SDSS image of M3. Every target star is indicated by a white rectangle, while the reference stars are shown in white circle. . . . .   | 82 |
| 6.6 | Color-magnitude diagram of the Ferraro et al. (1997) catalog of the globular cluster M3 with the 71 selected targets stars. The conversion from $B - V$ to $T_{\text{eff}}$ was done using relation of Sekiguchi & Fukugita (2000). . . . .   | 85 |
| 6.7 | Preliminary spectra of six observed stars of MS with the GTC (in black color) and their comparison with a theoretical normalized spectra at $T = 6,000$ K, $\log g = 4.2$ and the Reference abundance (in gray color). Left panels show the part corresponding to grism R2500U while right panels display that of the R2500V. Each panel is labeled with the identification of the star according to Table 6.2 in the blue part of the spectra (R2500U). On the spectra of the stars MS19 and MS28 are drawn the bandpasses central of the Lick/IDS indices, on the MS34 that reported by Pancino et al. (2010) and on the MS44 the indices defined in this work. . . . . | 87 |

# Index of Tables

|     |   |    |
|-----|---|----|
| 1.1 | Fraction of stars and summary of the main properties of the seven stellar populations of M2 reported by Milone et al. (2015). . . . .   | 10 |
| 1.2 | Parameters used by Sbordone et al. (2011) to generate the model atmospheres for the four mixtures. . . . .  | 14 |
| 1.3 | Abundances for selected elements in the four chemical compositions used for computing model atmospheres. . . . .  | 16 |
| 2.1 | Some important properties of M3 (Data obtained from Harris (1996)). .   | 20 |
| 3.1 | Number of models that converged within different threshold values. .  | 29 |
| 3.2 | Not converged models and their associated flux error. . . . .   | 31 |
| 4.1 | Lick/IDS index definitions. Indices 1 - 21 are from Table 2 of Trager et al. (1998) whereas indices 22 - 25 are from Table 1 of Worthey & Ottaviani (1997). . . . .   | 40 |
| 4.2 | Bandpass definition of the new spectroscopic indices defined in this work.  | 43 |
| 4.3 | Errors calculated by using a Monte Carlo technique for a spectra at $T = 6,000$ K and $\log g = 4.2$ . . . . .  | 46 |
| 5.1 | Adopted parameters of different evolutionary stages defined in the CMD of M3. . . . .   | 58 |
| 6.1 | Color criteria for extracting a preliminary sample of stars to observe. .   | 78 |
| 6.2 | Gaia coordinates and G-band magnitudes of the 71 selected targets + 5 reference stars. The label in the second column means, MS: Main Sequence, TO: Turn-off and RG: Red Giant Branch. The error is millisecond of arc (mas). . . . . | 83 |
| A.1 | Abundances for all elements in the considered mixtures. . . . .   | 91 |
| B.1 | All of the spectroscopic indices calculated for the three different set of physical conditions representing at the evolutionary stages MS-TO, RGB and HB of M3, extended over the entire range of effective temperature. . . . .      | 95 |



# References

- Baade, W. 1944, ApJ, 100, 137
- Bakos, G. A., Benko, J. M., & Jurcsik, J. 2000, AA, 350, 221
- Bastian, N., Cabrera-Ziri, I., & Salaris, M. 2015, MNRAS, 449, 3333
- Bastian, N., & Lardo, C. 2015, MNRAS, 453, 357
- Bedin, L. R., Piotto, G., Anderson, J., et al. 2004, ApJ, 605, L125
- Behr, B. B. 2003, ApJS, 149, 67
- Bellini, A., Bedin, L. R., Piotto, G., et al. 2010, AJ, 140, 631
- Bertone, E. 2001, PhD thesis, Università degli Studi di Milano
- Bertone, E., Buzzoni, A., Chávez, M., & Rodríguez-Merino, L. H. 2004, AJ, 128, 829
- Bertone, E., Buzzoni, A., Chávez, M., & Rodríguez-Merino, L. H. 2008, AJ, 485, 823
- Bertone, E., Chávez, M., Tapia-Schiavon, C., & Hernández-Águila, J. B. 2013, ASPC, 472, 179
- Binney, J., & Merrifield, M. 1998, Galactic Astronomy (Princeton University Press)
- Bragaglia, A., Carretta, E., Sollima, A., et al. 2015, A&A, 583
- Bressan, A., Marigo, P., Girardi, L., et al. 2012, MNRAS, 427, 127
- Buonanno, R., Corsi, C. E., Buzzoni, A., et al. 1994, A&A, 290, 69
- Burstein, D., Faber, S. M., Gaskell, C. M., & Krumm, N. 1984, ApJ, 287, 586
- Cabrera-Lavers, A. 2014, OSIRIS User Manual, version 3.1 edn., GRANTECAN S.A.
- Cacciari, C., Corwin, T. M., & Carney, B. W. 2005, AJ, 129, 267
- Caloi, V., & D'Antona, F. 2008, AJ, 673, 847
- Carretta, E., Bragaglia, A., Gratton, R. G., et al. 2006, A&A, 450, 523

- . 2010, A&A, 129
- Carretta, E., Gratton, R. G., Bragaglia, A., Bonifacio, P., & Pasquini, L. 2004, A&A, 416, 925
- Carretta, E., Bragaglia, A., Gratton, R. G., et al. 2009, A&A, 505, 117
- Castellani, M., Castellani, V., & Cassis, S. 2005, A&A, 437, 1017
- Castelli, F. 2005a, Mem. S.A.It. Suppl., 8, 25
- . 2005b, Mem. S.A.It. Suppl., 8, 34
- Castelli, F., & Kurucz, R. L. 2003, IAU Symposium, 210, 20
- Catelan, M., Grundahl, F., Sweigart, A. V., Valcarce, A. A. R., & Cortés, C. 2009, AJ, 695, L97
- Cohen, J. G. 1978a, ApJ, 223, 487
- . 1978b, ApJ, 223, 487
- Cohen, J. G., & Meléndez, J. 2005, AJ, 129, 303
- Corwin, T. M., & Carney, R. W. 2001, ApJ, 122, 3183
- Dalessandro, E., Salaris, M., Ferraro, F. R., Mucciarelli, A., & Cassisi, S. 2013, MNRAS, 430, 459
- Decressin, T., Meynet, G., Charbonnel, C., Prantzos, N., & Ekström, S. 2007, A&A, 464, 1029
- D'Antona, F., & Caloi, V. 2008, MNRAS, 390, 693
- D'Ercole, A., Vesperini, E., D'Antona, F., McMillan, S. L. W., & Recchi, S. 2008, MNRAS, 391, 825
- Faber, S. M., Burstein, D., & Dressler, A. 1977, AJ, 82, 941
- Faber, S. M., Friel, E. D., Burstein, D., & Gaskell, C. M. 1985, ApJS, 57, 711
- Fall, S. M., & Zhang, Q. 2001, AJ, 561, 751
- Ferraro, F. R., Carretta, E., Corsi, C. E., et al. 1997, A&A, 320, 757
- Freeman, K. C., & Rodgers, A. W. 1975, ApJ, 201, L71
- Gaia-Collaboration, Brown, A. G. A., Vallenari, A., et al. 2016, A&A, 595
- García-Hernández, D. A., Mészáros, S., Monelli, M., et al. 2015, ApJ, 815

- Goldsbury, R., Richer, H. B., Anderson, J., et al. 2010, AJ, 140, 1830
- Gomez-González, V. M. A., Mayya, Y. D., & Rosa-González, D. 2016, MNRAS, 460, 1555
- Gratton, R. G., Carretta, E., & Bragaglia, A. 2012, A&A Rev., 20
- Gratton, R. G., Sneden, C., & Carretta, E. 2004, ARA&A, 42, 385
- Gratton, R. G., Lucatello, S., Sollima, A., et al. 2015, A&A, 573
- Grevesse, N., & Noels, A. 1993, in Origin and evolution of the elements, eds. N. Prantzos, E. Vangioni-Flam, & M. Casse, 15
- Gruyters, P., Casagrande, L., Milone, A. P., et al. 2017, A&A, 603
- Harbeck, D., Smith, G. H., & Grebel, E. K. 2003, AJ, 125, 197
- Harris, W. E. 1996, AJ, 112, 1487
- Husser, T. O., von Berg, S. W., Dreizler, S., et al. 2013, A&A, 533
- Jofré, P., & Weiss, A. 2011, A&A, 533
- Johnson, C. I., Kraft, R. P., Pilachowski, C. A., et al. 2005, PASP, 117, 1308
- Jordi, C., Gebran, M., Carrasco, J. M., et al. 2010, A&A, 523
- Jurcsik, J., Smitola, P., Hajdu, G., et al. 2017, MNRAS, 523, 1317
- Kayser, A., Hilker, M., Greber, E. H., & Willemse, P. G. 2008, A&A, 486, 437
- Krause, M., Charbonnel, C., Decressin, T., Meynet, G., & Prantzos, N. 2013, A&A, 552
- Kurucz, R. L. 1970, SAO Special Report, 309
- . 1979, ApJS, 40, 1
- . 1992, RMxAA, 23, 45
- Lardo, C. 2013, PhD thesis, Università di Bologna - Dipartimento di Fisica e Astronomia
- Lee, J.-W. 2010, MNRAS, 405, L36
- Lee, Y.-W., Joo, J.-M., Sohn, Y.-J., et al. 1999, Nature, 402, 55
- Massari, D., Lapenna, E., Bragaglia, A., et al. 2016, MNRAS, 458, 4162

- Milone, A. P., Piotto, G., Bedin, L. R., et al. 2012, *ApJ*, 744, 58
- Milone, A. P., Marino, A. F., Piotto, G., et al. 2013, *ApJ*, 767, 120
- . 2015, *MNRAS*, 447, 927
- Mészáros, S., Martell, S. L., Shetrone, M., et al. 2015, *AJ*, 149, 153
- Norris, J. 1981, *ApJ*, 248, 177
- Norris, J., Cottrell, P. L., Freeman, K. C., & Costa, G. S. D. 1981, *ApJ*, 244, 205
- Norris, J., & Freeman, K. C. 1979, *ApJ*, 230, L179
- Norris, J. E. 2004, *ApJ*, 612, L25
- Oosterhoff, P. T. 1939, *The Observatory*, 62, 104
- Osborn, W. 1971, *The Observatory*, 91, 223
- Pancino, E., Rejkuba, M., Zoccali, M., & Carrera, R. 2010, *A&A*, 524
- Pietrinferni, A., Cassisi, S., & Castelli, F. 2006, *ApJ*, 642, 797
- Piotto, G., Milone, A. P., Marino, A. F., et al. 2013, *ApJ*, 775, 15
- Piotto, G., Villanova, S., Bedin, L. R., et al. 2005, *AJ*, 621, 777
- Piotto, G., Bedin, L. R., Anderson, J., et al. 2007, *ApJ*, 661, L53
- Piotto, G., Milone, A. P., Bedin, L. R., et al. 2015, *AJ*, 149, 91
- Pryor, C., & Georges, M. 1993, *ASPC*, 50, 357
- Salaris, M., Weiss, A., Ferguson, J. W., & Fusilier, D. J. 2006, *ApJ*, 645, 1131
- Sarajedini, A., Bedin, L. R., Chaboyer, B., et al. 2007, *AJ*, 133, 1658
- Saxner, M., & Gustafsson, B. 1984, *A&A*, 140, 334
- Sbordone, L., Salaris, M., Weiss, A., & Cassisi, S. 2011, *A&A*, 534
- Sekiguchi, M., & Fukugita, M. 2000, *ApJ*, 120, 1072
- Smith, G. H., & Norris, J. 1982, *ApJ*, 254, 149
- Strom, S. E., & Kurucz, R. L. 1966, *ApJ*, 71, 181
- Trager, S. C., Worthey, G., Faber, S. M., Burstein, D., & González, J. J. 1998, *A&AS*, 116, 1

- Valcarce, A. A. R., Catelan, M., Alonso-García, J., Contreras-Ramos, R., & Alves, S. 2016, A&A, 589
- Villanova, S., Bidin, C. M., Mauro, F., Muñoz, C., & Monaco, L. 2017, MNRAS, 464, 2730
- Villanova, S., Piotto, G., King, I. R., et al. 2007, ApJ, 663, 296
- Worthey, G., Faber, S. M., González, J. J., & Burstein, D. 1994, ApJS, 94, 687
- Worthey, G., & Ottaviani, D. L. 1997, ApJS, 11, 377
- Wu, Z. Y., Wang, J. J., & Chen, L. 2002, Chin. J. Astron. Astrophys., 2, 216